

Functional characterization of the Wiskott Aldrich Syndrome Protein (WASP)

Lim, Rina Pei Zhi

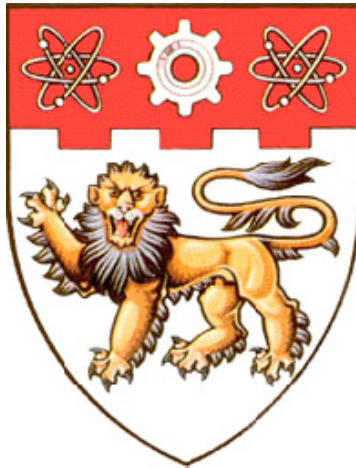
2011

Lim, R. P. Z. (2011). Functional characterization of the Wiskott Aldrich Syndrome Protein (WASP). Doctoral thesis, Nanyang Technological University, Singapore.

<https://hdl.handle.net/10356/46285>

<https://doi.org/10.32657/10356/46285>

Functional Characterization of the Wiskott Aldrich Syndrome Protein (WASP)



Lim Pei Zhi, Rina

**School of Biological Sciences
Nanyang Technological University**

2011

Functional Characterization of the Wiskott Aldrich Syndrome Protein (WASP)

Lim Pei Zhi, Rina

School of Biological Sciences

A thesis submitted to the Nanyang Technological University
in fulfillment of the requirement for the
degree of Doctor of Philosophy

2011

Acknowledgements

I would like to express my heartfelt gratitude to Dr Thiru for being such a wonderful supervisor, guardian and confidant. The four years in my PhD life was enriching and fulfilling but not entirely smooth-sailing. However, it was the optimism, constant encouragement and the words of wisdom from Dr Thiru that made it easier for me to get to the end of the arduous journey. For that, I am truly grateful.

My labmates Churou, Raodah, Swagata and Bhawana were a source of comfort and happiness. They made Mondays not as blue and work not as dull. I am thankful for the suggestions and help they provided when my experiments were failing and their generosity in the sharing of the equipment and reagents in the lab. Neeraj, my ‘collaborator’ was a great help and friend, raising new ideas that stirred my interest in our work. Mohan was an amazing senior, ever ready in providing help when my experiments reached a block and sharing his vast knowledge of everything that’s beyond the textbooks. Not forgetting the labmates in the earlier days of my PhD. Shangjuan, who is a sisterly figure to me. She was the one who helped to fit me into the lab, taught me the protocols and experiments and provided a listening ear when I was troubled. Zhanrui and Menglei, were ever helpful and cheerful, brightened up my days in the lab.

我要感谢我的父母。是他们的关爱及体量让我能专心的完成我的学业。妈妈每天煮的饭让我忘记每一天的疲惫和辛劳。爸爸每天不辞劳苦的送我去学校，我也感激不尽。I thank my sisters for being my pillars of support and making my home a place I look forward to returning to after a tiring day of work everyday. I thank Lester, for the help he has given in my work and the unfaltering support he has given to me in every aspect of my life.

I dedicate this dissertation to all who have made a difference in my life. For without them, it would have been impossible for me to reach this far in life today.

Contents

Acknowledgements	I
Contents	II
List of Figures	VI
List of Tables	VIII
Abbreviations	IX
Publications	XI
Abstract	XII
1. Introduction	1
1.1 The Cytoskeleton	1
1.1.1 Microtubules	2
1.1.2 Intermediate filaments	3
1.1.3 Actin Filaments	3
1.2 Arp2/3 complex and the actin nucleators	6
1.3 Nucleation promoting factors (NPFs)	10
1.4 Wiskott Aldrich Syndrome (WAS)	12
1.5 Wiskott Aldrich Syndrome protein (WASP)	13
1.6 Regulation of WASP	15
1.7 The Verprolin family of proteins	17
1.8 Physiological role of WASP	18
1.8.1 Function of WASP in lymphoid development	19
1.8.2 Function of WASP in the adaptive immune system	20
1.8.3 Function of WASP in the innate immune system	21
1.9 Phosphorylation of WASP and its significance	22
1.10 The Calpain family of proteases	26
1.10.1 Calpain and cell motility	28
1.10.2 Regulation of WASP by calpain	30
1.10.3 Role of WIP in the stability of WASP	31
1.10.4 Substrates of calpain	31
1.11 Objectives of project	32
2. Materials and Methods	35
2.1 Materials	35
2.1.1 Plasmids	35
2.1.2 Plasmid vectors	35
2.1.3 Bacterial strains	36
2.1.4 Yeast strains	36
2.1.5 Mammalian cell lines	36
2.1.6 Antibodies	36
2.1.7 Bacterial and yeast culture media	37
2.1.7.1 Luria-Bertani (LB) broth	37
2.1.7.2 LB agar plates	37
2.1.7.3 YPUAD medium	37
2.1.7.4 YPUAD agar plates	37
2.1.7.5 SD medium	38
2.1.7.6 SD agar plates	38
2.1.8 Mammalian cell culture media	39
2.1.9 Enzymes and kits	40

2.1.10	Polymerase chain reaction (PCR)	40
2.1.11	Chemicals and reagents	41
2.1.11.1	DNA work	41
2.1.11.2	Protein work	41
2.1.11.3	Others	41
2.1.12	General buffers and solutions	41
2.1.12.1	DNA subcloning experiments	41
2.1.12.1.1	50X Tris-acetate-EDTA (TAE)	41
2.1.12.1.2	Agarose gel	42
2.1.12.2	Western blots	42
2.1.12.2.1	10% SDS	42
2.1.12.2.2	10% Ammonium persulphate	42
2.1.12.2.3	5X Tris-glycine electrophoresis buffer	42
2.1.12.2.4	Transfer buffer	42
2.1.12.2.5	2X SDS-PAGE gel-loading buffer	42
2.1.12.2.6	1M Tris buffer	43
2.1.12.2.7	5M NaCl	43
2.1.12.2.8	1X Tris buffered saline (TBS)	43
2.1.12.2.9	Blocking solution	43
2.1.12.2.10	Wash solution	43
2.1.12.3	Gel staining	43
2.1.12.3.1	SDS PAGE gel destaining solution	43
2.1.12.3.2	SDS PAGE gel staining solution	44
2.1.13	Yeast reagents	44
2.1.13.1	10X LiAc	44
2.1.13.2	20% Tri-Chloro Acetic Acid (TCA)	44
2.1.13.3	50% PEG 3350	44
2.1.13.4	Loading dye (Urea buffer)	44
2.1.14	His tag pull-down assay	44
2.1.14.1	Equilibration buffer for Ni-NTA beads	44
2.1.14.2	Lysis Buffer (pull-down assay)	45
2.1.14.3	Elution Buffer for Ni-NTA beads	45
2.1.15	Tissue culture	45
2.1.15.1	Freezing media	45
2.1.15.2	Lysis buffer	45
2.1.15.3	Transfection reagent	46
2.2	Methods	46
2.2.1	<i>Escherichia coli</i> cells	46
2.2.1.1	Growth conditions and maintenance of <i>E. coli</i> cells	46
2.2.1.2	<i>E. coli</i> glycerol stocks preparation	46
2.2.1.3	Competent <i>E. coli</i> cells preparation	46
2.2.1.4	Transformation of <i>E. coli</i> cells	47
2.2.1.5	Plasmid DNA isolation from <i>E. coli</i> cells	47
2.2.2	<i>Saccharomyces cerevisiae</i> cells	48
2.2.2.1	Growth conditions and maintenance of <i>S. cerevisiae</i> cells	48
2.2.2.2	<i>S. cerevisiae</i> glycerol stocks preparation	48
2.2.2.3	Transformation of <i>S. cerevisiae</i> cells	48
2.2.2.4	Yeast two hybrid assay	49
2.2.2.5	Yeast cell lysis	50
2.2.2.6	Fluorescence visualization	51

2.2.3 Mammalian cell culture -----	51
2.2.3.1 Growth and maintenance of mammalian cells -----	51
2.2.3.2 Preparation of mammalian cell stocks -----	52
2.2.3.3 Transfection of adherent mammalian cells -----	52
2.2.3.4 Microporation of Jurkat cells -----	53
2.2.3.5 Ionomycin treatment of HEK 293T cells -----	53
2.2.3.6 Retrovirus vector mediated RNAi -----	53
2.2.3.7 Mammalian cell lysis -----	54
2.2.3.8 Actin staining of N-WASP ^{-/-} fibroblasts-----	55
2.2.3.9 Fluorescence visualization-----	55
2.2.3.10 Quantification of filopodia formation in N-WASP ^{-/-} fibroblasts-----	55
2.2.3.11 Fluorescence Resonance Energy transfer (FRET) assay-----	56
2.2.3.12 Flow cytometry-----	56
2.2.3.13 Analysis of Jurkat cell migration using the Dunn chemotaxis chamber-----	57
2.2.3.13.1 Washing of Dunn chamber and glass coverslips-----	57
2.2.3.13.2 Assembly of the Dunn chamber-----	58
2.2.3.13.3 Time-lapse microscopy-----	58
2.2.3.14 DNA manipulation-----	59
2.2.3.14.1 Agarose gel electrophoresis-----	59
2.2.3.14.2 DNA extraction from agarose gel -----	59
2.2.3.14.3 DNA subcloning -----	59
2.2.3.14.4 Verification of recombinant plasmid DNA constructs-----	60
2.2.3.14.5 Polymerase chain reaction (PCR)-----	60
2.2.3.14.5.1 Reverse transcription of RNA to cDNA -----	61
2.2.3.14.5.2 Real-time PCR (RT-PCR)-----	62
2.2.3.14.5.3 Site directed mutagenesis (SDM)-----	62
2.2.3.14.5.4 SDM kit-----	62
2.2.3.14.5.5 Overlap extension PCR-----	63
2.2.3.15 DNA precipitation-----	64
2.2.3.16 SDS-PAGE electrophoresis-----	64
2.2.3.17 Western blot analysis-----	65
2.2.3.18 His-tag pull down assay-----	64
2.2.3.19 GST protein expression and purification-----	67
2.2.3.20 Coomassie Staining-----	68
3. Results -----	69
3.1 Conformational analysis of WASP and its mutants using spilt YFP-----	69
3.1.1 Introduction-----	69
3.1.2 Bi-molecular Fluorescence Complementation (BiFC) -----	71
3.1.3 WIP and WIRE enhance YFP fluorescence from the WASP reporter -----	76
3.1.4 Toca1 and Nck1 reduce YFP fluorescence from the WASP reporter -----	80
3.1.5 Toca1 and Nck1 reduce YFP fluorescence even in the presence of WIP -----	84
3.1.6 Fluorescence from WASP reporter with mutations in WH1, GBD or VCA domain is not enhanced in the presence of WIP -----	86
3.1.7 WIP and WIRE enhance YFP fluorescence from the WASP reporter in mammalian cells-----	90
3.1.8 N-terminus of WIP is in close proximity to the C-terminus of WASP-----	92
3.2 Molecular characterisation of WASP ^{L270P} mutation related XLN-----	97
3.2.1 Introduction-----	97
3.2.2 WASP ^{L270P} adopts an open conformation-----	98

3.2.3	WASP with L270 mutation has increased phosphorylation in Tyr residues-----	99
3.2.4	Enhanced phosphorylation of WASP ^{L270P} is due to increased phosphorylation at residue 291-----	102
3.2.5	Phosphorylation causes WASP to adopt an open conformation-----	105
3.2.6	WASP mutants bearing mutations at Y291 are able to suppress growth defects of <i>las17Δ</i> cells-----	107
3.2.7	WASP knock down Jurkat T cells has impaired motility-----	108
3.2.8	WASP Y291 phosphorylation is crucial for T cell migration-----	114
3.2.9	WASP Y291 phosphorylation is required for filopodia induction in N-WASP ^{-/-} fibroblasts-----	119
3.3	Role of Calpain-mediated proteolysis of WASP in T cell function-----	124
3.3.1	Introduction-----	124
3.3.2	Fine mapping of WASP-WIP interaction site-----	125
3.3.3	<i>In vitro</i> proteolysis of WASP by calpain-----	128
3.3.4	Ionomycin treatment decreases the stability of WASP-----	129
3.3.5	WASP ⁹⁵⁻⁵⁰³ has reduced proteolysis by calpain-----	130
3.3.6	Mapping out the calpain cleavage site in WASP-----	133
3.3.7	Generation of a Calpain-resistant mutant of WASP-----	134
3.3.8	WASP ^{WRG} is resistant to calpain <i>in vitro</i> -----	137
3.3.9	WASP ^{WRG} mutant adopts an open conformation-----	138
3.3.10	WASP ^{WRG} mutant is able to form a functional complex with WIP-----	139
3.3.11	WASP ^{WRG} mutant induces filopodia to the same extent as WT WASP-----	140
3.3.12	Expression of WASP but not WASP ^{WRG} rescued impaired migration of WASP-deficient T cells-----	142
4	Discussion -----	145
4.1	Conformational analysis of WASP-----	145
4.1.1	Bi-molecular fluorescence complementation (BiFC) -----	145
4.1.2	WASP adopts an autoinhibited conformation-----	146
4.1.3	WIP and WIRE stabilize WASP in the autoinhibited conformation-----	147
4.1.4	Toca1 and Nck1 disrupt the autoinhibitory conformation of WASP-----	149
4.1.5	Mutations in WH1, GBD and VCA domains prevent stability of WASP in the closed conformation-----	150
4.1.6	N-terminus of WIP interacts with C-terminus of WASP-----	152
4.2	Role of phosphorylation of Tyr291 in the regulation of WASP-----	154
4.2.1	Differential phosphorylation of WASP ^{L270P} by different kinases-----	156
4.2.2	Phosphorylation affects the conformation of WASP-----	157
4.2.3	Dysregulation of phosphorylation in WASP with mutation associated with XLN leads to defects in T cell migration-----	159
4.3	Function of Calpain-mediated proteolysis of WASP-----	163
4.3.1	Role of WASP and calpain in cell motility-----	163
4.3.2	Calpain proteolysis of WASP-----	164
4.3.3	Role of Calpain-mediated proteolysis of WASP in cell motility-----	167
4.4	Future directions-----	170
4.4	Conclusion-----	172
5.	References -----	178

Appendix 1: Plasmids used in this study-----	194
Appendix 2: Primers used for constructs-----	199
Appendix 3: Protein sequence of WASP-----	202
Appendix 3: cDNA sequence of WASP-----	202

List of Figures

Introduction

Figure 1.1 The three types of cytoskeletal filaments-----	2
Figure 1.2 The structure of Arp2/3 complex and a model for nucleation and branching of actin-----	7
Figure 1.3 The three classes of nucleation factors-----	8
Figure 1.4 Schematic Figure showing the difference in association of Class I and II NPFs with the Arp2/3 complex-----	11
Figure 1.5 Class I and II NPFs-----	12
Figure 1.6 Schematic diagram illustrating the common domains shared by the WASP family of proteins-----	14
Figure 1.7 Sequence alignment of EVH1 domains from Mena, VASP, Ena and WH1 domain from WASP-----	15
Figure 1.8 Schematic diagram showing functional domains of WASP and its conformation in presence of different regulators-----	16
Figure 1.9 Regulation of WASP by phosphorylation-----	26
Figure 1.10 Schematic diagram showing the domain structures of the members of the calpain family of proteases-----	28

Materials and Methods

Figure 2.1 The assembled Dunn chamber-----	58
Figure 2.2 Schematic diagram of the overlap extension PCR-----	63

Results 3.1

Figure 3.1 Schematic illustration of the FRET assay-----	70
Figure 3.2 Schematic diagram showing fusion constructs used -----	72
Figure 3.3 Bi-molecular fluorescence complementation observed in <i>S. cerevisiae</i> cells-----	75
Figure 3.4 Schematic diagram showing fusion constructs used-----	76
Figure 3.5 WIP and WIRE enhance fluorescence signals from the WASP reporter-----	78
Figure 3.6 Schematic diagram showing fusion constructs used-----	79
Figure 3.7 NLS-WIP, NLS-WIRE and NLS-CR16 are localized in the nuclei of <i>S. cerevisiae</i> cells-----	79
Figure 3.8 Schematic diagram showing fusion constructs used-----	81
Figure 3.9 Toca1 or Nck1 reduced fluorescence signals from WASP reporter-----	82
Figure 3.10 Schematic diagram showing fusion constructs used-----	83
Figure 3.11 Toca1, Nck1 and Cdc42 are localized in the nuclei of <i>S. cerevisiae</i> cells-----	83
Figure 3.12 Toca1 or Nck1 reduced fluorescence signals from WASP reporter even in the presence of WIP-----	85
Figure 3.13 Diagram showing the mutations generated in the WASP gene-----	87
Figure 3.14 The selected mutations did not affect the conformation of WASP-----	88
Figure 3.15 Co-expression of WIP did not enhance fluorescence signals from WASP ^{A134T} , WASP ^{L270P} , WASP ^{D485N} or WASP ^{ΔVCA} -----	89

Figure 3.16 Schematic diagram showing fusion constructs used -----	91
Figure 3.17 WIP and WIRE enhanced fluorescence signals from WASP reporter in HEK 293T cells-----	91
Figure 3.18 N-terminus of WIP interacts with C-terminus of WASP to produce increased emission of CFP after photobleaching of YFP-----	94
Figure 3.19 Co-expression of YFP-WIP and CFP did not produce increased emission of CFP after photobleaching of YFP-----	95
Figure 3.20 N-terminus of WIP interacts with C-terminus of WASP to produce increased emission of CFP after photobleaching of YFP-----	96
Results 3.2	
Figure 3.21 WASP ^{L270P} adopts an open conformation-----	99
Figure 3.22 BTK, HCK and Tec induced increased tyrosine phosphorylation of WASP ^{L270P} ---	101
Figure 3.23 Increased phosphorylation of WASP ^{L270P} by BTK is due to increased phosphorylation at residue 291-----	103
Figure 3.24 Increased phosphorylation of WASP ^{L270P} by HCK is due to increased phosphorylation at residue 291-----	104
Figure 3.25 Phosphorylation causes WASP to adopt an open conformation-----	106
Figure 3.26 Co-expression of WT WASP or its mutants and WIP suppress the growth defects of <i>las17Δ</i> cells-----	108
Figure 3.27 Suppression of endogenous WASP expression by shRNA-----	110
Figure 3.28 shRNA was specific to WASP-----	111
Figure 3.29 WASP downregulation impairs the motility of Jurkat cells (A)-----	112
Figure 3.30 WASP downregulation impairs the motility of Jurkat cells (B)-----	113
Figure 3.31 WASP with mutations rendering it resistant to the shRNA-----	114
Figure 3.32 WASP Y291 phosphorylation is crucial for T cell migration (A)-----	117
Figure 3.33 WASP Y291 phosphorylation is crucial for T cell migration (B)-----	118
Figure 3.34 WASP Y291 phosphorylation is crucial for T cell migration (C)-----	119
Figure 3.35 WASP promotes formation of filopodia formation in N-WASP ^{-/-} fibroblasts in the presence of WIP-----	122
Figure 3.36 WASP Y291 phosphorylation is required for filopodia formation in N-WASP ^{-/-} fibroblasts-----	123
Results 3.3	
Figure 3.37 WASP expression stabilised after deletion of WH1 domain-----	126
Figure 3.38 Deletion constructs of WASP for analysis of interaction with WIP and stability of expression in the presence of calpain-----	126
Figure 3.39 Interaction of WASP and WIP was abolished when first 100 residues of WASP was deleted-----	127
Figure 3.40 WASP is a substrate of calpain-----	128
Figure 3.41 WASP expression reduced after ionomycin treatment of 293T cells-----	130
Figure 3.42 WASP ⁹⁵⁻⁵⁰³ has increased expression in presence of calpain-----	132
Figure 3.43 Mapping the calpain cleavage sites of WASP-----	134
Figure 3.44 Schematic diagram showing all the mutations generated in the WH1 domain of WASP-----	136
Figure 3.45 WASP with mutations at residues 102, 111 and 112 has reduced proteolysis by calpain-----	137
Figure 3.46 WASP ^{WRG} is resistant to calpain in vitro-----	138
Figure 3.47 WASP ^{WRG} mutant adopts an open conformation-----	139
Figure 3.48 Co-expression of both WT WASP or WASP ^{WRG} mutant and WIP	

suppress the growth defects of <i>las17Δ</i> cells-----	140
Figure 3.49 WASP ^{WRG} mutant induces filopodia comparable to WT WASP-----	141
Figure 3.50 Expression of WT WASP but not WASP ^{WRG} mutant rescued impaired migration of Jurkat WASP ^{KD} T cells (A)-----	143
Figure 3.51 Expression of WT WASP but not WASP ^{WRG} mutant rescued impaired migration of Jurkat WASP ^{KD} T cells (B)-----	144

Discussion

Figure 4.1 Principle of Bi-molecular fluorescence complementation used in this study-----	146
Figure 4.2 A model of WASP-WIP interaction-----	154
Figure 4.3 Summary of the findings in this study -----	176

Appendix

Figure A1 Schematic figure of WASP with point mutations generated in this study-----	201
--	-----

List of Tables

Table 1.1 Residues preferences of calpain near the cleavage site-----	32
Table 2.1 List of commercial vectors used-----	35
Table 2.2 List of primary antibodies used-----	36
Table 2.3 List of secondary antibodies used-----	37
Table 2.4 List of supplements used in the SD medium-----	38
Table 2.5 List of cell lines and the respective media used-----	39
Table 2.6 List of antibiotics used-----	39
Table 2.7 List of disposables used-----	39
Table 2.8 A summary of the antibodies used in Western blot and the respective dilutions-----	65

Abbreviations

ABPs	Actin-binding proteins
AR	Acidic region
Arp2/3	Actin-related protein
ARPC	Actin-related protein complex
BCR	B cell receptor
BR	Basic region
BSA	Bovine serum albumin
CFP	Cyan fluorescent protein
CH	Cofilin homology
Cobl	Cordon bleu
CR16	Glucocorticoid-regulated gene product
DAAMs	Dishevelled-associated activators of morphogenesis
DCs	Dendritic cells
DIA	Diaphanous
DTT	1, 4-Dithiothreitol
EBV	Epstein-Barr virus
EVH1	Ena/VASP homology domains in proteins like Ena/Mena and VASP
F-actin	Filamentous-actin
FH	Formin homology
FHODs	Formin homology domain proteins
FMNs	Formins
FRET	Fluorescence Resonance Energy transfer
FRLs	Formin-related protein in leukocytes
G-actin	Globular-actin
GBD	GTPase binding domain
GFP	Green fluorescent protein
Grb2	Growth Factor Receptor-Bound Protein 2
GST	Glutathione-S-transferase
HS1	Hematopoietic relative hematopoietic-specific protein 1
ICAM-1	Inter-cellular Adhesion molecule 1
INFs	Inverted formins
JMY	Junction-mediating regulatory protein
Jurkat ^{WASPkd}	Jurkat WASP knock down cells
LB	Luria-Bertani
LiAc	Lithium acetate
Lmod	Leiomodlin
LRR	Leu-rich repeats
MTOC	Microtubule organizing center
Nck	Nonbinding catalytic region of tyrosine kinase

NLS	Nuclear localization signal
NPFs	Nucleation promoting factors
N-WASP	Neural-WASP
PBS	Phosphate buffered saline
PCR	Polymerase chain reaction
PEI	Polyethyleneimine
PMSF	Phenylmethanesulfonyl fluoride
pN	Piconewton
PRDs	Proline rich domains
PRR	Proline rich region
RNAi	Retrovirus vector mediated
RT-PCR	Real-time PCR
SD	Synthetic Defined
SDM	Site directed mutagenesis
SDS-PAGE	Sodium dodecyl sulfate Polyacrylamide gel electrophoresis
SFM	Serum-free medium
TAE	Tris-acetate-EDTA
TBS	Tris buffered saline
TCR	T cell receptor
Toca1	Transducer of Cdc42-dependent actin assembly
VH	Verprolin homology
WAS	Wiskott Aldrich Syndrome
WASH	WASP and SCAR homologue
WASP	Wiskott Aldrich Syndrome protein
WASP ^{kd}	WASP knockdown
WASP _R	WASP resistant against shRNA
WAVE/SCAR	WASP family verprolin homologue 1-3
WBD	WASP binding domain
WH1/EVH1/PH	WASP homology domain 1/ Ena-VASP homology domain 1 / PH
Pleckstrin homology	PH
WH2	WASP homology 2
WHAMM	WASP homologue associated with actin, membranes and microtubules
WIP	WASP-interacting protein
WIRE	WIP related
WISH	WASP-interacting SH3 Protein
WT	Wildtype
XLN	X-linked severe congenital neutropenia
XLT	X-linked thrombocytopenia
YFP	Yellow fluorescent protein

Publications

The work in this study has been published in:

1. **Lim RP**, Misra A, Wu Z, Thanabalu T. (2007). Analysis of conformational changes in WASP using a split YFP. *Biochemical and Biophysical Research Communications*, 362(4), 1085-9.

Other publications:

1. Misra A, **Lim RP**, Wu Z, Thanabalu T. (2007). N-WASP plays a critical role in fibroblast adhesion and spreading. *Biochemical and Biophysical Research Communications*, 364(4), 908-12.
2. Misra A, Rajmohan R, **Lim RP**, Bhattacharyya S, Thanabalu T. (2010). The mammalian verprolin, WIRE induces filopodia independent of N-WASP through IRSp53. *Exp Cell Res*, 316(17):2810-24

Manuscript in preparation:

1. **Lim RP**, Jain N, Wong MH, Thanabalu T. (2011). Role of calpain-mediated proteolysis of WASP in T cell chemotaxis.

Abstract

Wiskott Aldrich Syndrome (WAS) is an X-linked recessive disease with clinical symptoms such as thrombocytopenia, eczema and recurrent infections due to immune deficiency. Identification of the WASP gene led to the discovery of other WAS-related diseases, X-linked thrombocytopenia (XLT) and X-linked congenital neutropenia (XLN) that present milder symptoms of WAS. WASP is a 502 –residue multidomain protein, comprising of, from the N to the C terminus, WH1 domain, basic region (BR), GTPase binding domain (GBD), proline rich region (PRR) and the VCA domain. The two fragments of YFP (Yellow Fluorescent Protein) molecule (YFP₁₋₁₅₄ and YFP₁₅₅₋₂₃₈) were fused to the N- and C-terminus of WASP respectively as a probe (WASP Reporter) for Bi-molecular fluorescence complementation (BiFC) to elucidate the conformation of WASP inside the cell. When WASP adopts a closed conformation, the two fragments of YFP are close to each other resulting in fluorescence and reduction in fluorescence indicates that WASP is in an open conformation. WASP was found to be in a closed conformation in yeast and this conformation was stabilized by WIP (WASP Interacting Protein) or WIRE (WIP related) as seen by the enhanced the fluorescence from the WASP reporter. On the other hand, Toca1 (Transducer of cdc42-dependent actin assembly) or Nck1 (Nonbinding catalytic region of tyrosine kinase) caused a reduction in YFP fluorescence, suggesting that SH3 domain-containing proteins altered the conformation to an open one. Cells expressing WASP reporter with mutations in WH1, GBD and VCA domains showed reduced fluorescence even in the presence of WIP suggesting that the conformation was affected by these mutations.

The mutation L270P in WASP (WASP^{L270P}) causes XLN and BiFC assay showed that WASP^{L270P} is in an open conformation, correlating with earlier studies which showed that WASP^{L270P} is constitutively active. WASP^{L270P} had enhanced phosphorylation at residue Tyr291. Jurkat^{WASPkd} (WASP knock down) had impaired chemotaxis towards SDF-1 α and decreased velocities (0.0383 μ m/sec) compared to WT Jurkat cells (0.0986 μ m/sec). Expression of WASP in Jurkat^{WASPkd} rescued both cell motility (0.0709 μ m/sec) and chemotaxis, while expression of WASP^{L270P} rescued the cell motility (0.0817 μ m/sec) but not chemotaxis towards SDF-1 α . WASP and WASP^{L270P} induced filopodia in N-WASP^{-/-} fibroblasts however WASP^{L270P} was more efficient than WASP. WASP^{L270P/Y291E} and WASP^{L270P/Y291F} rescued the growth defect of *las17* Δ cells just like WT WASP and WASP^{L270P}. WASP^{L270P/Y291F} was not able to rescue both the motility (0.0554 μ m/sec) and chemotaxis defect of Jurkat^{WASPkd}, and was inefficient in inducing filopodia in fibroblasts. On the other hand, WASP^{L270P/Y291E} rescued the impaired motility of Jurkat^{WASPkd} cells (0.0952 μ m/sec) but not the chemotaxis defect. WASP^{L270P/Y291E} induced filopodia in fibroblasts to a lesser extent than WASP^{L270P}. These results indicate that the activity of WASP requires cyclical phosphorylation and dephosphorylation and XLN mutation probably causes the disease by enhancing phosphorylation.

WASP is a substrate of calpain, a calcium-dependent protease. However the role of calpain in regulating WASP activity has not been elucidated due to the lack of calpain resistant WASP. To generate calpain resistant WASP, the putative cleavage site was mapped and subsequently site directed mutagenesis was carried out to generate

WASP^{WRG} (Y102W, T111R, P112G). WASP^{WRG} was more stable than WASP in both *in vitro* and *in vivo* proteolysis assays. WASP and WASP^{WRG} suppressed the growth defects of *las17Δ* cells in the presence of WIP, indicating that WASP^{WRG} is able to form a functional complex with WIP. WASP^{WRG} was able to induce filopodia in N-WASP^{-/-} fibroblasts just like WT WASP. Expression of WASP but not WASP^{WRG} rescued the impaired motility of the Jurkat^{WASPkd} T cells towards SDF-1 α . The results suggest a novel role of calpain-mediated proteolysis of WASP in Jurkat T cell motility.

1. Introduction

The cell is the basic functional unit of life and it contains all of the critical hereditary information that defines a species. Cells can be categorized into two basic types; the eukaryotic cells and prokaryotic cells. Despite the evolutionary differences, eukaryotic and prokaryotic cells share similarities in the structural organization of the cell and mechanisms in which cellular processes are carried out. How molecular components within a cell work together to produce complex cell behaviours can be better understood, perhaps by examining the mechanisms behind remodelling of the cytoskeleton.

1.1 The Cytoskeleton

The cytoskeleton serves as a scaffold and spatially organizes the contents within a cell which gives the cell its shape, assists in the communication of the cell with the external environment and provides coordinate forces required for the cell to change its morphology in response to the signals it receives (Fletcher and Mullins, 2010). There are three types of cytoskeletal filaments in eukaryotic cells; actin filaments, microtubules and intermediate filaments (Figure 1.1). All three types of filaments are made up of smaller subunits that can self associate either from end to end or side to side to form elongated structures. The differences in their mechanical properties and the network they form can be attributed to the differences in the structure of their subunits, their method of assembly and the associated proteins (Bruce Alberts, 2002). The effectiveness of the cytoskeletal system also relies on the accessory proteins that associate with these filaments. There are several classes of accessory proteins which include the nucleation-promoting factors, capping proteins, depolymerizing factors, severing factors, crosslinkers and stabilizing

proteins (Fletcher and Mullins, 2010). These three types of cytoskeletal filaments, together with their regulatory proteins are capable of forming a dynamic network that can disassemble and reassemble efficiently in response to both internal and external stimuli, and yet at the same time maintain the integrity of intracellular components (Bruce Alberts, 2002).

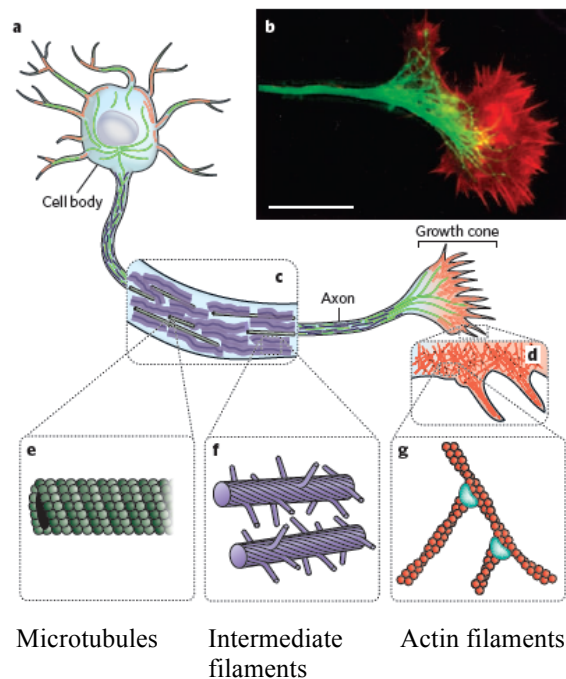


Figure 1.1 The three types of cytoskeletal filaments. Adapted from (Fletcher and Mullins, 2010).

1.1.1 Microtubules

Microtubules are polymers made up of 13 protofilaments linked tightly to form a stiff hollow tube. Each protofilament is made up of an assembly of α - β -tubulin heterodimers. Both α -tubulin and β -tubulin can bind to GTP. However, β -tubulin binds to GTP at a lower affinity and this contributes to the filament assembly and disassembly dynamics. Microtubules emanate from a microtubule organizing center (MTOC) and are involved in

long-range intracellular transport, mitosis and cell movement (Kavallaris, 2010). Microtubules are also the stiffest and least flexible of the three types of filaments, as indicated by their persistence length of about 5 μ m (Fletcher and Mullins, 2010).

1.1.2 Intermediate filaments

Intermediate filaments are the least stiff of the three kinds of cytoskeletal filaments and are made up of tetrameric subunits formed by monomers with a central α -helical domain. Two monomers associate in parallel to each other forming a dimer. A tetrameric subunit is then formed through antiparallel association of two dimers, resulting in the absence of polarity in the intermediate filaments unlike actin filaments and microtubules. Intermediate filaments function to resist mechanical forces in a cell. The most well-known class of intermediate filaments is the nuclear lamins which lies below the nuclear envelope that maintains the integrity of the nucleus (Tsai et al., 2006). Intermediate filaments can be bundled together and also be cross-linked to actin filaments and microtubules through cross-linking proteins such as plectins (Wiche, 1998).

1.1.3 Actin Filaments

Actin filaments make up the last type of cytoskeletal polymers and they complement microtubules and intermediate filaments in eukaryotic cells. Actin is one of the most abundant and highly conserved proteins on earth, evident from the presence of actin counterparts in prokaryotic cells. Eukaryotic cells depend on actin filaments for a myriad of processes like cell movement, mechanical support and transport of intracellular materials. The dynamic nature of the actin cytoskeleton facilitates these crucial processes.

Actin exists in two states; the monomeric globular-actin (G-actin) and the filamentous-actin (F-actin), which is formed through the self-assembly of G-actin. G-actin is made up of two major domains, which have two smaller subdomains each (Graceffa and Dominguez, 2003). The association of the four subdomains gives rise to two clefts; the large cleft which binds ATP while the other cleft, also known as the target-binding cleft binds to most actin-binding proteins (ABPs) (Dominguez, 2004). Actin filaments are asymmetrical as each actin monomer is rotated at 166° in the filaments. They are made up of two helices of head-to-tail bound actin subunits (Lee and Dominguez, 2010). The actin monomers are oriented in the same direction which gives actin filaments a polarized characteristic, similar to microtubules.

The process of actin polymerization can be divided into three distinct steps. The first step is actin nucleation, which is the rate-limiting step. In this step, an aggregate of three actin monomers is formed and serves as the nucleus for actin polymerisation. Next is the elongation step where actin monomers are added reversibly to both sides of the filament. The rate of elongation depends on the concentration of actin monomers available. However, the barbed (+) end of the filament grows faster than the pointed (-) end. During the elongation step, ATP-bound G-actin is preferentially added to the barbed (+) end and lost through the pointed (-) end in the ADP-bound state. This results in F-actin growing at the barbed end and shortening at the pointed end (Lee and Dominguez, 2010). Actin is an ATPase and through the hydrolysis of ATP that occurs along the way, the difference in free energy in the association and dissociation reactions, at the barbed and pointed end

respectively, drives the treadmilling process (Bruce Alberts, 2002). Finally, further growth of the filament could be stopped at the equilibrium step (Maly and Borisy, 2001).

Many biological processes depend on actin polymerization and cellular motility is one of the most well-known example. Pools of actin monomers are assembled at specific subcellular locations rapidly in response to cellular signals. These assembled actin filaments can cause a change in the cell shape, forming protrusions that assist cell movements. Each assembled actin filament can produce piconewton (pN) forces (Kovar and Pollard, 2004), which allow the leading edge of the cell to move forward. Cell migration is an essential process required in immune cells to search and destroy foreign pathogens. It is also crucial during embryo development and in the cell process extension of nerve cells (Pollard and Cooper, 2009). Actin filaments have also been shown to be involved in cytokinesis, where a contractile ring, consisting of actin filaments and myosin II, work together in segregation of the cell into two at the last stage of cell division in all cells (Pollard and Cooper, 2009). During the process of endocytosis, assembly of network of actin filaments and proteins are also required to induce curvature in the cell membranes. (Doherty and McMahon, 2009).

Actin polymerisation can be initiated from free barbed ends or by *de novo* filament nucleation. Free barbed ends can be generated either by uncapping of existing filaments or severing of filaments (Condeelis, 2001). *De novo* nucleation refers to the spontaneous assembly of actin from a pool of free monomers. However, the formation of an actin trimer, which is the first step of nucleation, is kinetically unfavourable (Sept and

McCammon, 2001). Thus, in order to overcome this barrier, cells make use of a variety of actin nucleators to regulate the timing and location of actin assembly.

1.2 Arp2/3 complex and the actin nucleators

Arp2/3 (Actin-related protein) complex is the first identified major nucleator. It is a 220 kDa complex that is made up of seven proteins, Arp2, Arp3 and subunits ARPC1-5 (Actin-related protein complex 1-5). The Arp2/3 complex promotes actin polymerization of a new filament from a pre-existing filament at an angle of 70°, generating branched actin networks (Figure 1.2) (Campellone and Welch, 2010). Arp2/3 complex caps the actin filament at the pointed end and actin is elongated at the barbed end. Studies have indicated that subunits ARPC2 and ARPC4 form contacts with the pre-existing filament while Arp2 and Arp3 interact with the pointed end of the new filament (Rouiller et al., 2008). Arp2/3 complex has low nucleation activity on its own (Mullins et al., 1998), however, binding to filaments and phosphorylation of tyrosine and threonine residues in Arp2 (LeClaire et al., 2008) can increase its activity. Another contributor that enhances the activity of the Arp2/3 complex involves the interaction of nucleation promoting factors (NPFs) with the Arp2/3 complex. These proteins induce conformational changes in Arp2/3 complex, bringing Arp2 and Arp3 in closer proximity, which mimics an actin dimer. Actin monomers are then recruited to the complex by the NPFs (Chesarone and Goode, 2009). These crucial steps help to overcome the kinetically unfavourable barrier during nucleation.

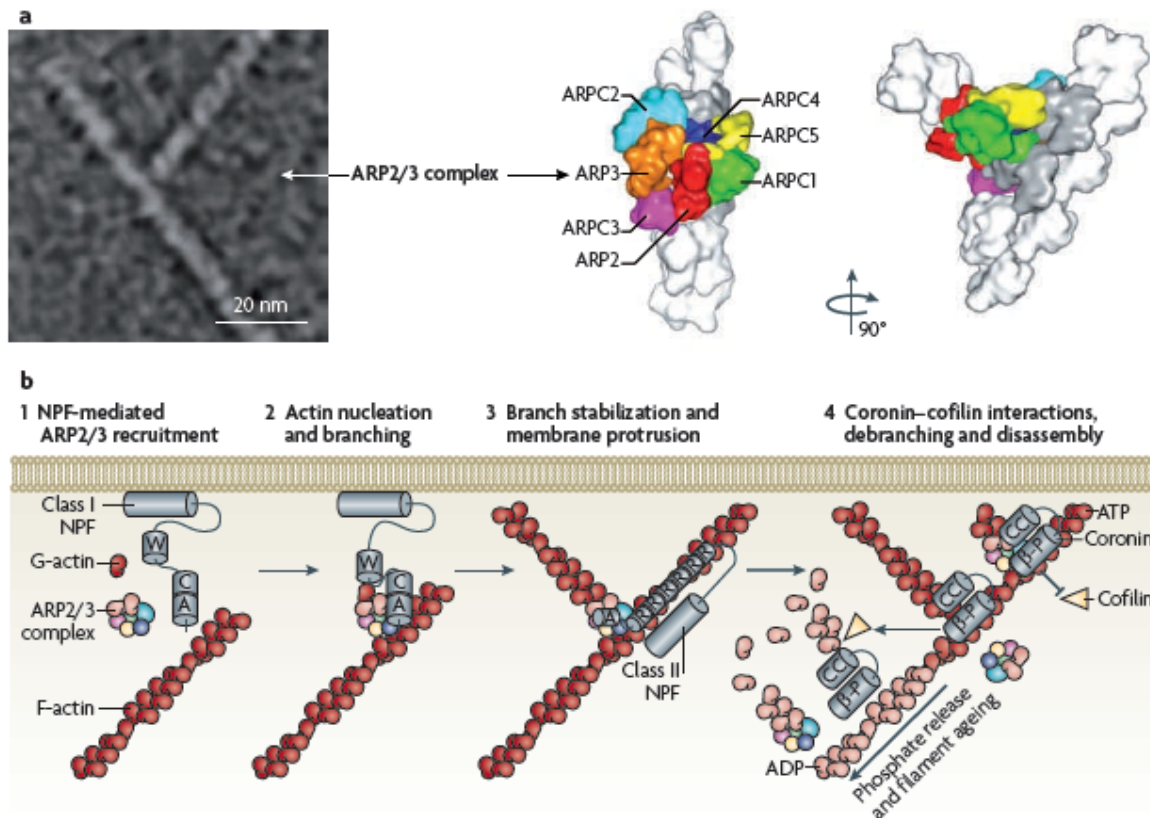


Figure 1.2 The structure of Arp2/3 complex and a model for nucleation and branching of actin. Adapted from (Campellone and Welch, 2010).

(A) The Arp2/3 complex is made up of seven proteins, including Arp2, Arp3, Arpc1-5. The electron micrograph shows the structure of a Y-branched actin filament and the Arp2/3 complex.

(B) Model depicting the sequence and proteins involved in the nucleation and branching of actin filaments.

Other than the Arp2/3 complex, there are two more classes of actin nucleators. Formins, which form the second group of nucleators, catalyse the formation of unbranched actin and assemble actin networks like stress fibres, filopodia and contractile rings during cytokinesis (Faix and Grosse, 2006; Goode and Eck, 2007). Formins contain the conserved formin homology (FH) domains, FH1 and FH2. Based on the FH2 sequence divergence, formins are classified into seven subclasses; Diaphanous (DIA), formin-related protein in leukocytes (FRLs), Dishevelled-associated activators of morphogenesis (DAAMs), forming homology domain proteins (FHODs), formins (FMNs), delphilin and inverted formins (INFs) (Higgs and Peterson, 2005). The FH2 domains in these proteins

bind to the barbed ends of actin filaments, unlike the Arp2/3 complex, and stabilize the actin dimers and trimers that are formed spontaneously (Figure 1.3) (Pring et al., 2003). As a result, formins prevent the association of other capping proteins, allowing elongation of the filament to continue (Harris et al., 2004). Dimerisation of the FH2 domains has been shown to stabilize the association of two actin monomers and after nucleation, the FH2 domains remain associated with the growing barbed end, adding new actin subunits progressively (Chesarone and Goode, 2009).

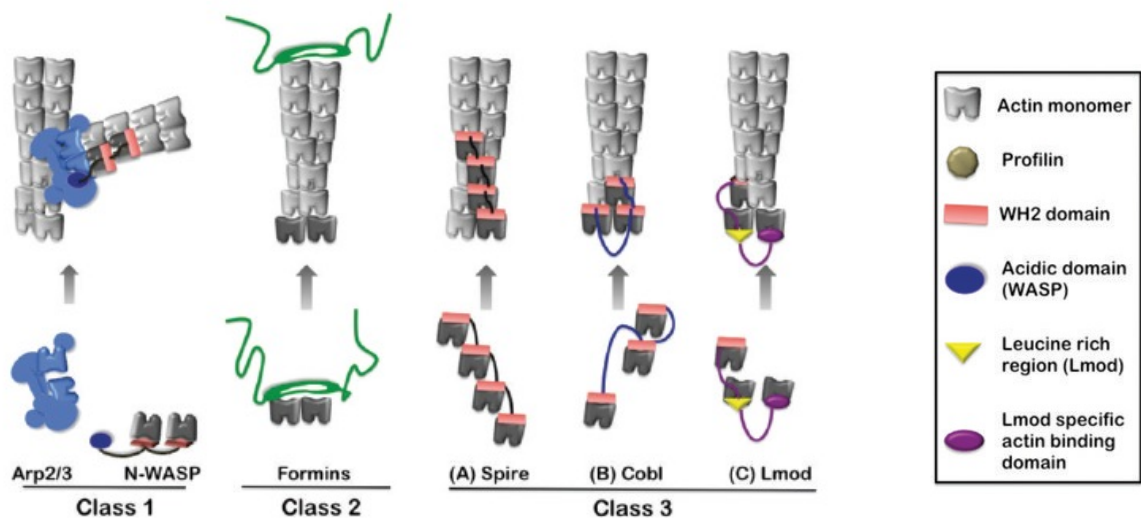


Figure 1.3 The three classes of nucleation factors. Adapted from (Chesarone and Goode, 2009).

Class I: Arp2/3 complex is recruited to the acidic domain of nucleating promoting factors (NPFs) like N-WASP. The WH2 domain of N-WASP, adjacent to the acidic domain, recruits actin monomers. The resulting complex is stabilized and actin polymerization occurs.

Class II: Formins bind to barbed ends of actin filaments and stabilizes actin dimers or trimers formed spontaneously.

Class III: Spire, Cobl and Lmod have between one to four tandem WH2 domains separated by linkers. The nucleation mechanisms used are similar but the actin nucleus generated varies.

The third class of nucleators includes the proteins Spire, Cordon bleu (Cobl), and Leiomodin (Lmod). Spire has four tandem Wasp Homology 2 (WH2) domains separated by short linkers. These four WH2 domains bind to four actin monomers cooperatively and the pre-nucleation complex formed resembles a short actin filament (Figure 1.3)

(Quinlan et al., 2005). It has been suggested that Spire caps the pointed ends of filaments to inhibit the disassembly (Quinlan et al., 2005). However, subsequent studies showed that Spire associates with barbed ends to prevent profilin-actin association after nucleation and severs filaments at the pointed end to enhance disassembly (Bosch et al., 2007). Importantly, it has also been indicated that Spire cooperates with Formins in actin assembly (Rosales-Nieves et al., 2006). Further biochemical and structural studies would be required to fully resolve the post-nucleation effects of Spire.

Nucleation of actin by Cobl involves three WH2 domains and the linker region between the last two WH2 domains. The length of the linker appears to be crucial for actin assembly. This suggests that the WH2 domains and the linker stabilize both short-pitch and long-pitch associations allowing the formation of a trimeric nuclei (Figure 1.3) (Campellone and Welch, 2010; Chesarone and Goode, 2009).

Lmod has a N-terminus that contain actin- and tropomyosin-binding helices, a central Leu-rich repeat (LRR) region and a C-terminus with a polyproline peptide, two predicted helices and a WH2 domain (Chereau et al., 2008). Full nucleation activity of Lmod requires the actin-binding elements in these domains. Two to three actin monomers are organized and stabilized at the pointed end, allowing elongation at the barbed end. However, little is known about how activities of Lmod are regulated and further characterization of the protein is needed (Campellone and Welch, 2010).

1.3 Nucleation promoting factors (NPFs)

The Arp2/3 complex, by itself, is a poor nucleator (Mullins et al., 1998). However, activation of the Arp2/3 complex via the interaction of NPFs can increase actin polymerization (Campellone and Welch, 2010). There are two classes of NPFs; Class I and II NPFs. They are classified based on the presence of binding sites for either G-actin or F-actin and the mechanisms used to activate the Arp2/3 complex.

Class I NPFs utilize a CA domain, which binds to the Arp2/3 complex, and an adjacent WH2 domain, which bind to G-actin, to stimulate Arp2/3 mediated nucleation (Figure 1.4). Activation of Arp2/3 by these proteins involves the formation of Arp2/3 complex-NPF-G-actin complex (Welch and Mullins, 2002). Within the complex, interaction between the Arp2/3 complex and the CA domain may cause a conformational change. Nucleation could then be initiated through the presentation of G-actin by the WH2 domain of the NPFs (Robinson et al., 2001). Mammalian class I NPFs include Wiskott Aldrich Syndrome protein (WASP), neural-WASP (N-WASP), WASP family verprolin homologue (WAVE/SCAR) 1-3, WASP and SCAR homologue (WASH), WASP homologue associated with actin, membranes and microtubules (WHAMM) and junction-mediating regulatory protein (JMY). These NPFs have diverse N-terminus sequences.

Class II NPFs, which includes cortactin and hematopoietic-specific protein 1 (HS1), possess acidic peptides at the N-termini that bind to Arp2/3, proline rich domains (PRDs) containing phosphorylation sites, SH3 domains that interact with proteins like N-WASP and repetitive sequences that bind to F-actin instead of G-actin (Campellone and Welch,

2010). It is hypothesized that the binding of the acidic peptides to the Arp2/3 complex may cause a conformational change that facilitates the binding of an existing filament, leading to activation of the Arp2/3 complex (Welch and Mullins, 2002)(Figure 1.4). Class II NPFs are weaker Arp2/3 activators compared to class I NPFs, however, cortactin can enhance Arp2/3 activation by N-WASP (Martinez-Quiles et al., 2004). Figure 1.5 shows schematic representations of the two classes of mammalian NPFs.

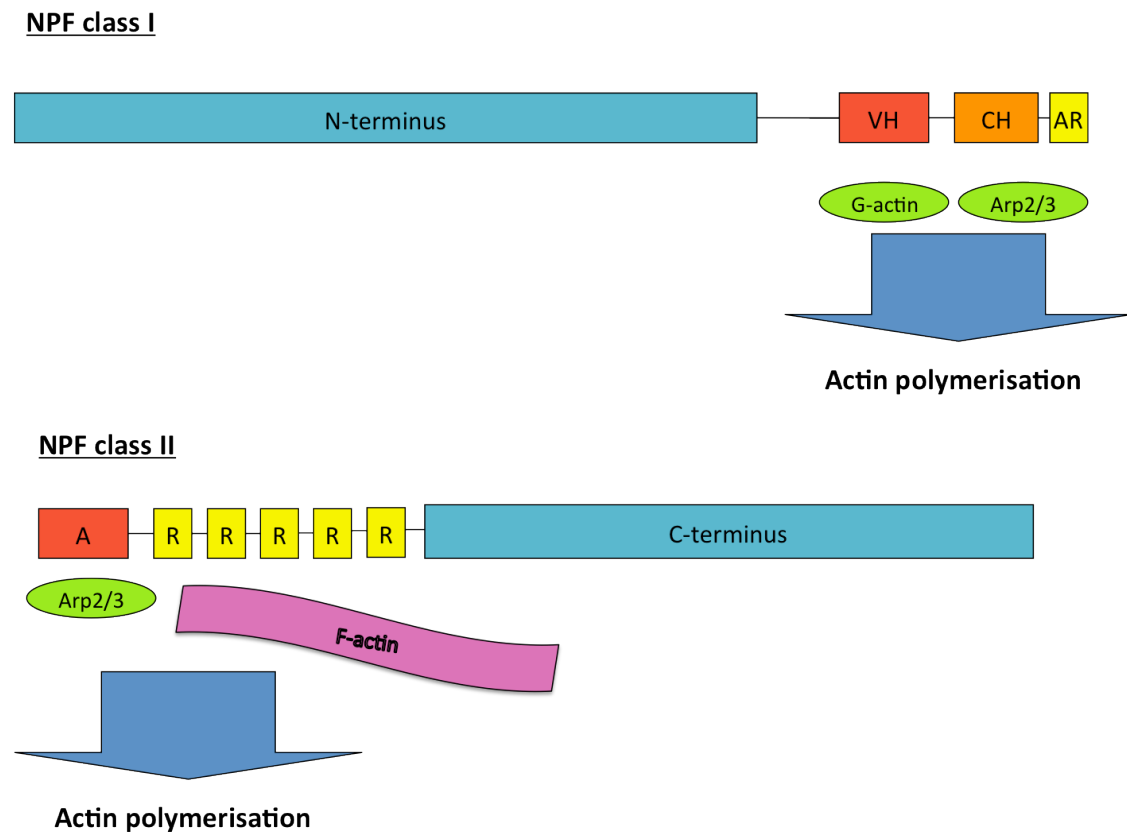


Figure 1.4 Schematic Figure showing the difference in association of Class I and II NPFs with the Arp2/3 complex. Class I NPFs utilize a CA domain, which binds to the Arp2/3 complex, and a WH2 (VH) domain which bind to G-actin to stimulate actin polymerisation. Class II NPFs utilize the acidic peptides at the N-terminus to bind to the Arp2/3 complex, which causes a conformational change that facilitates the binding of an existing filament to the repetitive sequences, leading to actin polymerisation.

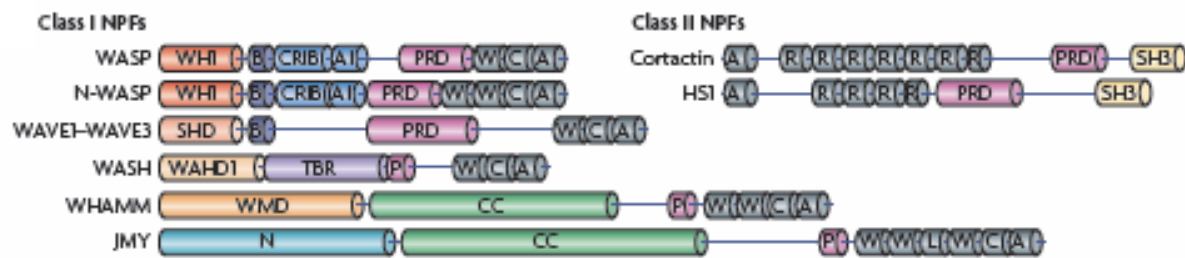


Figure 1.5 Class I and II NPFs. Adapted from (Campellone and Welch, 2010).

Class I NPFs contain WCA domains that bind to Arp2/3 complex and G-actin. Class II NPFs contain N-terminal acidic domains that bind ARP2/3 and central F-actin-binding repeats.

1.4 Wiskott Aldrich Syndrome (WAS)

One of the best characterized members of the class I NPFs is the Wiskott Aldrich Syndrome protein (WASP). WASP was identified as the protein mutated in Wiskott Aldrich syndrome and the gene was mapped to chromosome region Xp11.23 (Derry et al., 1994) and isolated by positional cloning. Since then, many reports showed several clinical phenotypes such as X-linked thrombocytopenia (XLT) and X-linked severe congenital neutropenia (XLN) (Devriendt et al., 2001; Villa et al., 1995) are associated with the missense mutations in different regions of this gene. The classic Wiskott Aldrich Syndrome (WAS) occurs at an incidence of between one and ten in a million individuals and is an X-linked recessive disorder. It is characterized by thrombocytopenia, eczema and immunodeficiencies (Ochs and Thrasher, 2006). Patients frequently suffer from recurrent infections, autoimmune diseases and hemorrhages (Thrasher, 2002). The severity of the disease is largely dependent on the mutation and resulting effect on the expression of WASP. Currently, the only curative treatment is hematopoietic stem cell transplantation where a related human leukocyte antigen-identical donor is needed to prevent higher rates of survival for the patients. Another fast emerging therapy that is still

undergoing trials is using the autologous gene therapy (Thrasher, 2009). Gene-corrected hematopoietic stem cells from the patients are transplanted back to themselves, avoiding rejection like in the case of mis-match donors.

1.5 Wiskott Aldrich Syndrome protein (WASP)

The Wiskott Aldrich Syndrome protein (WASP) belongs to the WASP/WAVE family of proteins which include N-WASP (neural-WASP) (Miki et al., 1996) and SCAR/WAVE1-3 (Suppressor of cAMP receptor/WASP-family verprolin homologous proteins) (Miki et al., 1998; Suetsugu et al., 1999). WASP is a 502- residue protein and has 1506 nucleotide residues. It is expressed predominantly in hematopoietic cells unlike N-WASP and SCAR/WAVE 1-3, which are expressed ubiquitously. The differences in expression patterns could be because of the different roles played by WASP and N-WASP in the cell types they are expressed in. WASP^{-/-} mice showed defects in T-cell activation and while N-WASP^{-/-} was an embryonic lethal mutation (Miki and Takenawa, 2003). Together with other studies, this indicates that WASP is crucial for hematopoietic cell functions while N-WASP is important for many cell types due to the ubiquitous expression (Miki and Takenawa, 2003; Snapper et al., 2001; Thrasher and Burns, 2010).

The five members of the WASP family (WASP, N-WASP, SCAR/WAVE1-3) share three common domains at the carboxy terminus; the verprolin homology (VH), cofilin homology (CH) and acidic region (AR). Collectively, these independent domains form the VCA module which is necessary for the activation of Arp2/3 dependent actin polymerization (Panchal et al., 2003). The WASP family proteins also share the basic

region (BR) and proline rich region (PRR) which are upstream of the VCA module. In addition, WASP and N-WASP possess a central GTPase binding domain (GBD) and a WASP homology domain 1/ Ena-VASP homology domain 1 / Pleckstrin homology (WH1/EVH1/PH) at the N-terminus (Callebaut et al., 1998) (Figure 1.6).

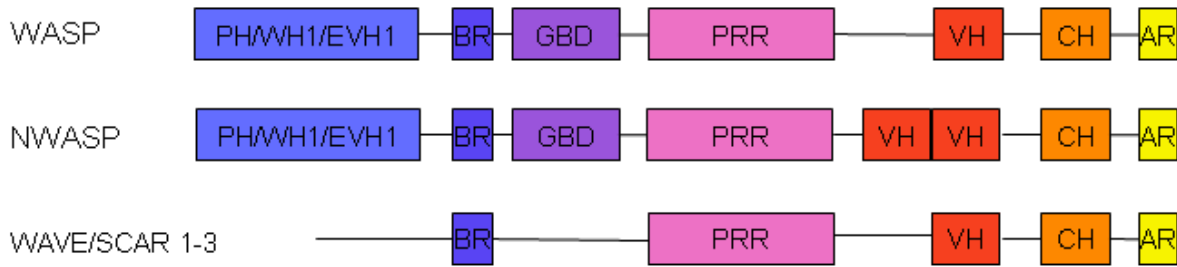


Figure 1.6 Schematic diagram illustrating the common domains shared by the WASP family of proteins. PH/WH1/EVH1: PH/WASP homology domain 1/ Ena-VASP homology domain1; BR: Basic Region; GBD: GTPase Binding Domain; PRR: Proline Rich Region; VH: Verprolin homology; CH: Cofilin homology; AR: Acidic Region.

The WH1 domain of WASP has been found to be structurally related to Ena/VASP homology (EVH1) domains in proteins like Ena/Mena and VASP (Vasodilator-stimulated phosphoprotein) (Figure 1.7) and has been found to bind to proline-rich motifs such as those found in the C-terminus of WASP-interacting protein (WIP), WIP related (WIRE) and glucocorticoid-regulated gene product (CR16) (Aspenstrom, 2002; Ho et al., 2001; Ramesh et al., 1997). Small GTPases like Cdc42 have also been shown to interact with WASP and mediate effects on actin cytoskeletal rearrangement by binding to the GBD region (Badour et al., 2003). The proline rich region of WASP encompasses several consecutive proline residues and PXXP motifs (where X can be any residue) that allows for binding of SH3 domain in effectors like Nonbinding catalytic region of tyrosine kinase (Nck), Growth Factor Receptor-Bound Protein 2 (Grb2) and WASP-interacting

SH3 Protein (WISH) (Badour et al., 2003). The V domain in the VCA region binds to an actin monomer while the CA domain binds to Arp2/3 complex. Upon the assembly of three actin monomers, in which two actin related molecules are from the Arp2/3 complex, actin polymerization can be initiated (Machesky and Insall, 1998).

		1	10	20	30	40	50	60	70									
MENA	1	MSEQSI	CQARA	AVMVY	DDANK---	KVVPAG	GSTGFS	RVHI	YHHTGN--	NTFRV	VGRKIQ	-DHQVV	INCA	IPKGL	-K	69		
VASP	1	MSETVIC	SSRAT	VMLY	DDGNK---	RMLPAG	TGPQAF	SRVQI	YHNPTA--	NSFRV	VGRKM	QPDQQV	VINCA	IVRGV	-K	71		
ENA	1	MTEQSI	IIGARAS	VMVY	DDNQK---	KVVP	SGSSS	-GLSKV	QIYHHQ	QN--	NTFRV	VGRKLQ	-DHEVV	INCS	ILKGL	-K	69	
WASP	39	LGRKCL	TLATA	AVVQLY	LALPP	GAEH	HTKEHC	----	GAVCF	VKDN	PQKSY	FIRLY	GLQAG	---	RLLWEQ	ELYSQ	-V	106
				80		90		100		110								
MENA	70	YNQATQ	-----	TFHOW	DAR-----	QVYGL	NFGSK	EDAN	VFASAM	MMHA	LEVLNS						113	
VASP	72	YNQATP	-----	NFHOW	DAR-----	QVWGL	NFGSK	EDAA	QFAAG	MASALE	ALEG						115	
ENA	70	YNQATA	-----	TFHOW	DSK-----	FVYGL	NFSSQ	NDAN	EFARAM	MMHA	LEVLSG						113	
WASP	107	YSTPTP	-----	FTHTF	AGDD-----	CQAGL	NFADE	DEDA	QAQAF	RALV	QEKIQ	KRNQ					150	

Figure 1.7 Sequence alignment of EVH1 domains from Mena, VASP, Ena and WH1 domain from WASP. Adapted from (Fedorov et al., 1999) Residues highlighted in red are the three fully conserved aromatics in the Ena/VASP and WASP WH1 domains that contact the proline-rich core of the peptide, as well as the four hydrophilic residues in the Ena/VASP family that form the binding pocket for Phe 1003. Residues highlighted in yellow are residues that contribute to the hydrophobic core in the EVH1 domains.

1.6 Regulation of WASP

The functional domains of WASP enables its interaction with numerous cytoplasmic molecules, resulting in successful integration of extracellular signals and activation of the Arp2/3 complex allowing reorganization of the actin cytoskeleton (Thrasher, 2002). WASP has been shown to adopt a closed conformation in which an autoinhibitory loop is formed through the binding of the VCA domain to the upstream BR domain. This prevents the VCA domain from interacting with actin monomers as well as the Arp2/3 complex (Kim et al., 2000) (Figure 1.8).

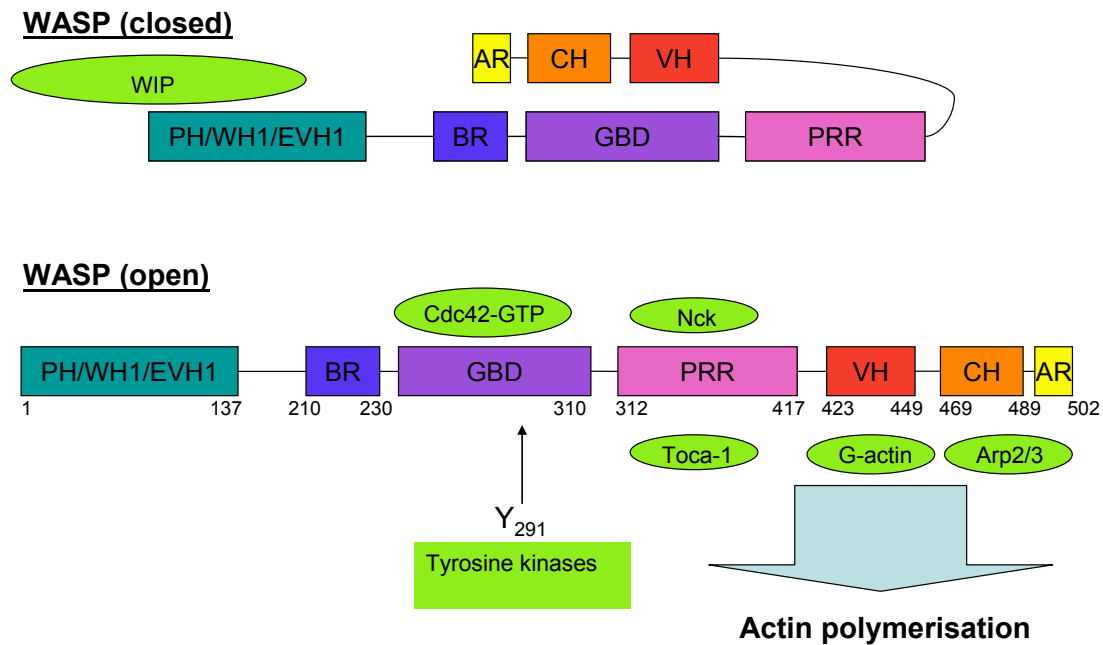


Figure 1.8 Schematic diagram showing functional domains of WASP and its conformation in presence of different regulators.

When WASP is in the closed conformation, an autoinhibitory loop is formed through interaction of the VCA and BR-GBD domains. Cdc42 activates WASP and dissociates the autoinhibitory loop, allowing the binding of G-actin and Arp2/3 complex resulting in actin polymerization.

The interaction of GTP-loaded Cdc42 with the GBD domain of WASP is postulated to be one of the mechanisms of WASP activation. The resulting dissociation of the autoinhibitory loop can facilitate the interaction and activation of the Arp2/3 complex (Imai et al., 2003a). Cdc42 is a member of the Rho family of GTPase that is known to regulate the formation of filopodia, cell-substrate adhesion and chemotaxis (Jaffe and Hall, 2005). However, recent studies showed that Cdc42 alone is insufficient for the activation of WASP. Transducer of Cdc42-dependent actin assembly (Toca1) is found to be required for Cdc42-dependent actin polymerization (Ho et al., 2004). Other regulators of WASP include SH3 domain-containing proteins that interact with the PRR domain of WASP. One such adaptor protein, Nck has been shown to be able to promote actin nucleation in presence of N-WASP and Arp2/3 complex (Rohatgi et al., 2001).

Phosphatidylinositol-4,5-bisphosphate (PtdIns(4,5)P₂) may cooperatively activate WASP and N-WASP together with Nck to regulate actin polymerization (Rivera et al., 2009). Dimerisation of WASP has also been shown to increase the affinity of WASP for the Arp2/3 complex, significantly enhancing actin assembly, adding another level of regulation (Padrick et al., 2008). Two other mechanisms of WASP activation include tyrosine phosphorylation on Y291 residue and the regulation of WASP degradation. Because of the similar structure, domains and biochemical interactions between WASP and N-WASP, many experimental findings from N-WASP have been extrapolated to WASP.

1.7 The Verprolin family of proteins

The human verprolin family of proteins, consisting of WASP-interacting protein (WIP), Glucocorticoid-regulated gene product (CR16) and WIP-related (WIRE), have been shown to be involved in the regulation of actin cytoskeleton. The effects of the verprolins are primarily mediated by the WASP family of proteins (Aspenstrom, 2005). WIP and WIRE are expressed ubiquitously while the expression of CR16 is restricted to the brain, heart, lung and colon (Aspenstrom, 2002; Kato et al., 2002; Ramesh et al., 1997; Weiler et al., 1996). The verprolins are proline-rich proteins with N-terminal proline-rich motifs, XPPPPP (where X can be Ala, Leu, Ser or Gly) that has been implicated in the binding to profilin (Holt and Koffer, 2001; Purich and Southwick, 1997). The proline-rich motifs can also bind to SH3 domains. WIP and WIRE have been reported to bind to SH3 domains-containing proteins like Nck and cortactin (Anton et al., 1998; Aspenstrom, 2002; Kinley et al., 2003). Additionally, these verprolins contain WASP homology 2

(WH2) motifs at the N-terminus and a C-terminal WASP binding domain (WBD). In verprolin WH2 motif 1, a consensus sequence RXALLXdIXkGXkLkK (The capital letters denote identical amino-acid residues and the lowercase letters denote conserved amino acid replacements or the amino acid residue found predominantly in the position, observed after alignment of WH2 domain of verprolins from different species) is found where kLkK is essential for the binding of verprolins to actin (Aspenstrom, 2005).

WIP is a cytosolic protein that is expressed in many tissues particularly in lymphoid tissues (Ramesh et al., 1997). Interaction between WIP and WASP is mediated through WASP binding domain (WBD) at the C-terminus of WIP and to the WH1 domain of WASP (Chou et al., 2006). Approximately eighty percent of mutations of WASP in Wiskott Aldrich syndrome patients are in the WH1 domain (Imai et al., 2003a) and some of these mutations have been shown to abolish the interactions between WASP and WIP (Stewart et al., 1999). This suggests the importance of the interaction of the WH1 domain of WASP with WIP, for WASP activity. However, it has also been proposed that the binding of WIP to WASP stabilizes the inactive conformation of WASP (Martinez-Quiles et al., 2001).

1.8 Physiological role of WASP

WASP is expressed in all hematopoietic cell lineages. In order to study the functional importance of WASP, WASP-deficient mice have been generated by several groups to study the development of hematopoietic cells and the function of WASP in the various immune cells (Snapper et al., 1998; Zhang et al., 1999).

1.8.1 Function of WASP in lymphoid development

Development of the early progenitors of several hematopoietic cell lineages appears to be normal in WASP-deficient mice (Cotta-de-Almeida et al., 2007; Meyer-Bahlburg et al., 2008; Snapper et al., 1998; Zhang et al., 1999). Also, there are no consistent defects observed in the hematopoiesis in humans. This may be due to the presence of other WASP family members that result in the redundancy and compensation in the absence of WASP (Cotta-de-Almeida et al., 2007). However, development of mature differentiated WASP-deficient hematopoietic cells is impaired. T cells numbers are reduced in the thymus of WASP-deficient mice as maturation is altered from the double positive thymocytes stage onwards. Reduction of peripheral T lymphocytes was also observed (Zhang et al., 1999). B cell development, on the other hand, appears to be normal as numbers of splenic and bone marrow B cells populations are comparable between the WT and WASP^{-/-} mice. However, similar to the T cells, peripheral B cell populations are significantly reduced (Zhang et al., 1999). Further studies need to be done to investigate the effects of WASP on the different subsets of B cells.

Somatic mosaicism has been found in Wiskott Aldrich Syndrome patients, in which reversion mutations restore the expression of WASP, indicating that there is a selective advantage for cells that express WASP in humans. However, this occurs only in mature lymphocytes like T cells, B cells and natural killer (NK) cells but not for cells of myeloid lineages (Ariga et al., 2001; Davis and Candotti, 2009).

1.8.2 Function of WASP in the adaptive immune system

The presence of WASP in all hematopoietic cells conveys the importance of WASP in humoral and cellular immunity. Other than its effects on hematopoiesis, deficiency of WASP also affects proper functions of these cells and directly impacts the efficiency of the mounting of immune responses.

In WASP-deficient T cells, there is a marked reduction of response towards chemokines (Snapper et al., 2005), resulting in impaired homing of T cells to secondary lymphoid tissues (Gunn et al., 1999). This may also explain the reduction in numbers of peripheral T cells. Deficiency of WASP also causes impaired actin polymerization and recruitment of proteins to the immunological synapse upon stimulation of the T cell receptor (TCR) (Sasahara et al., 2002). Proliferation and production of IL-2 upon TCR activation is similarly impaired due to defective TCR signaling (Molina et al., 1993; Snapper et al., 1998) as WASP functions as a scaffold protein within a signaling complex. Lentiviral gene therapy, which restores WASP expression, has been shown to rescue the defects in proliferation (Charrier et al., 2007). WASP may also have an indirect effect on the transcription of genes in T cells as WASP-deficient T cells fail to produce cytokines upon TCR activation (Morales-Tirado et al., 2004).

WASP deficiency causes selective subsets of mature B cells in the splenic marginal zone to be significantly reduced (Meyer-Bahlburg et al., 2008). It may have resulted from impaired homing of B cells or the retention of them in the marginal zone. This is evident from a study that have shown that WASP-deficient B cells failed to respond to

sphingosine 1 phosphate which is involved in marginal zone homing (Meyer-Bahlburg et al., 2008). Also, B cell retention in the marginal zone requires WASP, which enables integrin clustering following B cell receptor (BCR) activation. Due to the latter reason, WASP-deficient B cells have defects in immunological synapse formation. Thus, WASP plays an important role in B cell homeostasis as well as humoral immunity.

1.8.3 Function of WASP in the innate immune system

The importance of WASP in phagocytosis has been verified by studies that showed impaired phagocytosis in various cells of myeloid lineages that are deficient in WASP (Leverrier et al., 2001; Lorenzi et al., 2000). During phagocytosis, WASP is required for the formation of phagocytic cups that are enriched in actin (Tsuboi and Meerloo, 2007). These structures undergo internalisation, allowing ingestion of extracellular particles, forming phagosomes in the cell (Swanson, 2008). Defects in phagocytosis have been discovered in macrophages, neutrophils and dendritic cells (DCs) (Leverrier et al., 2001; Westerberg et al., 2003; Zhang et al., 1999).

Human WASP-deficient macrophages and DCs fail to form podosomes as efficiently as the WT cells (Burns et al., 2001). Podosomes are structures containing an actin core, surrounded by focal adhesion proteins like vinculin, talin and paxillin (Thrasher and Burns, 2010). The lack of podosomes in WASP deficient DCs and macrophages results in a defect in the clustering of the $\beta 2$ integrins (e.g. talin and paxillin), causing a decrease in cell binding to ICAM-1 (Inter-cellular Adhesion molecule 1), a ligand for $\beta 2$ integrins (Burns et al., 2004). This suggests that WASP may play a crucial role in integrin

clustering, allowing integrin activation in response to extracellular signals. Filopodia and lamellipodia formation at the leading edges of these cells are defective, suggesting that WASP and Cdc42 are in the same signaling pathway (Thrasher et al., 2000). Also, macrophages and DCs lacking in WASP has impaired chemotactic response towards specific chemoattractants, like macrophage chemoattractant CSF-1. Restoration of WASP expression, however, rescued this defect (Jones et al., 2002). Impaired migration of these cells is probably the cause of abnormal homing of WASP-deficient immune cells to inflammatory sites and effective mounting of adaptive immune responses in secondary lymphoid tissues (Thrasher and Burns, 2010).

1.9 Phosphorylation of WASP and its significance

Regulation of WASP activity by Cdc42 and SH3 domains containing proteins like Nck has been well-characterised by many groups. In recent years, post-translational modification of WASP has been discovered to play a crucial role in its regulation as well. WASP has been found to be substrates of many kinases, including the Src family of kinases like HCK (Cory et al., 2002b) and Fyn (Badour et al., 2004a) and Tec family tyrosine kinases like Itk (Bunnell et al., 1996) and BTK (Baba et al., 1999). Phosphorylation of both serine (such as Ser483 and Ser484) and tyrosine residues (such as Tyr291), have been reported on several distinct sites on WASP (Blundell et al., 2009; Cory et al., 2003; Cory et al., 2002b). Using a phosphomimetic mutation and a non-phosphorylatable mutation, by mutating Tyr to a negatively charged Glu residue (Y291E) and mutating Tyr to Phe residue (Y291F) respectively, many groups have studied the importance of phosphorylation in WASP. These mutations are useful as they only alter

the charges on the residues but have no effect on the binding of other WASP interactors. The Y291E mutation enhanced actin polymerization and filopodia formation in macrophages when compared to WASP or WASP^{Y291F}, indicating that phosphorylation regulates WASP positively (Cory et al., 2002b). Increased podosome assembly rate also occurred when WASP^{Y291E} was overexpressed (Dovas et al., 2009). In mice, Y293E mutation (Y291 in human WASP) also enhanced actin polymerization. However, the *in vivo* data showed that Y291E knockin mice shared many similar traits as WASP knockout mice and Y291F knockin mice (Blundell et al., 2009). These data indicate that tyrosine phosphorylation plays a critical role in the proper function of WASP. Also, the expression levels of WASP^{Y291E} was markedly reduced but could be partially restored by proteasome inhibitors treatment, suggesting that phosphorylation may target WASP for degradation by proteasomes (Blundell et al., 2009).

Tyr291 residue lies in the GBD domain of WASP and when WASP is in the autoinhibitory conformation, Tyr291 is located at the interface of two hydrophobic sheets (Cory et al., 2002b). Introduction of a negatively charged group, like the phosphate group, can destabilize the autoinhibited loop formed through the interaction of the BR-GBD and VCA domain (Kim et al., 2000). This can possibly stabilize the open conformation, exposing the VCA domain for Arp2/3 complex binding and thus, enhances actin polymerization.

In view of the results obtained by these studies, a model has been proposed as to how WASP is regulated *in vivo*. The binding of Cdc42 to WASP destabilizes the autoinhibited

conformation, allowing kinases to gain access to the Tyr291 residue. Phosphorylation of Tyr291 increases the instability of the contacts between the BR-GBD and VCA domains. This in turn enhances the activation of the Arp2/3 complex, increasing actin polymerization (Torres and Rosen, 2003, 2006). Additionally, the autoinhibited conformation of phosphorylated WASP can be disrupted by the binding of SH2 domains within the SH2-SH3 domains in the Src family kinases, leading to WASP activation (Torres and Rosen, 2003, 2006). When Cdc42 signal is deactivated before the kinases, WASP would return to the autoinhibited conformation. This denies the access of phosphatases to Tyr291, allowing the retention of phosphorylation of WASP for longer period of times. Subsequently, WASP can regain complete activation again via the binding of Cdc42 without the presence of the kinases (Torres and Rosen, 2003). Figure 1.9 summarises the regulation of WASP by phosphorylation. However, there have been contradictory findings in which Arp2/3 mediated actin polymerization by WASP after phosphorylation by Fyn, can occur independent of Cdc42 (Badour et al., 2004a). It may be because alternative pathways of activation of WASP exist.

The three mutations I294T, L270P and S272P causes XLN (Ancliff et al., 2006; Beel et al., 2009; Devriendt et al., 2001) and they are located closed to the site of phosphorylation at Tyr291. Furthermore, the mutation L270P causes WASP to adopt a constitutively open conformation (Devriendt et al., 2001). It would be interesting to study whether these mutations can affect phosphorylation at Tyr291 and in turn contribute to the pathology of XLN.

Serine phosphorylation in WASP has also been reported in two sites, Ser 483 and Ser484 in the VCA domain, which is mediated by casein kinase II (Cory et al., 2003). Phosphorylation of these two residues enhances the affinity of the VCA domain for Arp2/3 complex and is required for optimal activity of WASP (Cory et al., 2003). The role of phosphorylation of these two serine residues has not been well-characterised. Further studies have to be done to elucidate the mechanism of how serine phosphorylation regulates WASP activity.

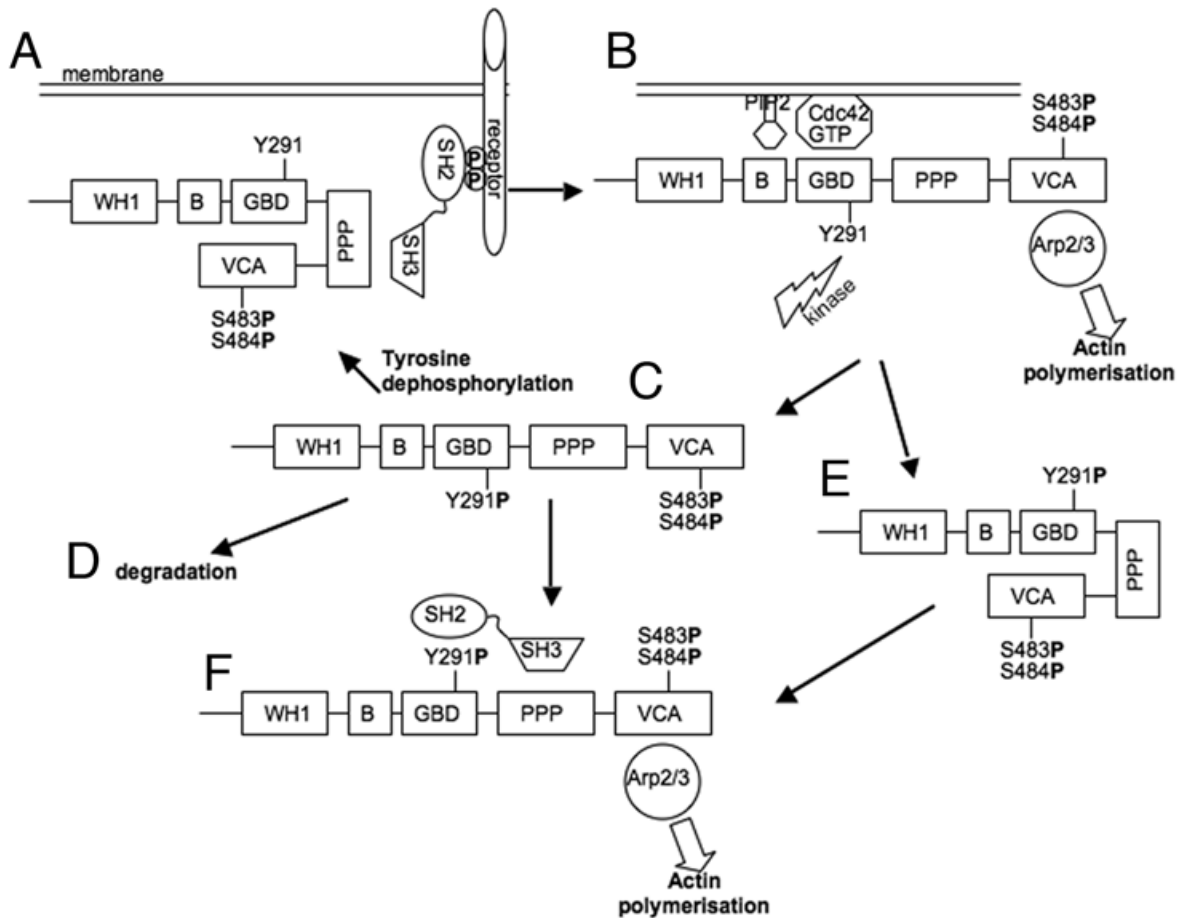


Figure 1.9 Regulation of WASP by phosphorylation. Adapted from (Dovas and Cox, 2010).

- A)** Recruitment of WASP, in the autoinhibited conformation, to the site of receptor signaling complex by SH3 domains containing proteins.
- B)** Activation of WASP by Cdc42 and PIP₂ allows phosphorylation of WASP by kinases.
- C)** Phosphorylated WASP may undergo dephosphorylation via phosphatases to return to (A) where it can be reactivated again or
- D)** It can be degraded by proteasomes
- E)** Termination of Cdc42 signal prior to the kinases allows the phosphorylation in WASP to be retained where it can be reactivated again (F)
- F)** Further activation of WASP by SH2 domain containing proteins.

1.10 The Calpain family of proteases

The calpain family of proteases consists of a group of cysteine proteases that are calcium dependent. Some of these proteases are ubiquitously expressed while the expressions of others are tissue-specific. Calpains share a common structural domain, domain II, which

can be further subdivided into IIa and IIb. This common element bears the catalytic triad residues, Cys, which is on subdomain IIa, as well as His and Arg which are present on subdomain IIb (Huang and Wang, 2001). It has been hypothesized that upon calcium binding, conformational changes would bring subdomains IIa and IIb together to form a catalytic pocket (Huang and Wang, 2001). Domain III is hypothesized to maintain the inactive state of the catalytic core but can also stabilize the active form of it (Reverter et al., 2001). Domain IV contains five sets of EF-hand structures and is responsible for calcium binding (Saez et al., 2006) (Figure 1.10). Calpains are classified according to the presence of the EF-hand module. Typical calpains contain the EF-hand domains while atypical calpains do not.

The most well studied members of the calpain family are the μ -calpain (calpain 1) and m-calpain (calpain 2). Both members are among the classical or typical calpains have different sensitivities to calcium. As indicated by their names, μ -calpain is activated by μ M levels of calcium while m-calpain is activated by mM levels of calcium (Saez et al., 2006).

The classical calpains have been associated with many diseases. Mutations in calpain-3 causes limb-girdle muscular dystrophy (Jia et al., 2001) and increased activity of calpain 2 causes cataracts due to enhanced cleavage of lens crystalline proteins (Biswas et al., 2005). Expression of calpain is upregulated in many types of cancers like brain and breast cancers causing the degradation of many cytoskeletal proteins like the WASP family of

proteins, focal adhesion kinase (FAK), integrins and oncogenes eg. c-Fos, c-Jun (Saez et al., 2006).

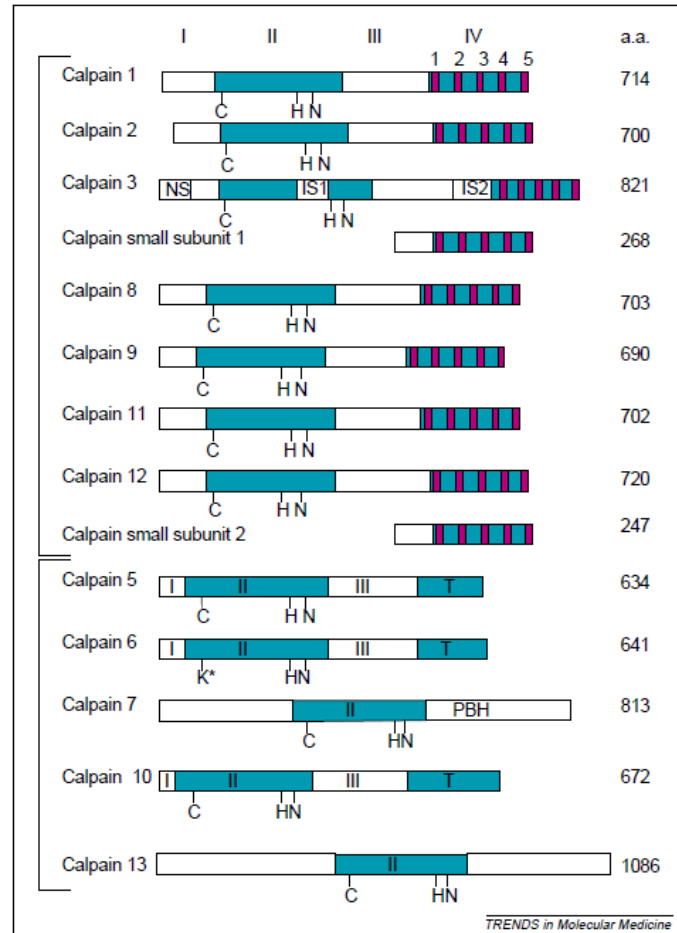


Figure 1.10 Schematic diagram showing the domain structures of the members of the calpain family of proteases. Adapted from (Huang and Wang, 2001).

1.10.1 Calpain and cell motility

Cell migration is a multi-step process which involves numerous proteins and complex regulatory pathways (Ridley et al., 2003). The first step in cell migration is the polarization of cells where several proteins are directed towards the leading edge where formation of adhesion and protrusions occurs (Lauffenburger and Horwitz, 1996). Focal complexes are first assembled and actin polymerization takes place where WASP/WAVE

proteins regulate the formation of actin filaments (Welch and Mullins, 2002). Protrusions are further stabilized by attachment of integrins and other proteins to the ECM (Geiger et al., 2001), forming focal adhesions which anchor the cell more tightly . At the rear end of the cell, adhesions are released, allowing the cell to move forward, completing the migration process (Ridley et al., 2003). In dendritic cells (Calle et al., 2006a), macrophages (Linder et al., 1999), and osteoclasts (Calle et al., 2004), podosomes are formed, in addition to focal complexes and focal adhesions. Podosomes are made up of an actin-rich core surrounded by proteins such as gelsolin, paxillin, vinculin, talin, WASP and other adaptor proteins that are linked to integrins (Calle et al., 2006a).

Proper regulation of the cell migration process is required for immune responses and pathological processes like metastasis of cancer cells. Calpain has been shown to be one of the critical players taking part in the regulatory process. Proteolytic degradation of cytoskeletal proteins, including filamins, vinculin, talin, cortactin and WASP family of proteins by calpain is thought to regulate the assembly and disassembly of adhesion structures (Lebart and Benyamin, 2006).

Expression of calpain is abundant in T cells and stimulation by phorbol ester or anti-CD3 increased the protein and mRNA levels (Deshpande et al., 1995). One study has shown that calpain plays a central role in the clustering of LFA-1, facilitating the adhesion to ICAM-1 (Stewart et al., 1998). LFA-1 associates with the cytoskeleton and it is likely that calpain cleaves a key protein which releases LFA-1, allowing it to move in the membrane (Kucik et al., 1996; Stewart et al., 1998).

1.10.2 Regulation of WASP by calpain

Inhibition of calpain by peptide inhibitors has been shown to reduce the turnover rates of podosomes and reduce the motility of dendritic cells (Calle et al., 2006b). Analysis of the cleavage of WASP, which is a podosomal protein, by calpain revealed that calpain inhibitors reduced the cleavage products of WASP (Calle et al., 2006b). This indicates that WASP is a substrate for calpain in migrating dendritic cells. Furthermore, WASP has been shown to be important for podosome formation through RNAi studies (Olivier et al., 2006). Loss of WASP expression abrogated podosome formation and increased the formation of focal adhesions that lack WASP (Olivier et al., 2006). The cleavage products of WASP have been suggested to also play a role in the formation of actin filaments although the biological functions remain unknown (Calle et al., 2006b). Localization of WASP is also found to be regulated by calpain (Calle et al., 2006b).

WASP and N-WASP appear to have differing sensitivities to calpain (Shcherbina et al., 2001). N-WASP, unlike WASP is not cleaved by calpain (Shcherbina et al., 2001). Since early stages of platelets activation remain normal in WASP-null platelets, it has been postulated that N-WASP plays a major role in the organization of actin cytoskeleton in the early events. Abnormal late-phase stages like aberrant regulation of calcium and procalpain levels in WASP null platelets indicate that WASP may play a role in adhesion and protrusion formation in response to changes in calpain levels (Shcherbina et al., 2001).

1.10.3 Role of WIP in the stability of WASP

WIP^{-/-} dendritic cells (DCs) have similar phenotypes as WASP^{-/-} dendritic cells, both display a lack of podosome formation and abnormal integrin clustering (Chou et al., 2006). WIP^{-/-} DCs have decreased expression of WASP but not vice versa, suggesting that WASP is protected from degradation by WIP. This may be due to the binding of WASP binding domain of WIP to the WH1 domain of WASP, preventing the exposure of the domain to proteases (Volkman et al., 2002). Further studies indicate that WIP protects WASP from calpain cleavage as inhibition of calpain in WIP null DCs, B and T cells resulted in the stabilization of WASP (Chou et al., 2006; de la Fuente et al., 2007).

1.10.4 Substrates of calpain

Calpain cleaves a wide diversity of proteins and these substrates include cytoskeletal proteins, transcription factors, receptors and enzymes (Lebart and Benyamin, 2006; Wang et al., 1989). Knowledge of substrate recognition and the determination of cleavage sites by calpain is crucial in the understanding of the function of both calpain and its substrates. Tompa and co-workers have compiled 106 substrate cleavage sites to analyse the cleavage recognition by calpain (Tompa et al., 2004). They found that the primary structure of the substrate is important around the scissile bond. Table 1 shows 11 residues, P₄ to P₇', that have been found around the scissile bond. In position P₁, Tyr, Lys and Arg occur at higher frequencies while Ser, Ala and Thr residues are preferred in position P₁'. However, it should be noted that other than the primary structure, calpain also recognizes the secondary structure and PEST regions of the substrates.

	P ₄	P ₃	P ₂	P ₁	P ₁ '	P ₂ '	P ₃ '	P ₄ '	P ₅ '	P ₆ '	P ₇ '
Trp	0.00	2.34^a	0.00	0.00	0.00	0.00	3.12^a	0.79	0.00	2.38^a	0.79
Tyr	0.90	0.00	0.30	2.69^a	0.00	0.30	0.60	0.60	1.81	1.52^b	0.30
Phe	0.23	0.23	0.23	1.84	0.46	0.46	0.23	1.39	0.00	0.94	1.17
Leu	0.59	0.59	2.97^a	0.59	0.59	0.40	0.20	0.40	0.90	0.60	1.01
Ile	0.32	1.13	0.81	0.16	0.65	0.65^b	0.97	0.33	0.33	0.33	0.99
Val	0.71	1.57	2.00^a	0.14	0.71	0.71	0.57	1.58	1.01	1.16	0.29
Ala	1.11	0.74	0.12	0.25	1.73	1.36	0.99	1.00	0.75	0.88	0.88
Gly	0.69	0.83	0.14	1.24	0.69	1.24	0.55	1.25	1.53	0.84	1.26
Ser	1.20	1.60	0.93	0.80	3.33	1.87	0.80	1.08	1.88	1.36	1.49
Thr	2.03^a	1.02	2.71^a	1.86	1.86^b	0.68	0.85	1.71	1.03	1.55	0.69
Pro	1.54	2.32^a	0.77	0.58	0.19	2.89^a	5.59^{a,b}	2.92^{a,b}	1.75	1.77	1.18
Asp	0.72	0.36	0.54	0.36	0.18	0.72	0.36	0.73	0.73	0.92	0.73
Glu	1.31	1.60	0.73	0.44	0.73	1.31	0.73	0.29	0.88	0.89	0.89
Gln	1.68	0.48	0.72	0.96	1.20	1.68	1.44	0.97	0.48	1.22	0.73
Asn	1.08	0.65	1.30	0.65	0.43	0.65	0.65	1.53	1.75	0.88	0.66
Lys	1.11	1.42	0.47	2.84^a	1.11	1.42	1.42	0.96	0.96	0.81	1.45
Arg	1.45	1.09	0.36	2.54^a	1.82	0.36	0.91	0.55	0.92	0.74	2.22^{a,b}
His	1.68	0.84	0.00	1.26	0.42	0.42	0.84	0.85	0.85	0.85	0.85
Cys	0.00	0.00	1.75	0.00	0.00	0.58	0.00	0.59	1.18	2.37	0.00
Met	0.80	0.40	0.40	1.59	0.80	0.40	1.19	0.00	0.00	0.00	1.22

^a Values exceeding 2.00 are in bold.

^b Values corresponding to the consensus calpastatin inhibitory segment in positions P₁'-P₇' (i.e. TIPPXYR) are underlined.

Table 1.1 Residues preferences of calpain near the cleavage site. Adapted from (Tompa et al., 2004). Scores represent the frequency of amino acid occurring at each position around the cleavage site.

1.11 Objectives of project

The Wiskott Aldrich Syndrome (WAS) is a rare but fatal disease in which treatments, other than bone marrow transplantation, are still poorly defined. Classic WAS is characterized by thrombocytopenia, eczema and immunodeficiencies and current therapies used are still not effective in lowering the mortality rates in WAS patients. WAS is caused by mutations in the Wiskott Aldrich Syndrome protein (WASP), which is found only in cells of hematopoietic lineage. Understanding the molecular basis of the disease could aid in uncovering new methods to treat the disease.

WASP is known to adopt two different conformations; open or close, depending on the interaction with various regulators. The Bi-molecular fluorescence complementation assay is a simplified method of the FRET assay where complementation of the two halves of YFP, that are fused to either of the two ends of WASP, will cause fluorescence of YFP. I propose to adopt this assay to simplify the study of the conformation of WASP and the

changes in its conformation upon interaction with various regulators. This assay will be developed in the *Saccharomyces cerevisiae* to eliminate other mammalian regulators that would otherwise affect the conformation of WASP. The verprolin family of proteins has emerged as important regulators of the actin cytoskeleton and they mediate their effects through the members of the WASP family. Other known activators of WASP including Rho-GTPase Cdc42, Toca1 and Nck1, could also potentially induce conformational changes in WASP. The BiFC assay will be utilized to examine how their interactions affect the conformation of WASP.

There are three mutations identified in WASP, in X-linked neutropenia patients, namely WASP^{L270P}, WASP^{S272P} and WASP^{I294T}. These mutations have been reported to cause a constitutively active WASP. Also, these mutations lie near the Tyr291 residue, which has been shown to be crucial in the positive regulation of WASP activity and for optimal activity in WASP through its phosphorylation. I hypothesize that the increase in activity of these mutant WASPs is caused by dysregulation of phosphorylation levels. The mutation WASP^{L270P} was selected to be used in the study of the role of phosphorylation in XLN. A phosphomimetic mutation, Y291E and a non-phosphorylatable mutation, Y291F, in the presence of L270P mutation will be used. I propose to use these mutations to analyse how phosphorylation in WASP^{L270P} affects the motility of Jurkat T cells and filopodia induction in fibroblasts, in order to characterize the XLN-causing mutation, WASP^{L270P}.

WASP degradation is another method in which WASP is regulated and WASP is known to be a substrate of calpain. In order to analyse the importance of the effects exerted by calpain on WASP, I propose to first generate a WASP mutant that is resistant to calpain cleavage. Using this mutant, I will examine if calpain proteolysis of WASP is important for the chemotactic response and motility in Jurkat T cells.

Together, these findings will enable a deeper understanding of the functions of the different domains of WASP. Also, the dynamics of WASP and its regulators, as well as mechanisms of the regulation of WASP studied in this project can potentially aid in uncovering new methods to treat the WAS, XLT and XLN

2. Materials and Methods

2.1 Materials

2.1.1 Plasmids

The list of plasmids used are listed in Appendix 1.

2.1.2 Plasmid vectors

For DNA subcloning experiments, vectors pUC19 and pUC18 were used. Vector pGEX was used for expression in the BL21 (DE3) strain of bacteria. For yeast two hybrid assays, vectors pACT2 and pAS2-1 were used for the expression of Gal4p Activation domain and the Gal4p Binding domain respectively. Vectors YEplac112, YEplac181 and YEplac195, which contain different selective markers, were used to express proteins in *Saccharomyces cerevisiae* cells. For expression of proteins in mammalian cells, vectors pFIV-H1/U6-copGFP and PEPCG were used. Table 2.1 summarized the commercial vectors used and their applications.

Vector	Resistant gene	Selective marker	Expression host	Used in
pGEX	Amp	-	Bacteria	Expression in bacteria cells
pUC18	Amp	-	Bacteria	DNA subcloning
pUC19	Amp	-	Bacteria	DNA subcloning
pACT2	Amp	Leu	Bacteria/Yeast	Yeast two hybrid
pAS2-1	Amp	Trp	Bacteria/Yeast	Yeast two hybrid
YEplac112	Amp	Trp	Bacteria/Yeast	Expression in yeast cells
YEplac181	Amp	Leu	Bacteria/Yeast	Expression in yeast cells
YEplac195	Amp	Ura	Bacteria/Yeast	Expression in yeast cells
pcDNA 3.1	Amp	-	Bacteria/Mammalian	Expression in mammalian cells
pFIV-H1/U6	Amp	-	Bacteria/Mammalian	Expression in mammalian cells
PEPCG-CopNeo	Kan	-	Bacteria/Mammalian	Expression in mammalian cells

Table 2.1. List of commercial vectors used.

2.1.3 Bacterial strains

The bacterial strain, *Escherichia coli* (*E. coli*) DH5 α , was used for plasmids amplification and DNA subcloning. *E. coli* BL21 (DE3) strain was used for protein expression.

2.1.4 Yeast strains

Yeast strain PJ69 (*Mat a his3 leu2 ura3 trp1 gal 4 Δ gal80 Δ met2::GAL7-lacZ GAL2-ADE2 LYS2::GAL1-HIS3*) used is described in (James et al., 1996). IDY166 (*Mat a his3 leu2 ura3 trp1 las17 Δ ::URA3*) used is described in (Naqvi et al., 1998).

2.1.5 Mammalian cell lines

HEK 293T, Cos7, Jurkat (clone E6-1) were from American Type Culture Collection (ATCC, USA). N-WASP deficient (N-WASP^{-/-}) mouse embryonic 6TC fibroblast cell line was a kind gift from Prof. Scott Snapper (Harvard Medical School, Boston, MA).

2.1.6 Antibodies

The antibodies used in this project are listed as follows:

Primary antibodies:

Antibody	Source
Anti-GFP mouse polyclonal antibody	Clontech Laboratories, Mountain View, CA, USA
Anti-GAPDH mouse monoclonal antibody	Ambion, Austin, TX, USA
Anti-His rabbit polyclonal antibody	Delta biolabs, Gilroy, CA, USA
Anti-WASP rabbit polyclonal antibody	Kindly provided by A/Prof Thirumaran Thanabalu
4G10	Upstate biotechnology, Lake placid, NY, USA

Table 2.2 List of primary antibodies used.

Secondary antibodies:

Antibody	Source
Anti-mouse IgG	Sigma, St. Louis, Mo, USA
Anti-rabbit IgG	Sigma, St. Louis, Mo, USA

Table 2.3 List of secondary antibodies used.

2.1.7 Bacterial and yeast culture media

2.1.7.1 Luria-Bertani (LB) broth

1% bacto-tryptone, 0.5% bacto-yeast extract and 0.5% NaCl was dissolved in distilled water and autoclaved.

2.1.7.2 LB agar plates

2% of bacto-agar was added to LB broth and autoclaved. Medium was left at room temperature to cool to below 60°C and 25 ml of medium was poured into each plate and left to solidify.

2.1.7.3 YPUAD medium

2% of bacto-peptone, 1% of bacto-yeast extract, 0.008% of adenine hemisulphate and 0.004% of uracil were dissolved in distilled water and autoclaved.

2.1.7.4 YPUAD agar plates

2% of bacto-agar was added to YPUAD medium and autoclaved. Medium was left at room temperature to cool to below 60°C and 25 ml of medium was poured into each plate and left to solidify.

2.1.7.5 SD medium

0.67% of Yeast Nitrogen base, 2% of Glucose and the different concentrations of the dropout supplements as described in Table 2.4 were dissolved in distilled water and autoclaved.

Supplements	Amount in dropout powder (g)	Final working concentration (mg/L)
Adenine	2.5	40
L-arginine (HCl)	1.2	20
L-aspartic acid	6.0	100
L-glutamic acid (monosodium salt)	6.0	100
L-histidine	1.2	20
L-isoleucine	1.8	30
L-leucine	3.6	60
L-lysine (mono-HCl)	1.8	30
L-methionine	1.2	20
L-phenylalanine	3.0	50
L-serine	22.5	375
L-threonine	12.0	200
L-tryptophan	2.4	40
L-tyrosine	1.8	30
L-valine	9.0	150
Uracil	1.2	20

Table 2.4 List of supplements used in the SD medium (Baker, 1993).

2.1.7.6 SD agar plates

2% of bacto-agar was added to SD medium and autoclaved. Medium was left at room temperature to cool to below 60°C and 25 ml of medium was poured into each plate and left to solidify.

For Yeast Two Hybrid assay, SD agar plates with 2 mM 3-AT but without histidine were used. 3-AT (1M stock concentration dissolved in distilled water) was filter-sterilised and added to SD medium without histidine to a final concentration of 2 mM. 2% of bacto-

agar was added to the SD medium containing 2mM 3-AT but without histidine, and autoclaved. Medium was left at room temperature to cool to below 60°C and 25 ml of medium was poured into each plate and left to solidify.

2.1.8 Mammalian cell culture media

Cell lines	Media
HEK 293T	Dulbecco's Minimal Eagles medium (DMEM) - Hyclone (Thermo Scientific)
Cos 7	Roswell Park Memorial Institute medium (RPMI-1640) – Hyclone (Thermo Scientific)
Jurkat (Clone E6-1)	Roswell Park Memorial Institute medium (RPMI-1640) – Hyclone (Thermo Scientific)
N-WASP ^{-/-} mouse embryonic 6TC fibroblast	Dulbecco's Minimal Eagles medium (DMEM) – Hyclone (Thermo Scientific)

Table 2.5 List of cell lines and the respective media used.

Supplements/ Antibiotics	Source
Fetal Bovine serum (FBS)	Hyclone (Thermo Scientific)
Penicillin-streptomycin	Hyclone (Thermo Scientific)
Puromycin	Sigma (USA)
Ionomycin	Sigma (USA)
PMA	Sigma (USA)
SDF-1 α	Sigma (USA)
G418	PAA Laboratories

Table 2.6 List of antibiotics used.

Disposables	Source
Tissue Culture plates	Iwaki or Nunc
Tissue Culture flasks	Corning or TPP
Pipettes	Costar

Table 2.7 List of disposables used.

2.1.9 Enzymes and kits

The restriction endonucleases obtained from Fermentas (Hanover, MD, USA) or New England Biolabs (NEB) (Ipswich, MA, USA) and T4 DNA ligase and buffer from Fermentas (Hanover, MD, USA) were used for DNA subcloning. For site directed mutagenesis (SDM) experiments, QuikChange Site-Directed Mutagenesis kit was purchased from Stratagene (La Jolla, CA, USA). For isolation of plasmid DNA from *E. coli* cells, QIAprep Spin Miniprep Kit (Qiagen) (Valencia, CA, USA) was used while for the isolation of RNA from mammalian cells, RNeasy Minikit (Qiagen) was used. QIAquick Gel extraction Kit (Qiagen) was used to extract DNA from agarose gels. The Bradford assay (Bio-Rad DC protein assays) used for measuring protein concentration was purchased from Bio-Rad (Hercules, CA, USA). The kits used for developing in Western blot include Millipore Immobilon Western (Millipore Corp, Billerica, MA, USA) and Amersham ECL Plus (GE healthcare, Buckinghamshire, UK). The Microporation kit and instrument used for Jurkat microporation was purchased from Digital Bio Technology (Digitalbiotechnology, Seoul, South Korea).

2.1.10 Polymerase chain reaction (PCR)

DNA polymerase KAPA HiFi from KAPA biosystems (Woburn, MA, USA) or DNA polymerase from BIOTOOLS (Madrid, Spain) were used. dNTPs (dTTP, dATP, dGTP and dCTP) mixtures were obtained from Invitrogen (Carlsbad, CA, USA).

2.1.11 Chemicals and reagents

2.1.11.1 DNA work

DNA loading ladder and 6X DNA loading buffer were obtained from NEB (Ipswich, MA, USA). Ampicillin and Kanamycin used in selective plates and medium were purchased from Sigma-Aldrich (St. Louis, Mo, USA).

2.1.11.2 Protein work

Phenylmethylsulfonyl fluoride (PMSF), 1, 4-Dithiothreitol (DTT) and protease inhibitors complete-mini protease tablets used in cell lysis were bought from Roche (Indianapolis, IN, USA). Protein molecular weight marker, Dual Color was purchased from Bio-Rad Laboratories (Hercules, CA, USA) and nitrocellulose membrane used for Western blot was obtained from Bio-Rad (Hercules, CA, USA).

2.1.11.3 Others

For actin staining in fibroblasts, Alexa-488-conjugated phalloidin from Molecular Probes (Eugene, OR, USA) was used. The rest of the chemicals used were purchased from Sigma Aldrich (St. Louis, Mo, USA) and were of analytical grade.

2.1.12 General buffers and solutions

2.1.12.1 DNA subcloning experiments

2.1.12.1.1 50X Tris-acetate-EDTA (TAE)

- 242 g of Tris base
- 57.1 ml of glacial acetic acid
- 100ml of 0.5 M EDTA (pH 8.0)
- Deionised water (topped up to 1 litre)

2.1.12.1.2 Agarose gel

1% agarose was added in 1 X TAE buffer (diluted from 50X TAE in deionised water) and microwaved till agarose dissolved.

2.1.12.2 Western blots

2.1.12.2.1 10% SDS

10 g of SDS was dissolved in 10 ml of deionised water.

2.1.12.2.2 10% Ammonium persulphate

1 g of ammonium persulphate was dissolved in 10 ml of deionised water.

2.1.12.2.3 5X Tris-glycine electrophoresis buffer

- 15.1g of Tris
- 94 g of glycine
- 5g of SDS
- Deionised water (topped up to 1 litre)

2.1.12.2.4 Transfer buffer

- 7.57g of Tris
- 36.1g of Glycine
- 0.625g of SDS
- Deionised water (topped up to 1 litre)

2.1.12.2.5 2X SDS-PAGE gel-loading buffer

- 100 mM Tris-HCl (pH 6.8)
- 200 mM dithiothreitol
- 4% SDS
- 0.2% Bromophenol blue
- 20% glycerol

2.1.12.2.6 1M Tris buffer

121.12 g of Tris was dissolved in 1 litre of deionised water and the pH of the solution was adjusted to 8.0 using HCl.

2.1.12.2.7 5M NaCl

292 g of NaCl was dissolved in 1 litre of deionised water.

2.1.12.2.8 1X Tris buffered saline (TBS)

- 10ml 1M Tris
- 30ml 5M NaCl
- 0.05% Triton X-100
- Deionised water (topped up to 1litre)

2.1.12.2.9 Blocking solution

5%, 3% or 1% of non-fat milk powder was dissolved in 1X Phosphate buffered saline to make the blocking solution. For western blot detecting phospho-proteins, 5% of Bovine serum albumin (BSA) was dissolved in 1X TBS.

2.1.12.2.10 Wash solution

To make the wash solution, 5 ml of 10% Triton-X was added to 995ml of 1X Phosphate buffered saline. For western blot detecting phospho-proteins, 1X TBS was used.

2.1.12.3 Gel staining

2.1.12.3.1 SDS PAGE gel destaining solution

- Methanol
- Deionised water
- glacial acetic acid

mixed in the ratio of 450:450:100

2.1.12.3.2 SDS PAGE gel staining solution

0.25 g of Brilliant Blue R-250 was dissolved in 100 ml of destaining solution.

2.1.13 Yeast reagents

2.1.13.1 10X LiAc

1 M lithium acetate solution was prepared in deionised water.

2.1.13.2 20% Tri-Chloro Acetic Acid (TCA)

20 g of TCA was dissolved in 100 ml of sterile deionized water.

2.1.13.3 50% PEG 3350

50 g of PEG 3350 was dissolved in 100 ml of sterile deionized water.

2.1.13.4 Loading dye (Urea buffer)

- 8 M Urea
- 50 mM Tris, pH 6.8
- 2% SDS
- 0.04% Bromophenol

2.1.14 His tag pull-down assay

2.1.14.1 Equilibration buffer for Ni-NTA beads

1. 50mM Tris(pH 8)
2. 100mM NaCl

2.1.14.2 Lysis Buffer (pull-down assay)

- 50mM Tris (pH 8)
- 100mM NaCl

The following was added fresh (to equilibration buffer),

- 5% NP40 (50ul in 1ml)
- 200mM PMSF stock(5 ul in 1ml)
- protease inhibitor stock (5ul in 100 ul)

2.1.14.3 Elution Buffer for Ni-NTA beads

- 50mM Tris (pH 8)
- 100mM NaCl

(varying concentrations of imidazole was added to the equilibration buffer)

- A. 10mM Imidazole
- B. 25mM Imidazole
- C. 50mM
- D. 100mM
- E. 150mM
- F. 250mM
- G. 500mM
- H. 1M mM

2.1.15 Tissue culture

2.1.15.1 Freezing media

The freezing media was prepared by adding 10% of dimethyl sulfoxide (DMSO) in FBS and was filter sterilized through a 0.2µm filter.

2.1.15.2 Lysis buffer

- 50 mM Tris-HCl, pH 7.5,
- 200 mM NaCl,
- 1% Triton X-100,
- 0.1% SDS,
- 0.5% sodium deoxycholate,
- 10% glycerol,
- 1 mM EDTA,
- 1mM phenylmethylsulfonyl fluoride (PMSF),
- protease inhibitor cocktail containing 10 µg/ml of leupeptin, pepstatin, and aprotinin each.

2.1.15.3 Transfection reagent

A 25% solution of Polyethyleneimine PEI (branched) (Sigma, St. Louis, Mo, USA) was prepared in deionised water. The 25% solution was then diluted to give a 10X solution by adding 0.9ml in 50ml of deionised water. The 10X solution was then filter sterilized through a 0.2µl filter.

2.2 Methods

2.2.1 *Escherichia coli* cells

2.2.1.1 Growth conditions and maintenance of *E. coli* cells

E. coli was either cultured in LB broth or maintained on LB agar plates at 37°C. *E. coli* transformed with plasmids containing ampicillin or kanamycin selection marker were cultured in LB-broth or grown on LB agar plates supplemented with 75 µg/ml ampicillin or kanamycin.

2.2.1.2 *E. coli* glycerol stocks preparation

A single colony of *E. coli* was inoculated in 5 ml of LB broth and grown until log phase. 800 µl of the bacterial culture was aliquoted out and added to 200 µl of 80% glycerol. The mixture was stored in a cryo-vial at -80°C.

2.2.1.3 Competent *E. coli* cells preparation

Competent *E. coli* cells were prepared using the CaCl₂ method. A single colony of *E. coli* was inoculated in 5 ml of LB broth and grown (incubated with shaking) overnight at 37°C. The bacterial culture was diluted to an OD₆₀₀ of 0.01 in 200 ml of LB broth the

next day and grown (incubated with shaking) to an OD₆₀₀ of 0.4 at 37°C. The cells were spun down at a speed of 4470 g at 4°C for 15 minutes. After decanting the supernatant, the pellet was resuspended in 100ml of ice-cold 100mM MgCl₂ that has been sterile filtered. The cells were spun down again at a speed of 4470 g at 4°C for 15 minutes. After decanting, the cell pellet was resuspended in 10 ml of ice-cold 100 mM CaCl₂ that has been sterile filtered. Cells were incubated in CaCl₂ on ice for 1-2 hours to become transformation competent. 5 ml of sterile ice-cold 75% glycerol was added to the cell suspension and mixed briefly. The cell suspension was aliquoted out in eppendorf tubes and froze in liquid nitrogen immediately. They were stored at -80 °C until further use.

2.2.1.4 Transformation of *E. coli* cells

Frozen competent cells in eppendorf tubes were first thawed on ice. For DNA amplification, 1 µl of DNA was added to 50 µl of competent cells. For subcloning of plasmids, 1 µl of DNA was added to 100 µl of competent cells. The tubes were incubated on ice for 20 minutes and heated at 42°C in a water bath for 90 seconds. They were then placed on ice immediately for 5 minutes. Cells were plated on LB agar plates containing the selective antibiotic and incubated at 37°C overnight.

2.2.1.5 Plasmid DNA isolation from *E. coli* cells

A single colony of *E. coli* was inoculated in 5 ml of LB broth containing selective antibiotic and grown (incubated with shaking) at 37°C overnight. The cells were spun down at 4470 g at 4°C for 5 minutes. Isolation of plasmid DNA from the cells was

carried out using the Miniprep kit, according to the instructions given in the manufacturer's manual.

2.2.2 *Saccharomyces cerevisiae* cells

2.2.2.1 Growth conditions and maintenance of *S. cerevisiae* cells

S. cerevisiae cells were either cultured in YPUAD or maintained on YPUAD agar plates at 30°C. *S. cerevisiae* cells transformed with plasmids containing selection markers were cultured in Synthetic Defined (SD) or grown on SD agar plates at 30°C.

2.2.2.2 *S. cerevisiae* glycerol stocks preparation

A single colony of *S. cerevisiae* was streaked on a YPUAD agar plate and grown at 30°C for 3 to 4 days. A loopful of cells was inoculated in a cryo-vial containing 500 µl of YPUAD and 20% glycerol. The cells were then stored at -80°C.

2.2.2.3 Transformation of *S. cerevisiae* cells

Transformation of *S. cerevisiae* cells were performed using the lithium acetate protocol (Thanabalu and Munn, 2001). A loopful of cells was inoculated in 25ml of YPUAD and grown (incubate with shaking) overnight at 30°C. The culture was diluted to an OD₆₀₀ of 0.2 in 25 ml of LB broth the next day and grown (incubated with shaking) to an OD₆₀₀ of 0.8 at 30°C. The cells were spun down at a speed of 1000 g at room temperature (RT) for 5 minutes. After decanting the supernatant, the cell pellet was washed once with deionised water. The cells were spun down at 1000 g at RT for 5 minutes and the supernatant was decanted. The cell pellet was resuspended in 500 µl of 100 mM (1X)

Lithium acetate (LiAc) and transferred to an eppendorf tube. The cells were spun at 14,300 g for 15s and LiAc was removed. Cells were resuspended with 250 µl of 100 mM LiAc. The cell suspension was vortexed and 50 µl of cell suspension was aliquoted into each tube. The cells were spun down at 14,300 g for 30s and LiAc was removed again. Each tube of cells was added with 240 µl of 50 % PEG, 36 µl of 1 M (10X) LiAc, 5 µl of sonicated salmon sperm DNA, 1 µl of plasmid DNA containing selection marker and 74 µl of deionised water. The control tube was added with 75 µl of deionised water without plasmid DNA. The tubes were vortexed for 1 minute and incubated at RT for 30 mins. After incubation, cells were heat-shocked in the waterbath at 42°C for 20 mins and spun down at 3332g for 15 s. The supernatant was discarded and 200 µl of deionised water was added into each tube. 100 µl of the cells were plated in the selective SD plates and grown at 30°C for 3-4 days.

2.2.2.4 Yeast two hybrid assay

The yeast two hybrid assay was used to identify protein-protein interaction. Proteins, whose interactions were to be verified, were cloned into these two plasmids, pAS2-1 or pACT2 which contain Gal4 Binding domain and Gal4 Activation domain respectively. The interaction of the proteins would bring the binding domain and the activation domain in close proximity and drive the transcription of the reporter gene, HIS3.

S. cerevisiae strain PJ69-4A was first transformed with bait plasmid pAS2-1 and prey plasmid pACT2, with proteins of interest cloned in, and grown on SD plates lacking Trp and Leu. Patching of the transformed *S. cerevisiae* cells were done on 2 different plates,

SD plates lacking Trp and Leu as a control and SD plates lacking Trp, Leu, His and supplemented with 2 mM 3AT to check for the interactions between the proteins. 3AT act as an inhibitor for non-specific activation of the transcription of the reporter genes.

2.2.2.5 Yeast cell lysis

A loopful of cells was inoculated in 25ml of YPUAD and grown (incubate with shaking) overnight at 30°C. The culture was diluted to an OD₆₀₀ of 0.2 in 25 ml of LB broth the next day and grown (incubated with shaking) to an OD₆₀₀ of 0.8 at 30°C. OD₆₀₀ of 7 units of cells were harvested by centrifugation of the cells at 4470 g for 5 minutes at RT. The supernatant was decanted and the cell pellet was washed once with deionised water. The cells were spun down at 4470 g at RT for 5 minutes and the supernatant was discarded. The cell pellet was resuspended in 1 ml of 1X PBS and transferred to an eppendorf tube. The cells were spun at 14,300 g for 30s and PBS was removed. The cell pellet was resuspended with 240 µl mixture containing 1.85 M NaOH and 1.06 M β-mercaptoethanol and incubated on ice for 10 mins. An equal volume of 20% of TCA was added to the tube and was incubated on ice for an additional 10 mins. The resulting pellet was obtained by centrifuging at 14,300 g for 10 mins and was washed in ice-cold acetone and spun at 14,300 g for 10 mins. The pellet was then resuspended in 100 µl of loading dye (urea buffer). 15 µl of sample was loaded in SDS-PAGE gel when Western blot analysis was required.

2.2.2.6 Fluorescence visualisation

Cells were grown to exponential phase and were harvested. They were washed twice with PBS, resuspended in PBS and applied to a microscope slide. Fluorescence imaging was performed using an Olympus microscope with CoolSNAPHQ camera (Roper Scientific). Fluorescence intensities of 100 cells were quantified using the metamorph software.

2.2.3 Mammalian cell culture

2.2.3.1 Growth and maintenance of mammalian cells

HEK 293T and N-WASP deficient (N-WASP^{-/-}) mouse embryonic 6TC fibroblast cell line were maintained in DMEM and 10% FBS, supplemented with penicillin-streptomycin. Cos7 and Jurkat (clone E6-1) cells were maintained in RPMI and 10% FBS, supplemented with penicillin-streptomycin.

The cells were cultured at 37°C in a 5% CO₂ incubator. HEK 293T, N-WASP^{-/-} fibroblasts and Cos7 cells were trypsinised and split once every 2-3 days at 1:7 dilution when they become confluent. Jurkat cells were split once every 2-3 days. Splitting was done by centrifuging the cell culture at 400 g for 4 mins and the old growth media was discarded. 10ml of fresh media was added to the cell pellet to resuspend the cells. 2 ml of the Jurkat cell suspension was added to a new dish that contains 8 ml of media.

For stable WASP expression, Jurkat cells were microporated with WASP constructs and selected with 2mg/ml G418 after 2 days. Media with G418 was changed once every 2 to 3 days for a week until WASP was stably expressed in the cells.

2.2.3.2 Preparation of mammalian cell stocks

For adherent cells, cells were first trypsinised and then resuspended in the appropriate growth media. For both the adherent and suspension cells, the number of cells and cell viability were determined using the hemacytometer, cell counter and Trypan Blue exclusion. 5×10^6 to 1×10^7 cells (per ml of freezing medium) were spun down at 400 g at 4 mins. The supernatant was discarded and the cell pellet was resuspended with cold freezing medium. The cell suspension was then aliquoted into cryogenic storage vials and stored at -80°C in an isopropanol cryobox, that has a controlled freezing rate, overnight. The frozen cells were transferred to liquid nitrogen tank.

2.2.3.3 Transfection of adherent mammalian cells

HEK 293T, N-WASP^{-/-} fibroblasts and Cos7 cells were grown in 6-well plates or seeded in coverslips in the 6-well plates to 80% confluency for one day before transfection. 3.5µg of DNA was added to 15µl of serum-free medium (SFM). The mixture was then added to 1.3 µl of PEI and 98.7µl of SFM and resuspended. The mixture was allowed to stand for 1 hr at RT. The old growth media was discarded and replaced with new complete growth media. When the morphology of the cells has reverted to the normal state, the reaction mixture was added dropwise onto the cells. The cells were incubated for 12 hrs at 37°C in the humidified chamber before changing the media to new growth media. After 36 hrs of incubation at 37°C in a 5% CO_2 -humidified incubator, cells were ready for further analysis.

2.2.3.4 Microporation of Jurkat cells

Jurkat cells were resuspended in new growth media a day before microporation. The number of cells and cell viability were determined using the hemacytometer, cell counter and Trypan Blue exclusion. 5×10^6 cells were spun down at 400 g at 4 mins. The supernatant was discarded and the cell pellet was resuspended in 100 μ l of Resuspension buffer R and 10 μ g of DNA. Microporation was performed at RT, at 1500 voltage, 10ms and 3 pulses. After which, cells were distributed into 6-well plates containing 3 ml of growth media and incubated at 37 °C in a 5% CO₂-humidified incubator. After 36 hrs of incubation, cells were ready for further analysis.

2.2.3.5 Ionomycin treatment of HEK 293T cells

HEK 293T cells were transfected according to Methods 2.2.3.3. 36 hours after transfection, the old growth media was discarded and HEK 293T cells were washed once with PBS. New growth media supplemented with 1mg/ml of ionomycin was replaced in the wells. The cells were incubated for 4 hours at 37 °C in a 5% CO₂-humidified incubator. Thereafter, cells were lysed for western blot analysis.

2.2.3.6 Retrovirus vector mediated RNAi

3 wells (6-well plate) of HEK 293T were transfected with 1.75 μ g PCL-ampho and 1.75 μ g shRNA (Refer to Appendix 2) (Total: 3.5 μ g) for each well, according to Methods 2.2.3.3. After 48 hrs, the supernatant was pooled together from the 3 wells and spun down at 2861 g for 4mins to remove the cell debris. The supernatant was filtered together with 10 μ g/ml of polybrene, with a 0.45 μ m filter. 2ml of fresh DMEM was added back

into the wells for collection the next day. A new 6-well plate was coated with 10 µg/ml fibronectin (650 µl per well) for 1 hr at 37°C prior to the addition of the supernatant. The plate was washed once with sterile 1X PBS. The virus containing supernatant was added to the well and spun down at 2861 g for 45 mins at 4°C. 1×10^6 Jurkat cells were spun down and resuspended in 2 ml of RPMI. The supernatant was removed from the well after centrifugation and the Jurkat cell suspension was added into the well. The cells were incubated at 37 °C in a 5% CO₂-humidified incubator for 24 hrs and were spun down at 400 g for 4 mins and resuspended in new media. Supernatant from the previous plate containing HEK 293T cells was spun down again on fibronectin-coated plate for 2861 g for 45 mins at 4°C. Jurkat cell suspension was added into the new well and incubated at 37 °C in a 5% CO₂-humidified incubator for 3-4 days. When the infected cells were confluent, cells with green fluorescent were sorted using FACS Aria cell sorter using the FL1-FITC filter. These cells were further grown at 37 °C in a 5% CO₂-humidified incubator for 3-4 days before analysis of endogenous WASP expression or expressing WASP mutants.

2.2.3.7 Mammalian cell lysis

Adherent cells were trypsinised and resuspended in the appropriate growth media. For both the adherent and suspension cells, the number of cells and cell viability were determined using the hemacytometer, cell counter and Trypan Blue exclusion. 2×10^6 were spun down at 400 g at 4 mins. The supernatant was discarded and the cell pellet was resuspended in 50 µl of lysis buffer (Materials 2.1.15.2). Cells were left on ice for 1 hr and unlysed cells were removed by spinning down at 14,300 g for 2 mins. 50 µl (equal

amounts) of 2X loading dye and 2 µl of 1M dTT was added to the lysate. Protein concentration was quantified with Bio-Rad DC protein assays. The lysate was boiled at 100°C for 5 mins and stored at -20°C until further use.

2.2.3.8 Actin staining of N-WASP^{-/-} fibroblasts

Fibroblasts were transfected in 6-well plates with coverslips, with the respective plasmid DNA. After 36 hrs, cells were washed 3 times with 1X PBS (10 mins per wash) and fixed with 3.7% formaldehyde for 20 mins at RT. Thereafter, the cells were permeabilised with 0.1% Triton-PBS for 20 mins at RT. Actin staining of the cells were then performed by incubating the cells with Alexa Fluor® 568 phalloidin (Invitrogen™, USA) (1:100 dilution in 0.1% Triton-PBS) for 45 mins in the dark. Cells were washed 3 times (10 mins per wash) with 0.1% Triton-PBS and mounted on microscope slides with Perma Fluor.

2.2.3.9 Fluorescence visualization

N-WASP^{-/-} fibroblasts on coverslips were transfected with the respective plasmid DNA. After 36 hrs, the cells were washed twice with 1X PBS and applied on a microscope slide. Fluorescence was visualized using an Olympus microscope with CoolSNAPHQ camera (Roper Scientific) with a 40X oil objective lens. Fluorescence and filopodia formation of the cells were analysed using the Metamorph software.

2.2.3.10 Quantification of filopodia formation in N-WASP^{-/-} fibroblasts

N-WASP^{-/-} fibroblasts were transfected with the respective plasmid DNA. After 36 hrs, filopodia formation for each cell was analysed. The cell was defined to have filopodia if it has 5 or more filopodia since the fibroblasts would contain a basal number of filopodia.

Filopodia were defined as cell protrusions and have a length of between 8µM to 15µM in length (Lim et al., 2008). For each set of experiment, 35 cells were analysed and the experiments were repeated thrice.

2.2.3.11 Fluorescence Resonance Energy transfer (FRET) assay

The FRET constructs were constructed by fusing YFP to the N-terminus of WIP (YFP-WIP) and fusing CFP to the C-terminus of WASP (WASP-CFP). These constructs were transfected into Cos7 cells. After 36 hrs, cells on the coverslips were mounted on microscope slides and were analysed by the CFP-YFP FRET by acceptor photobleaching method, using the Zeiss LSM 510 Meta confocal microscope where emission from CFP, excited at 458 nm, and YFP, excited at 514 nm were detected. A random cell was chosen and a boundary was drawn encompassing it to specify the area for photobleaching. The acceptor protein YFP was photobleached using the 514-nm laser line and the percentage change in fluorescence of the donor protein CFP was quantified by calculating the difference in intensity of the fluorescence before and after photobleaching $[(I_{\text{postbleach}} - I_{\text{prebleach}})/I_{\text{postbleach}} \times 100\%]$. The FRET values were quantified for at least 20 cells for each experiment and the experiments were repeated thrice.

2.2.3.12 Flow cytometry

The number of cells and cell viability were determined using the hemacytometer, cell counter and Trypan Blue exclusion. 3×10^6 cells were spun down at 400 g at 4 mins. The Cells were washed once with 1XPBS and centrifuged at 400 g at 4 mins. The cell pellet was resuspended with 1 ml of media and transferred to 12mmX 75mm polystyrene

round-bottom tubes (Falcon). Samples were analysed using FACS Calibur using the FL1-FITC filter.

2.2.3.13 Analysis of Jurkat cell migration using the Dunn chemotaxis chamber

2.2.3.13.1 Washing of Dunn chamber and glass coverslips

The glass coverslips (18 X 18 mm) (Hawksley & Sons Ltd, Lancing, Sussex, UK) were individually washed with detergent in deionised water and rinsed 6 times with deionised water. They were then soaked in fuming HCl for 10 mins and washed with deionised water to remove all traces of HCl. The coverslips were stored in 100% ethanol until further use.

The Dunn chamber (Weber Scientific International Ltd. West Sussex, UK) was cleaned immediately after use. It was first washed with detergent in deionised water and rinsed 6 times with deionised water. It was then placed in a beaker filled with 100% acetone to be washed for 10 mins with agitation. Thereafter, the chamber was rinsed 6 times with deionised water and soaked in 30% hydrogen peroxide for a further 10 mins. The chamber was then rinsed 6 times with deionised water again and was stored in 100% ethanol until further use. The bridge of the chamber was not touched at all times during the washing (Zicha et al., 1997).

2.2.3.13.2 Assembly of the Dunn chamber

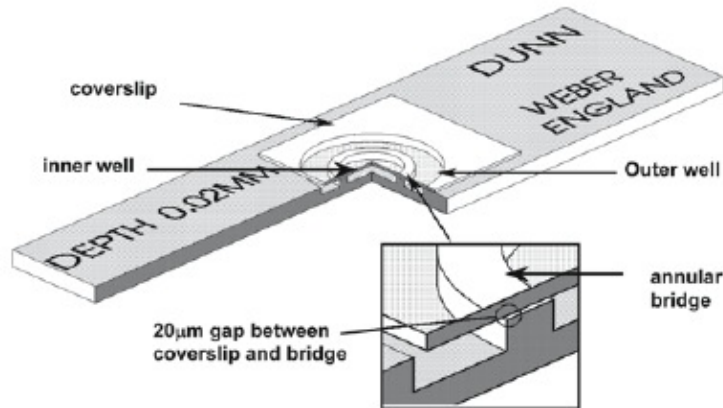


Figure 2.1. The assembled Dunn chamber (Zicha et al., 1997).

The Dunn Chamber contains a circular inner well and a circular outer well, separated by an annular bridge which is 20µm lower than the surrounding glass. This leaves a gap between the coverslip and the bridge, allowing the migration of cells across the bridge.

The coverslips stored in 100% ethanol were flamed until all the ethanol has evaporated. Jurkat cells suspended in RPMI 1640 supplemented with 9% FBS (2.25×10^6 in 120 µl) were loaded into both inner and outer wells of the chamber. The wells were covered with a coverslip, leaving a small slit at one edge and the medium in the outer well was replaced with the same medium but containing 5nM SDF-1 α . Cells were incubated for 3 hrs at 37°C in the 5% CO₂-humidified incubator.

2.2.3.13.3 Time-lapse microscopy

Migrating cells on the annular bridge between the inner and outer wells were observed using an inverted microscope (Olympus IX81) with 10X objective lens. Time-lapsed images were digitally captured every 30 seconds for a period of 50 mins using an Olympus CoolSNAP^{HQ} camera. Images were processed into videos using the Metamorph software. Migration paths of the cells were traced and analysed from the series of images

using Metamorph software. The data were plotted with Microsoft Excel. 20 cells were analysed for each set of experiment and experiment was repeated thrice.

2.2.3.14 DNA manipulation

2.2.3.14.1 Agarose gel electrophoresis

0.5 µg/ml of Ethidium Bromide was added to 1% agarose in 1X TAE and the gel was left to set. 6X DNA Loading buffer was added to the samples and they were loaded in the wells of the gel, submerged in 1X TAE. DNA was resolved by running the gel at 100V for 50 mins. DNA was visualized under the UV light.

2.2.3.14.2 DNA extraction from agarose gel

The agarose gel with DNA samples resolved was visualized under the UV light. The band of interest was cut out with a scalpel and the DNA fragment was extracted using the gel extraction kit according to the manufacturer's protocol.

2.2.3.14.3 DNA subcloning

The plasmid DNA was digested with appropriate restriction enzymes in the following reaction mixture:

Reaction mixture components	
Vector/Insert DNA	2µl /4µl
Enzyme 1	5 units
Enzyme 2	5 units
Buffer	2µl
BSA (1mg/ml)	0.5µl
Deionised water	Top up to 20 µl

The reaction mix was incubated at 37°C for 2 hours and the digested DNA was resolved by agarose gel electrophoresis. The DNA fragments of interest were cut out and purified. A ligation reaction mixture as follows was then set up to ligate the purified insert and vector DNA.

Ligation Reaction mixture components	
Vector DNA	1µl
Insert DNA	3µl
Ligation Buffer	2µl
T4 ligase	0.5µl
Deionised water	Top up to 20 µl

The ligation reaction mixture was incubated at RT for 2 hours and transformed into competent *E. coli* cells (Methods 2.2.1.4). The recombinant plasmid DNA was then isolated from the *E. coli* cells (Methods 2.2.1.5).

2.2.3.14.4 Verification of recombinant plasmid DNA constructs

The recombinant plasmid DNA was verified by checking with restriction enzymes that cut at restriction enzyme sites that are unique to it. The digested DNA was then resolved by agarose gel electrophoresis. The bands obtained in the gel were checked to verify if they are of the correct sizes.

2.2.3.14.5 Polymerase chain reaction (PCR)

All PCR reactions were performed using the Peltier Thermal Cycle PTC-100. A 25 µl reaction using KAPA HiFi system was set up as follows:

- 5µl of 5x KAPAHiFi Reaction Buffer
- 0.75µl of dNTP mix
- 0.75µl of 5' primer (10 µM)

- 0.75µl of 3' primer (10 µM)
- 0.5µl of Template DNA
- 0.5µl of KAPAHiFi DNA Polymerase (1 U/µL)
- Deionised water (topped up to 25 µl)

The cycle conditions used were:

- Initial Denaturation: 95°C for 10 mins
- Denaturation: 98°C for 20 sec
- Annealing: 55 °C for 15 sec (25 cycles)
- Extension: 72°C for 30 sec per kb
- Final Extension: 72°C for 5 min

2.2.3.14.5.1 Reverse transcription of RNA to cDNA

1- 5µg of RNA was added with 1µl of DEPC-treated water and 1µl of Random primers.

The mixture was incubated at 70°C for 5 mins and incubated on ice immediately for 5 mins. A reaction mixture prepared as follows was added to the RNA and incubated at 37°C for 5 mins.

Reaction mixture:

- 6 µl of 5X reaction buffer
- 3µl of 0.1M DTT
- 0.5 µl of 25mM dNTPs
- 9 µl of DEPC-treated water

The tube was transferred to the ice and incubated for 5 mins. 0.5 µl of Reverse Transcriptase was added to the tube and it was incubated for 60 mins at 42°C. The Reverse Transcriptase was then heat inactivated at 70°C for 5 mins. The tube containing the cDNA was stored at 4°C.

2.2.3.14.5.2 Real-time PCR (RT-PCR)

Total RNA was isolated from the cells using the RNAeasy kit and reversed-transcribed to cDNA according to Methods 2.2.3.14.5.1. A 25 µl Real-time PCR reaction was set up as follows:

- 12.5µl of SYBR Green Master Mix
- 0.25µl of cDNA
- 12.25µl of diluted primers (Forward + Reverse, 50nm in 25µl)

Each reaction was performed in triplicates and the primers used are listed in Appendix 2.

The RT-PCR was performed on 7500 Real-Time PCR system (Applied Biosystems) using the comparative C_T method and the relative quantification of WASP expression was calculated using the formulae below:

$$C_{t_{\text{target gene}}} - C_{t_{\text{Endogenous control}}} = \Delta C_t$$

$$C_{t_{\text{target gene}}} - C_{t_{\text{Reference sample}}} = \Delta\Delta C_t$$

The standard deviation was calculated using the following formula: $S = \sqrt{(S_1^2 + S_2^2)}$

2.2.3.14.5.3 Site directed mutagenesis (SDM)

Mutations were introduced in the gene of interest using the SDM kit or using the Overlap Extension technique.

2.2.3.14.5.4 SDM kit

SDM was performed according to the manufacturer's protocol provided. A single colony was picked from the LB plate containing selective antibiotics and the mutant plasmid DNA was isolated and sequenced to ensure the mutation has been introduced into the clone.

2.2.3.14.5.5 Overlap extension PCR

In the overlap extension PCR, as illustrated in Figure 2.2, two halves of the gene of interest are first amplified separately with an outer flanking primer and a mutagenesis primer each (primers a and b, primers c and d). The two mutagenesis primers are complementary to each other. The PCR products from the two PCR reactions (AB and CD) are purified and mixed together to be used as template for the third PCR reaction. In the third PCR reaction, the two outer flanking primers (primers a and d) are used to amplify the final full length PCR product (AD). Finally, the end product obtained is the gene of interest bearing the desired mutation.

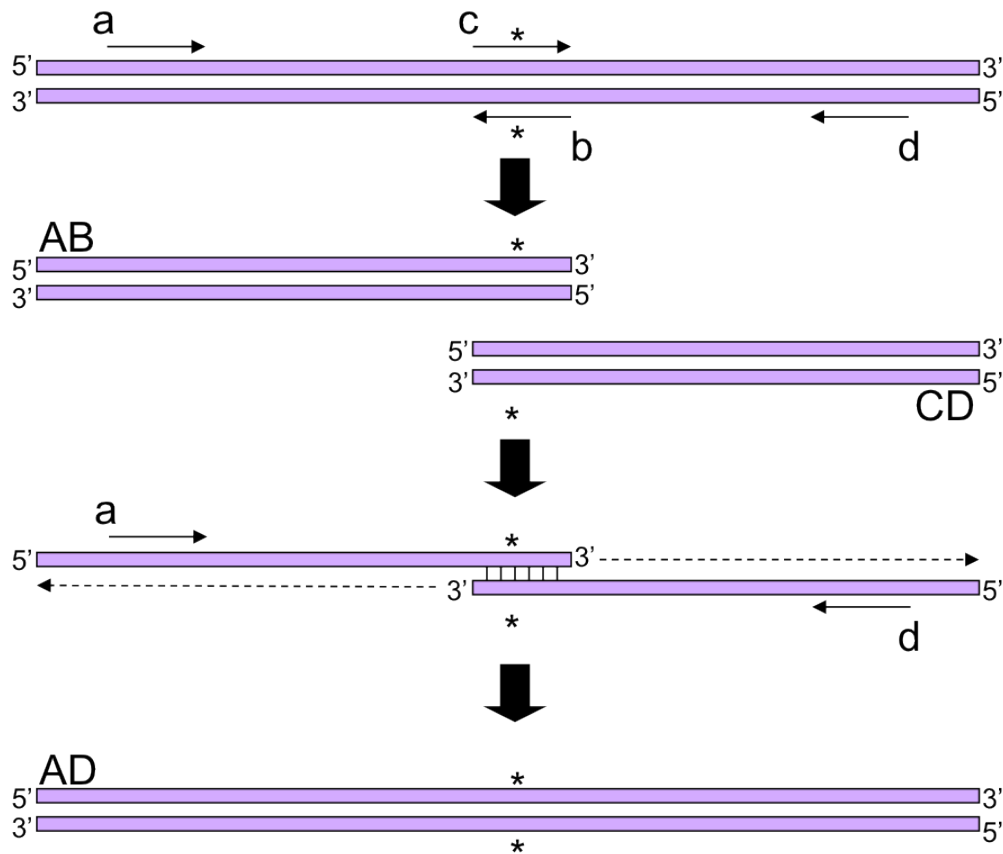


Figure 2.2 Schematic diagram of the overlap extension PCR.

b and c are the mutagenesis primers while a and d are flanking primers. AD is the final PCR product which contains the desired mutation.

2.2.3.15 DNA precipitation

For 20µl of DNA mix, 2.22 µl of NaOAc (1/10 of DNA mix) and 44.44 µl of 100% ethanol (2X of DNA and NaOAc mix) was added. The mixture was incubated at -20°C for 2 hours or more and spun down for 10 mins. The resulting pellet was washed with 70% ethanol and spun down for 10 mins. The pellet was air-dried and dissolved in appropriate amount of deionised water or 1X TE buffer according to the pellet size.

2.2.3.16 SDS-PAGE electrophoresis

A 10% SDS-PAGE gel was prepared as follows:

Resolving gel:

Components	ml
1.5 M Tris-HCl, pH 8.8	1.3
10% SDS	0.05
30% Acrylamide/Bis-acrylamide	1.7
10% ammonium persulfate (APS)	0.05
TEMED	0.002
H ₂ O	1.9

Stacking gel:

Components	ml
1.0 M Tris-HCl, pH 6.8	0.38
10% SDS	0.03
30% Acrylamide/Bis-acrylamide	0.5
10% ammonium persulfate (APS)	0.03
TEMED	0.003
H ₂ O	2.1

Proteins in samples were resolved by loading the appropriate amounts in the SDS-PAGE gel and the gel was run at 100V for 100mins, until the dye front has migrated past the end

of the gel. The gel was then further processed either for the staining of proteins or Western blot analysis.

2.2.3.17 Western blot analysis

Proteins resolved in the SDS-PAGE gel were transferred onto the nitrocellulose membrane using the semi-dry method. The nitrocellulose membrane and the gel were sandwiched between 6 filter papers, with 3 on each side and placed in a transfer cassette. The transfer cassette was submerged in the transfer buffer and transfer of the proteins was carried out at 90V for 90 mins. The membrane was then blocked for 30 mins at RT (Table 1). After blocking, the membrane was incubated on a roller with the appropriate primary (1°) antibody (Table 1) overnight at 4°C. The membrane was washed 3X with PBS-0.05% TritonX or 1X TBS (for detection of phospho-proteins) the next day and probed with the respective secondary (2°) antibody (Table 1) for 1 hr at RT. The membrane was subsequently washed 3X with PBS-0.05% TritonX or 1X TBS (for detection of phospho-proteins) and was detected with Millipore or Amersham detection kit according to manufacturer's protocol.

Blocking	1° Antibody	2° Antibody
3% milk in PBS	Anti-GFP in 3% milk (PBS) 1:10000 dilution	Anti-mouse IgG in 3% milk (PBS)
5% milk in PBS	Anti-GAPDH in 5% milk (PBS) 1:10000 dilution	Anti-mouse IgG in 5% milk (PBS)
3% milk in PBS	Anti-His in 3% milk (PBS) 1:1000 dilution	Anti-rabbit IgG in 3% milk (PBS)
5% milk in PBS	Anti-WASP in 5% milk (PBS) 1:1000 dilution	Anti-rabbit IgG in 5% milk (PBS)
5% BSA in TBS	4G10 in 5% BSA (TBS) 1:1000 dilution	Anti-mouse IgG in 5% BSA (TBS)

Table 2.8 A summary of the antibodies used in Western blot and the respective dilutions.

2.2.3.18 His-tag pull down assay

Mammalian cells transfected with appropriate DNA were lysed by adding 500 µl of lysis buffer (Materials 2.1.14.2) and incubating on ice for 1 hr. 200 µl beads were aliquoted into eppendorf tubes for each lysis sample. The Ni-NTA beads (Invitrogen, Carlsbad, CA, USA) were washed 3X with 1ml of deionised water at 100 g for 5mins. 500 µl of equilibration buffer (Materials 2.1.14.1) was then added to the beads and the tubes were rocked for 1hr at 4°C. The beads were further washed with 400 µl of equilibration buffer. Tubes containing the lysed cells were spun down at 6800 g for 5 mins to remove cells that were not lysed and the supernatant was transferred to a new tube. 30ul of the supernatant was aliquoted out as whole cell lysate. 500 µl of beads or equivalent amounts were added to the supernatant. The proteins were allowed to bind to the beads by rocking the tubes for 1hr at 4°C. The beads were spun down for 5mins at 100 g and the flow-through were stored in new tubes. Proteins were eluted from the beads with the elution buffers (Materials 2.1.14.3). 250ul of elution buffer containing 10mM imidazole was used for the first elution. The tubes were rocked at RT for 10 mins and spun down for 5 mins at 100 g. Eluted proteins in the supernatant were collected in new tubes. The elution was repeated with increasing concentrations of imidazole of elution buffer (25mM, 50mM, 100mM, 150mM, 250mM, 500mM, 1M). Elution buffer containing 50mM imidazole was determined to be the optimum concentration and was used for subsequent pull-down assays. Eluted proteins in the supernatant, flow-through and whole cell lysate were precipitated by adding an equal volume of 20% TCA (250ul) and incubated on ice for 10 mins. The tubes were spun down at 13,382 g for 10 mins to obtain a pellet. The pellets were washed in ice-cold acetone and spun at 13,382 g for 10 mins again. The

acetone was removed and the pellets were air-dried for 2 mins. The pellets were resuspended in 60 µl of 2X SDS-PAGE loading dye and 1M dTT (4µl in 100ul) and subsequently boiled at 100°C for 5 mins. The samples were stored at -20°C. 15µl of the samples were loaded in each lane of the SDS-PAGE gel and Western blot was performed the next day for analysis of the samples.

2.2.3.19 GST protein expression and purification

E. coli BL21 (DE3) cells were transformed with pGEX plasmids expressing proteins of interest. A single colony was picked and inoculated in 5 ml of LB broth supplemented with ampicillin (LB-amp) and grown (incubated with shaking) overnight at 37°C. The bacterial culture was diluted 1/100 (1ml in 100ml of LB-amp broth) and grown (incubated with shaking) to an OD₆₀₀ of 0.5 at 37°C. 1mM of IPTG was added to the culture and cells were induced by incubating with shaking at 30°C for 2-3 hours. The cells were spun down at a speed of 4470 g at RT for 20 minutes. After decanting the supernatant, the pellet was stored at -80°C (optional). 10 ml of PBS was (1/10 of original starting culture volume) added to the pellet and resuspended. The cells were sonicated (pulse on for 2s, pulse off for 2s and repeated 200-300 times) and aliquoted into eppendorf tubes. The cells were spun down at 13,328 g for 15 mins at 4°C. At the meantime, 500µl of Glutathione-sepharose beads (Sigma, USA) were aliquoted into eppendorf tubes for each sample and were washed 1X with 1ml of PBS and spun at 833 g for 5 mins. The supernatant from the cells were transferred to the beads and tubes were rolled at 4°C for 2 hours for binding of protein to the beads. The beads and supernatant were transferred to a column and the eluent was collected at stored at - 20°C. The column

was washed twice with PBS and proteins were eluted with 500 µl of reduced glutathione. A second elution was performed by adding 250 µl of reduced glutathione to the column again. 5 µl of eluent were aliquoted out and 100 µl of Bradford assay solution (5X dilution) was added to check for the presence of proteins. A last elution was performed to remove all the proteins bound on the beads by adding 250µl of reduced glutathione to the column. The column with the beads were washed 2X with 1X PBS and stored at 4°C. The protein concentration was measured using the Bradford assay and 2X loading dye was added to the sample. The proteins were then resolved by SDS-PAGE gel followed coomassie staining to check for the expression.

2.2.3.20 Coomassie Staining

After gel electrophoresis, the SDS-PAGE gel was soaked in 50 mL of the gel staining solution (Materials 2.1.12.3.2) for 30 mins with agitation. The solution was removed and the gel was washed with deionised water and soaked in 50 ml of gel destaining solution (Materials 2.1.12.3.1) for 2-3 hours. The gel was stored in 4°C in the destaining solution.

3. Results

3.1 Conformational analysis of WASP and its mutants using split YFP

3.1.1 Introduction

WASP has been suggested to adopt two different conformations; an autoinhibited and an open conformation, when interacting with different proteins. In the autoinhibited conformation, the VCA domain of WASP interacts with the BR and GBD domains and this autoinhibition can be relieved by the binding of GTP-loaded Cdc42 to the GBD (Kim et al., 2000). The conformation of WASP is crucial for its function. Thus, analyzing the conformation of WASP in the presence of different regulators or mutations occurring in WAS patients, will lead to elucidation of the mechanisms regulating WASP and the molecular defects giving rise to the disease.

The FRET assay has been utilized by many groups to study protein-protein interactions. In this assay, the two proteins of interest are tagged with different fluorophores in which one is a donor and the other an acceptor (Figure 3.1), where the fluorescence emission spectrum of the donor fluorophore overlaps with the absorption spectrum of the acceptor fluorophore (Kenworthy, 2001). The yellow fluorescent protein (YFP) (acceptor) and cyan fluorescent protein (CFP) (donor) are typically used for FRET. When the two proteins are not in close proximity, the emission from the donor is detected by excitation with appropriate wavelength. However, when the proteins are in close proximity (1-10nm), the emission from the acceptor is detected after donor excitation because of the result of FRET from the donor to acceptor fluorophore due to their close proximity. By

quantification of the quenching of donor fluorescence, protein-protein interactions can be detected (Kenworthy, 2001).

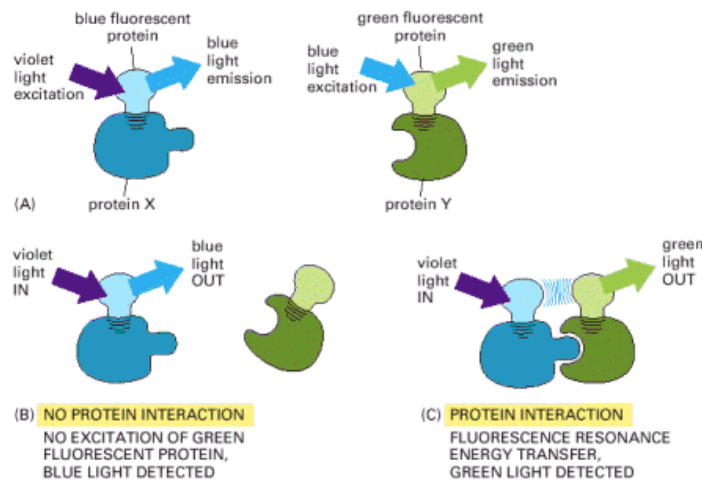


Figure 3.1 Schematic illustration of the FRET assay. Adapted from (Bruce Alberts, 2002).

Proteins tagged with fluorophores emit fluorescence upon excitation.

(A) When there is no protein interaction, donor emission is detected upon donor excitation. No emission is detected from acceptor fluorophores.

(B) When there is protein interaction, FRET occurs which results in acceptor fluorescence detection upon donor excitation.

However, FRET suffers from several drawbacks like spectral bleed-through, photobleaching and low background to noise ratio. New methods have since been developed which do not have the shortcomings of FRET assays. Hu and coworkers (Hu et al., 2002) have developed the Bi-molecular Fluorescence Complementation (BiFC) assay where fragments of fluorescent molecules are fused to separate proteins. Upon interactions of these proteins, the fluorescence would be reconstituted. Jeong and coworkers (Jeong et al., 2006) utilized the same method in which conformation of maltose binding protein was studied in vitro using the fluorescence complementation assay. Upon maltose binding, reconstitution of split green fluorescent protein (GFP) halves on each side of the protein occurs due to changes in conformation, resulting in

fluorescence (Jeong et al., 2006). YFP and CFP were each fused to the N-terminus and C-terminus of N-WASP respectively and FRET efficiency was examined to analyze conformational changes (Ward et al., 2004).

3.1.2 Bi-molecular Fluorescence Complementation (BiFC)

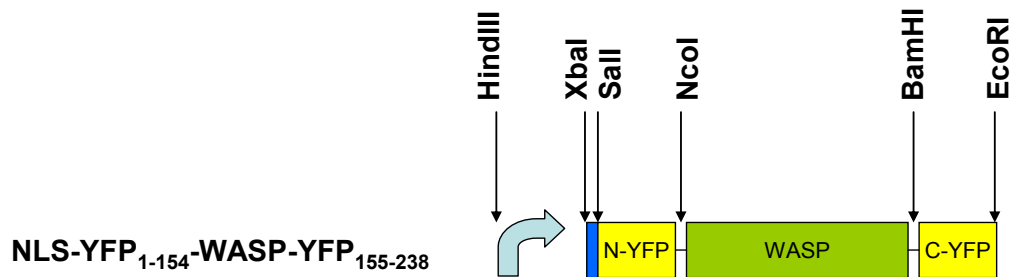
In order to study the changes in conformation of WASP, the Bi-molecular Fluorescence Complementation (BiFC) method was adopted. The YFP molecule is split into two halves and fused to the two termini of WASP, forming the WASP reporter. When WASP is in its closed conformation, YFP fluorescence is expected due to close proximity of the two YFP fragments, but upon activation, YFP fluorescence will be lost. Analysis of YFP fluorescence produced by the WASP reporter will allow us to determine the conformation of WASP.

WASP has been shown to be unstable in the cytoplasm in the absence of WIP (Rajmohan et al., 2006). Thus, in order to protect WASP from cytoplasmic proteases, WASP was targeted to the nucleus of *S. cerevisiae* by fusing a nuclear localization signal to the N-terminal of the WASP reporter (Figure 3.2A).

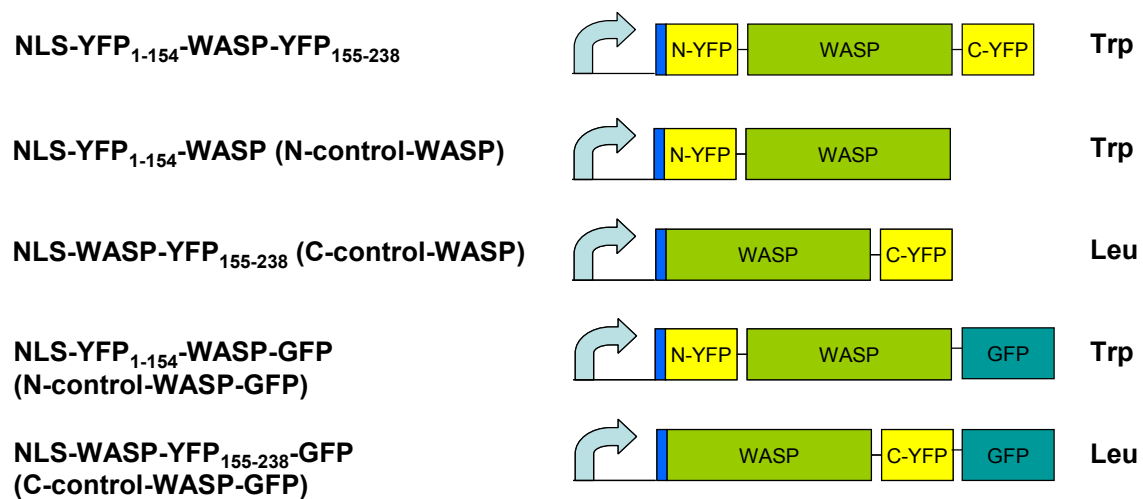
cDNA encoding the N-terminal fragment of YFP (YFP₁₋₁₅₄) and C-terminal fragment of YFP (YFP₁₅₅₋₂₃₈) was amplified using appropriate primers (Appendix 2). YFP₁₋₁₅₄ (*SalI/NcoI*) was fused to the N-terminus of WASP while YFP₁₅₅₋₂₃₈ (*BamHI/EcoRI*) was fused to the C-terminus of WASP. The nuclear localization signal (NLS) (*XbaI/SalI*) was

cloned upstream of YFP₁₋₁₅₄, under the control of Vrp1 promoter, forming the WASP reporter construct (Figure 3.2A).


A



B



Key

 : Vrp1 Promoter


 : Nuclear localization signal (NLS)

Figure 3.2 Schematic diagram showing fusion constructs used.

Constructs were cloned with NLS fused to the N-terminus, under the control of Vrp1 promoter. The fusion constructs were expressed either in YEplac112 (Trp) or YEplac181(Leu) plasmids.

WASP reporter in YEplac112 (Trp) plasmid was first transformed into *S. cerevisiae* cells that were grown to exponential phase. The transformants were selected on SD plates lacking tryptophan and grown to exponential phase in selective media at 24°C. These cells were subsequently analyzed using fluorescence microscopy.

YFP fluorescence was observed in the nuclei of the cells expressing the WASP reporter (Figure 3.3A), suggesting that the two halves of YFP were in close proximity. This could be due to either intermolecular or intramolecular interaction (Figure 3.3B). In order to clarify whether the fluorescence is due to intermolecular or intramolecular complementation, two additional constructs were made, namely N-control-WASP and C-control-WASP. N-control-WASP (YFP₁₋₁₅₄-WASP (Trp)) was cloned by fusing the N-terminal half of YFP to WASP while C-control-WASP (WASP-YFP₁₅₅₋₂₃₈ (Leu)) was made by fusing the C-terminal half of YFP to WASP. Both constructs were transformed into *S. cerevisiae* cells and selected on SD plate lacking tryptophan and leucine. The transformants were grown to exponential phase and analyzed using fluorescence microscopy. Fluorescence was not observed in the cells expressing both N-control-WASP and C-control-WASP (Figure 3.3A). However, this observation may be because N-control-WASP and C-control-WASP were not targeted to the nucleus.

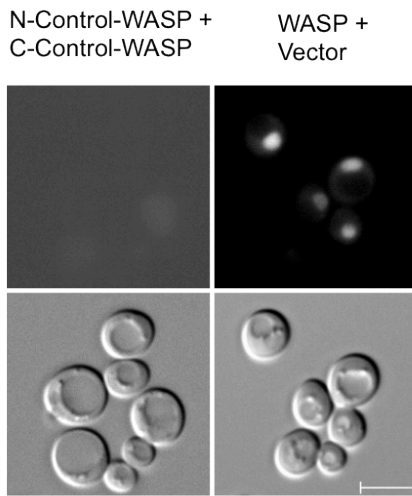
In order to verify that both N-control-WASP and C-control-WASP are localized to the nucleus, two constructs N-control-WASP-GFP (YFP₁₋₁₅₄-WASP-GFP (Trp)) and C-control-WASP-GFP (WASP-YFP₁₅₅₋₂₃₈-GFP (Trp)) were constructed. The plasmid constructs were transformed separately into *S. cerevisiae* cells and fluorescence was

analyzed. Both constructs were successfully targeted into the nucleus as shown in Figure 3.3C. This shows that both the N-control-WASP and C-control-WASP were in the nucleus. Western blot analysis showed the expression of both the proteins, N-control-WASP and C-control-WASP (Figure 3.3D). Thus, the lack of YFP fluorescence in the *S. cerevisiae* cells expressing N-control-WASP and C-control-WASP led to the conclusion that the YFP fluorescence observed in the *S. cerevisiae* cells expressing the WASP reporter (Figure 3.3A) is due to intramolecular complementation.

An explanation that inter-molecular YFP fluorescence was not observed is that when the two fragments of YFP were on different WASPs, either the orientation of the fragments was not correct or the two YFP fragments are not in close proximity, resulting in failure of complementation and fluorescence emission. Complementation of the two fragments of YFP only occurred when fused to the two ends of the same protein.

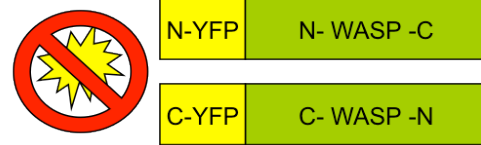
Together, the observations indicate that the sensor molecule is in an autoinhibited and closed conformation.

A

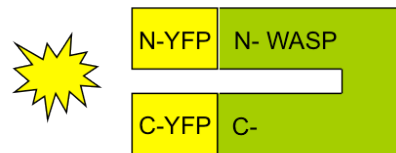


B

Intermolecular interaction



Intramolecular interaction



D

C

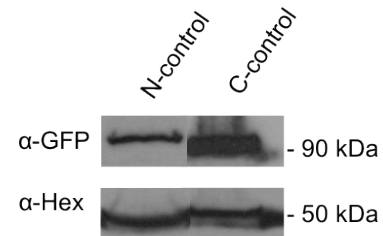
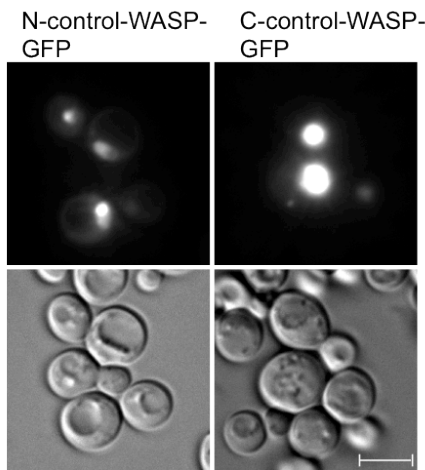


Figure 3.3 Bi-molecular fluorescence complementation observed in *S. cerevisiae* cells.

(A) *S. cerevisiae* cells were transformed with either YFP₁₋₁₅₄-WASP (Trp) together with (1) WASP-YFP₁₅₅₋₂₃₈ (Leu) or (2) YFP₁₋₁₅₄-WASP-YFP₁₅₅₋₂₃₈ (Trp) together with empty Leu plasmid and selected on SD (-Trp-Leu) plates. The transformants were grown to exponential phase at 24°C in selective media. YFP signals in these cells were subsequently analyzed using fluorescence microscopy. Bar = 5µm

(B) Schematic diagram explaining two possible models of YFP reconstitution. Fluorescence can occur through the complementation of the two fragments of YFP either from intermolecular or intramolecular interactions.

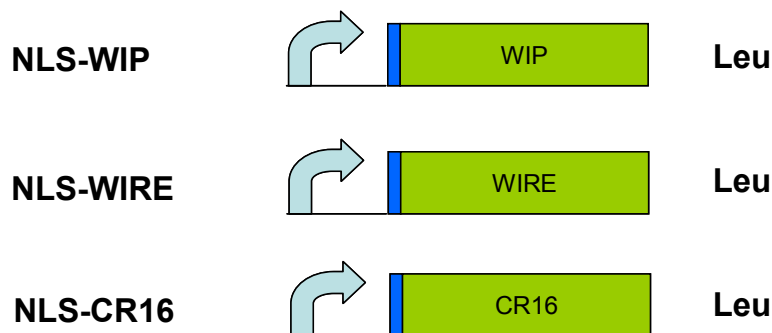
(C) *S. cerevisiae* cells were transformed with (1) YFP₁₋₁₅₄-WASP-GFP (Trp) or (2) WASP-YFP₁₅₅₋₂₃₈-GFP (Trp) and selected on SD (-Trp-Leu) plates. The transformants were grown to exponential phase at 24°C in selective media. GFP signals in these cells were subsequently analyzed using fluorescence microscopy. Bar = 5µm

(D) Western blot analysis of expression of WASP reporter in *S. cerevisiae* cells transformed with (1) YFP₁₋₁₅₄-WASP-GFP (Trp) or (2) WASP-YFP₁₅₅₋₂₃₈-GFP using anti-GFP (α-GFP) and anti-Hexokinase (α-Hex) as a loading control.

3.1.3 WIP and WIRE enhance YFP fluorescence from the WASP reporter

The verprolin family members (WIP, WIRE, CR16) have been shown to be involved in regulating the actin cytoskeleton and their effects are mainly mediated through the WASP family of proteins (Aspenstrom, 2005). Our laboratory has previously found that that human WASP is able to suppress the growth defects of *S. cerevisiae las17Δ* strain only in the presence of WIP, and WIP is able to mediate the cortical localization of WASP and stabilize WASP in these cells (Rajmohan et al., 2006).

In order to examine if the verprolin members are able to alter the conformation of WASP, WASP reporter (Trp) was transformed together with Leu plasmids expressing either NLS-WIP, NLS-WIRE or NLS-CR16 in *S. cerevisiae* cells (Figure 3.4).



Key



: Vrp1 Promoter



: Nuclear localization signal (NLS)

Figure 3.4 Schematic diagram showing fusion constructs used.

Constructs were cloned with NLS fused to the N-terminus, under the control of Vrp1 promoter. The fusion constructs were expressed in YEplac181 (Leu) plasmids.

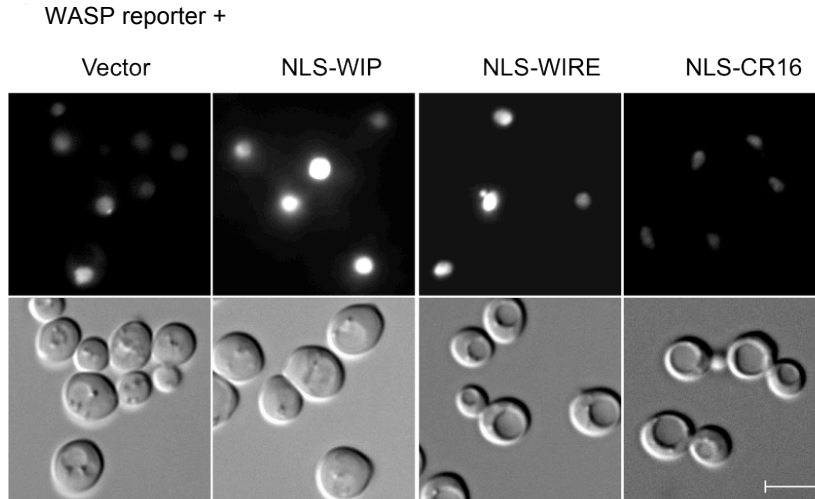
The cells were then selected on SD plates lacking Trp and Leu and transformants were grown to exponential phase. The cells were subsequently analyzed using fluorescence microscopy (Figure 3.5A). The fluorescence signals from 100 cells were quantified and plotted (Figure 3.5B). The YFP fluorescence from the WASP reporter was enhanced in the presence of either WIP or WIRE, while in the presence of CR16, the fluorescence from the WASP reporter did not change significantly (Figure 3.5A and B). Western blot analysis showed that cells transformed with all three verprolin proteins and the empty vector had equal expression of WASP reporter (Figure 3.5C), suggesting that the increase in fluorescence from WASP reporter + WIP or WASP reporter + WIRE was not due to increase in stability of the WASP reporter.

The lack of fluorescence signal enhancement from the WASP reporter in the presence of CR16 may be due to the lack of expression of CR16 or differential localization of the WASP reporter and CR16. CR16 may not have been targeted to the nucleus unlike WASP. Thus, in order to confirm that WIP, WIRE and CR16 are exerting their effects on WASP in the nucleus, three additional constructs were made in which the Leu plasmids expressing either NLS-WIP, NLS-WIRE or NLS-CR16 were fused with GFP at the C-terminus (Figure 3.6).

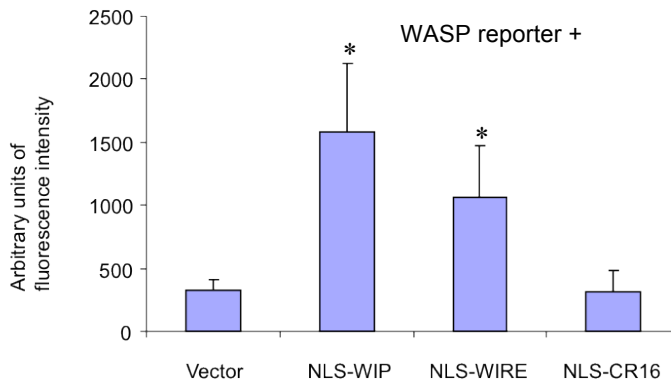
Cells expressing NLS-WIP-GFP, NLS-WIRE-GFP and NLS-CR16-GFP were analyzed using fluorescence microscopy. Fluorescence signal detected in the nucleus of these transformants showed that all three constructs were localized to the nucleus as well (Figure 3.7). Western blot analysis indicates that all the verprolins (WIP, WIRE, CR16)

were expressed in the cells. The interaction of WASP and the verprolins has been previously verified by yeast two hybrid assay in our laboratory (data not shown).

A



B



C

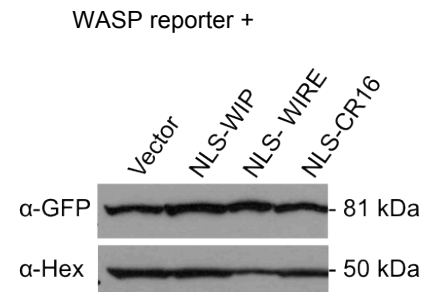
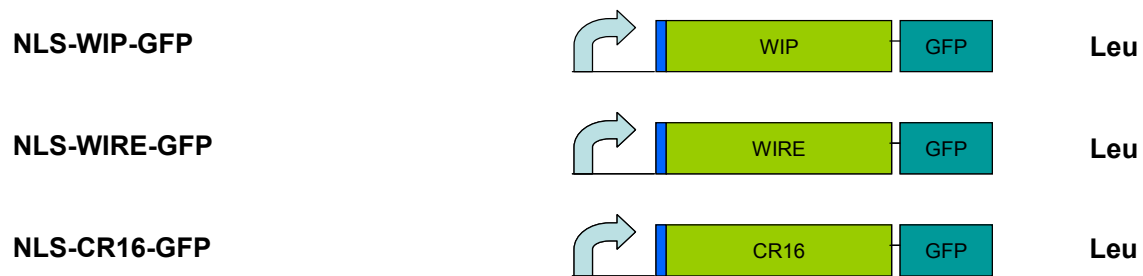


Figure 3.5 WIP and WIRE enhance fluorescence signals from the WASP reporter.

(A) *S. cerevisiae* cells were transformed with WASP reporter (Trp) together with (1) empty Leu plasmid, or Leu plasmids expressing (2) NLS-WIP, (3) NLS-WIRE or (4) NLS-CR16 and selected on SD (-Trp-Leu) plates. The transformants were grown to exponential phase at 24°C in selective media and YFP signals in these cells were subsequently analyzed using fluorescence microscopy. Bar = 5µm

(B) Fluorescence signal quantification from 100 *S. cerevisiae* cells expressing WASP reporter (Trp) together with (1) empty Leu plasmid, (2) NLS-WIP, (3) NLS-WIRE or (4) NLS-CR16 using metamorph software. *P<0.001 compared with WASP reporter + vector cells (unpaired student's t-test).

(C) Western blot analysis of expression of WASP reporter in *S. cerevisiae* cells transformed with WASP reporter (Trp) together with (1) empty Leu plasmid (2) NLS-WIP, (3) NLS-WIRE or (4) NLS-CR16 using anti-GFP (α-GFP) and anti-Hexokinase (α-Hex) as a loading control.



Key



 : Vrp1 Promoter
 : Nuclear localization signal (NLS)

Figure 3.6 Schematic diagram showing fusion constructs used

Constructs were cloned with NLS fused to the N-terminus, under the control of Vrp1 promoter. The fusion constructs were expressed in YEplac181 (Leu) plasmids.

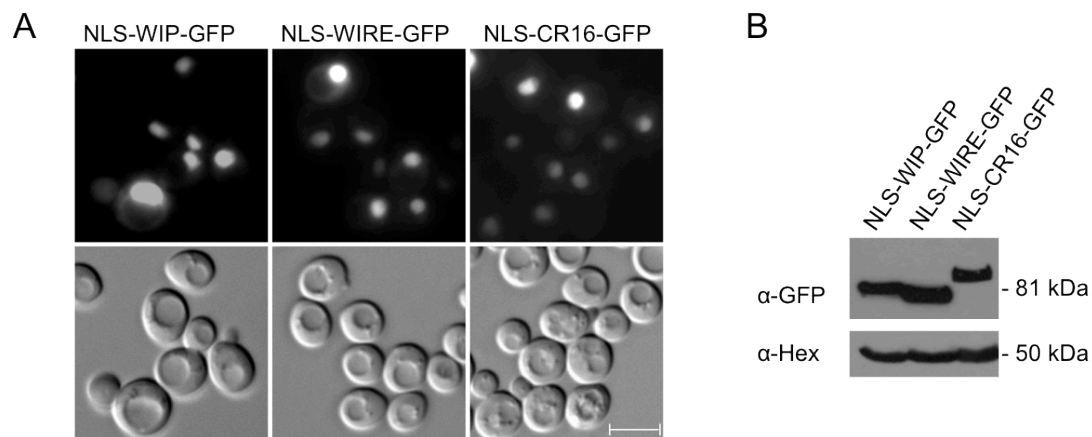


Figure 3.7 NLS-WIP, NLS-WIRE and NLS-CR16 are localized in the nuclei of *S. cerevisiae* cells

(A) *S. cerevisiae* cells were transformed with Leu plasmids expressing (1) NLS-WIP-GFP, (2) NLS-WIRE-GFP or (3) NLS-CR16-GFP and selected on SD (-Leu) plates. The transformants were grown to exponential phase at 24°C in selective media and YFP signals in these cells were subsequently analyzed using fluorescence microscopy. Bar = 5µm

(B) Western blot analysis of expression of (1) NLS-WIP-GFP, (2) NLS-WIRE-GFP or (3) NLS-CR16-GFP using anti-GFP (α -GFP) and anti-Hexokinase (α -Hex) as a loading control.

These results suggest that WIP and WIRE stabilize WASP in the autoinhibited conformation while CR16 has little or no effect on the conformation of WASP. This correlates with the observation that either WIP or WIRE can suppress the growth defect of *las17Δ* strain when expressed together with WASP, while CR16 expression together with WASP does not suppress the growth defect of *las17Δ* strain (Rajmohan et al. unpublished data). Although the expression level was higher for NLS-WIRE-GFP than NLS-WIP-GFP in Figure 3.7, the fluorescence levels detected from WASP reporter that was transfected with NLS-WIRE was lower than the WASP reporter transfected with NLS-WIP (Figure 3.5). This indicates that WIP exerts a greater effect on WASP, stabilizing WASP in the closed conformation, in comparison to WIRE.

3.1.4 Toca1 and Nck1 reduce YFP fluorescence from the WASP reporter

Other than the verprolin family of proteins, WASP interacts with many other cytoplasmic partners such as Cdc42, Toca1 and Nck1 that regulate its activity (Insall and Machesky, 2004; Kim et al., 2000; Rivero-Lezcano et al., 1995). Activated Cdc42 is known to be one of the interactors that is able to activate WASP by binding to its GBD domain (Kim et al., 2000). However, Toca1 has been found to bind to both Cdc42 and N-WASP and may act as an intermediate in the signaling pathway that links Cdc42 GTPase to the WASP family of proteins (Ho et al., 2004).

Thus, in order to examine the effect of Cdc42, Toca1 and Nck1 on WASP, WASP reporter (Trp) was transformed together with Leu plasmids expressing either Toca1,

Nck1 or Cdc42^{G12V}Δcaax in *S. cerevisiae* cells. G12V mutation was introduced in Cdc42 to render it constitutively active and the caax motif was deleted so that it does not associate with membranes in the cells. All constructs were again fused with NLS to target them to the nucleus (Figure 3.8).

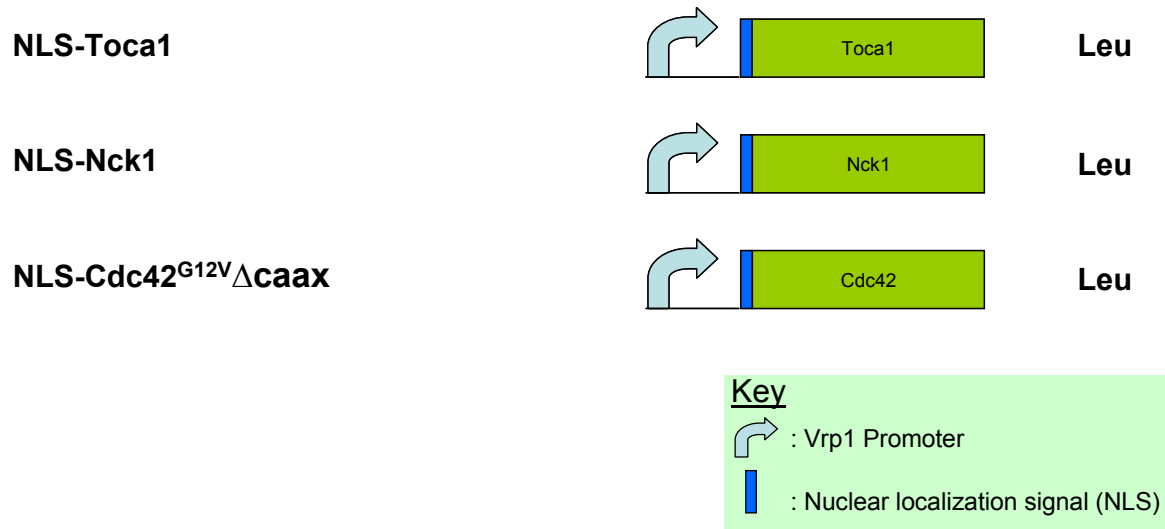


Figure 3.8 Schematic diagram showing fusion constructs used.

Constructs were cloned with NLS fused to the N-terminus, under the control of Vrp1 promoter. The fusion constructs were expressed in YEplac181 (Leu) plasmids.

After transformation, the cells were selected on SD plates lacking Trp and Leu and the transformants were grown to exponential phase. The fluorescence signals from the transformed cells were then examined using the fluorescence microscopy and the fluorescence intensities from 100 cells were quantified. From the analysis of fluorescence signal from the WASP reporter, it can be observed that both Toca1 and Nck1 reduced the fluorescence signal from the WASP reporter while Cdc42^{G12V}Δcaax did not affect the fluorescence signal from the WASP reporter (Figure 3.9A and B). Western blot analysis showed that cells transformed with all three proteins and the empty vector had equal expression of WASP reporter (Figure 3.9C). Thus, the reduction of YFP observed from

WASP reporter + Nck or WASP reporter + Toca1 is not due to reduced expression of the WASP reporter.

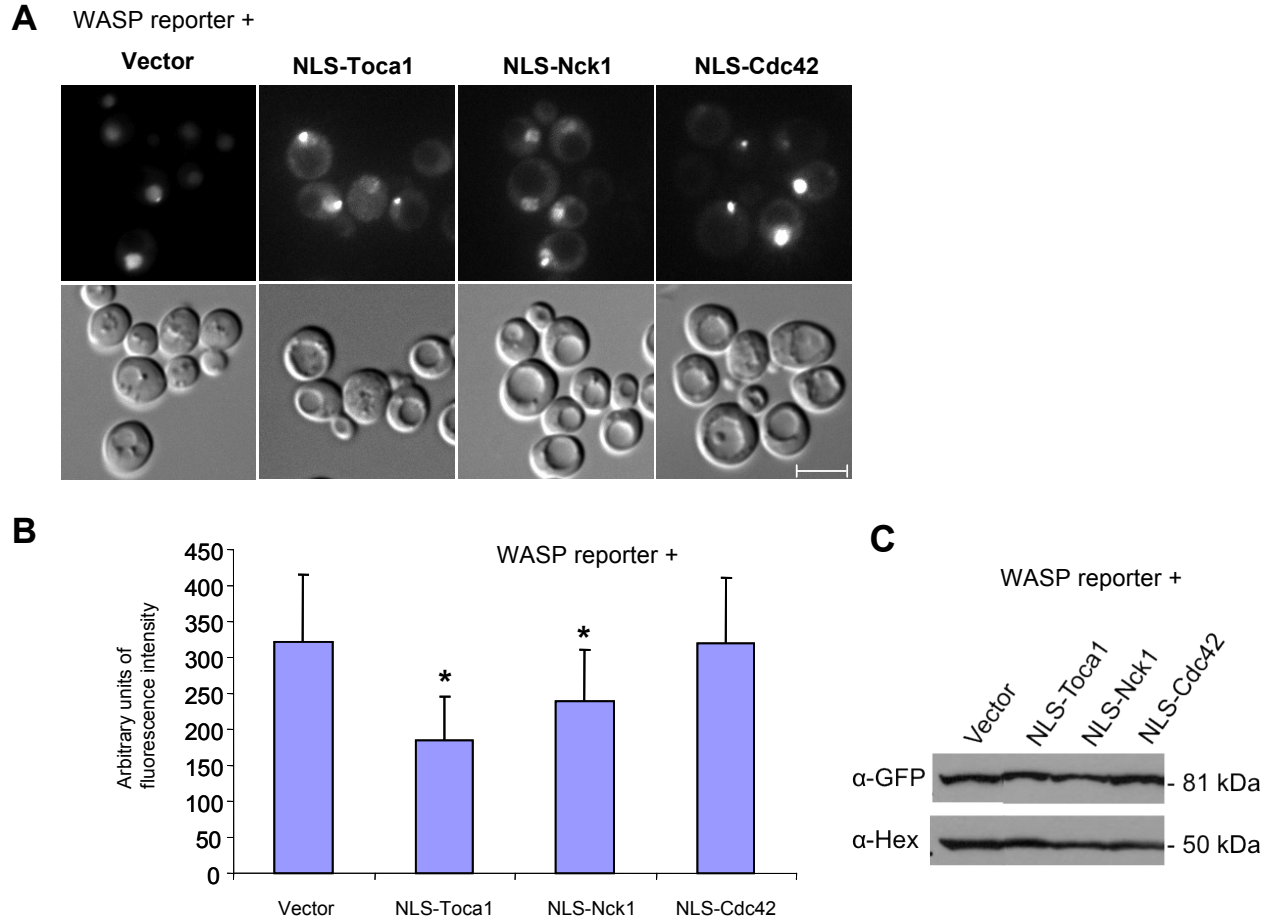


Figure 3.9 Toca1 or Nck1 reduced fluorescence signals from WASP reporter.

(A) *S. cerevisiae* cells were transformed with WASP reporter (Trp) together with (1) empty Leu plasmid, or Leu plasmids expressing (2) NLS-Toca1, (3) NLS-Nck1 or (4) NLS-Cdc42^{G12V}Δcaax and selected on SD (-Trp-Leu) plates. The transformants were grown to exponential phase at 24°C in selective media and YFP signals in these cells were subsequently analyzed using fluorescence microscopy. Bar = 5μm

(B) Fluorescence signal quantification from 100 *S. cerevisiae* cells expressing WASP reporter (Trp) together with (1) empty Leu plasmid, (2) NLS-Toca1, (3) NLS-Nck1 or (4) NLS-Cdc42^{G12V}Δcaax using metamorph software. *P<0.001 compared with WASP reporter + vector cells (unpaired student's t-test).

(C) Western blot analysis of expression of WASP reporter in *S. cerevisiae* cells transformed with WASP reporter (Trp) together with (1) empty Leu plasmid, or Leu plasmids expressing (2) NLS-Toca1, (3) NLS-Nck1 or (4) NLS-Cdc42^{G12V}Δcaax using anti-GFP (α-GFP) and anti-Hexokinase (α-Hex) as a loading control.

In order to verify that Toca1, Nck1 and Cdc42 were localized to the nuclei of the cells, GFP was tagged to the C-terminus of NLS-Toca1, NLS-Nck1 and NLS-Cdc42^{G12V}Δcaax (Figure 3.10) and were transformed into *S. cerevisiae* cells. Fluorescence signal was

detected in the nuclei of the transformants indicating that all three proteins, Toca1, Nck1 and Cdc42 were localized in the nucleus. Western blot analysis shows that all three proteins were expressed, indicating that the lack of any effect on the WASP reporter by Cdc42 is not due to lack of expression of Cdc42 (Figure 3.11).

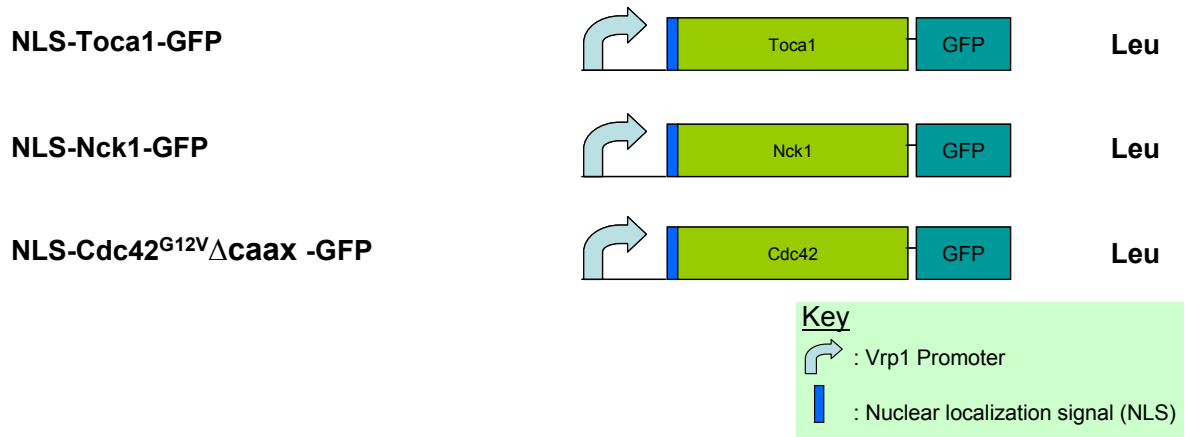


Figure 3.10 Schematic diagram showing fusion constructs used.

Constructs were cloned with NLS fused to the N-terminus, under the control of Vrp1 promoter. The fusion constructs were expressed in YEplac181 (Leu) plasmids.

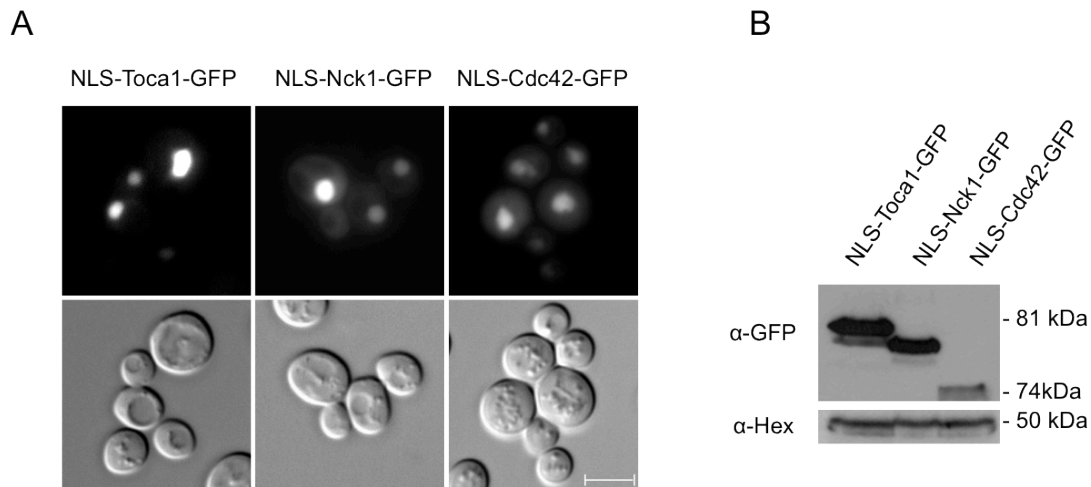


Figure 3.11 Toca1, Nck1 and Cdc42 are localized in the nuclei of *S. cerevisiae* cells.

(A) *S. cerevisiae* cells were transformed with (1) NLS-Toca1-GFP, (2) NLS-Nck1-GFP or (3) NLS-Cdc42^{G12V}Δcaax -GFP in Trp plasmids and selected on SD (-Trp-Leu) plates. The transformants were grown to exponential phase at 24°C in selective media and YFP signals in these cells were subsequently analyzed using fluorescence microscopy. Bar = 5μm

(B) Western blot analysis of expression of WASP reporter in *S. cerevisiae* cells transformed with (1) NLS-Toca1-GFP, (2) NLS-Nck1-GFP or (3) NLS-Cdc42^{G12V}Δcaax -GFP using anti-GFP (α-GFP) and anti-Hexokinase (α-Hex) as a loading control.

3.1.5 Toca1 and Nck1 reduce YFP fluorescence even in the presence of WIP

In extracts and resting cells, WASP/N-WASP is mainly found to be in complex with WIP (de la Fuente et al., 2007; Ho et al., 2004), adopting an autoinhibited conformation. Cdc42-GTP is thought to bind and induce conformational change in WASP (Sasahara et al., 2002). In order to investigate whether Toca1, Nck1 and Cdc42 can effectively change the conformation of WASP even when it is in complex with WIP, WASP reporter (Trp) was transformed together with WIP (Leu). The transformants were then co-transformed with Ura plasmids expressing either Toca1, Nck1 or Cdc42^{G12V}Δcaax in *S. cerevisiae* cells. The cells were then selected on SD plates deficient in Tryptophan, Leucine and Uracil and the transformants were grown to exponential phase at 24°C for analysis.

These cells were subsequently analyzed using fluorescence microscopy. Consistent with the results shown in Results 3.1.3, Toca1 and Nck reduced the fluorescence signal from the WASP reporter while Cdc42^{G12V}Δcaax had no effect (Figure 3.12A and B). This reduction in signal is not due to decreased expression of the WASP reporter as shown in the western blot analysis (Figure 3.12C). This result indicated that both Toca1 and Nck1 can disrupt the autoinhibitory loop of WASP and changing its conformation even in the presence of WIP while Cdc42 did not cause significant change in the conformation of WASP as analyzed using the BiFC method.

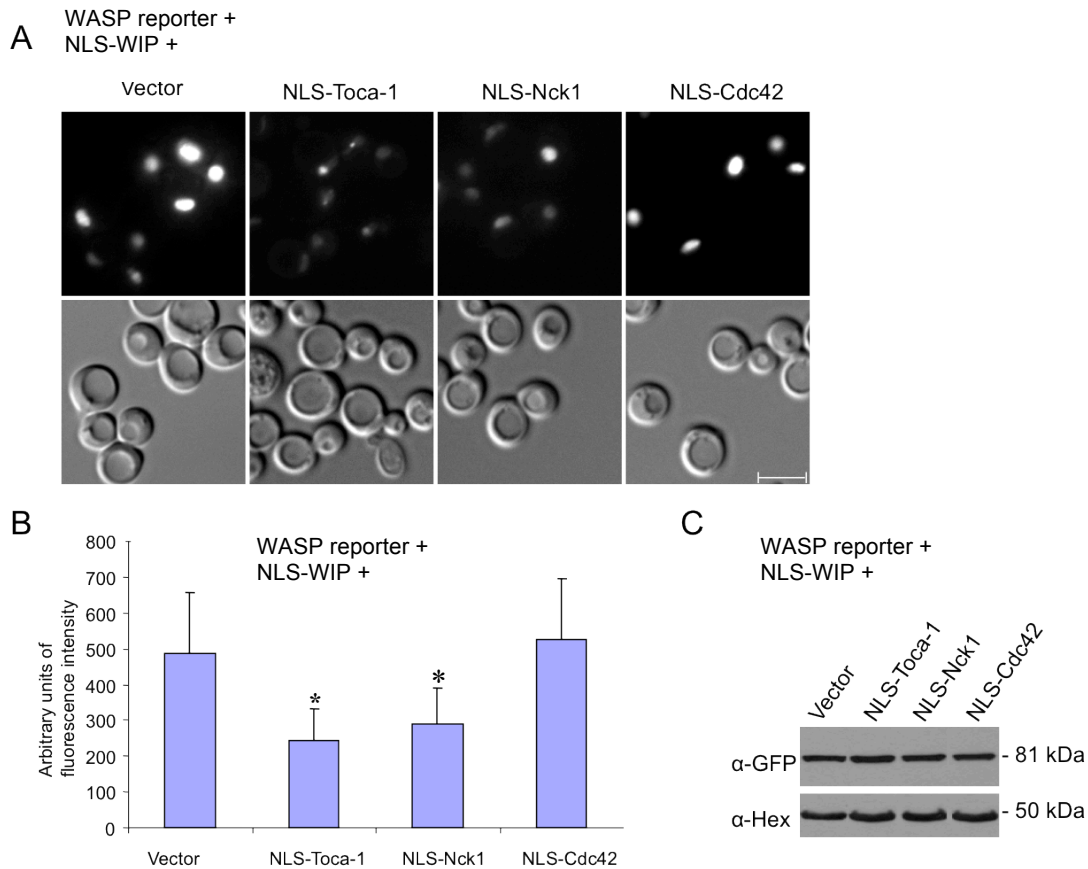


Figure 3.12 Toca1 or Nck1 reduced fluorescence signals from WASP reporter even in the presence of WIP.

(A) *S. cerevisiae* cells were transformed with WASP reporter (Trp) + NLS-WIP (Leu) together with (1) empty Ura plasmid, or Ura plasmids expressing (2) NLS-Toca1, (3) NLS-Nck1 or (4) NLS-Cdc42^{G12V}Δcaax and selected on SD (-Trp-Leu-Ura) plates. The transformants were grown to exponential phase at 24°C in selective media and YFP signals in these cells were subsequently analyzed using fluorescence microscopy. Bar= 5μm.

(B) Fluorescence signal quantification from 100 *S. cerevisiae* cells expressing WASP reporter (Trp) + NLS-WIP (Leu) together with (1) empty Ura plasmid, (2) NLS-Toca1, (3) NLS-Nck1 or (4) NLS-Cdc42^{G12V}Δcaax using metamorph software. *P<0.001 compared with WASP reporter + NLS-WIP+ vector cells (unpaired student's t-test).

(C) Western blot analysis of expression of the WASP reporter in *S. cerevisiae* cells transformed WASP reporter (Trp) together with (1) empty Leu plasmid, or Leu plasmids expressing (2) NLS-Toca1, (3) NLS-Nck1 or (4) NLS-Cdc42^{G12V}Δcaax using anti-GFP (α-GFP) and anti-Hexokinase (α-Hex) as a loading control.

3.1.6 Fluorescence from WASP reporter with mutations in WH1, GBD or VCA domain is not enhanced in the presence of WIP

It is known that missense mutations of the WASP gene can cause different degrees of severity of the Wiskott Aldrich Syndrome (Imai et al., 2003a), with the classic WAS as the most severe form while X-linked thrombocytopenia (XLT) and X-linked severe congenital neutropenia (XLN) are the milder forms (Devriendt et al., 2001; Villa et al., 1995). Thus, examining the effects of mutations in the different domains on the conformation of WASP would aid in elucidating the pathology of WAS.

One representative mutation from each domain was selected based on mutations identified in WAS/XLT/XLN patients and the residues were mutated using site directed mutagenesis (Imai et al., 2003a). In total, five mutations were selected, namely A134T (WH1 domain), G187C (BR region), L270P (GBD domain), P373S (PRR region) and D485N (CH domain) (Figure 3.13). Additionally, the VCA domain was also deleted from the WASP gene to analyze the effect on the conformation as the VCA domain is crucial for the formation of the autoinhibited conformation. These mutant WASP constructs were analyzed using the BiFC method where the two halves of YFP were fused to the N terminus and C-terminus of the WASP mutants. NLS was also fused to the N-terminus to these constructs to target them to the nucleus.

WASP

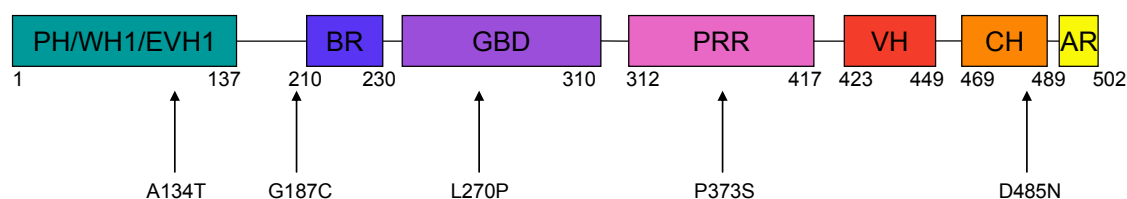


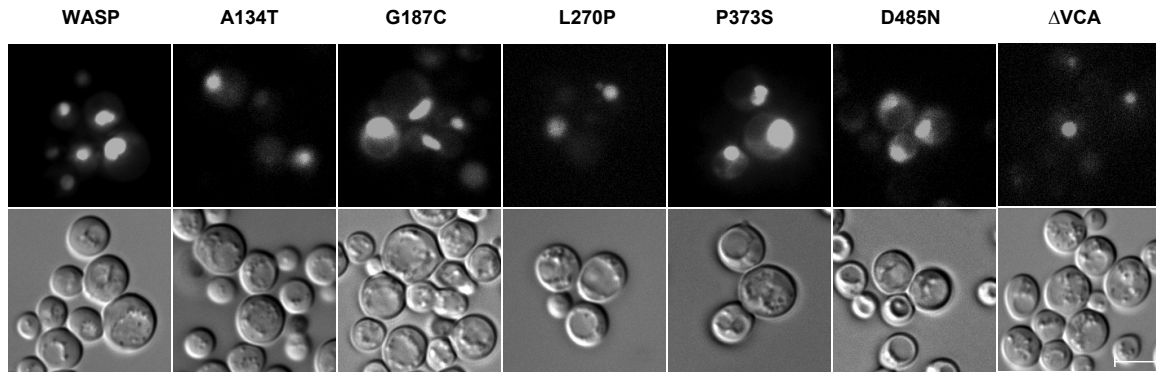
Figure 3.13 Diagram showing the mutations generated in the WASP gene.

The five mutant WASP reporters (A134T, G187C, L270P, P373S, D485N and Δ VCA) were each transformed separately together with empty Leu plasmids in *S. cerevisiae* cells. Fluorescence microscopy analysis of the transformants revealed that all the mutant WASP reporters and the VCA domain deleted WASP reporter did not have significantly reduced fluorescence signal (Figure 3.14A and B) when compared to WASP reporter. This may be due to the fact that the fluorescence signal of WASP reporter was low and any further reduction in signal was not significant.

Trp plasmids expressing the WASP mutants, WASP^{A134T}, WASP^{G187C}, WASP^{L270P}, WASP^{P373S}, WASP^{D485N} and WASP ^{Δ VCA} were transformed together with WIP (Leu) in *S. cerevisiae* cells to analyze how the mutations affect WASP in the natural state, in the presence of WIP. Fluorescence microscopy analysis of the cells revealed that fluorescence from the WASP reporter with mutations in the WH1, GBD, or CH domain is not enhanced even in the presence of WIP (Figure 3.15). This result suggests that mutations in these domains alter the conformation of WASP, disrupting its auto-

inhibitory conformation causing it to adopt an open conformation even in the presence of WIP.

A



B

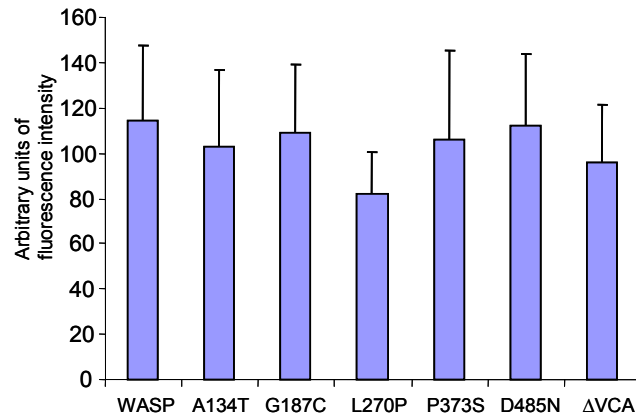


Figure 3.14 The selected mutations did not affect the conformation of WASP.

(A) *S. cerevisiae* cells were transformed with empty Leu plasmid together with (1) WASP reporter (Trp), (2) WASP^{A134T} sensor (Trp), (3) WASP^{G187C} sensor (Trp), (4) WASP^{L270P} sensor (Trp), (5) WASP^{P373S} sensor (Trp), (6) WASP^{D485N} sensor (Trp) or (7) WASP^{ΔVCA} sensor (Trp) and selected on SD (-Trp-Leu) plates. The transformants were grown to exponential phase at 24°C in selective media and YFP signals in these cells were subsequently analyzed using fluorescence microscopy. Bar=5μm

(B) Fluorescence signal quantification from 100 *S. cerevisiae* cells expressing 1) WASP reporter (Trp), (2) WASP^{A134T} sensor (Trp), (3) WASP^{G187C} sensor (Trp), (4) WASP^{L270P} sensor (Trp), (5) WASP^{P373S} sensor (Trp), (6) WASP^{D485N} sensor (Trp) or (7) WASP^{ΔVCA} sensor using metamorph software.

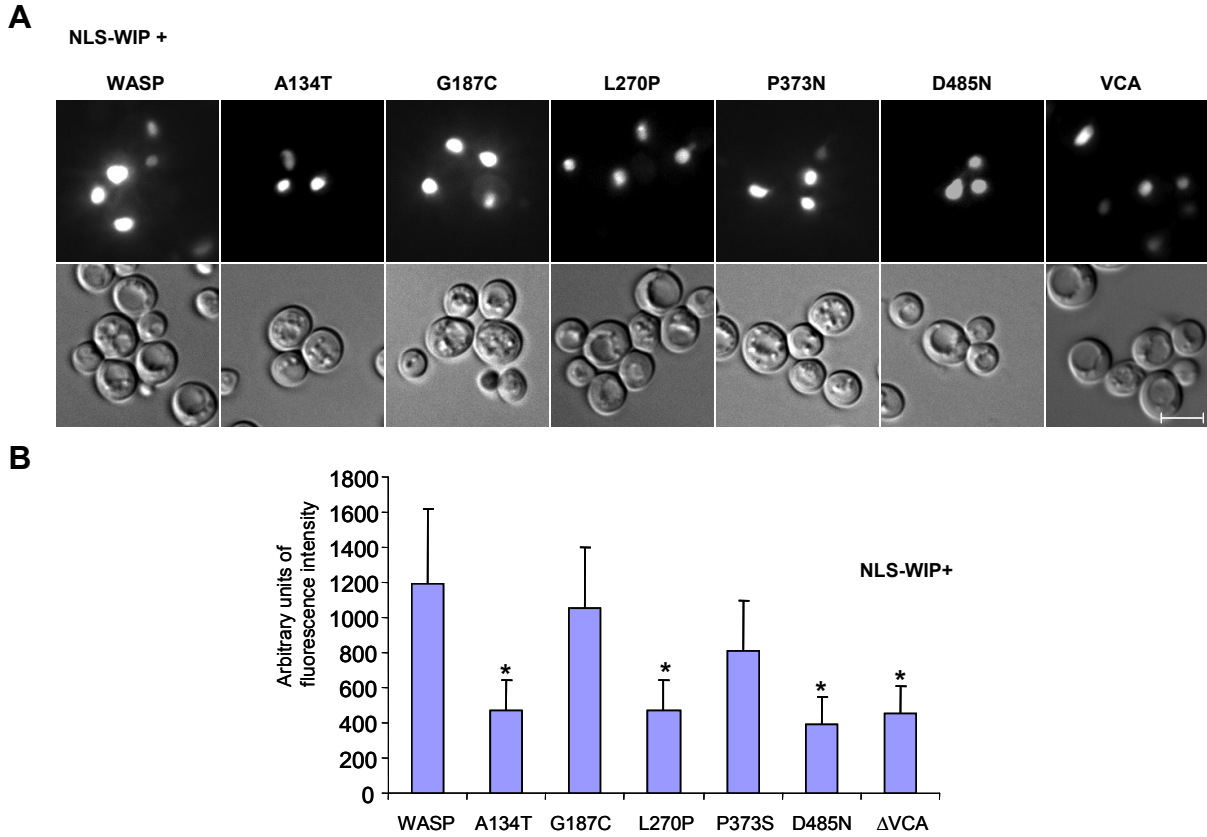


Figure 3.15 Co-expression of WIP did not enhance fluorescence signals from WASP^{A134T}, WASP^{L270P}, WASP^{D485N} or WASP^{ΔVCA}.

(A) *S. cerevisiae* cells were transformed with NLS-WIP (Leu) together with (1) WASP reporter (Trp), (2) WASP^{A134T} sensor (Trp), (3) WASP^{G187C} sensor (Trp), (4) WASP^{L270P} sensor (Trp), (5) WASP^{P373S} sensor (Trp), (6) WASP^{D485N} sensor (Trp) or (7) WASP^{ΔVCA} sensor and selected on SD (-Trp-Leu) plates. The transformants were grown to exponential phase at 24°C in selective media and YFP signals in these cells were subsequently analyzed using fluorescence microscopy. Bar = 5μm

(B) Fluorescence signal quantification from 100 *S. cerevisiae* cells expressing WIP (Leu) together with (1) WASP reporter (Trp), (2) WASP^{A134T} sensor (Trp), (3) WASP^{G187C} sensor (Trp), (4) WASP^{L270P} sensor (Trp), (5) WASP^{P373S} sensor (Trp), (6) WASP^{D485N} sensor (Trp) or (7) WASP^{ΔVCA} sensor using metamorph software. *P<0.001 compared with WASP reporter + NLS-WIP + vector cells (unpaired student's t-test).

3.1.7 WIP and WIRE enhance YFP fluorescence from the WASP reporter in mammalian cells

WIP and WIRE has been shown to enhance YFP fluorescence from the WASP reporter in *S. cerevisiae* cells, in results section 3.1.2. However, many of the regulators of WASP that are present in the mammalian cells are absent in the *S. cerevisiae* cells. Thus, to determine if similar observations of the regulation of conformation of WASP can be obtained in mammalian cells, the verprolins were expressed in HEK 293T cells together with the WASP reporter.

WASP reporter in pFIV vector was transfected in HEK 293T cells, together with WIP, WIRE or CR16 in pFIV vectors (Figure 3.16). After 36 hours, fluorescence of the cells was quantified with flow cytometry, using the FITC filter. The fluorescence signal of 10000 cells was analysed. Each experiment was performed thrice and the average signal obtained for each set was plotted.

From the results, WIP and WIRE increased the YFP fluorescence signal from the WASP reporter (Figure 3.17B) while CR16 did not cause a significant increase in the fluorescence signal. Western blot analysis (Figure 3.17C) showed that the expression level of WIRE is lower than WIP or CR16 in HEK 293T cells but was still able to induce a significant increase in the fluorescence levels of WASP reporter. The results show that WIP and WIRE stabilizes the close conformation of WASP while CR16 has minimal effect on the conformation of WASP. This finding is similar to the results obtained in *S. cerevisiae* cells (Figure 3.17) which indicates that the observations made on the

conformational changes in WASP, in the presence of the verprolins, in *S. cerevisiae* cells are relevant to the mammalian cells.

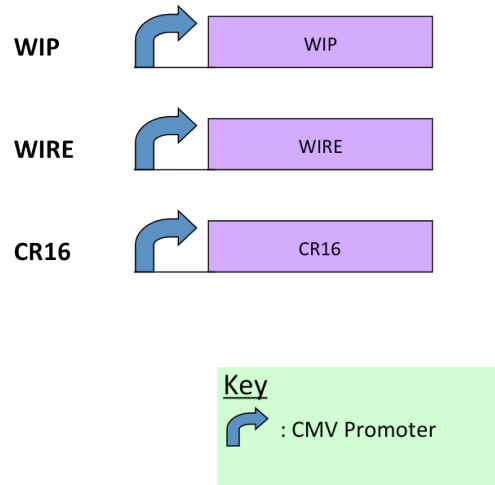


Figure 3.16 Schematic diagram showing fusion constructs used.

Constructs were cloned with the Verprolins under the control of CMV promoter. The fusion constructs were expressed in pFIV plasmids.

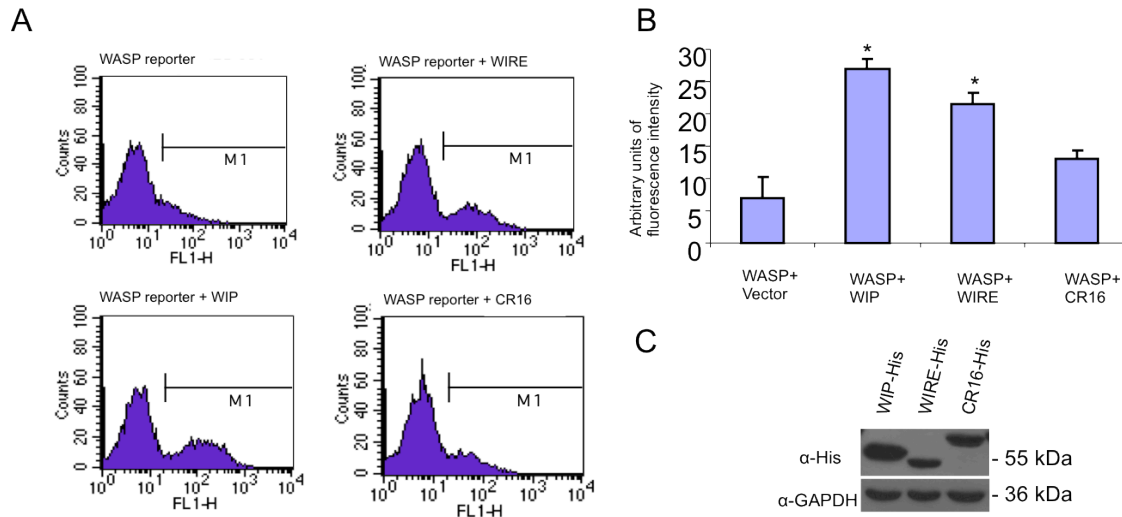


Figure 3.17 WIP and WIRE enhanced fluorescence signals from WASP reporter in HEK 293T cells.

(A) HEK 293T cells were transfected with WASP reporter together with (1) empty pFIV vector, or pFIV vector expressing (2) WIP, (3) WIRE or (4) CR16. 36 hours after transfection, YFP signals in these cells were analysed using flow cytometry.

(B) Fluorescence signal quantification from 10000 HEK 293T cells expressing YFP₁₋₁₅₄-WASP-YFP₁₅₅₋₂₃₈ (Trp) together with (1) empty pFIV vector, (2) WIP, (3) WIRE or (4) CR16. *P<0.001 compared with WASP reporter + vector cells.

(C) Western blot analysis of expression of (1) WIP-His, (2) WIRE-His or (3) CR16-His when transfected together with WASP reporter in HEK 293T cells using anti-His (α -His) and anti-GAPDH (α -GAPDH) as a loading control.

3.1.8 N-terminus of WIP is in close proximity to the C-terminus of WASP

Recent studies have shown that WASP and WIP function together and play important roles both in actin polymerization and IL-2 transcription (Dong et al., 2007). Interestingly, the BiFC assay in this project revealed that WASP is in a closed conformation in the presence of WIP (Results 3.1.2). We propose that the closed conformation of WASP is also functional and the interaction of WIP with WASP is crucial in the activity of WASP. The WBD domain of WIP is known to interact with the WH1 domain of WASP (Chou et al., 2006). However, since WASP has one less V domain in comparison to N-WASP, the extra V domain in WIP may compensate for it.

The BiFC assay was first used to study if the N-terminus of WIP is in close proximity with the C-terminus of WASP. YFP₁₋₁₅₄ was fused to the N-terminus of WIP (YFP₁₋₁₅₄-WIP) while YFP₁₅₅₋₂₃₈ was fused to the C-terminus of WASP (WASP-YFP₁₅₅₋₂₃₈) and transformed or transfected in either *S. cerevisiae* cells or HEK 293T cells respectively. However, low fluorescence levels were observed in both cell types. This observation could be because the two fragments of YFP were not oriented in the correct position for fluorescence complementation to take place, even if the two fragments are in close proximity. Hence, acceptor photobleaching FRET was used to examine the interaction between WIP and WASP.

In acceptor photobleaching FRET, the acceptor is first photobleached and the donor emission is measured. If the proteins are in close proximity, the donor emission would

increase (Kenworthy, 2001). Thus, analysis of the change in the intensity of the donor fluorescence would relate to the efficiency of energy transfer from the donor to the acceptor molecule.

In order to examine if the N-terminus of WIP is in close proximity with the C-terminus of WASP, FRET acceptor photobleaching was performed. YFP was fused to the N-terminus of WIP (YFP-WIP) while CFP was fused to the C-terminus of WASP (WASP-CFP) (Figure 3.20B). The two constructs were transfected into Cos7 cells and the YFP and CFP emission were analysed using confocal microscopy by acceptor photobleaching FRET after 36 hours (Figure 3.18). A control set was performed in parallel, in which YFP-WIP and CFP were transfected in Cos7 cells and analysed by FRET in a confocal microscope (Figure 3.19).

The analysis of the CFP emission from 60 cells after performing acceptor photobleaching FRET showed that there was a significant increase in the percentage of CFP emission in cells transfected with YFP-WIP and WASP-CFP in comparison to control cells transfected with YFP-WIP and CFP (Figure 3.20A). This showed that the hypothesis of N-terminus of WIP being in close proximity of C-terminus of WASP is correct (Figure 3.19B).

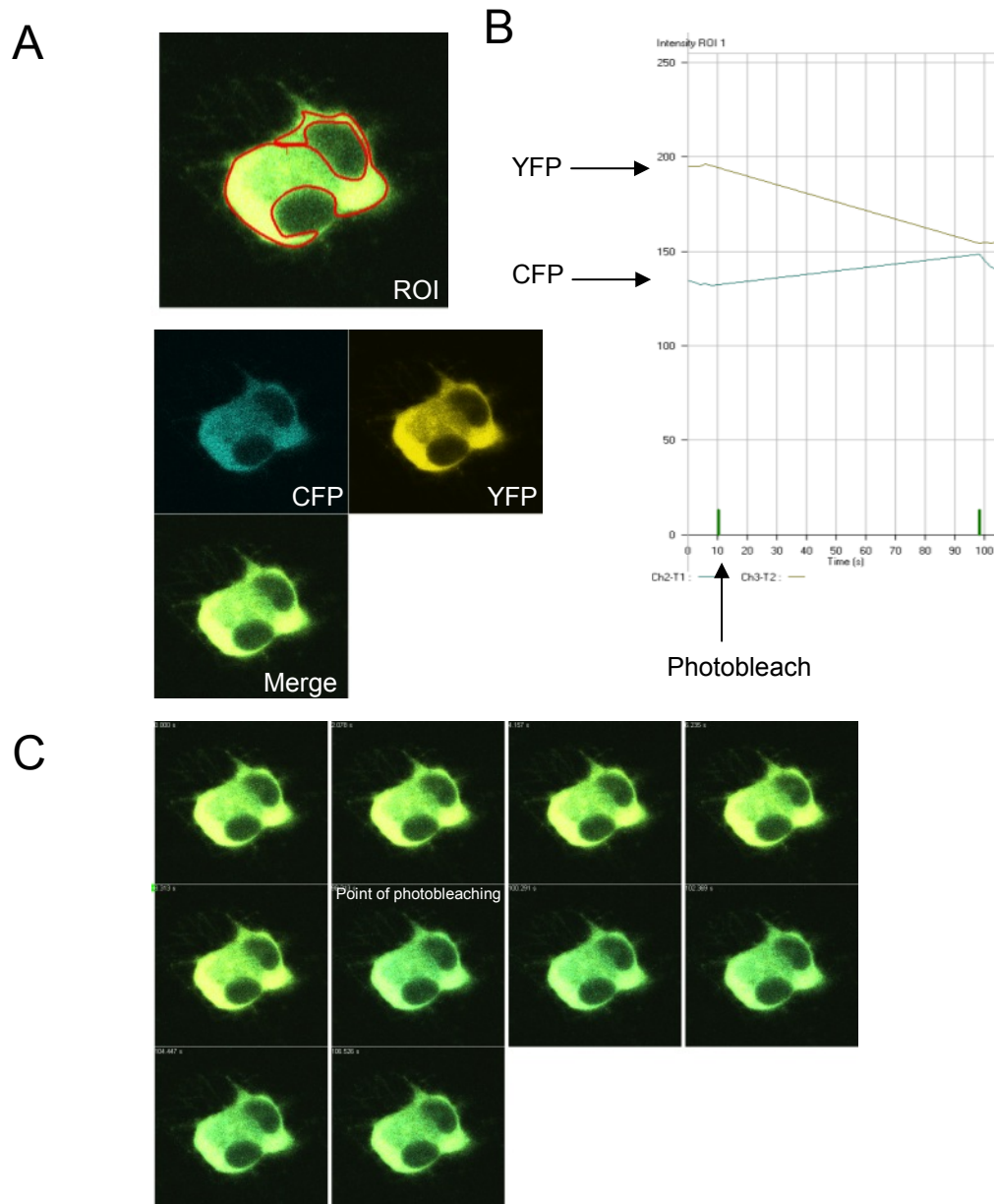


Figure 3.18 N-terminus of WIP interacts with C-terminus of WASP to produce increased emission of CFP after photobleaching of YFP.

(A) Cos7 cells were transfected with YFP-WIP and WASP-CFP. After 36 hrs, cells on the coverslips were mounted on microscope slides and were analysed using confocal microscopy by acceptor photobleaching FRET. A region of interest (ROI) was selected on the cell and the acceptor protein YFP was photobleached using the 514-nm laser line.

(B) The intensity of YFP and CFP emission in the ROI was analysed. The arrow indicates the point of photobleaching.

(C) A series of images of the cell was taken. The sixth frame shows the point of photobleaching.

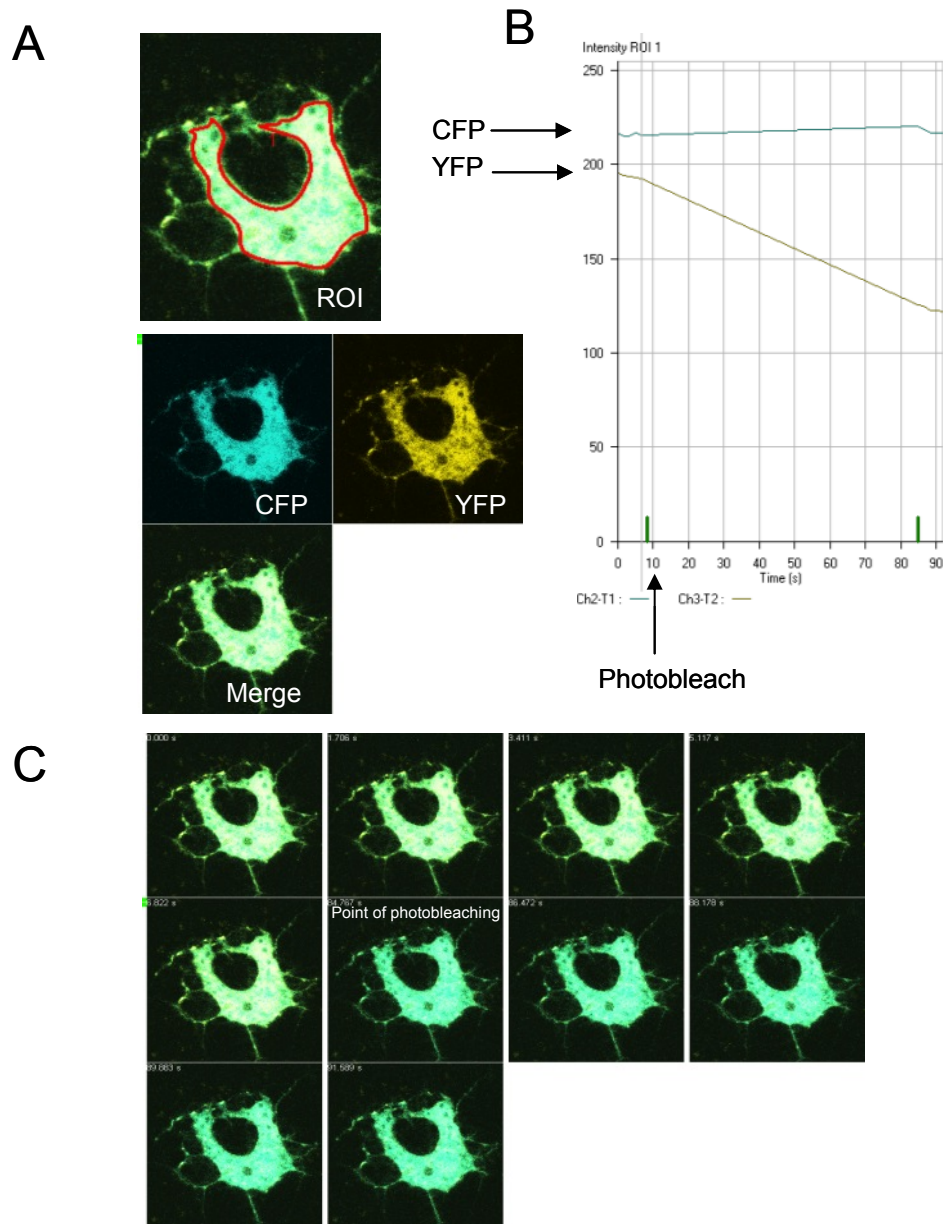


Figure 3.19 Co-expression of YFP-WIP and CFP did not produce increased emission of CFP after photobleaching of YFP.

(A) Cos7 cells were transfected with YFP-WIP and CFP. After 36 hrs, cells on the coverslips were mounted on microscope slides and were analysed using confocal microscopy by acceptor photobleaching FRET. A region of interest (ROI) was selected on the cell and the acceptor protein YFP was photobleached using the 514-nm laser line.

(B) The intensity of YFP and CFP emission in the ROI was analysed. The arrow indicates the point of photobleaching.

(C) A series of images of the cell was taken. The sixth frame shows the point of photobleaching.

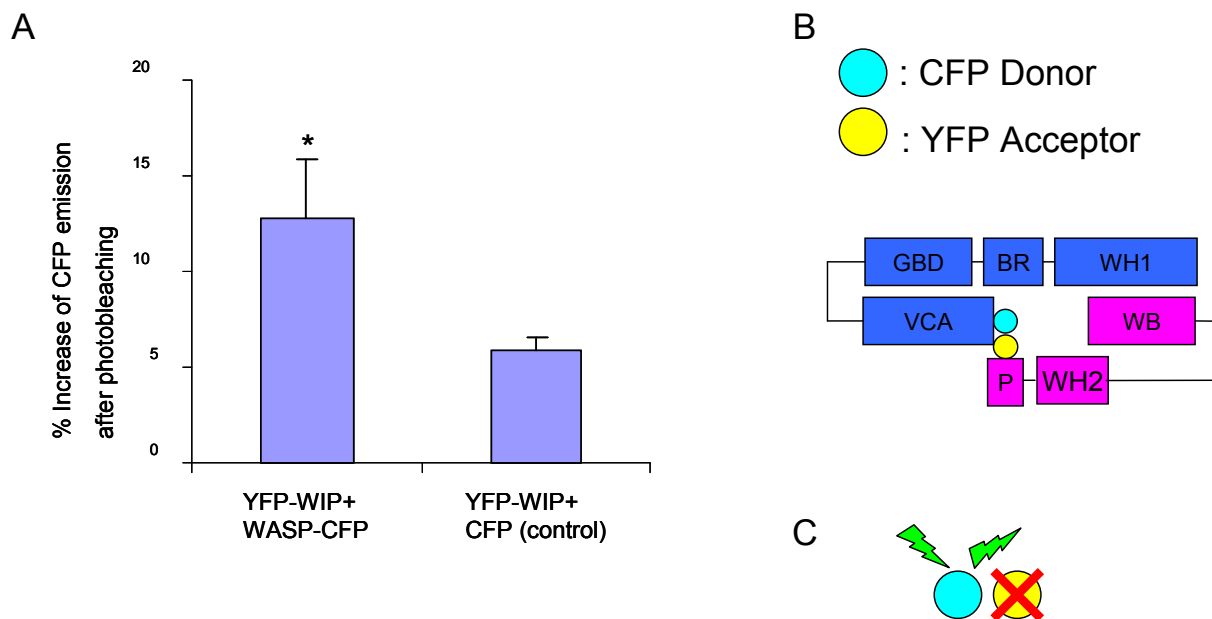


Figure 3.20 N-terminus of WIP interacts with C-terminus of WASP to produce increased emission of CFP after photobleaching of YFP.

(A) Cos7 cells were transfected with YFP-WIP and (1) WASP-CFP or (2) CFP. After 36 hrs, cells on the coverslips were mounted on microscope slides and were analysed using confocal microscopy by acceptor photobleaching FRET. The percentage increase in CFP emission after YFP photobleaching in 20 cells was tabulated by calculating the difference in intensity of the fluorescence before and after photobleaching $[(I_{\text{postbleach}} - I_{\text{prebleach}})/I_{\text{postbleach}} \times 100\%]$. The experiment was repeated thrice (n=3). *P<0.001 when compared to control cells.

(B) Schematic diagram illustrating the hypothesized conformation of WIP-WASP. WASP (blue) was fused with CFP (cyan) at the C-terminus while WIP (pink) was fused with YFP (yellow) at the N-terminus.

(C) Schematic diagram illustrating acceptor photobleaching FRET. When YFP (yellow) is close to CFP (cyan), after acceptor YFP photobleaching, the emission of CFP would increase as YFP can no longer undergo excitation.

Results 3.2

3.2 Molecular characterisation of WASP^{L270P} mutation related XLN

3.2.1 Introduction

WASP is predominantly in the autoinhibited, closed conformation in resting cells. The first activator of WASP that was identified is the Rho-GTPase Cdc42 (Aspenstrom et al., 1996). Recent studies suggest that Cdc42, acting cooperatively with Toca1, binds the GBD domain of WASP and (Ho et al., 2004) disrupts the interaction of the VCA domain and GBD domain in WASP, thereby converting to an open conformation. Importantly, the GBD domain of WASP hosts an important residue, Y291. The role of the phosphorylation of this tyrosine residue has been scrutinized in detail by many groups (Badour et al., 2004a; Blundell et al., 2009; Cory et al., 2002b). It is a major phosphorylation site in WASP as mutation of residue Y291 abolishes tyrosine phosphorylation of WASP (Cory et al., 2002b).

Many kinases such as the Src family kinases and Tec family kinases have been reported to phosphorylate WASP at residue Y291 (Baba et al., 1999; Badour et al., 2004a; Bunnell et al., 1996; Cory et al., 2002b). The phosphomimetic mutant Y291E displayed increased ability to enhance actin polymerization and filopodia formation in macrophages when compared to WASP or the non-phosphorylatable mutant Y291F (Cory et al., 2002b). These findings suggest the importance of phosphorylation in WASP activity.

The mutation L270P in WASP causes XLN and it has been suggested that this mutation causes WASP to be in a constitutively active conformation (Devriendt et al., 2001).

Because of the proximity of the residue L270 with the tyrosine residue Y291, we hypothesize that the mutation L270P can affect the phosphorylation at Y291. Also, the mutation L270P could mimic the effect of Cdc42 binding to WASP, which activates WASP. By coupling L270P mutation with Y291E or Y291F, a better understanding of the role of phosphorylation in the regulation of WASP and the molecular basis of XLN could be attained.

3.2.2 WASP^{L270P} adopts an open conformation

The three mutations, identified in XLN patients, L270P, S272P and I294T are all located within the GBD domain of WASP (Ancliff et al., 2006; Beel et al., 2009; Devriendt et al., 2001). These mutations disrupt the closed conformation of WASP through the disruption of the autoinhibitory loop. These constitutively active WASP mutants have been reported to have increased actin polymerizing activity (Ancliff et al., 2006; Beel et al., 2009; Devriendt et al., 2001).

In this study, the mutation L270P was selected as the representative mutation which causes XLN. First, the reported open conformation of L270P was verified in *S. cerevisiae* cells using the BiFC assay. The WASP reporter (Trp) and WASP^{L270P} sensor (Trp) constructs were each transformed separately together with NLS-WIP (Leu) plasmids in *S. cerevisiae* cells. Fluorescence microscopy analysis of the transformants revealed that the mutant WASP^{L270P} sensor had significantly reduced fluorescence signal (Figure 3.21A and B) when compared to WASP reporter. This confirms the postulation made by other

groups that reported that L270P mutation causes WASP to adopt an open conformation (Devriendt et al., 2001).

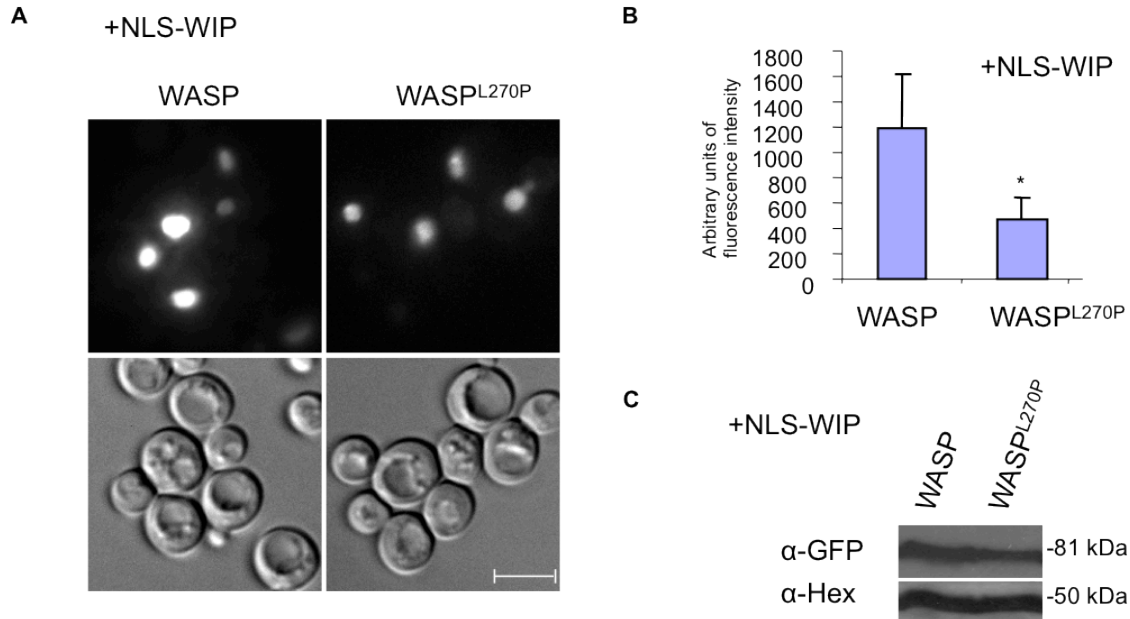


Figure 3.21 WASP^{L270P} adopts an open conformation.

(A) *S. cerevisiae* cells were transformed with NLS-WIP (Leu) together with (1) WASP reporter (Trp) or (2) WASP^{L270P} sensor (Trp) and selected on SD (-Trp-Leu) plates. The transformants were grown to exponential phase at 24°C in selective media and YFP signals in these cells were subsequently analyzed using fluorescence microscopy. Bar = 5μm

(B) Fluorescence signal quantification from 100 *S. cerevisiae* cells expressing NLS-WIP (Leu) together with (1) WASP reporter (Trp) or (2) WASP^{L270P} sensor (Trp), using metamorph software. * P<0.001 compared with WASP reporter + NLS-WIP cells.

(C) Western blot analysis of expression of the WASP reporter in *S. cerevisiae* cells transformed with WIP (Leu) together with (1) WASP reporter (Trp) or (2) WASP^{L270P} sensor (Trp) using anti-GFP (α-GFP) and anti-Hexokinase (α-Hex) as a loading control.

3.2.3 WASP with L270 mutation has increased phosphorylation in Tyr residues

The residue Y291 is sterically protected by the GBD-VCA domains when WASP is in the autoinhibited conformation (Torres and Rosen, 2003). It is proposed that in order for kinases to gain access to Y291, binding of an activator such as Cdc42, that can partially

destabilize the conformation, should first take place. If the mutation L270P is introduced in WASP, the open conformation adopted by WASP could bypass the requirement of an activator to destabilize the closed structure, for the access of kinases. To test this hypothesis, the ability of various kinases, previously shown to interact with WASP (Baba et al., 1999; Badour et al., 2004a; Cory et al., 2002b; Labno et al., 2003), to phosphorylate WASP or WASP^{L270P} was examined.

HEK 293T cells were transfected with WASP or WASP^{L270P} tagged with Histidine tag, together with Bruton's tyrosine kinase (BTK), Hematopoietic cell kinase (HCK), Tyrosine kinase expressed in hepatocellular carcinoma, (Tec), IL-2 inducible T cell kinase (ITK) and Fyn tagged with GFP. The transfected cells were lysed and his-tag pull-down assay was performed to isolate WASP or WASP^{L270P} from the lysates from cells with or without co-expression of the kinases. The tyrosine-phosphorylation levels of WASP or WASP^{L270P} was detected using phosphotyrosine specific antibody, 4G10. Western blot analysis revealed that BTK, HCK and Tec induced increased levels of tyrosine phosphorylation when mutation L270P was introduced in WASP (Figure 3.22A). The increased level of phosphorylated WASP mutant detected from cells co-expressing BTK, HCK and Tec, in comparison to the WT counterpart was not due to unequal levels of WASP or WASP^{L270P} isolated by the pull-down assay (Figure 3.22B). Low amounts of Tec were pulled down suggesting that the association of WASP and Tec may be transient or it may have been poorly expressed (Figure 3.22C). ITK and Fyn, on the other hand, did not induce increased tyrosine phosphorylation for WASP^{L270P} when compared to WASP. This could be because the increase in the phosphorylation levels of WASP^{L270P}

induced by these kinases was too low to be detected. No phosphorylation was detected when the cells were transfected with only WASP constructs, without any kinases, indicating that the phosphorylation levels detected in the western blots were due to exogenous kinases transfected (data not shown). The HEK 293T cells were treated by pervanadate, which is a phosphotyrosine phosphatase inhibitor, after transfection of WASP or WASP^{L270P} and the kinases to enhance tyrosine phosphorylation levels. However, pervanadate treatment caused non-specific tyrosine phosphorylation to be detected (data not shown). Together, these results indicate that WASP^{L270P} has increased phosphorylation in Tyr residues.

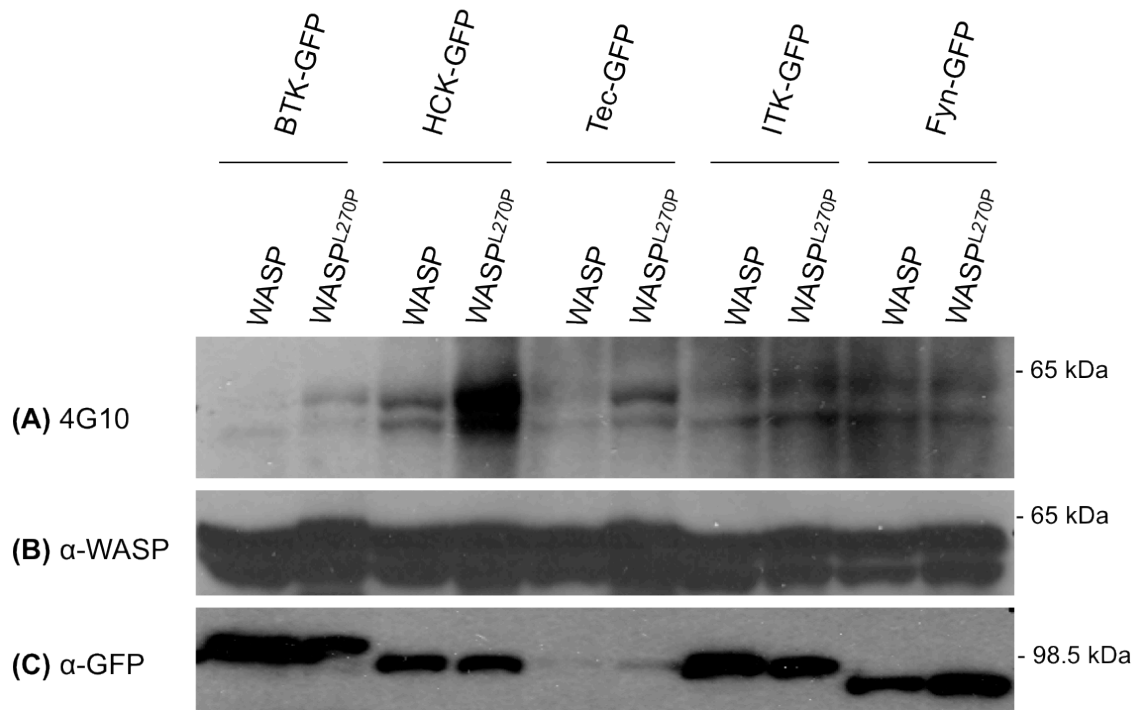


Figure 3.22 BTK, HCK and Tec induced increased tyrosine phosphorylation of WASP^{L270P}.
(A) HEK 293T cells were transfected with WASP-His or WASP^{L270P}-His together with (1) BTK-GFP, (2) HCK-GFP, (3) Tec-GFP, (4) ITK-GFP or (5) Fyn-GFP. WASP or WASP^{L270P} was isolated by His-tag pull-down assay. Western blot analysis of tyrosine-phosphorylation levels of WASP or WASP^{L270P} was performed using 4G10 antibody.
(B) Western blot analysis of levels of WASP or WASP^{L270P} isolated using anti-WASP (α-WASP).
(C) Western blot analysis of levels of kinases isolated using anti-GFP (α-GFP).

3.2.4 Enhanced phosphorylation of WASP^{L270P} is due to increased phosphorylation at residue 291

There are seven tyrosines residues in WASP, at amino acid residues 51, 83, 88, 102, 107, 212 and 291. However, mutation of all the tyrosine residues, except at residue Y291, did not cause a decrease in phosphorylation levels by HCK as compared to WT WASP (Baba et al., 1999). The consensus from the findings of many groups is that residue Y291 is the major phosphorylation site of WASP (Baba et al., 1999; Cory et al., 2002b).

To find out if the increase in tyrosine phosphorylation levels by BTK and HCK in WASP^{L270P} was due to phosphorylation at Y291, the mutation L270P was combined with a non-phosphorylatable Phe at 291 position, Y291F in WASP. HEK 293T cells were transfected with His-tag WASP^{L270P} or WASP^{L270P/Y291F} (WASP^{LP/YF}) together with GFP-tagged HCK or BTK (Figure 3.23 and 3.24). WASP^{L270P} or WASP^{LP/YF} was isolated by His-tag pull down assay and western blot analysis of the tyrosine phosphorylation levels of the WASP mutants showed that when Y291 was mutated to a non-phosphorylatable mutation Phe in WASP^{L270P}, the total tyrosine phosphorylation levels in WASP were reduced. The decrease in levels of phosphorylated WASP^{LP/YF} detected was not due to unequal levels of WASP mutant isolated by the pull-down assay or unequal amounts of HCK and BTK expressed (Figure 3.23 and 3.24). Similarly, when the mutation L270P was combined with a phosphomimetic mutation at Y291, L270P/Y291E (WASP^{LP/YE}), the tyrosine phosphorylation levels of WASP dropped (Figure 3.23 and 3.24). This results indicated that increased phosphorylation of WASP^{L270P} is due to increased phosphorylation at residue 291.

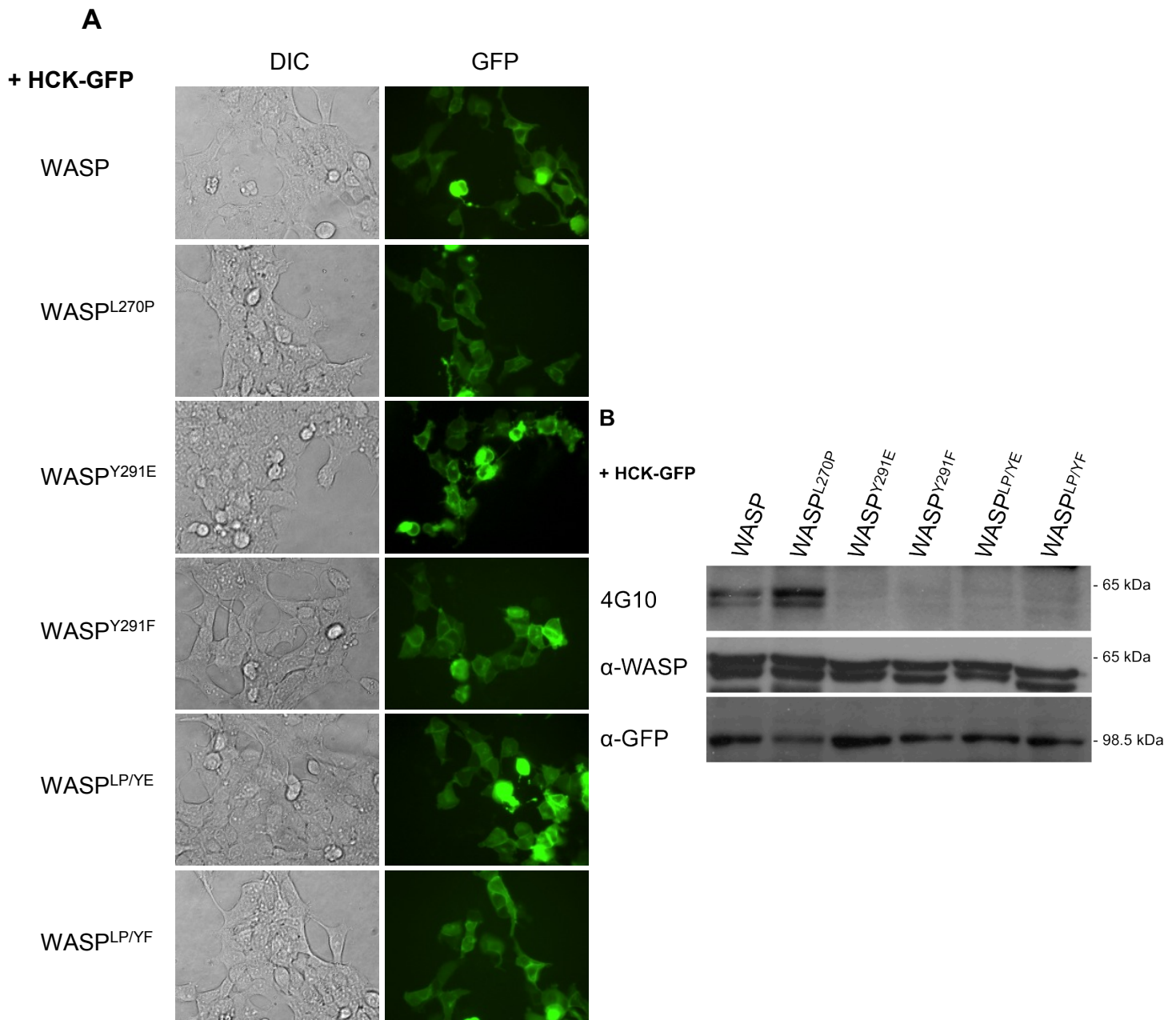


Figure 3.24 Increased phosphorylation of WASP^{L270P} by HCK is due to increased phosphorylation at residue 291.

(A) HEK 293T cells were transfected with HCK-GFP together with (1) WASP-His, (2) WASP^{L270P}-His, (3) WASP^{Y291E}-His, (4) WASP^{Y291F}-His, (5) WASP^{LP/YE}-His, (6) WASP^{LP/YF}-His. Transfection efficiencies of cells were analysed using fluorescence microscopy.

(B) HEK 293T cells were transfected with HCK-GFP together with (1) WASP-His, (2) WASP^{L270P}-His, (3) WASP^{Y291E}-His, (4) WASP^{Y291F}-His, (5) WASP^{LP/YE}-His, (6) WASP^{LP/YF}-His. The WASP mutants were isolated by His-tag pull-down assay. Western blot analysis of tyrosine-phosphorylation levels of WASP or WASP^{L270P} was performed using 4G10 antibody. Expression levels of WASP and BTK isolated in the pull-down assay were detected using anti-WASP (α -WASP) and anti-GFP (α -GFP) respectively.

3.2.5 Phosphorylation causes WASP to adopt an open conformation

Since phosphorylation is known to activate WASP, the conformation of phosphorylated WASP is hypothesized to be in the open conformation (Cory et al., 2002b). It would be interesting to analyse the conformation of WASP^{L270P} when additional mutations Y291E or Y291F is introduced.

WASP reporter (Trp) with mutations L270P, Y291E, Y291F, LP/YE or LP/YF was transformed together with NLS-WIP (Leu) in *S. cerevisiae* cells. The cells were then selected on SD plates lacking Trp and Leu and transformants were inoculated and grown to exponential phase. Subsequently, the cells were analyzed using fluorescence microscopy (Figure 3.25A). The fluorescence signals from 100 cells were quantified and plotted (Figure 3.25B). Western blot analysis showed that the transformed cells had equal expression of mutant WASP reporters (Figure 3.25C).

The fluorescence signal from cells transformed with WASP^{Y291F} was similar to fluorescence levels detected from cells transformed with WASP reporter, suggesting that the lack of phosphorylation causes WASP to adopt a closed conformation. On the other hand, mutation Y291E causes a reduction in the fluorescence levels from the mutant WASP reporter. Introduction of a glutamic acid residue, resembling the structure of a phospho group may have disrupted the autoinhibitory loop of WASP, causing it to adopt an open conformation, similar to the WASP^{L270P} sensor.

WASP^{LP/YF} sensor produced similar fluorescence levels as WASP^{L270P}, as the mutation Y291F has no effect on the conformation of WASP. WASP^{LP/YE} sensor surprisingly, had similar fluorescence levels as WASP^{L270P}. It could be due to the fact that WASP^{L270P} has already adopted an open conformation and the mutation Y291E had no further effect on the conformation of WASP.

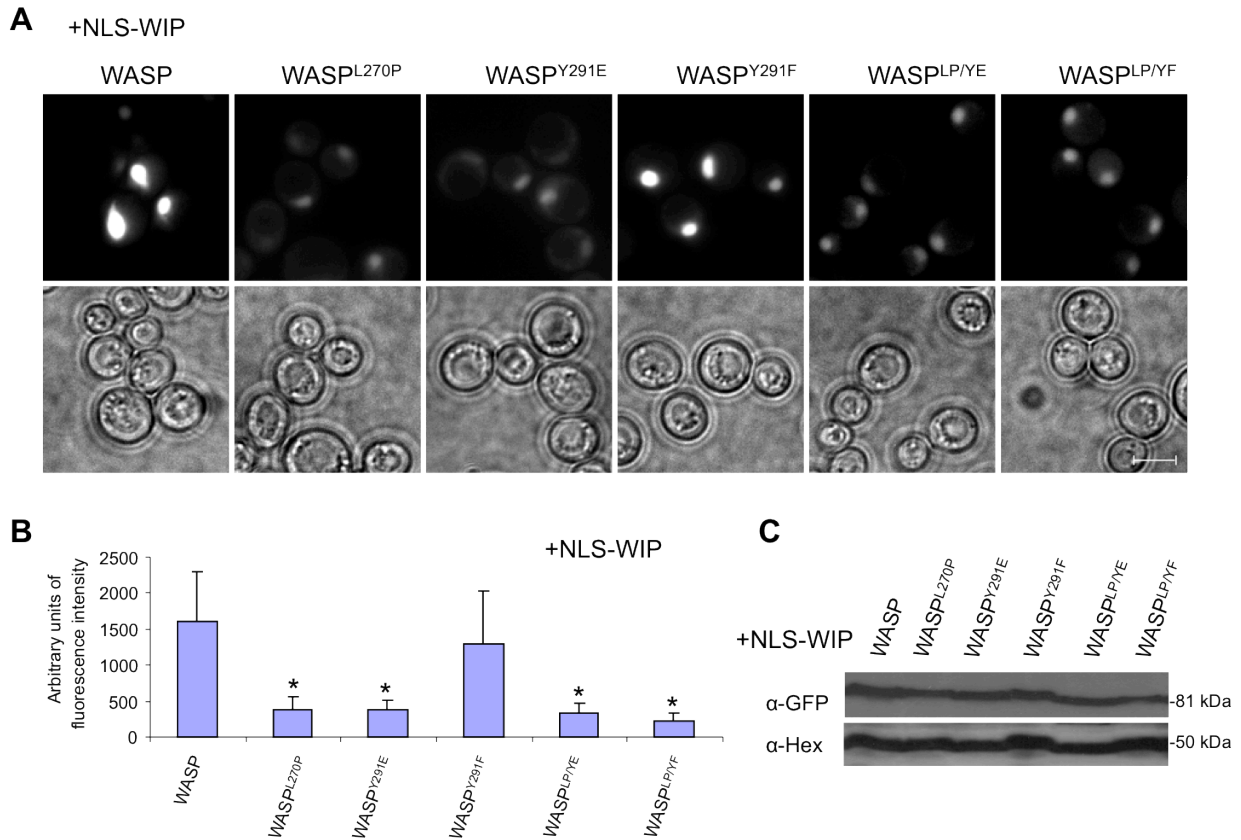


Figure 3.25 Phosphorylation causes WASP to adopt an open conformation.

(A) *S. cerevisiae* cells were transformed with NLS-WIP (Leu) plasmid together with (1) WASP reporter (Trp), (2) WASP^{L270P} sensor (Trp), (3) WASP^{Y291E} sensor (Trp), (4) WASP^{Y291F} sensor (Trp), (5) WASP^{L270P/Y291E} sensor (Trp) or (6) WASP^{L270P/Y291F} sensor (Trp) and selected on SD (-Trp-Leu) plates. The transformants were grown to exponential phase at 24°C in selective media and YFP signals in these cells were subsequently analyzed using fluorescence microscopy. Bar = 5μm

(B) Fluorescence signal quantification from 100 *S. cerevisiae* cells expressing NLS-WIP (Leu) plasmid together with (1) WASP reporter (Trp), (2) WASP^{L270P} sensor (Trp), (3) WASP^{Y291E} sensor (Trp), (4) WASP^{Y291F} sensor (Trp), (5) WASP^{L270P/Y291E} sensor (Trp) or (6) WASP^{L270P/Y291F} sensor (Trp) using metamorph software. *P<0.001 when compared to WASP reporter + NLS-WIP cells.

(C) Western blot analysis of expression of WASP mutant sensors in *S. cerevisiae* cells transformed with WIP (Leu) plasmid together with (1) WASP reporter (Trp), (2) WASP^{L270P} sensor (Trp), (3) WASP^{Y291E} sensor (Trp), (4) WASP^{Y291F} sensor (Trp), (5) WASP^{L270P/Y291E} sensor (Trp) or (6) WASP^{L270P/Y291F} sensor (Trp) using anti-GFP (α-GFP) and anti-Hexokinase (α-Hex) as a loading control.

3.2.6 WASP mutants bearing mutations at Y291 are able to suppress growth defects of *las17Δ* cells

Las17p is the yeast homologue of WASP and *S. cerevisiae* cells with the deletion of the gene have been shown to be unable to grow at elevated restrictive temperatures (Li, 1997). However, expression of human WASP together with human WIP in the *las17Δ* cells can suppress the growth defect and absence of the VCA domain of WASP or the V domain of WIP failed to suppress the growth defects in these cells (Rajmohan et al., 2006). This suggests that WASP and WIP have to form a functional complex for actin polymerization in order to suppress the growth defects of *las17Δ* cells.

The activity of WASP^{L270P}, WASP^{Y291E}, WASP^{Y291F}, WASP^{LP/YE} and WASP^{LP/YF} in *las17Δ* cells were examined in the presence of WIP in order to determine the effects of phosphorylation on the function of WIP-WASP complex. The mutants were transformed into *las17Δ* cells (IDY166) together with WIP. The transformants were streaked on YPUAD plates and grown at both 24°C and 37°C. All the mutations were able to rescue the growth defects of the *las17Δ* cells (Figure 3.26). The results indicate that although the mutations L270P, Y291E, LP/YE and LP/YF affected the conformation of WASP, these mutations did not affect the formation of a functional complex with WIP.

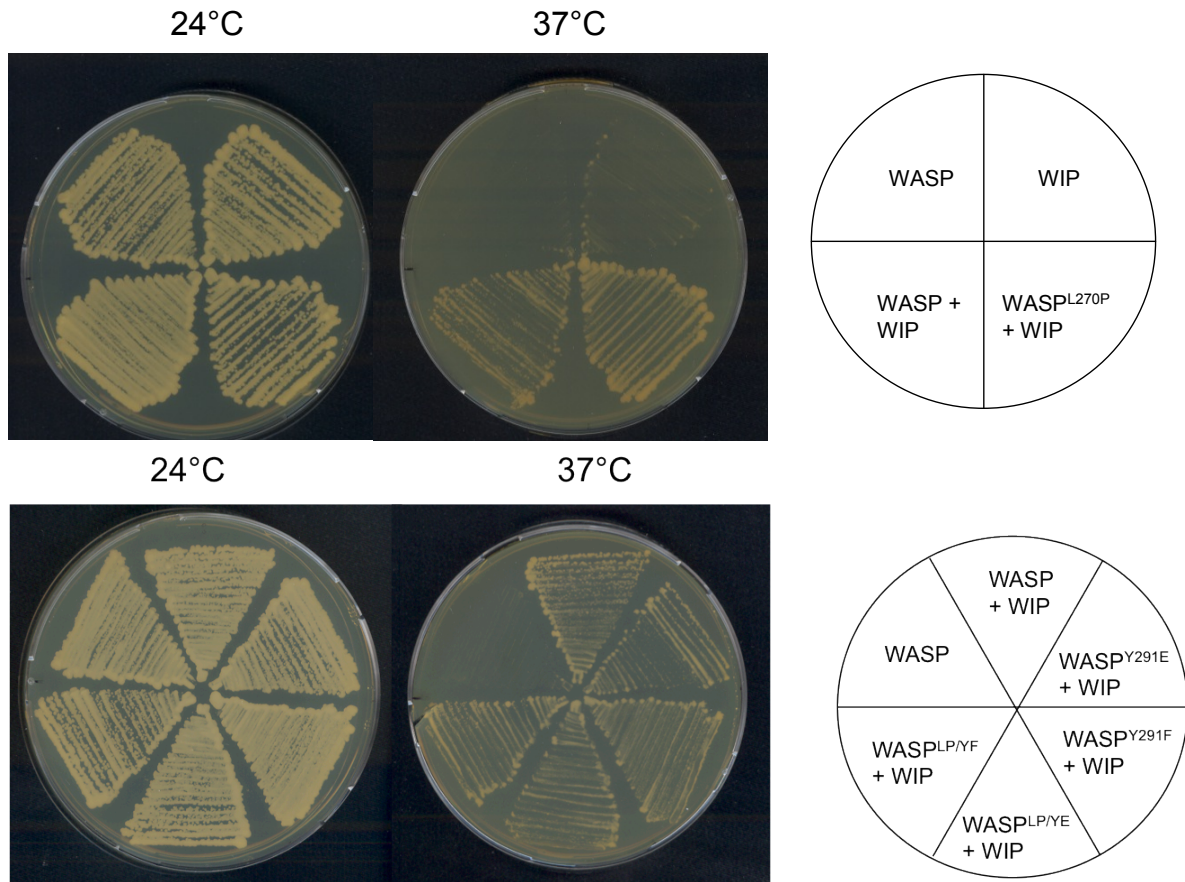


Figure 3.26 Co-expression of WASP or its mutants and WIP suppress the growth defects of *las17Δ* cells.

Las17Δ cells (IDY166) were transformed with plasmids expressing WASP or WASP mutants. The transformants were streaked on YPUAD plates and grown at both 24°C and 37°C. Photograph was taken after 3 days.

3.2.7 WASP knock down Jurkat T cells has impaired motility

Phosphorylation at Y291 has been shown to be indispensable for many roles of WASP in vivo (Dovas and Cox, 2010). It is required for podosome formation in dendritic cells and macrophages (Blundell et al., 2009; Dovas et al., 2009), crucial for phagocytic cup formation in macrophages (Tsuboi and Meerloo, 2007) and chemotaxis in dendritic cells (Blundell et al., 2009). However, little is known about the function of phosphorylation of WASP in T cells.

To determine if phosphorylation of WASP is important for T cell migration and if the mutation L270P in WASP affects T cell migration, a WASP-deficient Jurkat T cell line was first generated in order to express the phosphorylation mutants in the cell line for further characterization.

The RNAi method was used to generate the WASP knock down Jurkat T cell line, in which stable integration of lentiviral or retroviral vectors encoding shRNA or siRNA into the genome of the cells can downregulate the expression of WASP for long periods of time. Two lentiviral vectors encoding siRNA targeting the WASP coding region and 3' UTR were designed, W7si and W8si (Appendix 2) according to studies done by Olivier et al (Olivier et al., 2006). The efficacy of the siRNA vectors were tested in both HEK 293T cells and Jurkat T cells. However, both the siRNA vectors only effectively inhibited exogenous WASP expression in HEK 293T cells but not in Jurkat T cells (data not shown). Subsequently, lentiviral vectors encoding shRNA, W7, W8 and S1 (shRNA targeting another coding region of WASP) (Appendix 2) were designed and tested in both cell lines but similar results were obtained where no knockdown of WASP expression was observed in Jurkat T cells (data not shown). Double copies of the shRNAs in lentiviral vectors were constructed, W7-W7, W8-W8, S1-S1 but did not knock down the expression of WASP when transduced in Jurkat T cells (data not shown).

Epstein-Barr virus (EBV) based vectors have been shown to be maintained episomally after transduction into different cell lines (Hellebrand et al., 2006). EBV-based vector

harbouring the different shRNAs were constructed and transduced into Jurkat T cells but did not inhibit the expression of WASP effectively (data not shown).

Finally, retroviral vector encoding the WASP shRNA, S1 was used. The retroviral vector also encoded GFP to allow detection and sorting of the transduced cells. HEK 293T cells were transfected with the shRNA encoding vector to package the shRNA-containing viral particles. The viral particles were used to infect Jurkat T cells and target cells that were stably producing GFP were sorted by flow cytometry. The transduction was carried out once or twice to test if increasing transduction numbers would increase the efficiency of the knock-down of WASP expression. The shRNA effectively knocked down the expression of WASP in Jurkat T cells (Figure 3.27A). However, increasing the number of transduction did not increase the knockdown. Also, real-time PCR showed that mRNA level of WASP was down-regulated to over 2 folds as well (Figure 3.27B).

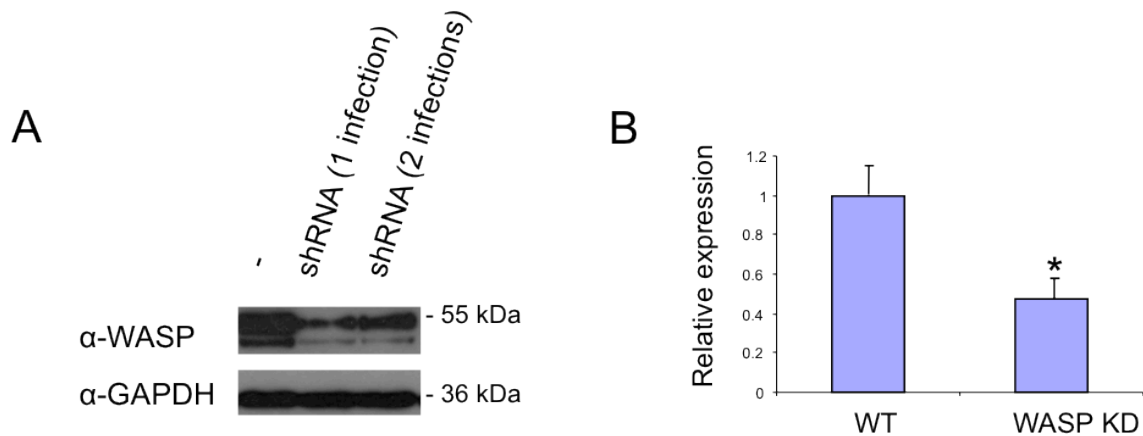


Figure 3.27 Suppression of endogenous WASP expression by shRNA.

(A) Western blot analysis of the expression level of WASP in Jurkat T cells transduced with shRNA vector using anti WASP (α -WASP) and anti GAPDH (α -GAPDH) as a loading control. Lane 1: WT Jurkat cells, lane 2: Jurkat cells transduced with WASP shRNA once, lane 3: Jurkat cells transduced with WASP shRNA twice. * $P < 0.001$ compared with WT cells.

(B) WASP mRNA levels quantified by real-time PCR in WT Jurkat and WASP knock down cells.

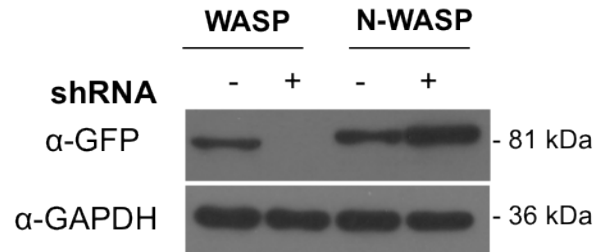


Figure 3.28 shRNA was specific to WASP.

Western blot analysis of expression of WASP and N-WASP in HEK 293T cells transfected with or without shRNA using anti GFP (α -GFP) and anti GAPDH (α -GAPDH) as a loading control.

N-WASP has more than 50% sequence homology with WASP (Derry et al., 1994). There was a possibility that the shRNA could target N-WASP as well. Thus, to check for the specificity of the shRNA, both WASP and N-WASP tagged with GFP were transfected in HEK 293T cells with or without the shRNA. The Western blot analysis showed that the shRNA was specific for WASP as N-WASP expression was unaffected by the shRNA (Figure 3.28).

In order to validate that WASP is important for the migration in T cells, and if partial down-regulation of WASP would be sufficient to impair migration in T cells, the chemotactic response of Jurkat T cells in response to SDF-1 α was analysed using Dunn chambers. Using time-lapse video microscopy, the migration tracks of the Jurkat T cells and Jurkat WASP knock down T cells (Jurkat^{WASPkd}) cells on the annular bridge of the Dunn chamber (Methods, 2.2.3.13.2) were traced. The Jurkat T cells preferentially migrated towards the source of SDF-1 α while the Jurkat^{WASPkd} had impaired movement. The chemotactic response of the Jurkat^{WASPkd} cells towards SDF-1 α was suppressed (Figure 3.29). Moreover, the migration velocities of the Jurkat^{WASPkd} (0.0383 μ m/sec) were significantly decreased (Figure 3.30A) in comparison to the Jurkat T cells

(0.0986 $\mu\text{m}/\text{sec}$). Additionally, circular histograms were plotted to analyse the overall directionality of migration of the cells (Figure 3.30B). 61.6% of the final positions of the Jurkat T cells lie in the 40° arc facing the chemokine source while only 26.6% of the Jurkat^{WASPkd} migrated to the region. This data indicated that the migrations of Jurkat^{WASPkd} were more random and they had impaired directionality movements towards SDF-1 α . Taken together, these data suggests that WASP plays an important role in the cell motility of Jurkat T cells and partial down regulation of WASP expression was sufficient to cause the impairment.

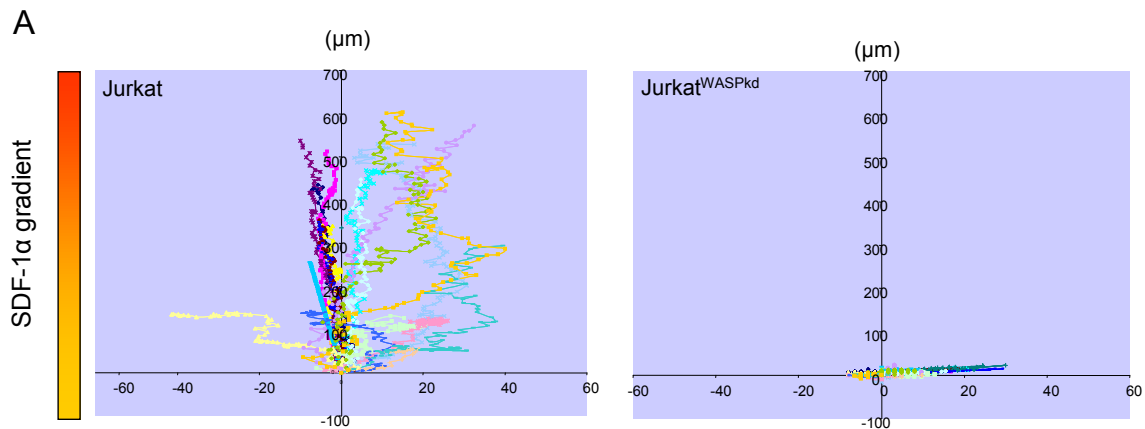
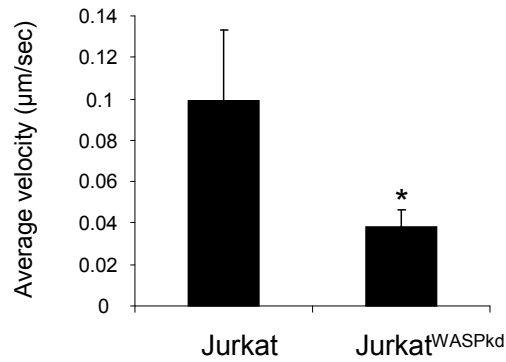


Figure 3.29 WASP downregulation impairs the motility of Jurkat cells (A)

Vector plots of migration paths of 20 randomly chosen cells from wildtype and Jurkat^{WASPkd} exposed to a gradient of SDF-1 α in the Dunn chamber. Time-lapsed images were captured over 50 mins at intervals of 30s. The starting point of each cell is at the intersection of the X and Y axes. The source of SDF-1 α was at the top.

A



B

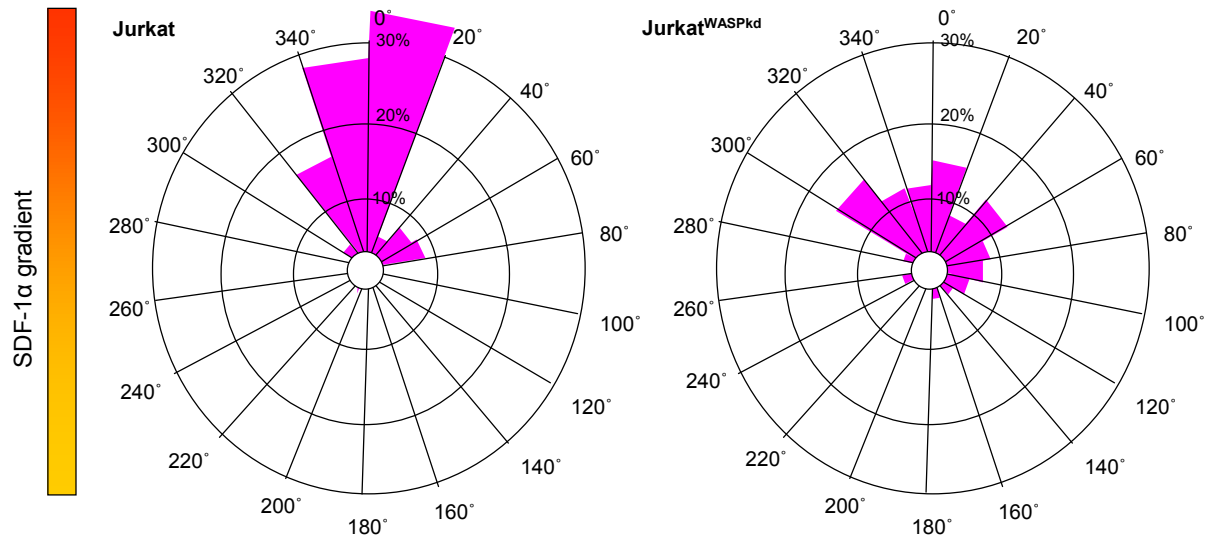


Figure 3.30 WASP downregulation impairs the motility of Jurkat cells (B)

(A) Migration velocity of each cell shown as a mean of velocities of 60 randomly chosen cells (20 cells each from 3 sets of experiments) * $P < 0.0001$ compared with WT cells (unpaired student's t-test)

(B) Circular histograms showing percentage of cells where the final positions of cells lie in each of the sectors (20°). The source of SDF-1 α was at the top.

From the results above, Jurkat^{WASPkd} cells were impaired in cell motility as compared to the Jurkat T cells. We hypothesize that reconstitution of WASP expression in the Jurkat^{WASPkd} cells will be able to rescue the impairment of chemotactic response of the cells towards SDF-1 α . However, a mutant version of WASP in which the shRNA cannot target, but is still able to be translated to WT WASP must first be cloned. 4 residues at the

target site of shRNA in WASP were mutated such that the respective amino acids were converted to be coded with the degenerate code (WASP_R) (Appendix 2) (Figure 3.31). The construct was tested in HEK 293T cells to verify if it was resistant to the shRNA. Western blot analysis showed that WASP_R could still expressed in the presence of the shRNA while WASP expression was down regulated when transfected together with the shRNA (Figure 3.31).

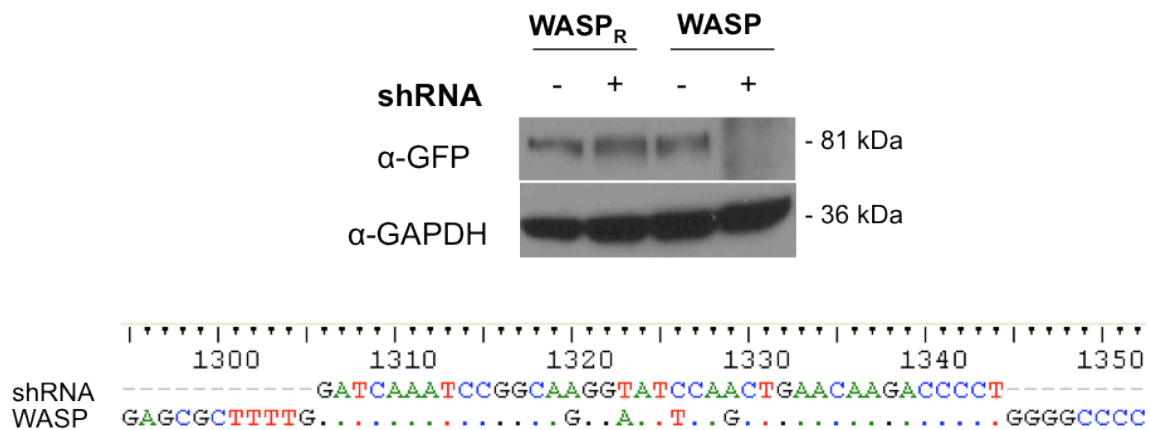


Figure 3.31 WASP with mutations rendering it resistant to the shRNA.

Western blot analysis of expression of WASP-GFP and WASP_R-GFP in HEK 293T cells transfected with or without shRNA using anti GFP (α-GFP) and anti GAPDH (α-GAPDH) as a loading control. WASP_R contains four mutations that rendered it resistant to the shRNA.

3.2.8 WASP Y291 phosphorylation is crucial for T cell migration

To ascertain the importance of phosphorylation of WASP in the chemotaxis of T cells, WASP_R or WASP_R bearing mutations L270P, Y291E, Y291F, L270P/Y291E (LP/YE) or L270P/Y291F (LP/YF) were tagged with RFP and expressed in Jurkat^{WASPkd}. The cells expressing the WASP mutants from neomycin resistant plasmids were selected for a week using G418. Subsequently, the chemotaxis responses of the cells towards SDF-1α were analysed in a Dunn Chamber using time-lapse microscopy.

Reconstitution of WASP expression in Jurkat^{WASPkd} (Jurkat^{WASPkd} + WASP_R) rescued the impairment in chemotactic response towards SDF-1 α (Figure 3.32), similar to the response of Jurkat T cells (Results 3.28). Jurkat^{WASPkd} + WASP_R^{L270P} cells behaved in a similar manner as Jurkat^{WASPkd} + WASP_R cells (Figure 3.32). The average velocity of the Jurkat^{WASPkd} + WASP_R^{L270P} cells (0.0817 μ m/sec) was similar to the Jurkat^{WASPkd} + WASP_R cells (0.0709 μ m/sec) (Figure 3.34A). However, the overall directionality of Jurkat^{WASPkd} + WASP_R^{L270P} cells, according to the circular histograms plotted, was impaired with only 18.2% of the final positions of the cells lying in the 40° arc facing the chemokine source, compared to 89% for the Jurkat^{WASPkd} + WASP_R cells (Figure 3.32). 25% of Jurkat^{WASPkd} + RFP cells were lying in the 40° arc facing the chemokine source compared to 18.2% of the Jurkat^{WASPkd} + WASP_R^{L270P} cells. The higher percentage of Jurkat^{WASPkd} + RFP cells lying in the region close to the chemokine source may be because the knockdown of the expression of WASP was not complete and WASP may still be exerting its effects. Expression of WASP^{L270P} may have dominant negative effect on the chemotaxis of Jurkat^{WASPkd} cells, resulting in less percentage of the cells lying in the 40° arc facing SDF-1 α compared to Jurkat^{WASPkd} + RFP cells.

Jurkat^{WASPkd} + WASP_R^{Y291F} cells and Jurkat^{WASPkd} + WASP_R^{Y291E} cells, on the other hand, had similar impairment in chemotaxis as Jurkat^{WASPkd} + RFP cells (Figure 3.32). The migration velocities of Jurkat^{WASPkd} + WASP_R^{Y291F} cells (0.0387 μ m/sec) were similar to Jurkat^{WASPkd} + RFP cells (0.0391 μ m/sec), significantly lower than the migration velocities of Jurkat^{WASPkd} + WASP_R cells (0.0709 μ m/sec) (Figure 3.34A). Jurkat^{WASPkd} + WASP_R^{Y291E} cells displayed intermediate velocities (0.0614 μ m/sec), in between that of

Jurkat^{WASPkd} + WASP_R and Jurkat^{WASPkd} cells (Figure 3.34A). The circular histograms showed that the directionality of migration of Jurkat^{WASPkd} + WASP_R^{Y291F} and Jurkat^{WASPkd} + WASP_R^{Y291E} cells were more random than Jurkat^{WASPkd} + WASP_R cells. 18.3% and 26.6% of the final positions of Jurkat^{WASPkd} + WASP_R^{Y291F} and Jurkat^{WASPkd} + WASP_R^{Y291E} cells respectively lie in the 40° arc facing the chemokine source while 89% of the final positions of Jurkat^{WASPkd} + WASP_R cells lie in the same region (Figure 3.33).

Coupling the Y291F mutation to WASP^{L270P} caused the average migration velocity of the Jurkat^{WASPkd} + WASP_R^{LP/YF} cells to decrease from 0.0817µm/sec to 0.0554µm/sec. The Y291E mutation increased the velocities of the Jurkat^{WASPkd} + WASP_R^{LP/YE} cells to 0.0952µm/sec. This increase in migration velocity is significantly higher than the average velocities of Jurkat^{WASPkd} + WASP_R cells (0.0709µm/sec) (Figure 3.34A). The circular histograms revealed that compared to Jurkat^{WASPkd} + WASP_R cells, both Jurkat^{WASPkd} + WASP_R^{LP/YF} and Jurkat^{WASPkd} + WASP_R^{LP/YE} cells showed more random migration, with only 13.3% (Jurkat^{WASPkd} + WASP_R^{LP/YF}) and 23.3% (Jurkat^{WASPkd} + WASP_R^{LP/YE}) of the final positions of the cells lying in the 40° arc facing the chemokine source (Figure 3.33). Western blot analysis showed that WASP and WASP mutants were expressed equally (Figure 3.34B), thus any difference observed was not due to the difference in the expression of the proteins.

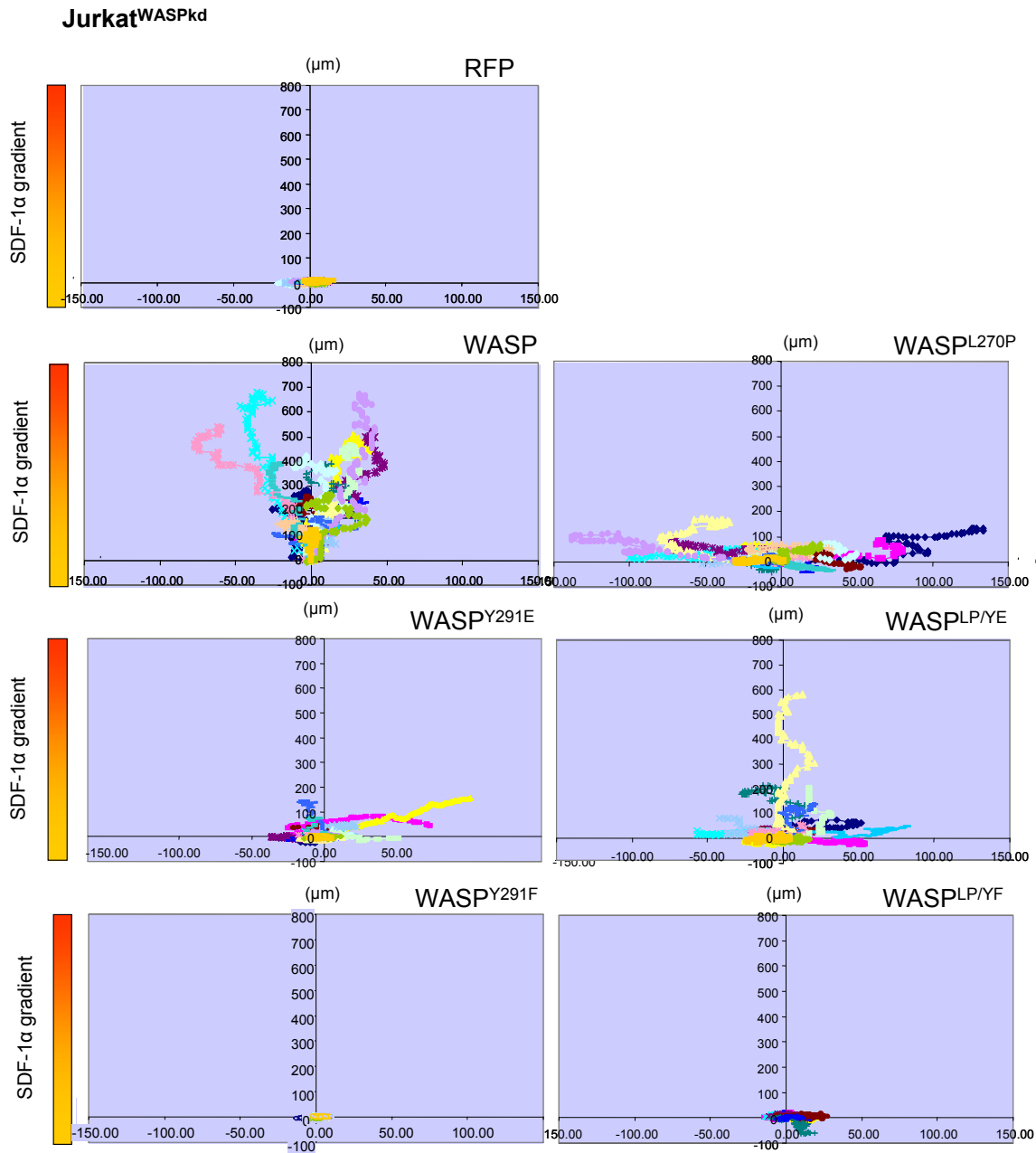


Figure 3.32 WASP Y291 phosphorylation is crucial for T cell migration (A)

Vector plots of migration paths of 20 randomly chosen cells from WASP knockdown cells expressing (1) RFP, (2) WASP_R-RFP, (3) WASP_R^{L270P}-RFP, (4) WASP_R^{Y291E}-RFP, (5) WASP_R^{Y291F}-RFP, (6) WASP_R^{L270P/Y291E}-RFP and (7) WASP_R^{L270P/Y291F}-RFP, exposed to a gradient of SDF-1 α in the Dunn chamber. Time-lapsed images were captured over 50 mins at intervals of 30s. The starting point of each cell is at the intersection of the X and Y axes. The source of SDF-1 α was at the top.

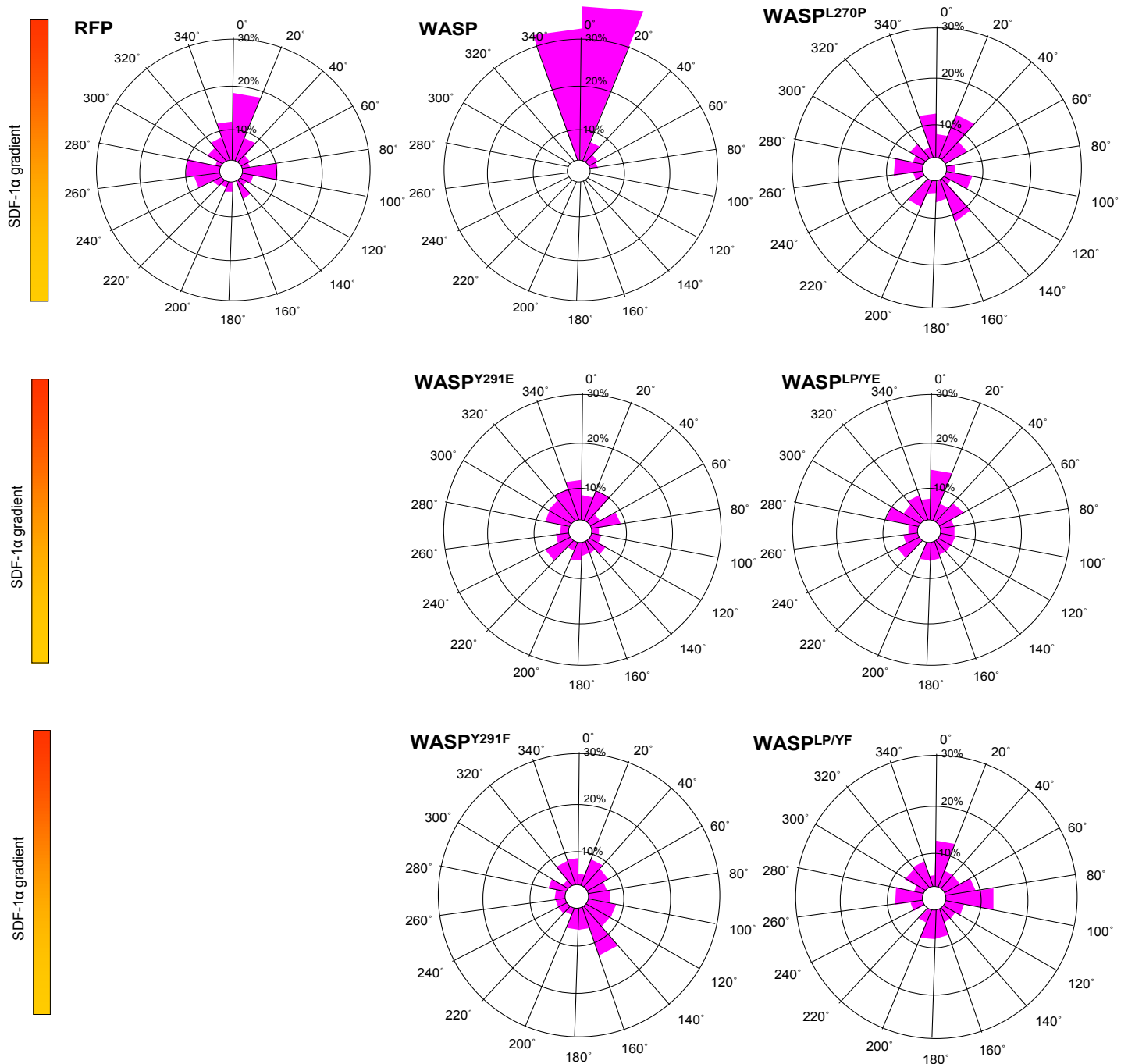


Figure 3.33 WASP Y291 phosphorylation is crucial for T cell migration (B)

WASP knockdown cells expressing (1) RFP, (2) WASP_R-RFP, (3) WASP_R^{L270P}-RFP, (4) WASP_R^{Y291E}-RFP, (5) WASP_R^{Y291F}-RFP, (6) WASP_R^{L270P/Y291E}-RFP and (7) WASP_R^{L270P/Y291F}-RFP, exposed to a gradient of SDF-1α in the Dunn chamber. Circular histograms showing percentage of cells where the final positions of cells lie in each of the sectors (20°). The source of SDF-1α was at the top.

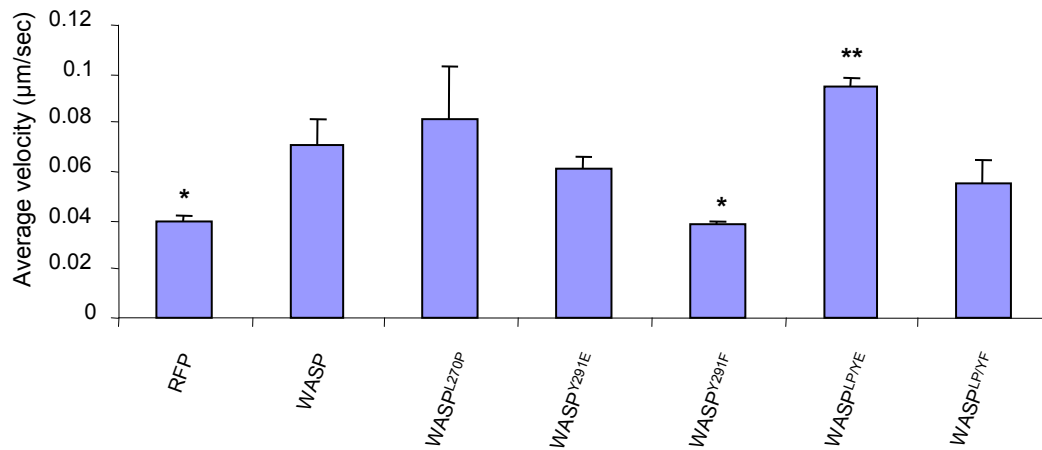
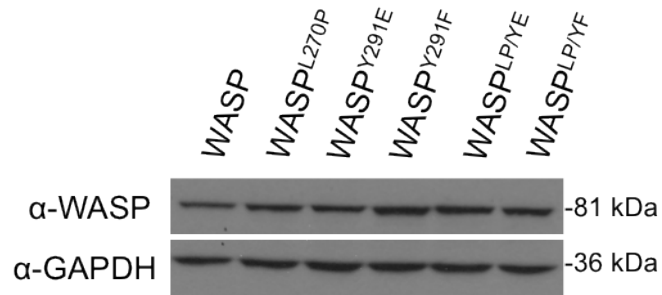
A**B**

Figure 3.34 WASP Y291 phosphorylation is crucial for T cell migration (C)

(A) Migration velocity of each cell shown as a mean of velocities of 60 randomly chosen cells (20 cells each from 3 sets of experiments) * $P < 0.01$, ** $P < 0.05$ compared with WASP_R-RFP cells (unpaired student's t-test).

(B) Western blot analysis of the expression levels of WASP in transfected cells after 36 hours using appropriate antibodies.

3.2.9 WASP Y291 phosphorylation is required for filopodia induction in

N-WASP^{-/-} fibroblasts

The inducible recruitment of WASP to the membrane has been shown to increase filopodia formation (Castellano et al., 1999). Since phosphorylation at Y291 of WASP is

crucial for T cell migration, it would be interesting to analyse the effects of phosphorylation of WASP on the actin cytoskeleton in the cells.

Filopodia formation induced by the WASP mutants was examined in N-WASP^{-/-} fibroblasts since these cells do not express both WASP and N-WASP (Misra et al., 2010). The effects observed in the cells could thus be mainly attributed to WASP or the mutants. Also, since N-WASP expression is absent in these cells, filopodia formation due to the interaction between N-WASP and WIP, when exogenous WIP is introduced, would be absent. N-WASP^{-/-} fibroblasts were seeded on coverslips and transfected with 3.5µg of appropriate DNA. After 36 hours, the cells were fixed and stained with phalloidin for actin. Thereafter, the cells on coverslips were mounted on microscope slides and analysed using fluorescence microscopy. WASP and WIP were first individually assessed for the ability to promote filopodia formation. Transfection of WASP-expressing construct caused significant promotion the formation of filopodia while the increase in filopodia formation by WIP was negligible (Figure 3.35). The co-expression of WASP and WIP increased the filopodia formation significantly. The expression levels of WASP are equal in cells transfected with WASP alone or WASP together with WIP (Figure 3.35C). Actin staining of the cells showed that actin was localized in the membrane projections that were identified as filopodia. Filopodia are defined as actin-rich membrane projections with length that is between 8µm to 20µm (Misra et al., 2010).

Subsequently, N-WASP^{-/-} fibroblasts seeded on coverslips were transfected with WASP mutants, WASP^{L270P}, WASP^{Y291E}, WASP^{Y291F}, WASP^{L270P/Y291E} (WASP^{LP/YE}),

WASP^{L270P/Y291F} (WASP^{LP/YF}) tagged with GFP (1.75µg of DNA) together with WIP (1.75µg of DNA), in order to examine how the mutations in WASP affect filopodia induction in the cells. After 36 hours, cells on the coverslips were mounted on microscope slides and analysed using fluorescence microscopy. The results showed that WASP^{L270P} induced filopodia formation in 48.37% of cells while WASP induced 26.43% of the cells. This suggests that WASP^{L270P} is more effective than WASP in inducing filopodia formation. WASP^{Y291E} (31.25%) also induced increased filopodia formation in the fibroblasts, albeit to a less extent than WASP^{L270P}, while WASP^{Y291F} was least efficient in promoting filopodia formation (21.07%) (Figure 3.36). This indicates that phosphorylation of WASP is important for filopodia induction in the fibroblasts. The percentage of cells with induced filopodia formation by WASP^{LP/YE} (38.69%) was in between that of WASP^{L270P} and WASP^{Y291E}. WASP^{LP/YF} (22.99%) on the other hand promoted significantly less filopodia than WASP^{L270P} (Figure 3.36). Western blot analysis showed that the difference in filopodia induction is not due to differences in expression levels of the WASP mutants (Figure 3.36C). The results suggest that phosphorylation of WASP^{L270P} plays a role in the increase in filopodia induction but it may not be the sole contributor.

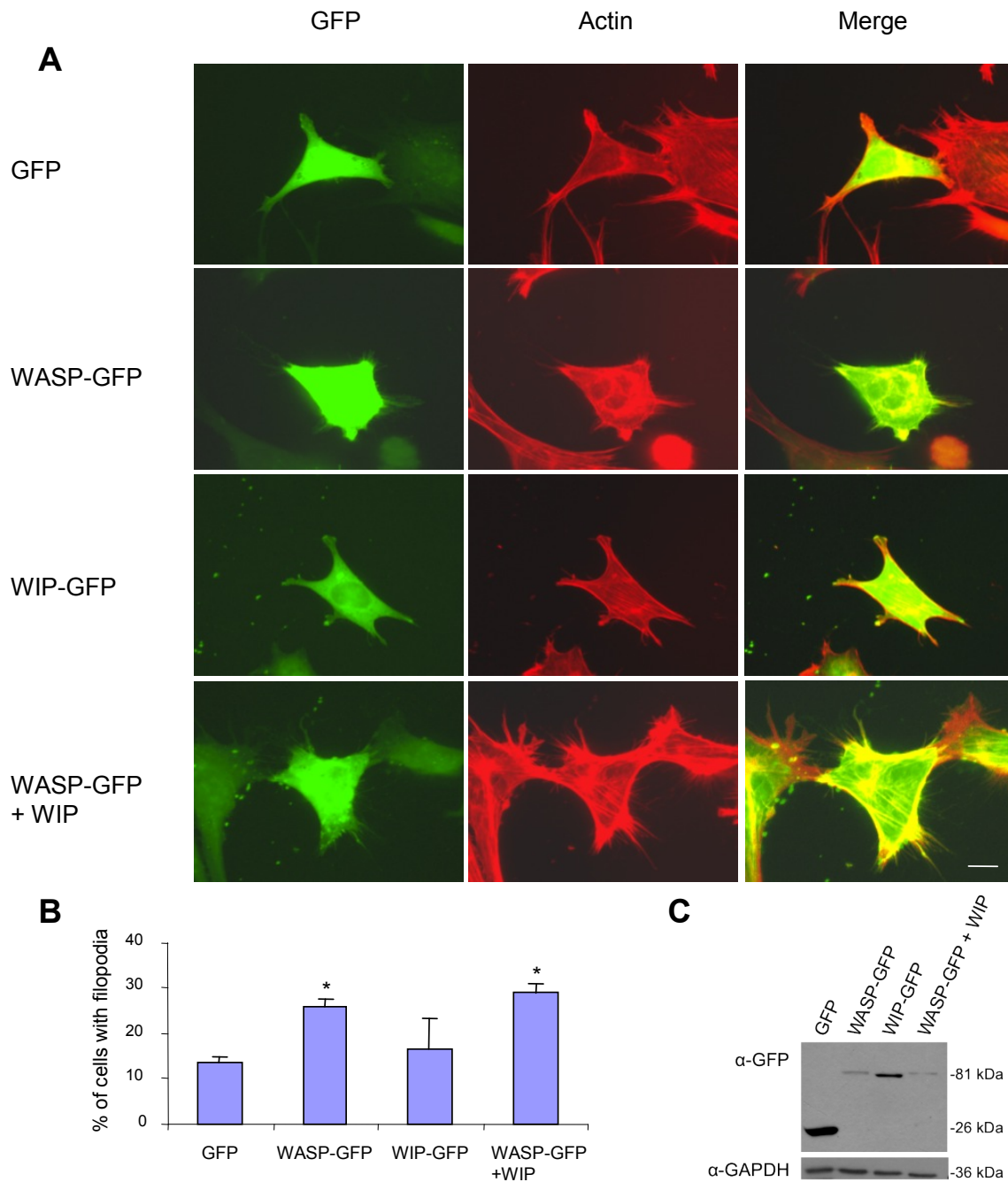


Figure 3.35 WASP promotes formation of filopodia formation in N-WASP^{-/-} fibroblasts in the presence of WIP.

(A) N-WASP^{-/-} fibroblasts were transfected with (1) GFP, (2) WASP-GFP, (3) WIP-GFP or (4) WASP-GFP together with WIP. After 36 hours, cells were fixed and stained with Alexa568-Phalloidin to visualize filamentous actin. Bar represents 15 μ m.

(B) Statistical analysis of 30 random transfected cells for filopodia induction was carried out as described Methods 2.2.3.10. Each experiment was repeated thrice. * $P < 0.01$ compared with cells transfected with only GFP (unpaired student's t-test). A cell was defined as having filopodia (8-20 μ m) if it contains 5 or more filopodia.

(C) Western blot analysis of the expression levels of WASP or WIP in transfected cells after 36 hours using appropriate antibodies.

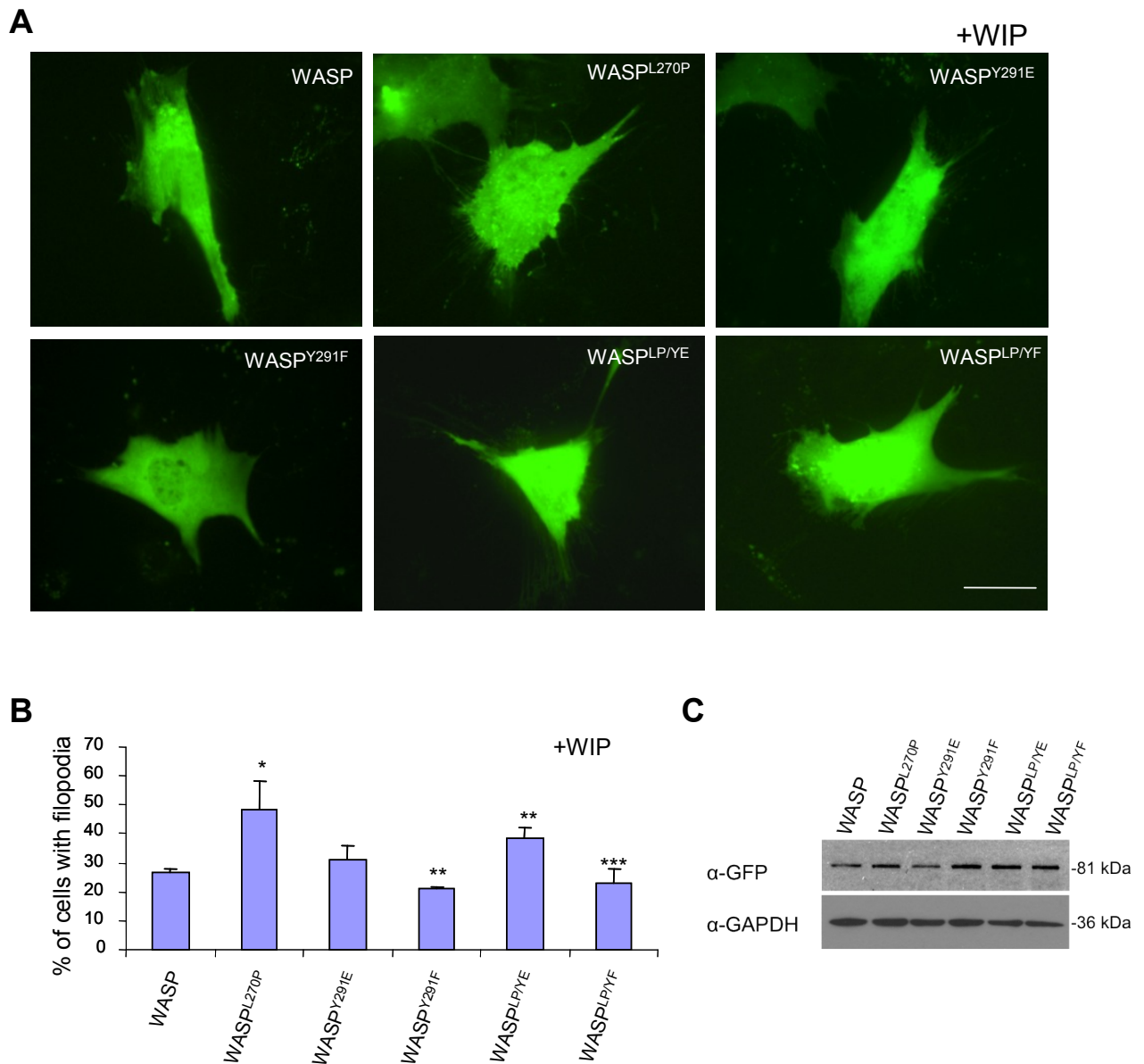


Figure 3.36 WASP Y291 phosphorylation is required for filopodia formation in N-WASP^{-/-} fibroblasts.

(A) N-WASP^{-/-} fibroblasts were transfected with (1) WASP-GFP, (2) WASP^{L270P}-GFP, (3) WASP^{Y291E}-GFP, (4) WASP^{Y291F}-GFP, (5) WASP^{L270P/Y291E}-GFP and (6) WASP^{L270P/Y291F}-GFP together with WIP. After 36 hours, cells were analysed for the presence of filopodia. Bar represents 15 μ m.

(B) Statistical analysis of 30 random transfected cells for filopodia induction was carried out as described Methods 2.2.3.10. Each experiment was repeated thrice. * $P < 0.01$, ** $P < 0.05$ compared with cells transfected with WASP-GFP. *** $P < 0.001$ compared with cells transfected with WASP^{L270P}-GFP (unpaired student's t-test). A cell was defined as having filopodia (8-20 μ m) if it contains 5 or more filopodia.

(C) Western blot analysis of the expression levels of WASP in transfected cells after 36 hours using appropriate antibodies.

Results 3.3

3.3 Role of Calpain-mediated proteolysis of WASP in T cell function

3.3.1 Introduction

Proper regulation of the cell migration is crucial for normal and pathological processes which involve a myriad of proteins and the coordination of the activity of these proteins to drive the actin polymerization machinery (Ridley et al., 2003). The formation of protrusions at the leading edge of cells relies on the regulation of actin filaments in cell adhesion structures. Calpain has been shown to be important in the cell migration process (Bhatt et al., 2002; Dourdin et al., 2001) and members of the Calpain family regulates the assembly and disassembly of adhesion structures through the proteolysis of cytoskeletal proteins, including filamins, vinculin, talin, cortactin and the WASP family of proteins (Lebart and Benyamin, 2006). The WASP family of proteins belongs to a class of nucleation promoting factors that activates the Arp2/3 complex and increases the rate of actin polymerization (Campellone and Welch, 2010). WASP activates the Arp2/3 complex through the binding of both the Arp2/3 complex and G-actin at the VCA domain of WASP (Machesky and Insall, 1998). This bypasses the actin nucleation step which is a rate-limiting step in actin polymerization. WASP has been shown to be a substrate of calpain as inhibition of calpain results in reduced cleavage products of WASP (Calle et al., 2006b). The aim of this study was to determine if calpain proteolysis of WASP is important for the regulation of cell migration and other functions in T cells. In order to characterize the role of calpain-mediated proteolysis of WASP in the function of T cells, the calpain cleavage sites in WASP must be mapped in order to generate a calpain-

resistant WASP. The calpain-resistant mutant can be used to study if these functions were impaired when regulation of WASP by calpain was inhibited.

3.3.2 Fine mapping of WASP-WIP interaction site

It has been shown that WIP acts as a chaperone for WASP and protect WASP from calpain-mediated degradation (de la Fuente et al., 2007) and it is likely that the binding of WASP binding domain (WBD) of WIP to the WH1 domain of WASP prevents the exposure of the cleavage sites to proteases (Volkman et al., 2002). Our laboratory has shown previously that deleting the WH1 domain of WASP renders WASP^{ΔWH1} to be very stable in yeast (Rajmohan et al., 2006). Furthermore, western blot analysis of the expression levels of WASP^{ΔWH1} showed that WASP^{ΔWH1} is expressed much more stably compared to WASP in HEK 293T cells transfected with WASP or WASP^{ΔWH1} (Figure 3.38). Thus, by analyzing the interaction of truncated WASP (with deletion at the WH1 region) and WIP, the region of WASP targeted by calpain could be narrowed down.

Deletion constructs of WASP were cloned, in which increasing number of residues were deleted from the WH1 domain of WASP. Primers that were designed to bind to specific sites in the WH1 domain (Appendix 2) were used together with a 3' primer, which binds to the end of WASP, to amplify the various length of truncated WASP (Figure 3.38)

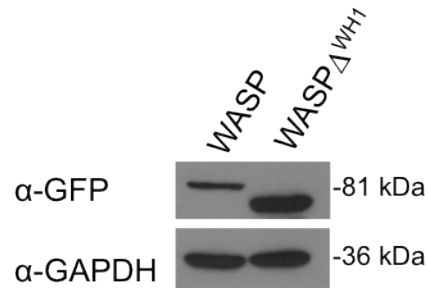


Figure 3.37 WASP expression stabilised after deletion of WH1 domain.

Western blot analysis of expression of WASP in 293T cells transfected with (1) WASP or (2) WASP^{ΔWH1} using anti GFP (α-GFP) and anti GAPDH (α-GAPDH) as a loading control.

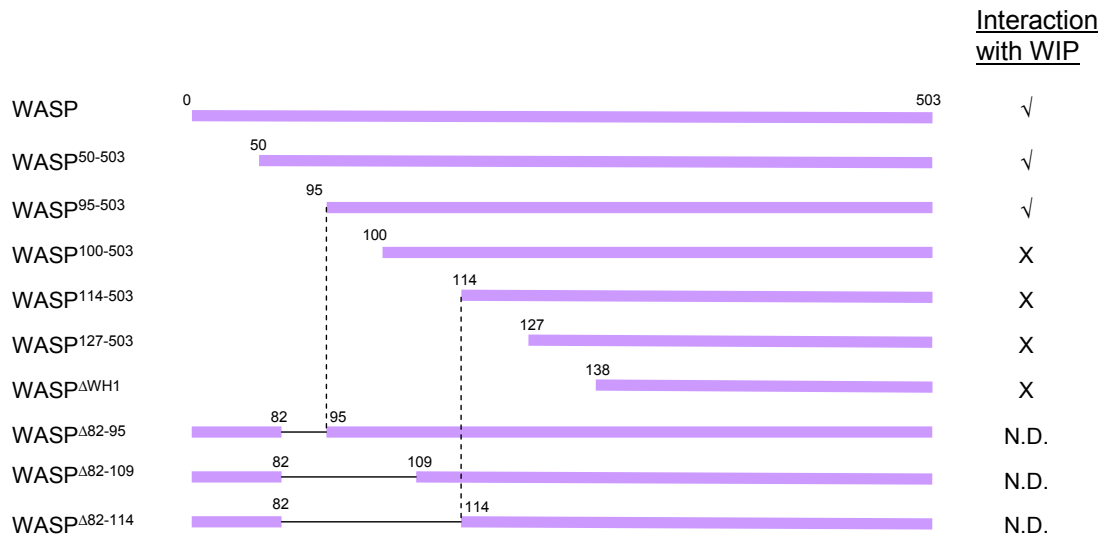


Figure 3.38 Deletion constructs of WASP for analysis of interaction with WIP and stability of expression in the presence of calpain.

The leftmost column indicates if there was positive or negative interaction of truncated WASP with WIP (✓ : positive interaction, X: negative interaction).

Full length WASP, WASP⁵⁰⁻⁵⁰³, WASP⁹⁵⁻⁵⁰³, WASP¹⁰⁰⁻⁵⁰³, WASP¹¹⁴⁻⁵⁰³, WASP¹²⁷⁻⁵⁰³, WASP^{ΔWH1} (WASP¹³⁸⁻⁵⁰³) were cloned into the bait plasmid pAS2-1 containing the

Gal4p Binding domain and WIP was cloned into the prey plasmid pACT2 that contained the Gal4p Activation domain. A yeast two hybrid assay was performed to check for the interaction between the truncated WASP and WIP (Methods 2.2.2.4).

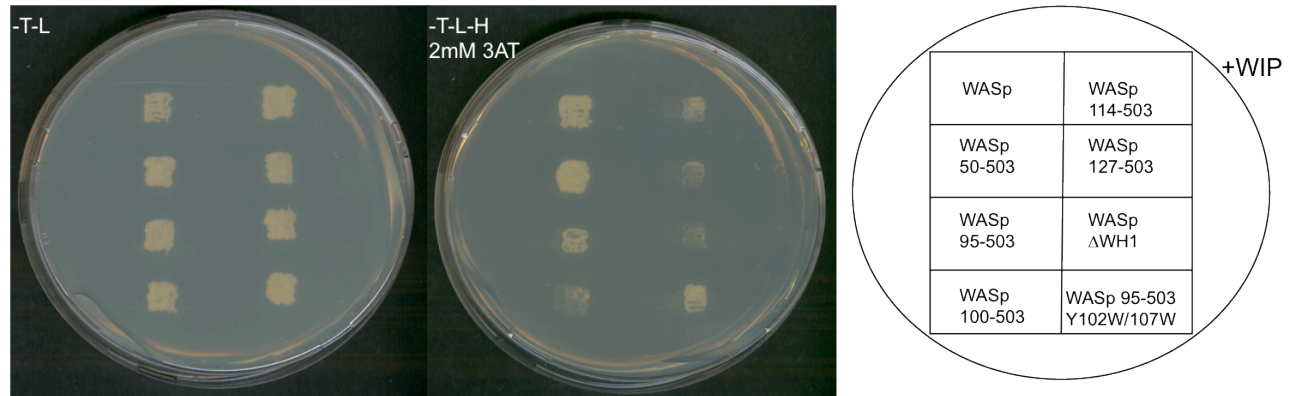


Figure 3.39 Interaction of WASP and WIP was abolished when first 100 residues of WASP was deleted.

Deletion constructs of WASP in bait plasmid pAS2-1(Trp) (1) full length WASP, (2) WASP⁵⁰⁻⁵⁰³, (3) WASP⁹⁵⁻⁵⁰³, (4) WASP¹⁰⁰⁻⁵⁰³, (5) WASP¹¹⁴⁻⁵⁰³, (6) WASP¹²⁷⁻⁵⁰³, (7) WASP^{ΔWH1} (WASP¹³⁸⁻⁵⁰³), (8) WASP^{95-503 Y102W/Y107W} were transformed together with prey plasmid pACT2-WIP (Leu) in *S. cerevisiae* cells and grown on SD (-Trp-Leu) plates at 37°C for 3 days. Transformants of cells expressing both truncated WASP and WIP were streaked on SD (-Trp-Leu) plates and SD (-Trp-Leu-His) plates supplemented with 2mM 3AT and incubated at 37°C for 5 days before analysis.

The yeast two hybrid assay showed that *S. cerevisiae* cells expressing full length WASP, WASP⁵⁰⁻⁵⁰³, WASP⁹⁵⁻⁵⁰³ together with WIP were able to grow on SD (-T-L-H) plates supplemented with 2mM 3AT. 3AT was added to act as an inhibitor for non-specific activation of the transcription of the HIS3 reporter gene. However, *S. cerevisiae* cells expressing WASP¹⁰⁰⁻⁵⁰³, WASP¹¹⁴⁻⁵⁰³ and WASP¹²⁷⁻⁵⁰³ and WASP^{ΔWH1} (WASP¹³⁸⁻⁵⁰³) together with WIP were not able to grow on SD (-T-L-H) plates supplemented with 2mM 3AT (Figure 3.39). This result indicates that when the first 100 residues of WASP were

deleted, the interaction of WASP and WIP was reduced. Also, the result correlated with existing findings that the WH1 domain is critical for WASP-WIP interaction (Chou et al., 2006). It could be hypothesized from the result of this assay that the region critical for the interaction of WASP and WIP lies between residues 95-114 of WASP. Indirectly, it could also be inferred that the calpain cleavage region of WASP resides within this region.

3.3.3 *In vitro* proteolysis of WASP by calpain

Previous studies have shown that inhibition of calpain reduced the expression of calpain cleavage products of WASP (Calle et al., 2006b). However, this could be due to the fact that calpain is required to activate other proteases, which degrade WASP. In order to determine if WASP is a direct substrate of calpain, WASP tagged with GST was expressed and purified in *E.coli*. GST-WASP⁹⁵⁻³²⁰ was used for purification as we could not purify the full length WASP, GST-WASP.

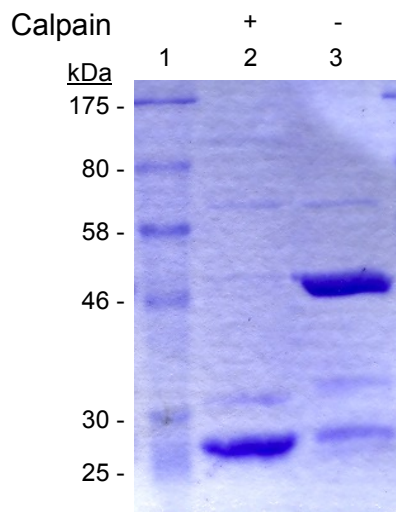


Figure 3.40 WASP is a substrate of calpain. GST-WASP⁹⁵⁻³²⁰ was purified from *E. coli* (BL21) cells after IPTG induction and resolved in a 10% SDS-PAGE gel, followed by staining with Coomassie blue. Lane 1 is the protein ladder, lane 2 is GST-WASP⁹⁵⁻³²⁰ that was incubated with calpain for 2 hours and lane 3 is the untreated GST-WASP⁹⁵⁻³²⁰.

GST-WASP⁹⁵⁻³²⁰ (50 kDa) was purified and incubated in cleavage buffer containing 100µg/ml calpain 1 (calpain μ) and CaCl₂ for 2 hours. Both calpain treated and untreated

GST-WASP⁹⁵⁻³²⁰ were resolved in SDS-PAGE gel and stained with Coomassie blue. In the untreated sample, a strong single band at about 50 kDa was detected which corresponded to the size of GST-WASP⁹⁵⁻³²⁰ (Figure 3.40 lane 3). After calpain treatment, the 50 kDa band was absent. This result shows that WASP is a substrate of calpain.

3.3.4 Ionomycin treatment decreases the stability of WASP

Ionomycin is a calcium ionophore that is known to activate calpain in the cells (Dreolini and Takei, 2007). In order to confirm if increased calcium levels in cells can activate calpain to increase degradation of WASP, HEK 293T cells were transfected with WASP tagged with GFP and treated with ionomycin for 4 hours before lysis. Expressions of WASP with and without ionomycin treatment of the cells were analysed using Western blot.

Stability of WASP decreased after ionomycin treatment of the HEK 293T cells. Additionally, the expression of WASP^{T111P} was also analysed. The mutation T111P causes WAS and lies in the WH1 region of WASP. This mutation abolished the ability of WASP to suppress the growth defect of *S cerevisiae las17Δ* cells in the presence of WIP (las17p is the yeast homologue of WASP) (Rajmohan et al., 2009). Co-expression of WASP and WIP can however, suppress the growth defects of these cells. Thus, it is likely that the mutation abolishes the interaction of WASP and WIP, causing WASP to be susceptible to degradation. Western blot analysis showed that similar to WASP, ionomycin treatment also reduced the expression of the WASP mutant (Figure 3.41). This

indicates that ionomycin treatment of HEK 293T cells increases the activity of calpain for the degradation of WASP.

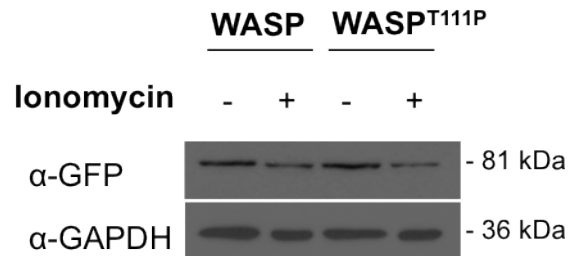


Figure 3.41 WASP expression reduced after ionomycin treatment of 293T cells.

Western blot analysis of expression of WASP in 293T cells transfected with (1) WASP or (2) WASP^{T111P} using anti GFP (α -GFP) and anti GAPDH (α -GAPDH) as a loading control. The transfected HEK 293T cells were first treated with 1 μ g/ml of ionomycin for 4 hours before lysis for western blot analysis.

3.3.5 WASP⁹⁵⁻⁵⁰³ has reduced proteolysis by calpain

The yeast two hybrid assay showed that when the first 100 residues of WASP were deleted, the interaction of WASP and WIP were abolished (Results 3.3.2). This suggests that the calpain cleavage sites in WASP may lie around this region. By analyzing the expression levels of the truncated WASP mutants in the presence of calpain, the region important for calpain proteolysis in WASP could be determined.

In order to verify if the expression levels of the mutant WASP was affected when the residues were deleted from the WH1 domain of WASP, HEK 293T cells were transfected with full length WASP, WASP⁵⁰⁻⁵⁰³, WASP⁹⁵⁻⁵⁰³, WASP¹⁰⁰⁻⁵⁰³, WASP¹¹⁴⁻⁵⁰³, WASP¹²⁷⁻⁵⁰³, WASP ^{Δ WH1} (WASP¹³⁸⁻⁵⁰³) tagged with GFP. The transfected cells were treated with ionomycin for 4 hours before lysis. The expression levels of the mutant WASP were subsequently analysed by Western blot.

Western blot analysis showed that WASP deleted in the first 95 residues (WASP⁹⁵⁻⁵⁰³) and 100 residues (WASP¹⁰⁰⁻⁵⁰³) had a slight increase in stability when compared to full length WASP (Figure 3.42). However, when 114 and 127 residues were deleted from the WH1 domain of WASP, the expression levels of the mutant WASPs increased to a level that was comparable to that of WASP^{ΔWH1} (WASP¹³⁸⁻⁵⁰³) (Figure 3.42). This indicated that by increasing the number of residues deleted from 100 (WASP¹⁰⁰⁻⁵⁰³) to 114 (WASP¹¹⁴⁻⁵⁰³), the expression and stability of WASP had increased.

In order to narrow down the region of calpain cleavage in WASP, three more deletion constructs were cloned, in which residues 82-95, 82-109 and 82-114 of the WH1 domain of WASP were deleted. The mutant WASP constructs, WASP^{Δ82-95}, WASP^{Δ82-109} and WASP^{Δ82-114}, were transfected into HEK 293T cells and treated with ionomycin for 4 hours before lysis and Western blot to check for the relative expression for the WASP mutants. As seen in the Western blots, expression levels of WASP^{Δ82-95}, WASP^{Δ82-109}, WASP^{Δ82-114} did not increase as significantly as WASP¹¹⁴⁻⁵⁰³ (Figure 3.42). A possible explanation is that by retaining the front portion of the WH1 domain of WASP, the sequence of the amino acids has been changed causing calpain to recognize a cleavage site at the portion of the WH1 domain that has been retained instead. This results in similar expression levels of WASP^{Δ82-95}, WASP^{Δ82-109} and WASP^{Δ82-114} with WASP. Figure 3.38 summarised the expression levels of the mutant WASPs and the interaction with WIP.

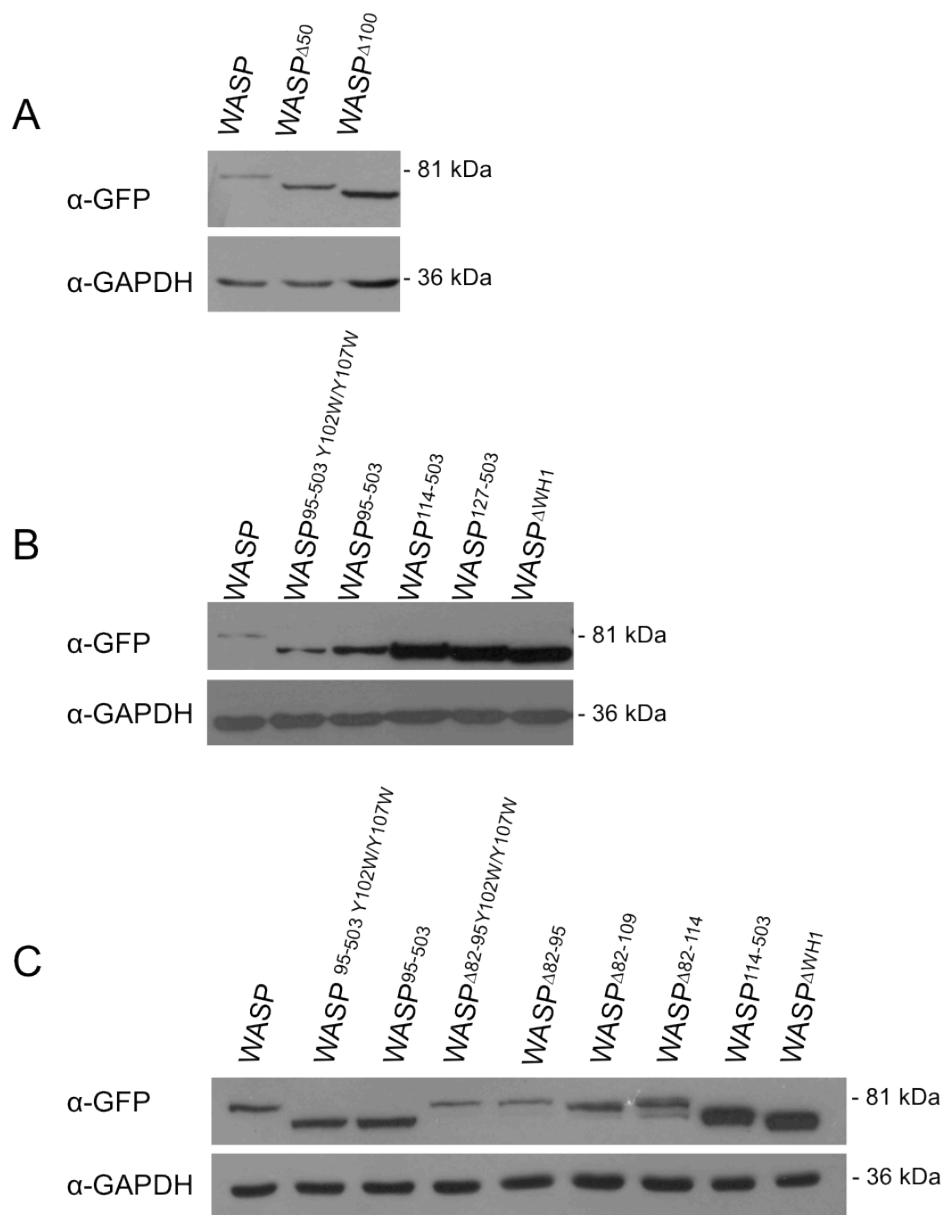


Figure 3.42 WASP⁹⁵⁻⁵⁰³ has increased expression in presence of calpain.

Western blot analysis of expression of WASP mutants in HEK 293T cells transfected with

(A) (1) full length WASP, (2) WASP^{Δ50}, (3) WASP^{Δ100}

(B) (1) full length WASP, (2) WASP^{95-503 Y102W/Y107W}, (3) WASP⁹⁵⁻⁵⁰³, (4) WASP¹¹⁴⁻⁵⁰³, (5) WASP¹²⁷⁻⁵⁰³, (6) WASP^{ΔWH1} (WASP¹³⁸⁻⁵⁰³)

(C) (1) full length WASP, (2) WASP^{95-503 Y102W/Y107W}, (3) WASP⁹⁵⁻⁵⁰³, (4) WASP^{Δ82-95Y102W/Y107W}, (5) WASP^{Δ82-95}, (6) WASP^{Δ82-109}, (7) WASP^{Δ82-114}, (8) WASP¹¹⁴⁻⁵⁰³, (9) WASP^{ΔWH1} (WASP¹³⁸⁻⁵⁰³)

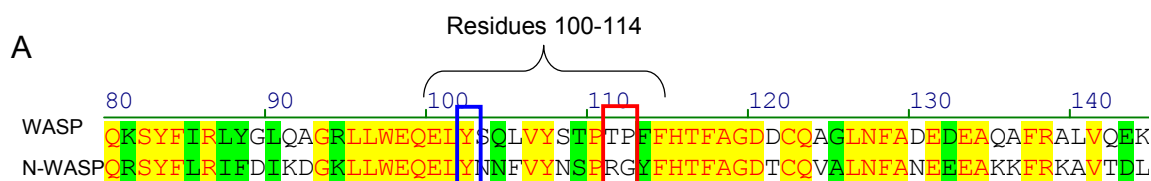
using anti GFP (α-GFP) and anti GAPDH (α-GAPDH) as a loading control. The transfected HEK 293T cells were first treated with 1μg/ml of ionomycin for 4 hours before lysis for western blot analysis.

3.3.6 Mapping of the calpain cleavage site in WASP

The Western blot analysis (Results 3.3.5) showed an increase in the stability of WASP between the deletion of 100 residues and 114 residues at the N-terminus of WASP, when transfected cells were treated with ionomycin before lysis. This indicated that the region critical for calpain cleavage in WASP lies between residue 100 to 114, in the WH1 domain.

N-WASP (Neural WASP), unlike WASP, has been reported to be non-susceptible to cleavage by calpain (Shcherbina et al., 2001). Given the high sequence similarity between the two proteins, this finding was surprising. Thus, closer examination and comparison between the two sequences would be useful in determining residues which are responsible for the susceptibility of WASP to calpain.

Figure 3.43A shows the sequence alignment of N-WASP and WASP from residue 80 to 140 of WASP. Within residues 100 to 114, there were a number of residues that were not conserved between WASP and N-WASP, including residues S103, Q104, L105, S108, T109, T111, P112 and F113. The occurrence of Lys and Tyr at position P₁ of the calpain cleavage site were the highest (Figure 3.43B) and in residues 100 to 114 of WASP, there were 2 Tyr residues, Y102 and Y107. Taken together, the findings and analysis indicate that the calpain cleavage site of WASP occurs within residues 100-114 in the WH1 domain.



B

Determinants of Calpain Cleavage 20779

TABLE II
Amino acid preferences of calpain around the cleavage site

The occurrence of each residue in positions P₄–P₇' for all 106 cleavage sites (Table I) has been counted and normalized to the frequency of the same amino acid in Swiss-Prot and TrEMBL.

	P ₄	P ₅	P ₆	P ₁	P ₁ '	P ₂ '	P ₃ '	P ₄ '	P ₅ '	P ₆ '	P ₇ '
Trp	0.00	2.34 ^a	0.00	0.00	0.00	0.00	3.12 ^a	0.79	0.00	2.38 ^a	0.79
Tyr	0.90	0.00	0.30	2.69 ^a	0.00	0.30	0.60	0.60	1.81	1.52 ^a	0.30
Phe	0.23	0.23	0.23	1.84	0.46	0.46	0.23	1.39	0.00	0.94	1.17
Leu	0.59	0.59	2.97 ^a	0.59	0.59	0.40	0.20	0.40	0.90	0.60	1.01
Ile	0.32	1.13	0.81	0.16	0.65	0.65 ^b	0.97	0.33	0.33	0.33	0.99
Val	0.71	1.57	2.00 ^a	0.14	0.71	0.71	0.57	1.58	1.01	1.16	0.29
Ala	1.11	0.74	0.12	0.25	1.73	1.36	0.99	1.00	0.75	0.88	0.88
Gly	0.69	0.83	0.14	1.24	0.69	1.24	0.55	1.25	1.53	0.84	1.26
Ser	1.20	1.60	0.93	0.80	3.33	1.87	0.80	1.08	1.88	1.36	1.49
Thr	2.03 ^a	1.02	2.71 ^a	1.86	1.86 ^b	0.68	0.85	1.71	1.03	1.55	0.69
Pro	1.54	2.32 ^a	0.77	0.58	0.19	2.89 ^a	5.59 ^{a,b}	2.92 ^{a,b}	1.75	1.77	1.18
Asp	0.72	0.36	0.54	0.36	0.18	0.72	0.36	0.73	0.73	0.92	0.73
Glu	1.31	1.60	0.73	0.44	0.73	1.31	0.73	0.29	0.88	0.89	0.89
Gln	1.68	0.48	0.72	0.96	1.20	1.68	1.44	0.97	0.48	1.22	0.73
Asn	1.08	0.65	1.30	0.65	0.43	0.65	0.65	1.53	1.75	0.88	0.66
Lys	1.11	1.42	0.47	2.84 ^a	1.11	1.42	1.42	0.96	0.96	0.81	1.45
Arg	1.45	1.09	0.36	2.54 ^a	1.82	0.36	0.91	0.55	0.92	0.74	2.22 ^{a,b}
His	1.68	0.84	0.00	1.26	0.42	0.42	0.84	0.85	0.85	0.85	0.85
Cys	0.00	0.00	1.75	0.00	0.00	0.58	0.00	0.59	1.18	2.37	0.00
Met	0.80	0.40	0.40	1.59	0.80	0.40	1.19	0.00	0.00	0.00	1.22

^a Values exceeding 2.00 are in bold.
^b Values corresponding to the consensus calpastatin inhibitory segment in positions P₁'–P₇' (i.e. TIPPXYR) are underlined.

Figure 3.43 Mapping the calpain cleavage sites of WASP.

(A) Sequence alignment between WASP and N-WASP. Residues highlighted in yellow are conserved while residues that are non-highlighted or highlighted in green or are non-conserved. Residue Y102 (Blue box) and Residues T111 and P112 (Red box) of WASP are residues that were mutated which increased the resistance of WASP against calpain.

(B) Table showing occurrence of residues at calpain cleavage sites of 106 substrates of calpain. At P₁ position, occurrence of Lys and Tyr residues were the highest. Adapted from (Tompa et al., 2004).

3.3.7 Generation of a Calpain-resistant mutant of WASP

To determine which residues were crucial for calpain cleavage in WASP, a series of site directed mutants were generated by mutating residues around or within 100 to 114 of the WH1 domain. The aim of mutating these critical residues was to abolish the calpain cleavage sites in WASP to achieve a WASP mutant that was resistant to calpain proteolysis and it would be useful for further studies. Also, in order to achieve a WASP mutant that was able to retain its biochemical properties, site directed mutant WASPs were preferred to be used over truncated WASP mutants.

Trp residues were reported to have nil occurrence at the P₁ position of the calpain cleavage site (Figure 3.43). Thus, Tyr residues within residues 100 to 114 of WASP, including Y88, Y102 and Y107, were mutated to Trp (Y88W, Y102W, Y107W). Additionally, Y107 was mutated to Cys (Y107C) as this mutation was known to cause the WAS (Imai et al., 2003a). This mutation may have an effect on the expression or stability of WASP that is caused by calpain mediated degradation. Also, four other residues, S103, S108, T111 and P112 were mutated to the respective residues aligned in N-WASP (S103N, S108N, T111R and P112G). T111 was mutated to proline as well, as this mutation was also known to cause WAS (Imai et al., 2003a). The mutations were used in various combinations subsequently to achieve a mutant WASP that was as resistant to calpain proteolysis as possible. Figure 3.44 summarised the location of the mutations. The mutant WASPs, WASP^{Y88W}, WASP^{Y102W}, WASP^{Y107C}, WASP^{Y107W}, WASP^{T111P}, WASP^{T111R/P112G} and WASP^{S103N/S108N} were tagged with GFP and transfected into HEK 293T cells. The transfected cells were treated with ionomycin for 4 hours. Subsequently, the cells were lysed (Methods 2.2.3.7) and Western blot analysis was performed.

The Western blot analysis (Figure 3.45) showed that WASP^{Y88W} and WASP^{Y107W} did not have any significant increase in stability, in comparison to the expression of WASP, after ionomycin treatment. On the other hand, WASP^{Y102W}, WASP^{Y107C}, WASP^{T111R/P112G} and WASP^{S103N/S108N} had significantly enhanced expression when compared to WASP. The expression levels, however, were not as high as WASP^{ΔWH1} (WASP¹³⁸⁻⁵⁰³). Thus, the mutations that conferred enhanced stability to WASP were combined in order to achieve a mutant WASP that was more resistant to calpain proteolysis.

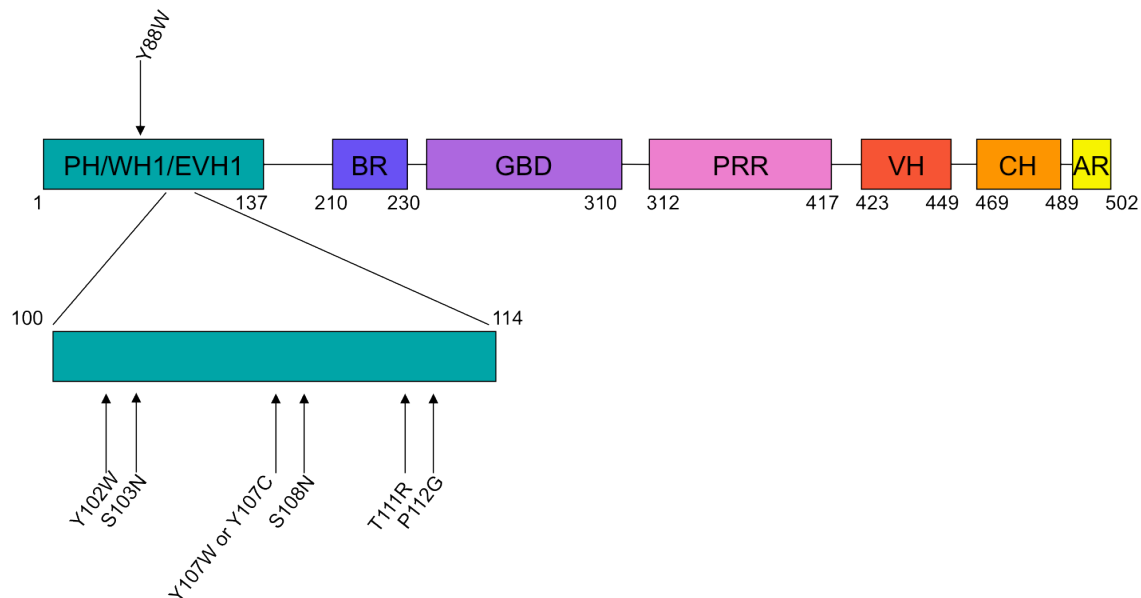


Figure 3.44 Schematic diagram showing all the mutations generated in the WH1 domain of WASP.

WASP^{Y88W/Y102W}, WASP^{Y102W/Y107W}, WASP^{Y102W/T111R/P112G} (WASP^{WRG}) and WASP^{S103N/S108N/T111R/P112G} were fused to GFP and transfected into HEK 293T cells. Similarly, the cells underwent 4 hours of ionomycin treatment and were lysed for Western blot analysis. The Western blot showed that among the mutant WASPs, the expression level of WASP^{WRG} was the highest (Figure 3.45). These mutations were also introduced to the truncated WASP, WASP⁹⁵⁻⁵⁰³ (WASP^{95-503 Y102W/T111R/P112G}). However, the mutations did not increase the stability of WASP and may be because of the shifting of the calpain cleavage site in the WH1 region due to the removal of the first 95 residues of WASP. The mutant WASP^{WRG} was then selected to be used for subsequent studies to analyse the function of calpain and WASP in T cells.

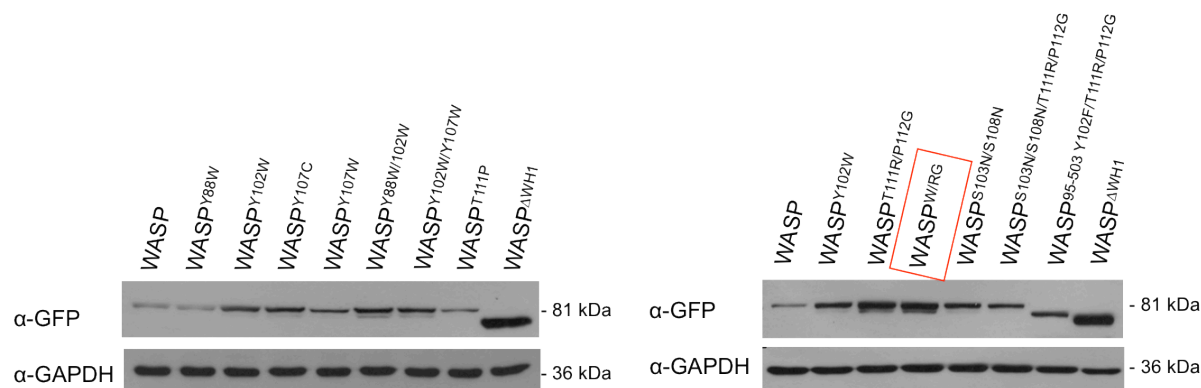


Figure 3.45 WASP with mutations at residues 102, 111 and 112 has reduced proteolysis by calpain.

Western blot analysis of expression of WASP mutants in HEK 293T cells transfected with (1) full length WASP, (2) WASP^{Y88W}, (3) WASP^{Y102W}, (4) WASP^{Y107C}, (5) WASP^{Y107W}, (6) WASP^{Y88W/Y102W}, (7) WASP^{Y102W/Y107W}, (8) WASP^{T111P}, (9) WASP^{T111R/P112G}, (10) WASP^{WRG}, (11) WASP^{S103N/S108N}, (12) WASP^{S103N/S108N/T111R/P112G}, (13) WASP^{95-503 Y102W/T111R/P112G} and WASP^{ΔWH1} (WASP¹³⁸⁻⁵⁰³), using anti GFP (α-GFP) and anti GAPDH (α-GAPDH) as a loading control. The transfected HEK 293T cells were first treated with 1 μg/ml of ionomycin for 4 hours before lysis for western blot analysis.

3.3.8 WASP^{WRG} is resistant to calpain *in vitro*

In order to confirm if WASP^{WRG} is susceptible to calpain degradation, the ability of calpain 1 to cleave purified WASP and WASP^{WRG} was tested using an *in vitro* cleavage assay. GST-WASP95-320 and GST-WASP95-320WRG were purified from *E. coli* (BL21) cells and incubated in cleavage buffer containing calpain 1 and CaCl₂ for 2 hours. Coomassie blue staining revealed that WASP^{WRG} had reduced proteolysis by calpain 1 as compared to WASP (Figure 3.46). This data demonstrates the region of calpain cleavage site in the WH1 region of WASP and the mutant is resistant to calpain proteolysis.

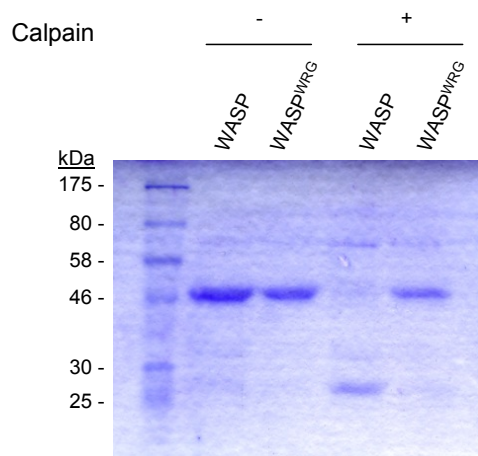


Figure 3.46 WASP^{WRG} is resistant to calpain *in vitro*.

GST-WASP⁹⁵⁻³²⁰ and GST-WASP⁹⁵⁻³²⁰WRG were purified from *E. coli* (BL21) cells after IPTG induction. Purified proteins were incubated with calpain in cleavage buffer containing CaCl₂. Samples were then resolved in a 10% SDS-PAGE gel, followed by staining with Coomassie blue.

3.3.9 WASP^{WRG} mutant adopts an open conformation

The introduction of 3 mutations in the WH1 domain of WASP decreased the level of WASP proteolysis by calpain. They may have an effect on the conformation of WASP. In order to study the effects of the mutations on the calpain-resistant WASP mutant, the BiFC assay was utilized to study its conformation.

WASP reporter (Trp) or WASP^{WRG} (Trp) was transformed together with WIP (Leu) in *S. cerevisiae* cells. The transformants were analysed for fluorescence signals using fluorescence microscopy after selection on SD plates lacking Trp and Leu. Statistical analysis of the fluorescence of 100 cells showed that the average fluorescence signal from WASP^{WRG} cells were lower than signals from cells transformed with WASP (Figure 3.47B), although the transformed cells expressed similar amounts of WASP (Figure

3.47C). This data suggests that the calpain resistant WASP mutant adopts an open conformation.

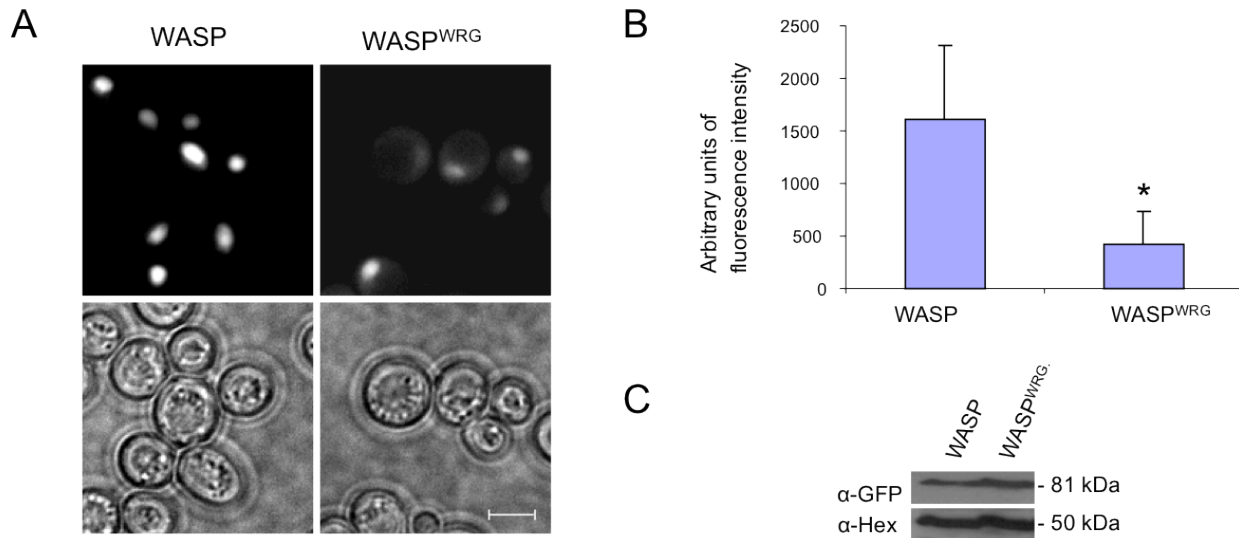


Figure 3.47 WASP^{WRG} mutant adopts an open conformation.

(A) *S. cerevisiae* cells were transformed with WIP (Leu) plasmid together with (1) WASP reporter (Trp) or (2) WASP^{WRG} sensor (Trp) and selected on SD (-Trp-Leu) plates. The transformants were grown to exponential phase at 24°C in selective media and YFP signals in these cells were subsequently analyzed using fluorescence microscopy. Bar = 5 μm.

(B) Fluorescence signal quantification from 100 *S. cerevisiae* cells expressing WIP (Leu) plasmid together with (1) WASP reporter (Trp) or (2) WASP^{WRG} sensor (Trp) using metamorph software.

(C) Western blot analysis of expression of WASP mutant sensors in *S. cerevisiae* cells transformed with WIP (Leu) plasmid together with (1) WASP reporter (Trp) or (2) WASP^{WRG} sensor (Trp) using anti-GFP (α-GFP) and anti-Hexokinase (α-Hex) as a loading control.

3.3.10 WASP^{WRG} mutant is able to form a functional complex with WIP

Additionally, to find out if the 3 mutations can affect the interaction of WASP with WIP, WASP or WASP^{WRG} was transformed into *las17Δ* cells (IDY166) together with WIP. The transformants were streaked on YPUAD plates and were grown at both 24°C and 37°C. The mutations Y102W/T111R/P112G did not affect the ability of WASP to rescue the growth defect of *las17Δ* cells (Figure 3.48), indicating that these mutations do not affect the formation of a functional complex with WIP.

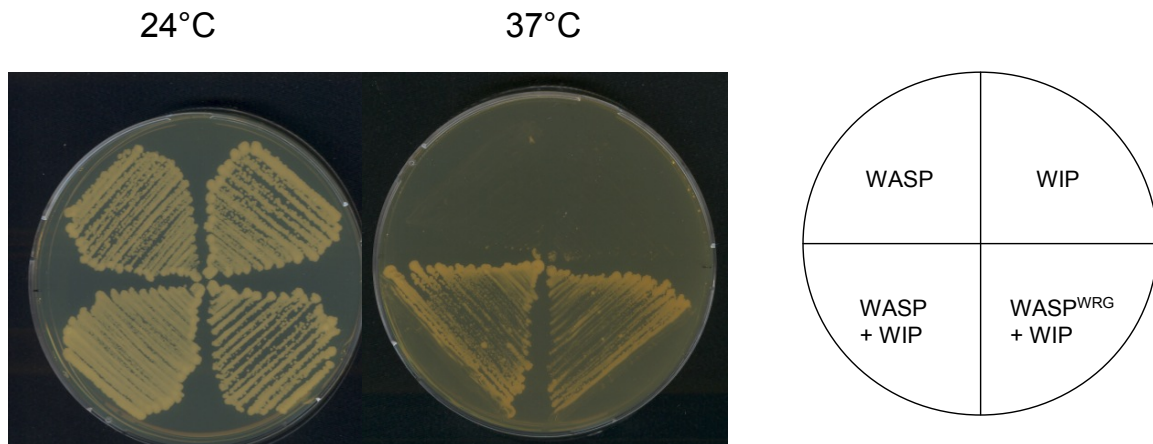


Figure 3.48 Co-expression of both WASP or WASP^{WRG} mutant and WIP suppress the growth defects of *las17Δ* cells.

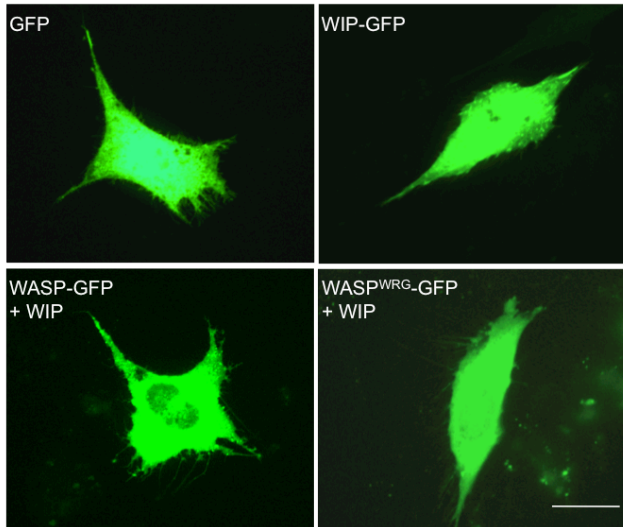
Las17Δ cells (IDY166) were transformed with plasmids expressing (1) WASP alone, (2) WIP alone or WIP together with (3) WASP, (4) WASP^{WRG}. The transformants were streaked on YPUAD plates and grown at both 24°C and 37°C. Photograph was taken after 3 days.

3.3.11 WASP^{WRG} mutant induces filopodia to the same extent as WASP

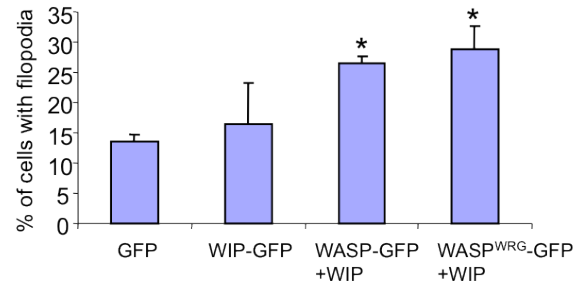
In order to further validate if WASP^{WRG} mutant is functional, filopodia induction by the mutant was assessed in N-WASP^{-/-} fibroblasts. The absence of expression of both WASP and N-WASP in N-WASP^{-/-} fibroblasts provides a simplified environment, where increased filopodia formation could be directly attributed to WASP or the mutant when expressed. WASP-GFP or WASP^{WRG}-GFP was expressed in N-WASP^{-/-} fibroblasts, together with WIP. The WASP^{WRG} mutant caused similar induction of filopodia formation in the fibroblasts with 26.2% compared to WASP, which induced filopodia formation in 27.3% of the cells (Figure 3.49A and B). The expression levels of both WASP and WASP^{WRG} were equal (Figure 3.49C). Membrane projections that were identified as filopodia contained actin. Filopodia were further defined as actin-rich membrane projections with length that is between 8μm to 20μm. This data indicates that

the mutations introduced in the calpain resistant WASP mutant did not affect the ability to induce filopodia formation and this mutant is fully functional.

A



B



C

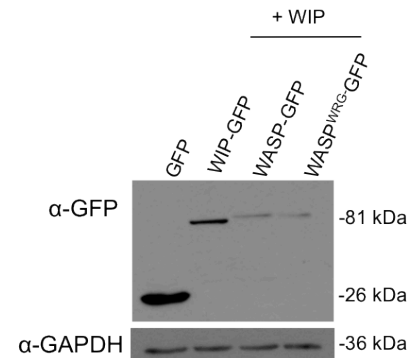


Figure 3.49 WASP^{WRG} mutant induces filopodia comparable to WASP.

(A) N-WASP^{-/-} fibroblasts were transfected with WIP together with (1) WASP-GFP alone (2) WIP-GFP alone, or WIP together with (3) WASP-GFP or (4) WASP^{WRG}-GFP. After 36 hours, cells were analysed for the presence of filopodia. Bar represents 15 μm.

(B) Statistical analysis of 30 random transfected cells for filopodia induction was carried out as described Methods 2.2.3.10. Each experiment was repeated thrice. * P<0.01 compared with cells transfected with only GFP (unpaired student's t-test). A cell was defined as having filopodia (8-20 μm) if it contains 5 or more filopodia.

(C) Western blot analysis of the expression levels of WASP in transfected cells after 36 hours using appropriate antibodies.

3.3.12 Expression of WASP but not WASP^{WRG} rescued impaired migration of WASP-deficient T cells

To determine whether calpain-mediated proteolysis of WASP is crucial for the migration of T cells, the chemotactic responses of Jurkat^{WASPkd} + WASP_R^{WRG} or Jurkat^{WASPkd} + WASP_R, towards SDF-1 α were characterized using the Dunn chamber. RFP, WASP_R-RFP or WASP_R^{WRG}-RFP in neomycin-resistant constructs was microporated in Jurkat^{WASPkd} and cells were selected with G418 for a week. The migration ability of the cells was assayed using the Dunn chamber and time-lapse microscopy. From the results, Jurkat^{WASPkd} + RFP had impaired migration towards the source of the chemokine, similar to the migration of Jurkat^{WASPkd} + WASP_R^{WRG} cells (Figure 3.50). Cells expressing Jurkat^{WASPkd} + WASP_R rescued the impaired migration and chemotaxis of Jurkat^{WASPkd} cells (Figure 3.50). In contrast, expression of Jurkat^{WASPkd} + WASP_R^{WRG} failed to rescue the impairment of the migration and the suppression of the chemotactic response towards SDF-1 α was similar to that of Jurkat^{WASPkd} + RFP cells (Figure 3.50). The migration velocities ($\mu\text{m}/\text{sec}$) of the Jurkat^{WASPkd} + WASP_R^{WRG} were significantly decreased (0.0445 $\mu\text{m}/\text{sec}$) (Figure 3.50B) in comparison to Jurkat^{WASPkd} + WASP_R cells (0.0709 $\mu\text{m}/\text{sec}$). Circular histograms analysing the overall directionality of the cell motility showed that 89.9% of the final positions of the Jurkat^{WASPkd} + WASP_R cells lie in the 80° arc facing the chemokine source while only 21.6% of the Jurkat^{WASPkd} + WASP_R^{WRG} cells migrated to the region (Figure 3.51A). Western blot analysis showed that expressions of WASP_R and WASP_R^{WRG} are equal (Figure 3.51B), indicating that any difference observed is not due to difference in the expression of the proteins. Hence, the data showed that expression of WASP^{WRG} mutant is unable to rescue the impaired cell

motility of Jurkat^{WASP^{KD}} cells towards SDF-1 α . Taken together, these data suggests that the proteolysis of WASP by calpain plays an important role in the cell motility of Jurkat cells.

A

Jurkat^{WASP^{KD}}

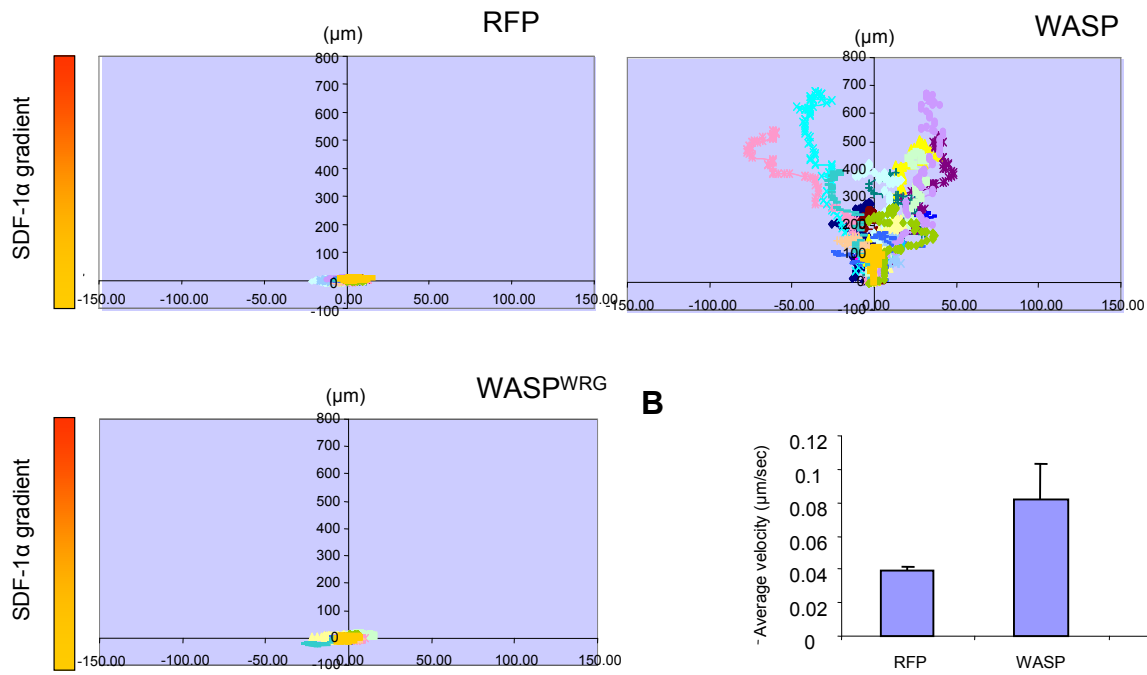


Figure 3.50 Expression of WASP but not WASP^{WRG} mutant rescued impaired migration of Jurkat^{WASP^{KD}} cells (A)

(A) Vector plots of migration paths of 20 randomly chosen cells from WASP knockdown cells expressing RFP, WASP_R-RFP or WASP_R^{WRG}-RFP, exposed to a gradient of SDF-1 α in the Dunn chamber. Time-lapsed images were captured over 50 mins at intervals of 30s. The starting point of each cell is at the intersection of the X and Y axes. The source of SDF-1 α was at the top.

(B) Migration velocity of each cell shown as a mean of velocities of 60 randomly chosen cells (20 cells each from 3 sets of experiments) * P<0.01 compared with WASP_R-RFP cells (unpaired student's t-test).

A

Jurkat^{WASP^{KD}}

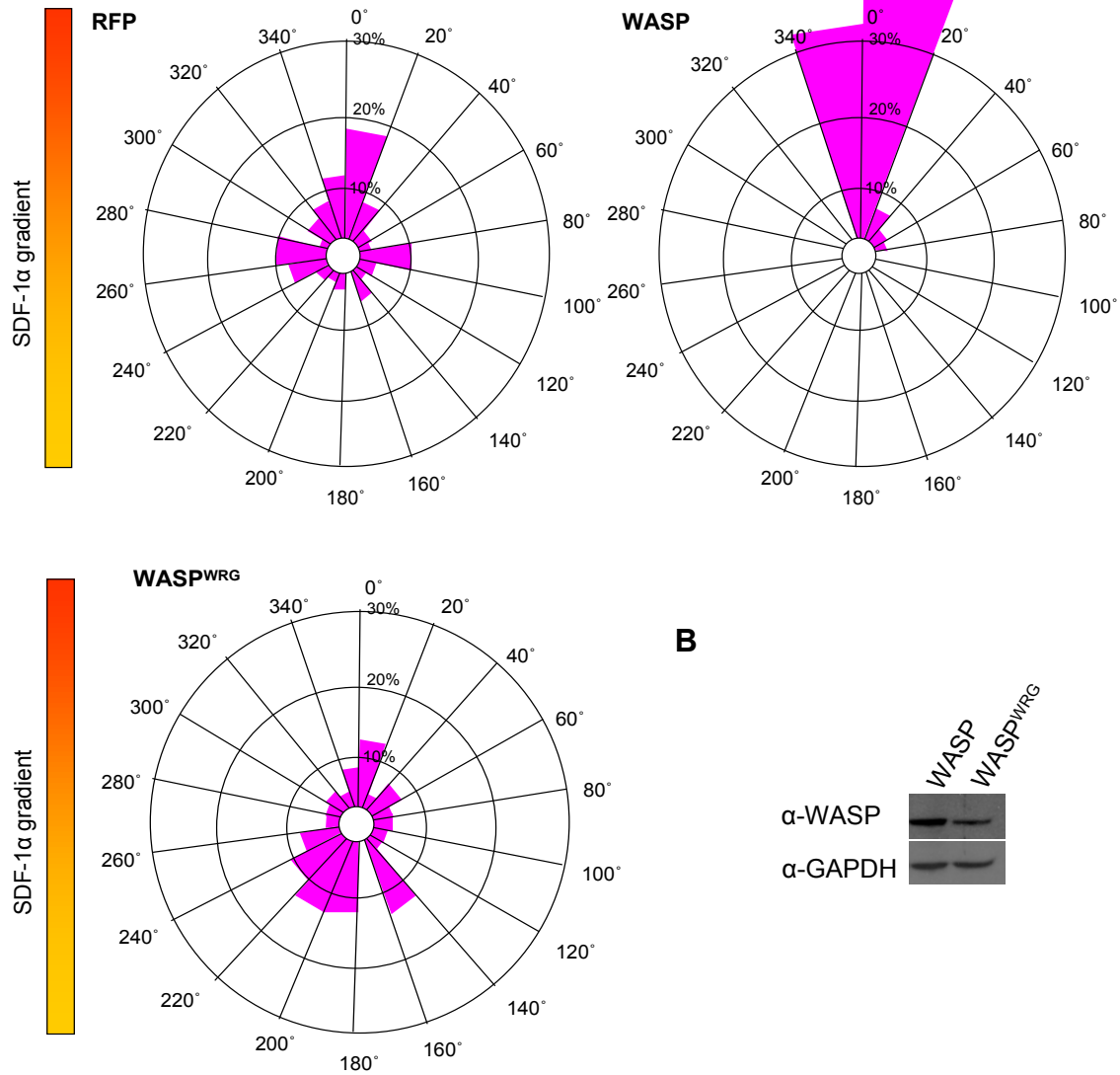


Figure 3.51 Expression of WASP but not WASP^{WRG} mutant rescued impaired migration of Jurkat WASP^{KD} T cells (B)

(A) Circular histograms showing percentage of cells where the final positions of cells lie in each of the sectors (20°). The source of SDF-1α was at the top.

(B) Western blot analysis of the expression levels of WASP in transfected cells after 36 hours using appropriate antibodies.

4. Discussion

4.1 Conformational analysis of WASP

4.1.1 Bi-molecular fluorescence complementation (BiFC)

The BiFC assay has been adopted by many groups to visualize protein interactions or to determine the locations of the protein interactions (Anderie and Schmid, 2007; Hu et al., 2002). This approach is based on the complementation of two halves of a single YFP molecule which are initially non-fluorescence but fluorescence is restored when brought together. The two fragments of YFP can be fused to separate proteins such that when the two proteins interact, the two fragments will be brought closed together and fluorescence emission can occur. However, in this study, the two fragments of YFP are fused separately to the two ends of a single protein. Using this assay, we are able to study the conformational changes of WASP. When WASP adopts an open conformation, the two fragments of YFP cannot complement each other due to the distance and thus, no fluorescence can occur. However, when the conformation is altered such that it now forms a closed conformation, the two fragments are brought together in close proximity, allowing fluorescence emission to be restored (Figure 4.1).

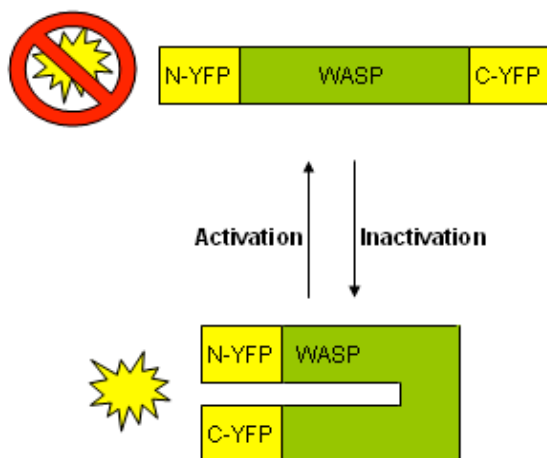


Figure 4.1 Principle of Bi-molecular fluorescence complementation used in this study.

When WASP is in the activated form, the two fragments of YFP are far apart, resulting in no fluorescence. However, when WASP is in the autoinhibition state, the two YFP fragments are brought close together to reconstitute a functional YFP resulting in fluorescence.

4.1.2 WASP adopts an autoinhibited conformation

In the inactivated form, WASP and N-WASP adopts the autoinhibitory conformation in which the GBD domain is in contact with the VCA domain (Kim et al., 2000). Activation of WASP and N-WASP relieves this autoinhibitory contact to allow the binding of actin monomers and the Arp2/3 complex resulting in actin polymerization.

The conformation of N-WASP has been studied previously using a FRET-based approach in which a YFP molecule was fused to the N-terminus while a CFP molecule was fused to the C-terminus (Ward et al., 2004). In the presence of a constitutively active Cdc42 mutant, FRET efficiency was reduced. However, as this study was performed in HEK 293T cells, full complement of N-WASP binding partners exists. Thus, it is difficult to determine if Cdc42 is the direct activator of N-WASP. Hence, conformational change of

WASP was chosen to be studied in *S. cerevisiae* cells which do not contain any of the known interactors of WASP. Also, by using the BiFC method, we can eliminate the problem of sources of non-FRET fluorescence contributing to the background noise in the FRET approach.

As WASP has been shown to be unstable in the cytoplasm of *S. cerevisiae* cells, it was tagged with NLS to be targeted to the nucleus, to prevent degradation by cytoplasmic proteases. Fluorescence signal was observed in the nuclei of *S. cerevisiae* cells expressing WASP reporter (Figure 3.3A). This showed that WASP can adopt an autoinhibited conformation which allowed the reconstitution of a functional YFP. Fluorescence signal observed is due to intramolecular interactions and not intermolecular interactions as cells expressing N-control-WASP (Trp) together with C-control-WASP (Leu) (Figure 3.3A) and did not produce any fluorescence. This is the first instance whereby the whole molecule of WASP is used to examine its conformational changes.

4.1.3 WIP and WIRE stabilize WASP in the autoinhibited conformation

The verprolin family of proteins consists of WIP, WIRE and CR16 which are known to be important effectors for the signaling to the actin cytoskeleton network. These actions are mainly mediated by the WASP family of proteins (Aspenstrom, 2005). All three members share a homologous region near the C-terminus which is important for the binding to the WH1 domain of WASP and N-WASP. Las17p is the yeast homologue of WASP and *S. cerevisiae* cells with the deletion of the gene have been shown to be unable to grow at elevated restrictive temperatures (Li, 1997). WIP together with WASP has

been shown to be able to suppress the growth defects in yeast deficient in Las17p (Rajmohan et al., 2006). However, when WASP alone was expressed or expressed together with CR16, these defects were not suppressed (data not shown).

Many groups have demonstrated that the binding of WIP can stabilize WASP (de la Fuente et al., 2007; Sawa and Takenawa, 2006; Tsuboi, 2007) but the conformation adopted by WASP when bound to WIP is not known. One group has postulated that the interaction between WASP and WIP may stabilize the closed conformation of WASP because WIP slows down the rate of actin polymerization upon Cdc42 activation (Martinez-Quiles et al., 2001).

In this study, expression of WASP reporter together with WIP or WIRE in *S. cerevisiae* cells produced enhanced fluorescence signal from the WASP reporter while co-expression with CR16 had no significant effects (Figure 3.5). Also, similar result was obtained in HEK 293T cells where increased fluorescence from the WASP reporter was observed in the presence of WIP or WIRE but not CR16 (Figure 3.17). This correlates with observations found in previous studies (Rajmohan et al., 2006). This result indicates that WASP is stabilized in the closed conformation when it is in complex with WIP or WIRE but not CR16. This raises an interesting question: Does the WASP molecule in complex with WIP or WIRE activate the Arp2/3 complex? WASP requires WIP for stabilization and cortical localization in *S. cerevisiae* cells (Rajmohan et al., 2006), suggesting that WASP exist in the closed conformation in the cortical patches of the *S.*

cerevisiae cells. This raises the possibility that WASP in the closed conformation, is able to suppress the growth defects of *las17Δ* strain by activating Arp2/3 complex.

4.1.4 Toca1 and Nck1 disrupt the autoinhibitory conformation of WASP

Many reports have provided evidence that the binding of Rho-GTPase Cdc42 to the GBD domain of WASP enables the release of WASP from its autoinhibited conformation, thereby allowing WASP to elicit its function (Kim et al., 2000; Rohatgi et al., 1999). However, more recent findings from Kirschner laboratory have identified a new protein Toca1 that interacts with both Cdc42 and WASP. The signaling pathway proposed is that Toca1 is first required to activate the WASP/N-WASP-WIP complex. Cdc42 in turn interacts with both Toca1 and WASP/N-WASP, leading to Arp2/3 mediated actin polymerization (Ho et al., 2004).

Other SH3-containing proteins like Nck and Grb2 interacts with the PRR region of WASP, regulating actin dynamics. Nck is able to act independently to promote WASP/N-WASP mediated nucleation of actin filaments, suggesting that Nck can regulate the activity of WASP/N-WASP (Rohatgi et al., 2001).

The results in this study has shown that expression of WASP reporter together with Cdc42, with or without WIP in *S. cerevisiae cells* did not lead to a reduction in the fluorescence signal from the WASP reporter (Figure 3.9 and 3.12). On the other hand, Toca1 when expressed with WASP reporter and WIP, was able to reduce the YFP fluorescence from the WASP reporter (Figure 3.12). This data is consistent with the

literature that Toca1 is required for Cdc42 to activate WASP. Interaction of Cdc42 with WASP failed to release the autoinhibitory loop but when Toca1 is bound, WASP changes to an open and active conformation. Nck1 likewise is able to reduce the YFP fluorescence signal from the WASP reporter when expressed together with WASP reporter and WIP (Figure 3.12). This interesting observation further reiterates that Nck1 can act in an independent pathway from Cdc42 (Badour et al., 2003). Thus, SH3 domain-containing proteins like Toca1 and Nck1 are able to bind to WASP, altering its conformation leading to Arp2/3 mediated actin polymerization.

4.1.5 Mutations in WH1, GBD and VCA domains prevent stability of WASP in the closed conformation

Missense, deletion, insertion and nonsense mutations in the WASP gene can give rise to different degree of severity in clinical phenotypes in patients. These include XLT and XLN which are allelic variants of classic WAS with milder phenotypes. Many groups have identified the positions and type of mutations found in these patients (Imai et al., 2003a; Jin et al., 2004). In order to examine how these mutations affect the conformation of WASP, one representative mutant was chosen from each domain to be cloned into the WASP reporter.

YFP fluorescence in WASP^{A134T}, WASP^{L270P} and WASP^{D485N} sensors transformed in *S. cerevisiae* cells were observed to be significantly reduced in the presence of WIP (Figure 3.15). The mutation of Ala134 to Thr occurs in the WH1 domain of WASP which has been reported to cause the classic WAS (Imai et al., 2003a). This mutation affects the

interaction of WIP with WASP (Rajmohan et al., 2006; Stewart et al., 1999), thereby affecting the stability of WASP. The mutation A134T causes WASP to adopt an open conformation as indicated by the BiFC assay. The YFP fluorescence signal from the mutant WASP reporter was not enhanced in the presence of WIP. This suggests that binding of WIP to WASP is essential for the stabilisation of the closed conformation of WASP.

The mutation L270P at the GBD domain has been reported to give rise to the XLN disease. This mutation gives rise to a constitutively active mutant as assayed by in vitro actin polymerization assay (Devriendt et al., 2001). Consistent with the literature, the data in this study showed a decrease in YFP fluorescence signal in the WASP^{L270P} sensor transformed in *S. cerevisiae* cells, in the presence of WIP (Figure 3.15). This suggests that L270P mutation keeps WASP in the constitutively active conformation even when it is bound to WIP.

The mutation Asp485 to Asn in the CH region within the VCA domain has been identified in both WASP and XLT patients. It is likely that the alteration of an acidic residue (Asp) to a neutral residue (Asn) can disrupt the interaction with the basic residues in the BR domain. The reduction in the fluorescence signal from the WASP mutant sensor (Figure 3.15) suggests that this mutation have disrupted the autoinhibitory loop that is formed between the BR-GBD domain and the VCA domain. Deletion of the whole VCA domain was observed to produce the same results. Expression of the WASP^{ΔVCA} sensor in *S. cerevisiae* cells resulted in lower fluorescence signal detected in the nuclei of

the transformants, in the presence of WIP (Figure 3.15). This validates the conclusion that the VCA domain is important to maintain the autoinhibited conformation of WASP.

G187C and P373S mutations in WASP have also been reported in some cases of XLT and WAS patients respectively (Imai et al., 2003a). However, these two mutations did not affect the conformation of WASP (Figure 3.15). This may be due to the locations of the mutations in the BR and PRR region which may not be critical for the formation of the autoinhibitory conformation that is reported to be made between the BR-GBD and VCA domain (Kim et al., 2000). Thus, these two mutations do not affect the conformation of WASP raising the possibility that these mutations cause the diseases because of failure of localization of WASP to areas such as immunological synapses and not because of failure of WASP to adopt an autoinhibited conformation.

4.1.6 N-terminus of WIP interacts with C-terminus of WASP

WASP and WIP function together to play important roles in actin polymerization. WIP regulates WASP-mediated actin polymerization through the regulation of the release from its autoinhibited conformation (Sasahara et al., 2002). Also, WIP has been shown to act as a chaperone of WASP by preventing its degradation (de la Fuente et al., 2007). Recently, Dong et al has also shown that the WIP-WASP complex is required for NFAT activation and the dissociation of WIP and WASP is not required (Dong et al., 2007). Interestingly, BiFC studies in this project revealed that interaction of WIP with WASP, keeps WASP in the close conformation. Deciphering the structural basis of WASP-WIP would thus provide more clues on how WASP and WIP function together.

The N-terminus of WIP has been found to be inhibitory and deletion of this region (1-60 residues) greatly enhanced the NFAT activity in T cells transfected with this mutant, when compared to deletion in other regions of WIP (Dong et al., 2007). The acceptor photobleaching FRET assay in this study revealed that the N-terminus of WIP is in close association with the C-terminus of WASP (Figure 3.20). This indicates that other than the interaction of the WBD domain (C-terminus) of WIP with the WH1 domain (N-terminus) of WASP (Chou et al., 2006), the N-terminus of WIP is also in close proximity of the C-terminus of WASP. Yamaguchi et al has shown that the two tandem V domains in N-WASP is a more potent activator of Arp2/3 complex induced actin polymerization when compared to the single V domain in other WASP family members like WASP (Yamaguchi et al., 2000). Both the VCA domain of WASP and the V domain of WIP bind to actin. If the N-terminus of WIP is in close proximity with the C-terminus of WASP and WASP-WIP forms a functional complex, it could be likely that the V domain in WIP can serve to compensate for the extra V domain that is found in N-WASP but not in WASP. This increases the efficiency of WASP-mediated activation of the Arp2/3 complex (Figure 4.2) in actin polymerisation. Full activation of WASP may take place upon interaction of other proteins like Cdc42 and Toca1. However, further studies are required to elucidate the mechanism of WASP-WIP mediated actin polymerization.

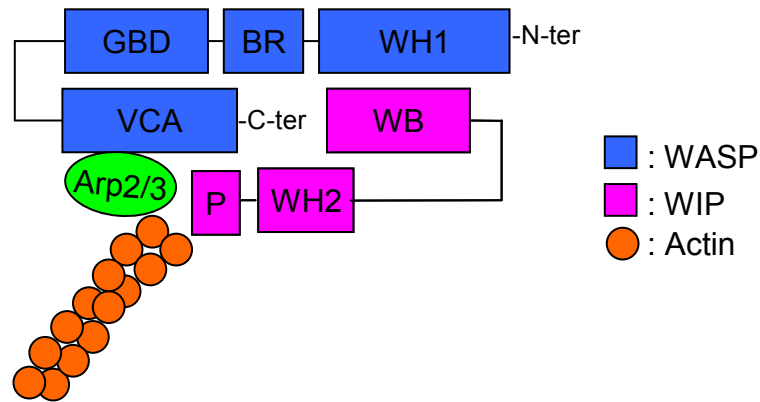


Figure 4.2 A model of WASP-WIP interaction.

4.2 Role of phosphorylation of Tyr291 in the regulation of WASP

Mutations in WASP that cause decreased WASP activity are associated with the Wiskott Aldrich syndrome and X-linked thrombocytopenia. On the other hand, mutations that induce enhanced WASP activity are linked to X-linked neutropenia (Ancliff et al., 2006; Beel et al., 2009; Devriendt et al., 2001). This suggests the importance of the precise regulation of WASP *in vivo*, which would otherwise manifest into different clinical phenotypes.

The most widely studied mechanism of WASP activation is through the interaction of Cdc42, which acts cooperatively with PIP₂ (Aspenstrom et al., 1996; Higgs and Pollard, 2000; Symons et al., 1996). However, contradictory findings from other groups showed that Cdc42-independent mechanisms of WASP activation also exist (Badour et al., 2004a). One possible mode of activation is through the SH3 containing protein, Nck which mediates the activation and recruitment of WASP to immunological synapse independent of Cdc42 (Zeng et al., 2003). Phosphorylation of WASP on residue Y291

has also been identified to be one of the crucial mechanisms, which regulate the activity of WASP. Introduction of a negatively charged phosphate group is thought to destabilize the autoinhibitory loop formed by the GBD and VCA domain. Many kinases have been described to phosphorylate Y291 in WASP, including BTK (Baba et al., 1999) and HCK (Cory et al., 2002a). BTK is a member of the Tec family of tyrosine kinases and its expression is limited to the B cells. It is involved in the pathogenesis of B cell deficiencies (Tsukada et al., 1993). HCK belongs to the Src family of kinases and is only expressed in the hemotopoietic cells. HCK functions to regulate actin-dependent processes such as adhesion and filopodia formation (Suen et al., 1999). These two kinases have been shown to be implicated in the regulation of WASP. However, it is unclear whether Cdc42 interaction is a requirement for the access of kinases to Y291 for the phosphorylation of WASP. The hierarchy of events leading to the activation of WASP still remains debatable.

Three mutations that render a constitutively active WASP have been identified in XLN namely, L270P, S272P and I294T (Westerberg et al., 2010). These three mutations are located in the GBD domain. When WASP is in a closed conformation, the GBD domain binds to the VCA domain of WASP, preventing the binding of the Arp2/3 complex. Cdc42 interacts with WASP through the binding of the GBD domain, disrupting the autoinhibitory loop. This releases the VCA domain, allowing the binding of Arp2/3 complex and G-actin, leading to actin polymerization. Mutations within the GBD domain eg. L270P has been shown to result in the failure of autoinhibition (Thrasher, 2002). To study how phosphorylation of WASP can be affected in XLN, the mutation L270P was

selected to be used. In this study, the roles of phosphorylation in WASP^{L270P} have been addressed through the use of a phosphomimetic and non-phosphorylatable mutation at residue Y291, Y291E and Y291F respectively. Although these mutations alter the charge of the residues, they do not disrupt the binding of interactors such as Cdc42. The results (Section 3.2) in this study indicate the importance of phosphorylation in the regulation of WASP^{L270P}, through the conformation of WASP and in T cell functions.

4.2.1 Differential phosphorylation of WASP^{L270P} by different kinases

Many members of the Src family of kinases have been shown to phosphorylate WASP, including HCK (Cory et al., 2002b), Fyn (Badour et al., 2004a) and Lyn (Guinamard et al., 1998). Another group of kinases, Tec family tyrosine kinases including BTK (Baba et al., 1999) and Itk (Bunnell et al., 1996), have also been shown to interact with WASP. To determine the ability of the Src kinases and Tec kinases to phosphorylate WASP, five kinases were selected to study the phosphorylation levels of WASP or WASP^{L270P}, namely BTK, HCK, Tec, ITK and Fyn. From the results, increased phosphorylation in the presence of L270P in WASP was observed in cells co-expressing BTK, HCK or Tec but not when co-expressed with either ITK or Fyn (Figure 3.22).

The decreased tyrosine phosphorylation levels of WASP with Y291F or Y291E mutation shows that both BTK and HCK phosphorylates WASP on Y291 residue (Figure 3.22 and 3.23) correlating with existing literature (Baba et al., 1999; Cory et al., 2002b). BTK is only found in B lymphocytes and is important in normal B lymphocytes development (Tsukada et al., 1993), while expression of HCK is limited to hematopoietic cells, similar

to WASP. HCK has been shown to regulate chemotaxis of monocytes (Resnati et al., 1996), phagocytosis (Ghazizadeh et al., 1994) and adhesion of macrophages (Scholz et al., 2000). BTK and HCK induced phosphorylation of WASP were hypothesized to regulate WASP and promote actin polymerization activity in these cells. To substantiate this conclusion, the kinase assay in the yeast, in the presence and absence of WIP must be performed. Unfortunately, these experiments were not performed due to time constraints. The presence of the mutation L270P abolishes the requirement of Cdc42 to destabilise the GBD-VCA domain. As WASP^{L270P} adopts an open conformation (Figure 3.21), the accessibility of kinases to Tyr residues in WASP is increased. As predicted, in the presence of the kinases, BTK, HCK and Tec, increased tyrosine phosphorylation of WASP^{L270P} was detected as compared to WASP (Figure 3.22). To determine if Y291 is the target residue for phosphorylation in WASP^{L270P}, Y291F mutation that was non-phosphorylatable was introduced in WASP^{L270P}. The decrease in tyrosine phosphorylation levels observed in WASP^{LP/YF} indicates that the increased in phosphorylation levels in WASP^{L270P} by both HCK and BTK (Figure 3.22 and 3.23) was due to phosphorylated Y291. Similarly results were obtained for WASP^{LP/YE}.

4.2.2 Phosphorylation affects the conformation of WASP

The introduction of a negatively charged phosphate group potentially destabilizes the autoinhibitory loop formed between the BR-GBD and VCA domains of WASP and facilitates the binding of Arp2/3 complex and actin polymerization. In correlation to this, the phosphomimetic mutation Y291E caused a decrease in fluorescence signal produced by the WASP reporter in comparison to WASP. Conversely, the non-phosphorylatable

mutation Y291F causes the mutant WASP reporter to adopt a conformation similar to WASP reporter, as both produced similar levels of YFP fluorescence. This is because Tyr291 residue lies in the GBD domain of WASP and when WASP is in the autoinhibitory conformation, Tyr291 is located at the interface of two hydrophobic sheets (Cory et al., 2002b). Introduction of a negatively charged group, like the phosphate group, can destabilize the autoinhibited loop formed through the interaction of the BR-GBD and VCA domain (Kim et al., 2000). The introduced phenylalanine (F) residue at 291 would be buried between the two hydrophobic sheets. This verifies previous findings that phosphorylation causes the unfolding of WASP, releasing the VCA domain for Arp2/3 binding (Torres and Rosen, 2006).

WASP^{L270P} adopts an open conformation and is constitutively active. The introduction of the additional mutation Y291E however, did not lead to further decrease in the signal produced by WASP^{LP/YE} sensor (Figure 3.25). It could be due to the fact that WASP^{L270P} is already in an open conformation and the mutation Y291E had no further effect on the conformation of WASP. Similar fluorescence levels were observed in cells when Y291F was introduced in WASP^{L270P} (WASP^{LP/YF}) sensor (Figure 3.25), as compared to WASP^{L270P} and WASP^{LP/YE} sensors. L270 lies in the hydrophobic core of the GBD-VCA domain, when WASP is in the closed conformation (Devriendt et al., 2001) and it is likely that the substitution of L270 by proline increases the instability of the closed conformation of WASP. The open conformation of WASP^{L270P} increases the accessibility of kinases to its Tyr residues. These results suggest that phosphorylation keeps WASP in an open conformation but may not be essential to maintain the open conformation of

WASP^{L270P}. This may provide the explanation why the WASP^{Y291F} should adopt a close conformation as seen in the yeast BiFC assay (Figure 3.25).

4.2.3 Dysregulation of phosphorylation in WASP with mutation associated with XLN leads to defects in T cell migration

Three mutations, L270P, S272P and I294T that are located in the GBD domain of WASP have been identified to be responsible in causing XLN in patients (Ancliff et al., 2006; Beel et al., 2009; Devriendt et al., 2001). These mutations disrupt the autoinhibited conformation of WASP, causing increased actin polymerization (Ancliff et al., 2006; Beel et al., 2009; Devriendt et al., 2001). The symptoms of XLN include severe neutropenia, frequent bacterial infections and myelocytopenia caused by myelopoiesis arrest (Westerberg et al., 2010). The pathology and the complexity of the symptoms arising from the 3 mutations cannot be easily elucidated. This study focuses on how dysregulation of phosphorylation in WASP with an activating mutation, L270P, in T cells can be a possible mechanism in the pathology of XLN.

The actin cytoskeleton plays a central role in T cell morphology, adhesion and motility, which are important processes in the homing of T cells to tissues. The presence of WASP is crucial in the reorganization of the actin cytoskeleton in T lymphocytes and is found to play essential roles, together with WIP, in T cell chemotaxis and homing (Gallego et al., 2006). Recently, the covalent modification of Y291 in WASP by phosphorylation has emerged as an important level of regulation of WASP activity. The synthetic phosphomimicking mutant Y291E has been shown to enhance actin polymerization and

filopodia formation in macrophages (Cory et al., 2002b). Also, tyrosine phosphorylation has been reported to be required for T cell activation (Badour et al., 2004b).

In this study, Jurkat^{WASPkd} cells + WASP_R^{Y291F} cells behaved in a similar manner as Jurkat^{WASPkd} + RFP cells. Both of the cells, Jurkat^{WASPkd} cells and Jurkat^{WASPkd} cells + WASP_R^{Y291F} cells, displayed minimal movement towards SDF-1 α (Figure 3.32). The mutation Y291E rescued the impaired migration of Jurkat^{WASPkd} cells partially (Figure 3.32). The average velocities of the Jurkat^{WASPkd} + WASP_R^{Y291E} cells were increased minimally and overall directionality of the cells were more random than Jurkat^{WASPkd} + WASP_R (Figure 3.32). This result suggests that many levels of regulations of WASP exist and phosphorylation/dephosphorylation only acts as one of which that increase WASP activity.

The average velocities of Jurkat^{WASPkd} + WASP_R^{L270P} cells were similar to Jurkat^{WASPkd} + WASP_R cells (Figure 3.34). However, overall directionality of the cells was more random than Jurkat^{WASPkd} + WASP_R (Figure 3.33), indicating that WASP^{L270P} is unable to fully rescue the defects in the chemotaxis of Jurkat WASP^{KD} T cells. WASP^{L270P} suppressed the growth defects of *las17 Δ* strain in the presence of WIP (Figure 3.26) and is localized to the cortical patches (data not shown) in the yeast cells, indicating that WASP^{L270P} is able to form a functional complex with WIP. This suggests that although L270P is an activating mutation in WASP, the effect it exerts on the cells is not the same as WT WASP. This may in part be a contributing factor in the pathology of XLN caused by the point mutation, L270P. Tyrosine phosphorylation levels in both WASP^{LP/YF} and

WASP^{LP/YE} were reduced to a negligible level, indicating that the major phosphorylation site in WASP^{L270P} is at Y291 (Figure 3.23 and 3.24). The coupling of Y291F mutation to WASP^{L270P} decreased the chemotactic response and velocities of Jurkat WASP^{kd} + WASP^{LP/YF} cells towards SDF-1 α compared to Jurkat WASP^{kd} + WASP^{L270P} cells (Figure 3.33 and 3.34). Although mutations LP/YE rescued the impairment of cell motility, it was not as significant as L270P alone.

The analysis of the ability of the phosphorylation mutations in WASP to induce filopodia formation in N-WASP^{-/-} fibroblasts showed that phosphomimetic mutation (Y291E) increases filopodia formation while the non-phosphorylatable mutation (Y291F) did not lead to increase in filopodia formation (Results 3.35). This correlates with studies done by another group in which Y291E increased filopodia formation in macrophages (Cory et al., 2002b). These observations suggest that phosphorylation in Y291 enhances the ability of WASP to stimulate filopodia formation. However, the extent of induced filopodia was not as pronounced as cells that had expression of WASP^{L270P}. WASP^{LP/YF} induced significantly less filopodia in the fibroblasts than WASP^{L270P}. The combination of the two mutations L270P/Y291E caused decreased filopodia formation when compared to L270P, but was still higher than induction by Y291E (Results 3.35). This suggests that the increased activity of WASP^{L270P} may be attributed to more factors other than phosphorylation.

One major disadvantage of using phosphomimetic mutation is that it may not represent the phosphorylation process in its entirety. Both phosphorylation and dephosphorylation

may be needed in the regulation of cellular processes. Moreover, kinases like the Src family of kinases contain both SH3 and SH2 domains. The SH2 domain of Src kinase was reported to have a significant affinity for the phosphorylated GBD domain (Torres and Rosen, 2006). Binding of the SH2 could further aid in the disruption of the GBD-VCA domains. A phosphomimetic mutation may fail to emulate the interaction of the SH2 domains to the GBD domain in WASP. Nonetheless, the phosphomimetic mutation does not interfere with the interaction of other crucial factors like Cdc42. The activity of WASP may require cyclical phosphorylation and dephosphorylation and introducing the phosphomimicking mutation, Y291E cannot emulate this. This may explain the dampened effects of the mutation Y291E on WASP in chemotaxis response of Jurkat cells towards SDF-1 α and the filopodia induction in N-WASP^{-/-} cells.

To draw this conclusion, it is necessary to establish all the conditions under which WASP can be phosphorylated. The critical aspect of whether WASP phosphorylation is WIP dependent is not established in this study. It is a dilemma whether WASP can be phosphorylated in the WASP-WIP complex where WASP adopts a closed conformation. While the WIP-WASP complex leads to actin polymerization, the phosphorylation of WASP may serve as another function if WASP prevents WASP from being phosphorylated by HCK (BTK). The characteristic of the WASP^{Y291F} mutant could provide an important clue.

In summary, the results from this study suggest that both WASP and WASP^{L270P} are phosphorylated by different kinases and proper regulation of the phosphorylation levels

of WASP is important for the chemotaxis of Jurkat cells and filopodia formation. The absence of phosphorylatable WASP in Jurkat cells impairs cell motility and directionality toward SDF-1 α , and also the ability to stimulate filopodia formation in fibroblasts. The results also indicate that increased phosphorylation levels in WASP^{L270P} is one of the factors that induces a constitutively active WASP, affecting chemotactic responses and filopodia formation. Other than disrupting the autoinhibitory conformation of WASP, phosphorylation may play other roles like regulating the interaction of the SH2 domain of proteins with the GBD domain of WASP.

In conclusion, phosphorylation plays an important role in the regulation of the activity of WASP, which is required for proper cell migration, and formation of membrane protrusions. Failure in the proper regulation of phosphorylation in WASP directly impacts proper cell functions for eg. homing of T cells, which can manifest into symptoms observed in XLN patients. The enhancement of phosphorylation by the XLN mutation is probably a cause of the disease.

4.3 Function of Calpain-mediated proteolysis of WASP

4.3.1 Role of WASP and calpain in cell motility

Polarised cell motility in response to a stimulus is important for both immune and pathological processes. Regulated formation of membrane protrusions like lamellipodia and filopodia towards the stimulus is needed for the cell to propel itself forward in the correct direction. Calpains, which are a family of calcium-dependent cysteine proteases, regulate these membrane protrusions by regulating the actin cytoskeleton near the cell

membrane. Calpain knockdown cells display altered morphology, with increased filopodia observed, and reduction in cell migration (Wu et al., 2006). Cytoskeletal proteins like cortactin, talin and FAK are substrates of calpain and proteolysis of these substrates have been shown to be critical for proper regulation of cell migration (Chan et al., 2010; Franco et al., 2004; Perrin et al., 2006). This indicates that the regulation or turnover of these cytoskeletal proteins and focal adhesion components is critical in cell motility.

Both calpain and WASP have been thought to play important roles in cell motility in the immune response. Calpain regulates T cell adhesion and spreading (Glading et al., 2002; Rock et al., 2000) and WASP plays an essential role in the assembly of adhesion structures like podosomes in hematopoietic cells like macrophages, dendritic cells and osteoclasts (Burns et al., 2001; Calle et al., 2004; Linder et al., 1999). Through calpain inhibition studies, WASP has been identified to be a substrate of calpain (Calle et al., 2006b). However, whether calpain-mediated proteolysis of WASP is critical for membrane protrusion dynamics or cell motility has yet to be defined. Here, direct evidence shows that proteolysis of WASP by calpain regulates T cell migration.

4.3.2 Calpain proteolysis of WASP

The putative preferred calpain cleavage site of WASP was mapped by narrowing down the region in WH1 domain using deletion constructs of WASP (Figure 3.38). WIP has been reported to act as a chaperone for WASP and prevents its degradation by calpain (de la Fuente et al., 2007). This suggests that the preferred calpain cleavage site in WASP

would most likely lie in the region crucial for interaction between the two proteins. Hence, yeast two hybrid assays were performed to check for the interaction between the truncated WASP mutants and WIP to identify the region in the WH1 domain, which was protected by WIP (Figure 3.38). Finally, using site directed mutagenesis experiments, a WASP mutant (WASP^{Y102W/T111R/P112G}/ WASP^{WRG}) that was resistant to calpain was generated (Figure 3.45). Calpain-resistant WASP (WASP^{WRG}) contained three mutations; Y102W, T111R and P112G, located in the WH1 domain. Tyr291 has been mutated to Trp as Trp residues have nil occurrences at the P₁ position of the calpain cleavage site. Trp111 and Pro112 have been mutated to Arg and Gly respectively, according to residues found in N-WASP at the same positions. These mutations have not been found in WAS, XLN or XLT patients or known to cause any of the WAS associated phenotypes (Imai et al., 2003b). A WASP mutant whose expression that was as stable WASP^{ΔWH1} could not be achieved, possible explanations include the existence of more than one cleavage site in the WH1 domain or that the introduction of mutations shifted the preferred calpain cleavage sites. However, a mutant version of WASP with point mutations was preferred over a truncated WASP mutant because minimal biochemical properties differences between the WASP and mutant WASP was required to achieve a more realistic study. Despite the difference in stability between WASP^{WRG} and WASP^{ΔWH1}, phenotypic differences in the cells transfected with the two constructs could still be observed. Unfortunately, GST-WASP could not be expressed, which would have been useful in the study of the calpain cleavage of WASP. This could be because of the presence of secondary structures in the mRNA that inhibited translation or aggregation of misfolded protein in insoluble inclusion bodies (Baneyx, 1999).

The deletion of *las17* (yeast homologue of WASP) in *S. cerevisiae* cells causes it to be unable to grow at elevated restrictive temperatures (Li, 1997). However, suppression of the growth defect can be achieved by expression of human WASP together with human WIP in the *las17Δ* cells. Furthermore, the VCA domain of WASP and the V domain of WIP is crucial to suppress the growth defects, suggesting that WASP and WIP have to form a functional complex for actin polymerization in order to suppress the growth defects of *las17Δ* cells. The calpain-resistant WASP mutant retained its ability to rescue the growth defect of *las17Δ* cells together with WIP (Figure 3.48), indicating that like WT WASP, the mutant is able to form a functional complex with WIP. Filopodia formation induced by the mutant is also similar to the WT WASP (Figure 3.48). Thus, although the calpain-resistant WASP mutant has reduced proteolysis by calpain, it retained similar properties with the WT WASP.

The BiFC assay revealed that the WASP^{WRG} mutant adopts a more open conformation than WASP (Figure 3.47). However, despite of the difference in conformation, phenotypic differences could still be observed between them.

WASP degradation has been demonstrated to be effected by both calpain and proteasome. Inhibition of proteasome or calpain by their respective inhibitors increased the expression levels of WASP in activated T cells (de la Fuente et al., 2007). It is possible that the two system of degradation serve to complement each other. One group has shown that inhibition of proteasome activity reduced calpain-mediated protein degradation (Smith and Dodd, 2007). Furthermore, activation of calpain significantly increased the

proteolysis of proteins by proteasome (Smith and Dodd, 2007). These results indicate the dependency of proteasome activity by calpain and vice versa. It would be interesting to study the mechanism of WASP degradation by both calpain and proteasome. Sequential proteolytic pathways may act as an additional level of regulation of WASP activity.

The minimal fragment of WIP that was required for WIP-WASP interaction was not sufficient to protect WASP from calpain proteolysis (de la Fuente et al., 2007), suggesting the possibility that there may be other regions in WIP that prevents WASP degradation from calpain. The FRET assay utilized to study WASP-WIP interaction in this study demonstrated that the N-terminus of WIP interacts with the C-terminus of WASP (Results 3.1.8). Hence, other than the conventionally known interaction between the C-terminus (WBD domain) of WIP and the N-terminus (WH1 domain) of WASP, interaction of the N-terminus of WIP with the C-terminus of WASP may also serve as another level of regulation of WASP degradation.

4.3.3 Role of Calpain-mediated proteolysis of WASP in cell motility

In this study, a calpain cleavage site of WASP was mapped in the WH1 region and mutations were introduced in the region to generate a calpain-resistant WASP mutant. Expression of WASP but not calpain-resistant WASP (WASP^{WRG}) restored the defect in T cell migration in WASP knock down Jurkat cells (Figure 3.50).

Cell migration is a process that is comprised of a series of steps; the first is the polarised extension of a membrane protrusion followed by the stable attachment of the leading

edge of the protrusion that includes the formation of focal complexes and focal adhesions. The cell body then contracts, and with the release of the rear end of the cell, the cell moves forward. Calpain plays multiple roles in the cell migration process and may be involved in each step of the process. The importance of calpain in the initial step of migration where cell spreading and formation of forward extension protrusions was demonstrated by a group which showed that formation of lamellipodia and filopodia formation was reduced in fibroblasts when the cells were treated with calpain inhibitors (Potter et al., 1998). Also, when calpain activity was inhibited in CHO cells, an extended morphology was adopted by the cells, with many of them having elongated tails. This indicates the role calpain plays in regulating the release of the rear ends of these cells, most likely through the dissolution of the focal adhesions (Huttenlocher et al., 1997). These results suggest that calpain is crucial for the regulation of the multiple steps in cell migration.

The Rho-family GTPases, including Rho, Rac and Cdc42, play important roles in cell migration through the reorganisation of the actin cytoskeleton. Rho GTPase stimulates the formation of stress fibres which are required for cell contraction while Rac GTPase promotes the formation of lamellipodia and Cdc42 regulates formation of filopodia (Hall, 2005). Both lamellipodia and filopodia are necessary for the initial step of cell migration. These proteins stimulate the formation of the different types of membrane protrusions via actin nucleators like the Arp2/3 complex. Nucleation promoting factors (NPFs) like the WASP family of proteins act as an intermediate between the RhoGTPases and Arp2/3 complex. Together, the Rho-family GTPase and the WASP family members regulate the

dynamics of actin cytoskeleton reorganisation, which drives the formation of the membrane protrusions crucial to the migration of the cell.

From the results, it can be concluded that calpain-mediated proteolysis of WASP is involved in the tight regulation of the cell migration process. Other than WASP, many other cytoskeletal proteins involved in membrane protrusions like WAVE1,2,3 and cortactin have been reported to be proteolysed by calpain as well (Oda et al., 2005; Perrin et al., 2006). It is likely that calpain-mediated proteolysis of these substrates regulates the proper turnover of the actin-based protrusions like filopodia and hence cell migration.

The two major isoforms of the calpain family are μ -calpain (calpain 1) and m-calpain (calpain 2). Based on previous findings, μ -calpain is activated by 5–50 μ M of intracellular calcium levels while m-calpain is activated by 0.2–1 mM of calcium levels. Moreover, these two members appear to have different spatial distributions and specificities for substrates in different cell types (Moraczewski et al., 1996; Wu et al., 2006). These findings suggest that μ -calpain and m-calpain have different modes of activation and may play distinctive roles in the different cell types. Both isoforms are present in Jurkat T cells and may be expressed at different levels. However, this study did not address the specificity of the calpain subtype that was involved in the cleavage of WASP. The lack of inhibitors for specific calpain isoform limits the elucidation of the subtype that is involved in the cleavage of WASP and cell migration. Further studies like RNAi targeting specific isoforms of calpain can be used to address this issue.

SDF-1 α is a member of the CXC family of chemokines and is a ligand for the chemokine receptor CXCR4 (Loetscher et al., 1994). Both SDF-1 α and CXCR4 are widely expressed in many tissues. SDF-1 α is a potent chemoattractant for many cell types, including monocytes and CD34⁺ human progenitors and is involved in the homing and trafficking of these cells (Aiuti et al., 1997; Luster, 1998). In this study, overexpression of calpain-resistant WASP mutant in WASP-deficient T cells did not rescue the impaired motility towards stromal cell-derived factor 1 α (SDF-1 α) unlike WASP. In addition, the intracellular concentration of Ca²⁺ has been demonstrated to increase in response to SDF-1 α (CXCL12) by another group (Bach et al., 2007). This provides evidence that calpain is involved in the chemotaxis of Jurkat T cells in response to SDF-1 α through the proteolysis of WASP. Besides SDF-1 α , chemotactic responses of T cells towards chemokine CCL2 have also been reported and calpain has been shown to be involved in the process (Butler et al., 2009).

Taken together, this study demonstrates a novel role of calpain-mediated proteolysis of WASP in T cell migration. Cleavage of the WH1 domain between residues 102 to 112 of WASP, but not other regions, by calpain is critical for the chemotaxis of Jurkat T cells towards SDF-1 α .

4.4 Future Directions

Expression of WASP^{WRG} in Jurkat^{WASPkd} cells did not rescue the impaired migration of the cells unlike WASP. There could be a possibility that it is because WASP^{WRG} did not complement or was not functional in the Jurkat^{WASPkd} cells. In order to verify this,

WASP^{WRG} could be overexpressed in Jurkat cells. If expression of WASP^{WRG} leads to impairment in the migration ability of the cells, it would confirm that calpain-mediated proteolysis of WASP is crucial for T cell migration.

More assays such as adhesion assay and spreading assay of Jurkat^{WASPkd} cells expressing WASP^{WRG} could be performed to further analyse if adhesion and spreading of Jurkat^{WASPkd} cells expressing WASP^{WRG} could also be affected. Similarly, these assays could also be done for Jurkat^{WASPkd} cells expressing WASP^{L270P} and the phosphorylation mutants to enable a deeper understanding of how the migration of T cells are affected by the XLN-related mutation.

Besides T cells, WASP is also expressed in other hematopoietic cells. Both phosphorylation and calpain-mediated proteolysis of WASP should also be studied in these cells eg dendritic cells, macrophages and B cells. It would also be interesting to elucidate how calpain and proteasome degradation of WASP complement each other and how these systems are coordinated.

The regulation of WASP is hierarchical, in which two layers of regulation exist. The first layer is the allosteric regulation, which occurs through the formation of the inhibitory loop formed between the VCA domain and the BR-GBD domain of WASP. The second layer of regulation is the dimerization of WASP, which enhances the activation of the Arp2/3 complex significantly. It would be interesting to study how phosphorylation and calpain-proteolysis of WASP affect its dimerization or oligomerisation.

4.5 Conclusion

WASP is an important regulator of the actin cytoskeleton and deficiency or dysregulation of this protein causes WAS which is associated with a myriad of defects in cellular processes in the hematopoietic cells. The regulation of WASP activity is achieved through the regulation of its conformation. WASP adopts a closed conformation when the VCA domain is in contact with the GBD domain, forming an autoinhibitory loop. In this study, a BiFC assay was first established to study the conformation of WASP. Using this assay, two aspects of the regulation of WASP were also further studied in detail; phosphorylation and calpain degradation of WASP.

In this study, the BiFC assay has been used to analyse the regulation of the conformation of WASP upon interaction with its cytoplasmic partners. WASP is shown to be in a closed conformation and this conformation is stabilized by WIP and WIRE but not CR16, even though all three proteins bind to WASP. In this conformation, the V domain of WIP is in close proximity to the VCA domain in WASP, as determined by the FRET assay. Toca1 and Nck, on the other hand, cause WASP to adopt an open conformation even in the presence of WIP, leading to a more efficient activation of the Arp2/3 complex. Cdc42 surprisingly did not open the conformation of WASP, suggesting the need of Cdc42 to work synergistically with Toca1 to activate WASP.

There were some differences between the BiFC assays done in the different cell types; yeast (*S. cerevisiae*) and mammalian (HEK 293T) cells. The WASP reporter and verprolin constructs used in the yeast cells contained an additional NLS fused to the N-

terminal YFP fragment to target the proteins to the nucleus of the cells. In contrast, WASP reporter and verprolin constructs used in mammalian cells do not contain NLS. Additionally, the verprolin constructs used in mammalian cells contained His-tags to allow analysis of the expression levels of the verprolins, while the verprolins used in the yeast cells were not fused with His tags. Besides these differences, the yeast and mammalian cells have their intrinsic differences. Regulators of WASP (WIP, WIRE, CR16, Toca1, Nck1) are not present in the yeast cells, unlike the HEK293T cells, which provides a more accurate study of the regulation of WASP by the verprolins or interactors that were transformed together with WASP into the yeast cells. Despite these differences, studies on WASP done in the yeast cells provide a simplistic view of the complicated network of proteins in the mammalian cells. Despite these differences, the data from the BiFC assay in yeast cells can be extrapolated to the mammalian cells but it should be noted that in mammalian cells, there are many levels of regulation of WASP, tightly regulating its activity.

The mutation L270P has been identified as one of the mutation that causes XLN. Using this constitutively active mutation L270P, the effects of phosphorylation on WASP was studied to investigate if the increase in phosphorylation in WASP^{L270P} is one of the mechanisms causing XLN. BiFC assay showed that WASP^{L270P} is in an open conformation even in the presence of WIP. In this conformation, WASP^{L270P} is phosphorylated more efficiently by kinases, which may lead to more efficient activation of the Arp2/3 complex. Analysis of WASP phosphorylation in WASP^{L270P}, in the regulation of T cell motility and filopodia induction was conducted, using the

phosphomimetic mutation Y291E and non-phosphorylatable mutation Y291F. The importance of proper regulation by phosphorylation in WASP^{L270P} was evident in the impaired chemotactic response of the WASP^{L270P/Y291F} in the Jurkat^{WASPkd} cells and the filopodia formation in fibroblasts. The dysregulation of phosphorylation levels in WASP^{L270P} is a likely cause of XLN.

The role of calpain-mediated proteolysis of WASP in T cell motility has not been elucidated. In order to analyse this, the calpain cleavage site of WASP was mapped using yeast two hybrid assay and site-directed mutagenesis to generate a calpain-resistant WASP mutant (WASP^{WRG}). WASP-deficient Jurkat T cells (Jurkat^{WASPkd}) had impaired migration towards SDF-1 α and the expression of WASP^{WRG} in Jurkat^{WASPkd} cells did not rescue the defect, unlike WT WASP. The results showed that calpain-mediated proteolysis of WASP is critical for T cell motility and it is possible that calpain-mediated proteolysis of WASP leads to efficient disassembly of focal adhesions during cell migration. Taken together, the results showed that cyclical phosphorylation and dephosphorylation of WASP as well as calpain-mediated proteolysis of WASP are important regulations of WASP activity.

In conclusion, a possible mechanism of the regulation of WASP can be summarized from the findings in this study (Figure 4.3). Native WASP is predominantly associated with WIP and is in a closed conformation. Toca1 interacts with the PRR region of WASP and activates the WASP-WIP complex. Cdc42 in turn interacts with Toca1 and WASP-WIP. Alternatively, Nck1 binds to WASP and activates it, independently of Cdc42. This leads

to the destabilization of the autoinhibitory loop formed between the BR-GBD and VCA domains. The Y291 residue in the GBD domain is exposed and becomes susceptible to phosphorylation by Tyrosine kinases such as BTK, HCK or Tec. Phosphorylation of the Y291 residue increases the instability of the contacts between the BR-GBD and VCA domains, causing WASP to adopt an open conformation. In the open conformation, the VCA domain is exposed and binds to Arp2/3 complex and G-actin, leading to actin polymerisation. The mutation L270P (see asterisk in Figure 4.3) was identified to be responsible for causing XLN in patients. This mutation disrupts the closed conformation of WASP, allowing tyrosine kinases to gain access to the Y291 residue. This bypasses the need for activation by Cdc42 or Nck1. Enhanced phosphorylation levels on Y291 contribute partly to the constitutively active behaviour of WASP^{L270P}. Phosphorylation of WASP can induce filopodia formation as shown in this study. In T cells, phosphorylation of WASP enhances its activity, leading to cellular processes like T cell activation, phagocytosis and immunological synapse formation (Thrasher and Burns, 2010). Activity of WASP is also regulated through degradation by calpain. Increased levels of Ca²⁺ in the cytoplasm activate calpain, among other proteins. Calpain binds to the WH1 domain of WASP and cleavage of the WH1 domain (between residues 102 -112) occurs, leading to the degradation of WASP.

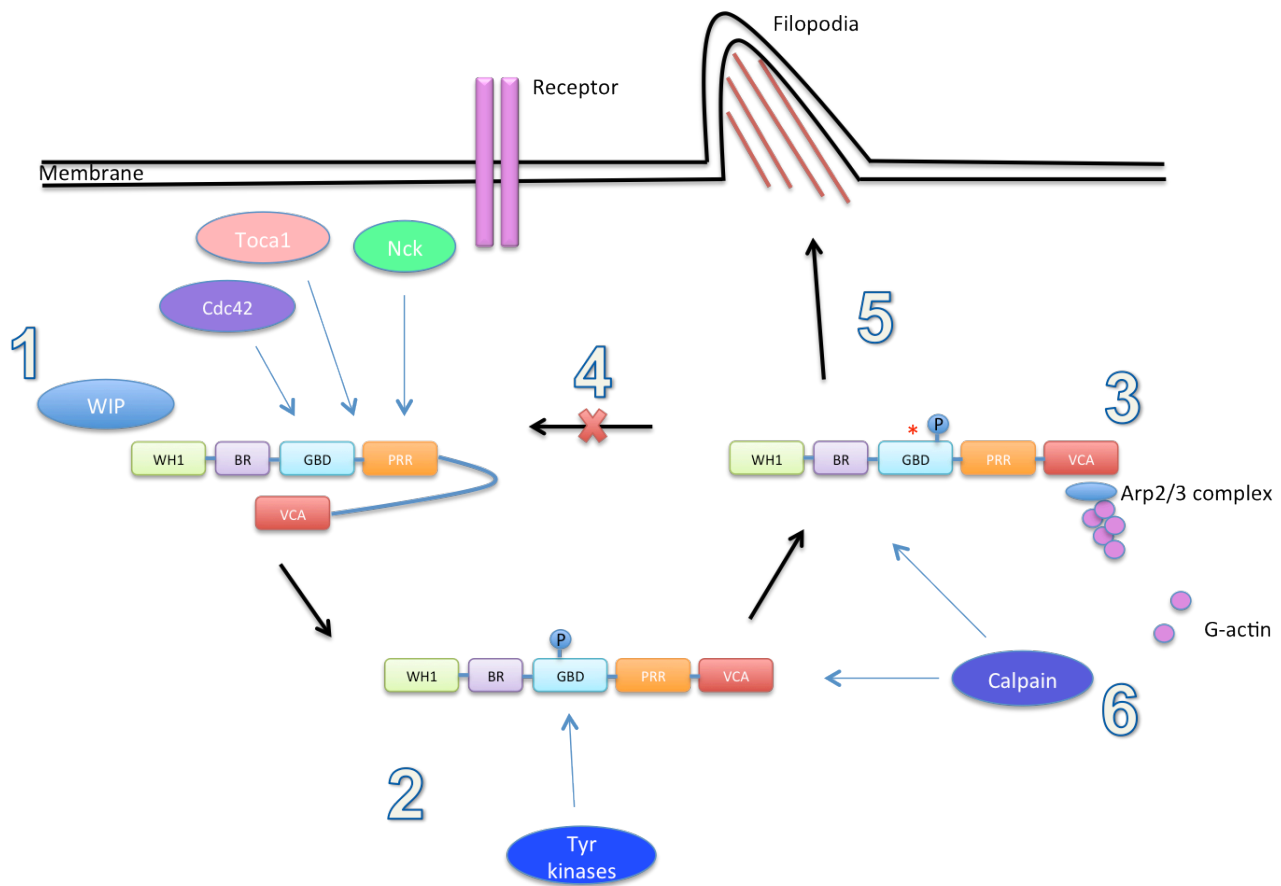


Figure 4.3 Summary of the findings in this study

1. Native WASP is predominantly associated with WIP and is in a closed conformation. Toca1 interacts with the PRR region of WASP and activates the WASP-WIP complex. Cdc42 in turn interacts with Toca-1 and WASP-WIP. Alternatively, Nck1 binds to WASP and activates it, independently of Cdc42. This leads to the destabilization of the autoinhibitory loop form between the BR-GBD and VCA domains.
2. The Y291 residue in the GBD domain is exposed and becomes susceptible to phosphorylation by Tyrosine kinases such as BTK, HCK or Tec. Phosphorylation of the Y291 residue increases the instability of the contacts between the BR-GBD and VCA domains, causing WASP to adopt an open conformation.
3. In the open conformation, the VCA domain is exposed and binds to Arp2/3 complex and G-actin, leading to actin polymerisation.
4. The mutation L270P (see asterisk) was identified to be responsible for causing XLN in patients. This mutation disrupts the closed conformation of WASP, allowing tyrosine kinases to gain access to Y291 residue. Enhanced phosphorylation levels on Y291 contribute partly to the constitutively WASP^{L270P}.
5. Phosphorylation of WASP induces filopodia formation.
6. Increased levels of Ca^{2+} activates Calpain. Calpain binds to the WH1 domain of WASP and cleavage of the WH1 domain (between residues 102 -112) occurs, leading to the degradation of WASP.

Presently, hematopoietic stem cells transplantation is the only curative therapy for WAS patients (Thrasher, 2009). However, transplantation of a bone marrow from a mismatched donor would lead to decreased survival rates (Bosticardo et al., 2009). WAS, XLT and XLN patients express either normal levels or diminished levels of WASP in their lymphocytes. Patients with decreased levels of WASP expressed in the lymphocytes, typically develop the classic WASP phenotype. In contrast, XLN patients have mutations in WASP that enhances actin polymerization. Because of the diverse phenotypes manifested in WAS, XLN and XLT patients, given the phenotype-genotype correlation, treatment of these patients should vary according to the molecular defect or the cause of the disease. Targeted therapies or transplantation of autologous gene-corrected hematopoietic stem cells would be more desirable than the current treatment for patients that fail to find matching donors. One such therapy could be to increase the stability of mutant WASP as diminished level of WASP in lymphocytes is the cause of the classic WAS. A deeper understanding of the molecular mechanism of WASP regulation would pave the way for individualized or personalised treatment for WAS, XLT and XLN patients.

5. References

- Aiuti, A., Webb, I.J., Bleul, C., Springer, T., and Gutierrez-Ramos, J.C. (1997). The chemokine SDF-1 is a chemoattractant for human CD34+ hematopoietic progenitor cells and provides a new mechanism to explain the mobilization of CD34+ progenitors to peripheral blood. *J Exp Med* 185, 111-120.
- Ancliff, P.J., Blundell, M.P., Cory, G.O., Calle, Y., Worth, A., Kempinski, H., Burns, S., Jones, G.E., Sinclair, J., Kinnon, C., *et al.* (2006). Two novel activating mutations in the Wiskott-Aldrich syndrome protein result in congenital neutropenia. *Blood* 108, 2182-2189.
- Anderie, I., and Schmid, A. (2007). In vivo visualization of actin dynamics and actin interactions by BiFC. *Cell Biol Int* 31, 1131-1135.
- Anton, I.M., Lu, W., Mayer, B.J., Ramesh, N., and Geha, R.S. (1998). The Wiskott-Aldrich syndrome protein-interacting protein (WIP) binds to the adaptor protein Nck. *The Journal of biological chemistry* 273, 20992-20995.
- Ariga, T., Kondoh, T., Yamaguchi, K., Yamada, M., Sasaki, S., Nelson, D.L., Ikeda, H., Kobayashi, K., Moriuchi, H., and Sakiyama, Y. (2001). Spontaneous in vivo reversion of an inherited mutation in the Wiskott-Aldrich syndrome. *J Immunol* 166, 5245-5249.
- Aspenstrom, P. (2002). The WASP-binding protein WIRE has a role in the regulation of the actin filament system downstream of the platelet-derived growth factor receptor. *Exp Cell Res* 279, 21-33.
- Aspenstrom, P. (2005). The verprolin family of proteins: regulators of cell morphogenesis and endocytosis. *FEBS Lett* 579, 5253-5259.
- Aspenstrom, P., Lindberg, U., and Hall, A. (1996). Two GTPases, Cdc42 and Rac, bind directly to a protein implicated in the immunodeficiency disorder Wiskott-Aldrich syndrome. *Curr Biol* 6, 70-75.
- Baba, Y., Nonoyama, S., Matsushita, M., Yamadori, T., Hashimoto, S., Imai, K., Arai, S., Kunikata, T., Kurimoto, M., Kurosaki, T., *et al.* (1999). Involvement of wiskott-aldrich syndrome protein in B-cell cytoplasmic tyrosine kinase pathway. *Blood* 93, 2003-2012.
- Bach, T.L., Chen, Q.M., Kerr, W.T., Wang, Y., Lian, L., Choi, J.K., Wu, D., Kazanietz, M.G., Koretzky, G.A., Zigmond, S., *et al.* (2007). Phospholipase cbeta is critical for T cell chemotaxis. *J Immunol* 179, 2223-2227.
- Badour, K., Zhang, J., Shi, F., Leng, Y., Collins, M., and Siminovitch, K.A. (2004a). Fyn and PTP-PEST-mediated regulation of Wiskott-Aldrich syndrome protein (WASp) tyrosine phosphorylation is required for coupling T cell antigen receptor engagement to WASp effector function and T cell activation. *J Exp Med* 199, 99-112.

Badour, K., Zhang, J., and Siminovitch, K.A. (2003). The Wiskott-Aldrich syndrome protein: forging the link between actin and cell activation. *Immunol Rev* 192, 98-112.

Badour, K., Zhang, J., and Siminovitch, K.A. (2004b). Involvement of the Wiskott-Aldrich syndrome protein and other actin regulatory adaptors in T cell activation. *Semin Immunol* 16, 395-407.

Baker, J. (1993). Current protocols in molecular biology.

Baneyx, F. (1999). Recombinant protein expression in *Escherichia coli*. *Current opinion in biotechnology* 10, 411-421.

Beel, K., Cotter, M.M., Blatny, J., Bond, J., Lucas, G., Green, F., Vanduppen, V., Leung, D.W., Rooney, S., Smith, O.P., *et al.* (2009). A large kindred with X-linked neutropenia with an I294T mutation of the Wiskott-Aldrich syndrome gene. *Br J Haematol* 144, 120-126.

Bhatt, A., Kaverina, I., Otey, C., and Huttenlocher, A. (2002). Regulation of focal complex composition and disassembly by the calcium-dependent protease calpain. *Journal of cell science* 115, 3415-3425.

Biswas, S., Harris, F., Dennison, S., Singh, J.P., and Phoenix, D. (2005). Calpains: enzymes of vision? *Med Sci Monit* 11, RA301-310.

Blundell, M.P., Bouma, G., Metelo, J., Worth, A., Calle, Y., Cowell, L.A., Westerberg, L.S., Moulding, D.A., Mirando, S., Kinnon, C., *et al.* (2009). Phosphorylation of WASp is a key regulator of activity and stability in vivo. *Proceedings of the National Academy of Sciences of the United States of America* 106, 15738-15743.

Bosch, M., Le, K.H., Bugyi, B., Correia, J.J., Renault, L., and Carlier, M.F. (2007). Analysis of the function of Spire in actin assembly and its synergy with formin and profilin. *Mol Cell* 28, 555-568.

Bosticardo, M., Marangoni, F., Aiuti, A., Villa, A., and Grazia Roncarolo, M. (2009). Recent advances in understanding the pathophysiology of Wiskott-Aldrich syndrome. *Blood* 113, 6288-6295.

Bruce Alberts, A.J., Julian Lewis, Martin Raff, Keith Roberts, and Peter Walter (2002). *Molecular Biology of the Cell*, 4th edition.

Bunnell, S.C., Henry, P.A., Kolluri, R., Kirchhausen, T., Rickles, R.J., and Berg, L.J. (1996). Identification of Itk/Tsk Src homology 3 domain ligands. *J Biol Chem* 271, 25646-25656.

Burns, S., Hardy, S.J., Buddle, J., Yong, K.L., Jones, G.E., and Thrasher, A.J. (2004). Maturation of DC is associated with changes in motile characteristics and adherence. *Cell Motil Cytoskeleton* 57, 118-132.

Burns, S., Thrasher, A.J., Blundell, M.P., Machesky, L., and Jones, G.E. (2001). Configuration of human dendritic cell cytoskeleton by Rho GTPases, the WAS protein, and differentiation. *Blood* 98, 1142-1149.

Butler, J.T., Samantaray, S., Beeson, C.C., Ray, S.K., and Banik, N.L. (2009). Involvement of calpain in the process of Jurkat T cell chemotaxis. *J Neurosci Res* 87, 626-635.

Calle, Y., Burns, S., Thrasher, A.J., and Jones, G.E. (2006a). The leukocyte podosome. *Eur J Cell Biol* 85, 151-157.

Calle, Y., Carragher, N.O., Thrasher, A.J., and Jones, G.E. (2006b). Inhibition of calpain stabilises podosomes and impairs dendritic cell motility. *Journal of cell science* 119, 2375-2385.

Calle, Y., Jones, G.E., Jagger, C., Fuller, K., Blundell, M.P., Chow, J., Chambers, T., and Thrasher, A.J. (2004). WASp deficiency in mice results in failure to form osteoclast sealing zones and defects in bone resorption. *Blood* 103, 3552-3561.

Callebaut, I., Cossart, P., and Dehoux, P. (1998). EVH1/WH1 domains of VASP and WASP proteins belong to a large family including Ran-binding domains of the RanBP1 family. *FEBS Lett* 441, 181-185.

Campellone, K.G., and Welch, M.D. (2010). A nucleator arms race: cellular control of actin assembly. *Nat Rev Mol Cell Biol* 11, 237-251.

Castellano, F., Montcourrier, P., Guillemot, J.C., Gouin, E., Machesky, L., Cossart, P., and Chavrier, P. (1999). Inducible recruitment of Cdc42 or WASP to a cell-surface receptor triggers actin polymerization and filopodium formation. *Curr Biol* 9, 351-360.

Chan, K.T., Bennis, D.A., and Huttenlocher, A. (2010). Regulation of adhesion dynamics by calpain-mediated proteolysis of focal adhesion kinase (FAK). *J Biol Chem* 285, 11418-11426.

Charrier, S., Dupre, L., Scaramuzza, S., Jeanson-Leh, L., Blundell, M.P., Danos, O., Cattaneo, F., Aiuti, A., Eckenberg, R., Thrasher, A.J., *et al.* (2007). Lentiviral vectors targeting WASp expression to hematopoietic cells, efficiently transduce and correct cells from WAS patients. *Gene Ther* 14, 415-428.

Chereau, D., Boczkowska, M., Skwarek-Maruszewska, A., Fujiwara, I., Hayes, D.B., Rebowski, G., Lappalainen, P., Pollard, T.D., and Dominguez, R. (2008). Leiomodin is an actin filament nucleator in muscle cells. *Science (New York, NY)* 320, 239-243.

Chesarone, M.A., and Goode, B.L. (2009). Actin nucleation and elongation factors: mechanisms and interplay. *Current opinion in cell biology* 21, 28-37.

Chou, H.C., Anton, I.M., Holt, M.R., Curcio, C., Lanzardo, S., Worth, A., Burns, S., Thrasher, A.J., Jones, G.E., and Calle, Y. (2006). WIP regulates the stability and localization of WASP to podosomes in migrating dendritic cells. *Curr Biol* 16, 2337-2344.

Condeelis, J. (2001). How is actin polymerization nucleated in vivo? *Trends Cell Biol* 11, 288-293.

Cory, G.O., Cramer, R., Blanchoin, L., and Ridley, A.J. (2003). Phosphorylation of the WASP-VCA domain increases its affinity for the Arp2/3 complex and enhances actin polymerization by WASP. *Mol Cell* 11, 1229-1239.

Cory, G.O., Garg, R., Cramer, R., and Ridley, A.J. (2002a). Phosphorylation of tyrosine 291 enhances the ability of WASp to stimulate actin polymerization and filopodium formation. Wiskott-Aldrich Syndrome protein. *The Journal of biological chemistry* 277, 45115-45121.

Cory, G.O., Garg, R., Cramer, R., and Ridley, A.J. (2002b). Phosphorylation of tyrosine 291 enhances the ability of WASp to stimulate actin polymerization and filopodium formation. Wiskott-Aldrich Syndrome protein. *J Biol Chem* 277, 45115-45121.

Cotta-de-Almeida, V., Westerberg, L., Maillard, M.H., Onaldi, D., Wachtel, H., Meelu, P., Chung, U.I., Xavier, R., Alt, F.W., and Snapper, S.B. (2007). Wiskott Aldrich syndrome protein (WASP) and N-WASP are critical for T cell development. *Proceedings of the National Academy of Sciences of the United States of America* 104, 15424-15429.

Davis, B.R., and Candotti, F. (2009). Revertant somatic mosaicism in the Wiskott-Aldrich syndrome. *Immunol Res* 44, 127-131.

de la Fuente, M.A., Sasahara, Y., Calamito, M., Anton, I.M., Elkhail, A., Gallego, M.D., Suresh, K., Siminovich, K., Ochs, H.D., Anderson, K.C., *et al.* (2007). WIP is a chaperone for Wiskott-Aldrich syndrome protein (WASP). *Proceedings of the National Academy of Sciences of the United States of America* 104, 926-931.

Derry, J.M., Ochs, H.D., and Francke, U. (1994). Isolation of a novel gene mutated in Wiskott-Aldrich syndrome. *Cell* 79, following 922.

Deshpande, R.V., Goust, J.M., Chakrabarti, A.K., Barbosa, E., Hogan, E.L., and Banik, N.L. (1995). Calpain expression in lymphoid cells. Increased mRNA and protein levels after cell activation. *J Biol Chem* 270, 2497-2505.

Devriendt, K., Kim, A.S., Mathijs, G., Frints, S.G., Schwartz, M., Van Den Oord, J.J., Verhoef, G.E., Boogaerts, M.A., Fryns, J.P., You, D., *et al.* (2001). Constitutively activating mutation in WASP causes X-linked severe congenital neutropenia. *Nat Genet* 27, 313-317.

Doherty, G.J., and McMahon, H.T. (2009). Mechanisms of endocytosis. *Annu Rev Biochem* 78, 857-902.

Dominguez, R. (2004). Actin-binding proteins--a unifying hypothesis. *Trends in biochemical sciences* 29, 572-578.

Dong, X., Patino-Lopez, G., Candotti, F., and Shaw, S. (2007). Structure-function analysis of the WIP role in T cell receptor-stimulated NFAT activation: evidence that WIP-WASP dissociation is not required and that the WIP NH2 terminus is inhibitory. *J Biol Chem* 282, 30303-30310.

Dourdin, N., Bhatt, A.K., Dutt, P., Greer, P.A., Arthur, J.S., Elce, J.S., and Huttenlocher, A. (2001). Reduced cell migration and disruption of the actin cytoskeleton in calpain-deficient embryonic fibroblasts. *The Journal of biological chemistry* 276, 48382-48388.

Dovas, A., and Cox, D. (2010). Regulation of WASp by phosphorylation: Activation or other functions? *Commun Integr Biol* 3, 101-105.

Dovas, A., Gevrey, J.C., Grossi, A., Park, H., Abou-Kheir, W., and Cox, D. (2009). Regulation of podosome dynamics by WASp phosphorylation: implication in matrix degradation and chemotaxis in macrophages. *Journal of cell science* 122, 3873-3882.

Dreolini, L., and Takei, F. (2007). Activation of LFA-1 by ionomycin is independent of calpain-mediated talin cleavage. *Biochem Biophys Res Commun* 356, 207-212.

Faix, J., and Grosse, R. (2006). Staying in shape with formins. *Developmental cell* 10, 693-706.

Fedorov, A.A., Fedorov, E., Gertler, F., and Almo, S.C. (1999). Structure of EVH1, a novel proline-rich ligand-binding module involved in cytoskeletal dynamics and neural function. *Nature structural biology* 6, 661-665.

Fletcher, D.A., and Mullins, R.D. (2010). Cell mechanics and the cytoskeleton. *Nature* 463, 485-492.

Franco, S.J., Rodgers, M.A., Perrin, B.J., Han, J., Bennin, D.A., Critchley, D.R., and Huttenlocher, A. (2004). Calpain-mediated proteolysis of talin regulates adhesion dynamics. *Nat Cell Biol* 6, 977-983.

Gallego, M.D., de la Fuente, M.A., Anton, I.M., Snapper, S., Fuhlbrigge, R., and Geha, R.S. (2006). WIP and WASP play complementary roles in T cell homing and chemotaxis to SDF-1alpha. *Int Immunol* 18, 221-232.

Geiger, B., Bershadsky, A., Pankov, R., and Yamada, K.M. (2001). Transmembrane crosstalk between the extracellular matrix--cytoskeleton crosstalk. *Nature reviews* 2, 793-805.

Ghazizadeh, S., Bolen, J.B., and Fleit, H.B. (1994). Physical and functional association of Src-related protein tyrosine kinases with Fc gamma RII in monocytic THP-1 cells. *J Biol Chem* 269, 8878-8884.

Glading, A., Lauffenburger, D.A., and Wells, A. (2002). Cutting to the chase: calpain proteases in cell motility. *Trends Cell Biol* 12, 46-54.

Goode, B.L., and Eck, M.J. (2007). Mechanism and function of formins in the control of actin assembly. *Annual review of biochemistry* 76, 593-627.

Graceffa, P., and Dominguez, R. (2003). Crystal structure of monomeric actin in the ATP state. Structural basis of nucleotide-dependent actin dynamics. *J Biol Chem* 278, 34172-34180.

Guinamard, R., Aspenstrom, P., Fougereau, M., Chavrier, P., and Guillemot, J.C. (1998). Tyrosine phosphorylation of the Wiskott-Aldrich syndrome protein by Lyn and Btk is regulated by CDC42. *FEBS Lett* 434, 431-436.

Gunn, M.D., Kyuwa, S., Tam, C., Kakiuchi, T., Matsuzawa, A., Williams, L.T., and Nakano, H. (1999). Mice lacking expression of secondary lymphoid organ chemokine have defects in lymphocyte homing and dendritic cell localization. *J Exp Med* 189, 451-460.

Hall, A. (2005). Rho GTPases and the control of cell behaviour. *Biochem Soc Trans* 33, 891-895.

Harris, E.S., Li, F., and Higgs, H.N. (2004). The mouse formin, FRLalpha, slows actin filament barbed end elongation, competes with capping protein, accelerates polymerization from monomers, and severs filaments. *The Journal of biological chemistry* 279, 20076-20087.

Hellebrand, E., Mautner, J., Reisbach, G., Nimmerjahn, F., Hallek, M., Mocikat, R., and Hammerschmidt, W. (2006). Epstein-Barr virus vector-mediated gene transfer into human B cells: potential for antitumor vaccination. *Gene therapy* 13, 150-162.

Higgs, H.N., and Peterson, K.J. (2005). Phylogenetic analysis of the formin homology 2 domain. *Molecular biology of the cell* 16, 1-13.

Higgs, H.N., and Pollard, T.D. (2000). Activation by Cdc42 and PIP(2) of Wiskott-Aldrich syndrome protein (WASp) stimulates actin nucleation by Arp2/3 complex. *J Cell Biol* 150, 1311-1320.

Ho, H.Y., Rohatgi, R., Lebensohn, A.M., Le, M., Li, J., Gygi, S.P., and Kirschner, M.W. (2004). Toca-1 mediates Cdc42-dependent actin nucleation by activating the N-WASP-WIP complex. *Cell* 118, 203-216.

Ho, H.Y., Rohatgi, R., Ma, L., and Kirschner, M.W. (2001). CR16 forms a complex with N-WASP in brain and is a novel member of a conserved proline-rich actin-binding protein family. *Proc Natl Acad Sci U S A* 98, 11306-11311.

Holt, M.R., and Koffer, A. (2001). Cell motility: proline-rich proteins promote protrusions. *Trends in cell biology* 11, 38-46.

Hu, C.D., Chinenov, Y., and Kerppola, T.K. (2002). Visualization of interactions among bZIP and Rel family proteins in living cells using bimolecular fluorescence complementation. *Molecular cell* 9, 789-798.

Huang, Y., and Wang, K.K. (2001). The calpain family and human disease. *Trends Mol Med* 7, 355-362.

Huttenlocher, A., Palecek, S.P., Lu, Q., Zhang, W., Mellgren, R.L., Lauffenburger, D.A., Ginsberg, M.H., and Horwitz, A.F. (1997). Regulation of cell migration by the calcium-dependent protease calpain. *J Biol Chem* 272, 32719-32722.

Imai, K., Nonoyama, S., and Ochs, H.D. (2003a). WASP (Wiskott-Aldrich syndrome protein) gene mutations and phenotype. *Curr Opin Allergy Clin Immunol* 3, 427-436.

Imai, K., Nonoyama, S., and Ochs, H.D. (2003b). WASP (Wiskott-Aldrich syndrome protein) gene mutations and phenotype. *Current opinion in allergy and clinical immunology* 3, 427-436.

Insall, R.H., and Machesky, L.M. (2004). Regulation of WASP: PIP2 Pipped by Toca-1? *Cell* 118, 140-141.

Jaffe, A.B., and Hall, A. (2005). Rho GTPases: biochemistry and biology. *Annu Rev Cell Dev Biol* 21, 247-269.

James, P., Halladay, J., and Craig, E.A. (1996). Genomic libraries and a host strain designed for highly efficient two-hybrid selection in yeast. *Genetics* 144, 1425-1436.

Jeong, J., Kim, S.K., Ahn, J., Park, K., Jeong, E.J., Kim, M., and Chung, B.H. (2006). Monitoring of conformational change in maltose binding protein using split green fluorescent protein. *Biochemical and biophysical research communications* 339, 647-651.

Jia, Z., Petrounevitch, V., Wong, A., Moldoveanu, T., Davies, P.L., Elce, J.S., and Beckmann, J.S. (2001). Mutations in calpain 3 associated with limb girdle muscular dystrophy: analysis by molecular modeling and by mutation in m-calpain. *Biophys J* 80, 2590-2596.

Jin, Y., Mazza, C., Christie, J.R., Giliani, S., Fiorini, M., Mella, P., Gandellini, F., Stewart, D.M., Zhu, Q., Nelson, D.L., *et al.* (2004). Mutations of the Wiskott-Aldrich

Syndrome Protein (WASP): hotspots, effect on transcription, and translation and phenotype/genotype correlation. *Blood* 104, 4010-4019.

Jones, G.E., Zicha, D., Dunn, G.A., Blundell, M., and Thrasher, A. (2002). Restoration of podosomes and chemotaxis in Wiskott-Aldrich syndrome macrophages following induced expression of WASp. *Int J Biochem Cell Biol* 34, 806-815.

Kato, M., Miki, H., Kurita, S., Endo, T., Nakagawa, H., Miyamoto, S., and Takenawa, T. (2002). WICH, a novel verprolin homology domain-containing protein that functions cooperatively with N-WASP in actin-microspike formation. *Biochemical and biophysical research communications* 291, 41-47.

Kavallaris, M. (2010). Microtubules and resistance to tubulin-binding agents. *Nature reviews* 10, 194-204.

Kenworthy, A.K. (2001). Imaging protein-protein interactions using fluorescence resonance energy transfer microscopy. *Methods* 24, 289-296.

Kim, A.S., Kakalis, L.T., Abdul-Manan, N., Liu, G.A., and Rosen, M.K. (2000). Autoinhibition and activation mechanisms of the Wiskott-Aldrich syndrome protein. *Nature* 404, 151-158.

Kinley, A.W., Weed, S.A., Weaver, A.M., Karginov, A.V., Bissonette, E., Cooper, J.A., and Parsons, J.T. (2003). Cortactin interacts with WIP in regulating Arp2/3 activation and membrane protrusion. *Curr Biol* 13, 384-393.

Kovar, D.R., and Pollard, T.D. (2004). Insertional assembly of actin filament barbed ends in association with formins produces piconewton forces. *Proceedings of the National Academy of Sciences of the United States of America* 101, 14725-14730.

Kucik, D.F., Dustin, M.L., Miller, J.M., and Brown, E.J. (1996). Adhesion-activating phorbol ester increases the mobility of leukocyte integrin LFA-1 in cultured lymphocytes. *J Clin Invest* 97, 2139-2144.

Labno, C.M., Lewis, C.M., You, D., Leung, D.W., Takesono, A., Kamberos, N., Seth, A., Finkelstein, L.D., Rosen, M.K., Schwartzberg, P.L., *et al.* (2003). Itk functions to control actin polymerization at the immune synapse through localized activation of Cdc42 and WASP. *Curr Biol* 13, 1619-1624.

Lauffenburger, D.A., and Horwitz, A.F. (1996). Cell migration: a physically integrated molecular process. *Cell* 84, 359-369.

Lebart, M.C., and Benyamin, Y. (2006). Calpain involvement in the remodeling of cytoskeletal anchorage complexes. *FEBS J* 273, 3415-3426.

LeClaire, L.L., 3rd, Baumgartner, M., Iwasa, J.H., Mullins, R.D., and Barber, D.L. (2008). Phosphorylation of the Arp2/3 complex is necessary to nucleate actin filaments. *The Journal of cell biology* 182, 647-654.

Lee, S.H., and Dominguez, R. (2010). Regulation of actin cytoskeleton dynamics in cells. *Molecules and cells*.

Leverrier, Y., Lorenzi, R., Blundell, M.P., Brickell, P., Kinnon, C., Ridley, A.J., and Thrasher, A.J. (2001). Cutting edge: the Wiskott-Aldrich syndrome protein is required for efficient phagocytosis of apoptotic cells. *J Immunol* 166, 4831-4834.

Li, R. (1997). Bee1, a yeast protein with homology to Wiskott-Aldrich syndrome protein, is critical for the assembly of cortical actin cytoskeleton. *J Cell Biol* 136, 649-658.

Lim, K.B., Bu, W., Goh, W.I., Koh, E., Ong, S.H., Pawson, T., Sudhakaran, T., and Ahmed, S. (2008). The Cdc42 Effector IRSp53 Generates Filopodia by Coupling Membrane Protrusion with Actin Dynamics. *J Biol Chem* 283, 20454-20472.

Linder, S., Nelson, D., Weiss, M., and Aepfelbacher, M. (1999). Wiskott-Aldrich syndrome protein regulates podosomes in primary human macrophages. *Proceedings of the National Academy of Sciences of the United States of America* 96, 9648-9653.

Loetscher, M., Geiser, T., O'Reilly, T., Zwahlen, R., Baggiolini, M., and Moser, B. (1994). Cloning of a human seven-transmembrane domain receptor, LESTR, that is highly expressed in leukocytes. *J Biol Chem* 269, 232-237.

Lorenzi, R., Brickell, P.M., Katz, D.R., Kinnon, C., and Thrasher, A.J. (2000). Wiskott-Aldrich syndrome protein is necessary for efficient IgG-mediated phagocytosis. *Blood* 95, 2943-2946.

Luster, A.D. (1998). Chemokines--chemotactic cytokines that mediate inflammation. *N Engl J Med* 338, 436-445.

Machesky, L.M., and Insall, R.H. (1998). Scar1 and the related Wiskott-Aldrich syndrome protein, WASP, regulate the actin cytoskeleton through the Arp2/3 complex. *Curr Biol* 8, 1347-1356.

Maly, I.V., and Borisy, G.G. (2001). Self-organization of a propulsive actin network as an evolutionary process. *Proceedings of the National Academy of Sciences of the United States of America* 98, 11324-11329.

Martinez-Quiles, N., Ho, H.Y., Kirschner, M.W., Ramesh, N., and Geha, R.S. (2004). Erk/Src phosphorylation of cortactin acts as a switch on-switch off mechanism that controls its ability to activate N-WASP. *Mol Cell Biol* 24, 5269-5280.

Martinez-Quiles, N., Rohatgi, R., Anton, I.M., Medina, M., Saville, S.P., Miki, H., Yamaguchi, H., Takenawa, T., Hartwig, J.H., Geha, R.S., *et al.* (2001). WIP regulates N-WASP-mediated actin polymerization and filopodium formation. *Nature cell biology* 3, 484-491.

Meyer-Bahlburg, A., Becker-Herman, S., Humblet-Baron, S., Khim, S., Weber, M., Bouma, G., Thrasher, A.J., Batista, F.D., and Rawlings, D.J. (2008). Wiskott-Aldrich syndrome protein deficiency in B cells results in impaired peripheral homeostasis. *Blood* 112, 4158-4169.

Miki, H., Miura, K., and Takenawa, T. (1996). N-WASP, a novel actin-depolymerizing protein, regulates the cortical cytoskeletal rearrangement in a PIP2-dependent manner downstream of tyrosine kinases. *EMBO J* 15, 5326-5335.

Miki, H., Suetsugu, S., and Takenawa, T. (1998). WAVE, a novel WASP-family protein involved in actin reorganization induced by Rac. *Embo J* 17, 6932-6941.

Misra, A., Rajmohan, R., Lim, R.P., Bhattacharyya, S., and Thanabalu, T. (2010). The mammalian verprolin, WIRE induces filopodia independent of N-WASP through IRSp53. *Experimental cell research* 316, 2810-2824.

Molina, I.J., Sancho, J., Terhorst, C., Rosen, F.S., and Remold-O'Donnell, E. (1993). T cells of patients with the Wiskott-Aldrich syndrome have a restricted defect in proliferative responses. *J Immunol* 151, 4383-4390.

Moraczewski, J., Piekarska, E., Bonavaud, S., Wosinska, K., Chazaud, B., and Barlovatz-Meimon, G. (1996). Differential intracellular distribution and activities of mu- and m-calpains during the differentiation of human myogenic cells in culture. *C R Acad Sci III* 319, 681-686.

Morales-Tirado, V., Johansson, S., Hanson, E., Howell, A., Zhang, J., Siminovitch, K.A., and Fowell, D.J. (2004). Cutting edge: selective requirement for the Wiskott-Aldrich syndrome protein in cytokine, but not chemokine, secretion by CD4⁺ T cells. *J Immunol* 173, 726-730.

Mullins, R.D., Heuser, J.A., and Pollard, T.D. (1998). The interaction of Arp2/3 complex with actin: nucleation, high affinity pointed end capping, and formation of branching networks of filaments. *Proceedings of the National Academy of Sciences of the United States of America* 95, 6181-6186.

Naqvi, S.N., Zahn, R., Mitchell, D.A., Stevenson, B.J., and Munn, A.L. (1998). The WASp homologue Las17p functions with the WIP homologue End5p/verprolin and is essential for endocytosis in yeast. *Curr Biol* 8, 959-962.

Ochs, H.D., and Thrasher, A.J. (2006). The Wiskott-Aldrich syndrome. *J Allergy Clin Immunol* 117, 725-738; quiz 739.

Oda, A., Miki, H., Wada, I., Yamaguchi, H., Yamazaki, D., Suetsugu, S., Nakajima, M., Nakayama, A., Okawa, K., Miyazaki, H., *et al.* (2005). WAVE/Scars in platelets. *Blood* 105, 3141-3148.

Olivier, A., Jeanson-Leh, L., Bouma, G., Compagno, D., Blondeau, J., Seye, K., Charrier, S., Burns, S., Thrasher, A.J., Danos, O., *et al.* (2006). A partial down-regulation of WASP is sufficient to inhibit podosome formation in dendritic cells. *Mol Ther* 13, 729-737.

Padrick, S.B., Cheng, H.C., Ismail, A.M., Panchal, S.C., Doolittle, L.K., Kim, S., Skehan, B.M., Umetani, J., Brautigam, C.A., Leong, J.M., *et al.* (2008). Hierarchical regulation of WASP/WAVE proteins. *Molecular cell* 32, 426-438.

Panchal, S.C., Kaiser, D.A., Torres, E., Pollard, T.D., and Rosen, M.K. (2003). A conserved amphipathic helix in WASP/Scar proteins is essential for activation of Arp2/3 complex. *Nat Struct Biol* 10, 591-598.

Perrin, B.J., Amann, K.J., and Huttenlocher, A. (2006). Proteolysis of cortactin by calpain regulates membrane protrusion during cell migration. *Mol Biol Cell* 17, 239-250.
Pollard, T.D., and Cooper, J.A. (2009). Actin, a central player in cell shape and movement. *Science (New York, NY)* 326, 1208-1212.

Potter, D.A., Tirnauer, J.S., Janssen, R., Croall, D.E., Hughes, C.N., Fiocco, K.A., Mier, J.W., Maki, M., and Herman, I.M. (1998). Calpain regulates actin remodeling during cell spreading. *J Cell Biol* 141, 647-662.

Pring, M., Evangelista, M., Boone, C., Yang, C., and Zigmond, S.H. (2003). Mechanism of formin-induced nucleation of actin filaments. *Biochemistry* 42, 486-496.

Purich, D.L., and Southwick, F.S. (1997). ABM-1 and ABM-2 homology sequences: consensus docking sites for actin-based motility defined by oligoproline regions in *Listeria* ActA surface protein and human VASP. *Biochemical and biophysical research communications* 231, 686-691.

Quinlan, M.E., Heuser, J.E., Kerkhoff, E., and Mullins, R.D. (2005). *Drosophila* Spire is an actin nucleation factor. *Nature* 433, 382-388.

Rajmohan, R., Meng, L., Yu, S., and Thanabalu, T. (2006). WASP suppresses the growth defect of *Saccharomyces cerevisiae* las17Delta strain in the presence of WIP. *Biochemical and biophysical research communications* 342, 529-536.

Rajmohan, R., Raodah, A., Wong, M.H., and Thanabalu, T. (2009). Characterization of Wiskott-Aldrich syndrome (WAS) mutants using *Saccharomyces cerevisiae*. *FEMS Yeast Res* 9, 1226-1235.

Ramesh, N., Anton, I.M., Hartwig, J.H., and Geha, R.S. (1997). WIP, a protein associated with wiskott-aldrich syndrome protein, induces actin polymerization and redistribution in lymphoid cells. *Proc Natl Acad Sci U S A* 94, 14671-14676.

Resnati, M., Guttinger, M., Valcamonica, S., Sidenius, N., Blasi, F., and Fazioli, F. (1996). Proteolytic cleavage of the urokinase receptor substitutes for the agonist-induced chemotactic effect. *EMBO J* 15, 1572-1582.

Reverter, D., Strobl, S., Fernandez-Catalan, C., Sorimachi, H., Suzuki, K., and Bode, W. (2001). Structural basis for possible calcium-induced activation mechanisms of calpains. *Biol Chem* 382, 753-766.

Ridley, A.J., Schwartz, M.A., Burridge, K., Firtel, R.A., Ginsberg, M.H., Borisy, G., Parsons, J.T., and Horwitz, A.R. (2003). Cell migration: integrating signals from front to back. *Science (New York, NY)* 302, 1704-1709.

Rivera, G.M., Vasilescu, D., Papayannopoulos, V., Lim, W.A., and Mayer, B.J. (2009). A reciprocal interdependence between Nck and PI(4,5)P(2) promotes localized N-WASP-mediated actin polymerization in living cells. *Molecular cell* 36, 525-535.

Rivero-Lezcano, O.M., Marcilla, A., Sameshima, J.H., and Robbins, K.C. (1995). Wiskott-Aldrich syndrome protein physically associates with Nck through Src homology 3 domains. *Mol Cell Biol* 15, 5725-5731.

Robinson, R.C., Turbedsky, K., Kaiser, D.A., Marchand, J.B., Higgs, H.N., Choe, S., and Pollard, T.D. (2001). Crystal structure of Arp2/3 complex. *Science (New York, NY)* 294, 1679-1684.

Rock, M.T., Dix, A.R., Brooks, W.H., and Roszman, T.L. (2000). Beta1 integrin-mediated T cell adhesion and cell spreading are regulated by calpain. *Exp Cell Res* 261, 260-270.

Rohatgi, R., Ma, L., Miki, H., Lopez, M., Kirchhausen, T., Takenawa, T., and Kirschner, M.W. (1999). The interaction between N-WASP and the Arp2/3 complex links Cdc42-dependent signals to actin assembly. *Cell* 97, 221-231.

Rohatgi, R., Nollau, P., Ho, H.Y., Kirschner, M.W., and Mayer, B.J. (2001). Nck and phosphatidylinositol 4,5-bisphosphate synergistically activate actin polymerization through the N-WASP-Arp2/3 pathway. *J Biol Chem* 276, 26448-26452.

Rosales-Nieves, A.E., Johndrow, J.E., Keller, L.C., Magie, C.R., Pinto-Santini, D.M., and Parkhurst, S.M. (2006). Coordination of microtubule and microfilament dynamics by *Drosophila* Rho1, Spire and Cappuccino. *Nat Cell Biol* 8, 367-376.

Rouiller, I., Xu, X.P., Amann, K.J., Egile, C., Nickell, S., Nicastro, D., Li, R., Pollard, T.D., Volkman, N., and Hanein, D. (2008). The structural basis of actin filament branching by the Arp2/3 complex. *The Journal of cell biology* 180, 887-895.

Saez, M.E., Ramirez-Lorca, R., Moron, F.J., and Ruiz, A. (2006). The therapeutic potential of the calpain family: new aspects. *Drug Discov Today* 11, 917-923.

Sasahara, Y., Rachid, R., Byrne, M.J., de la Fuente, M.A., Abraham, R.T., Ramesh, N., and Geha, R.S. (2002). Mechanism of recruitment of WASP to the immunological synapse and of its activation following TCR ligation. *Mol Cell* 10, 1269-1281.

Sawa, M., and Takenawa, T. (2006). *Caenorhabditis elegans* WASP-interacting protein homologue WIP-1 is involved in morphogenesis through maintenance of WSP-1 protein levels. *Biochemical and biophysical research communications* 340, 709-717.

Scholz, G., Cartledge, K., and Dunn, A.R. (2000). Hck enhances the adherence of lipopolysaccharide-stimulated macrophages via Cbl and phosphatidylinositol 3-kinase. *J Biol Chem* 275, 14615-14623.

Sept, D., and McCammon, J.A. (2001). Thermodynamics and kinetics of actin filament nucleation. *Biophys J* 81, 667-674.

Shcherbina, A., Miki, H., Kenney, D.M., Rosen, F.S., Takenawa, T., and Remold-O'Donnell, E. (2001). WASP and N-WASP in human platelets differ in sensitivity to protease calpain. *Blood* 98, 2988-2991.

Smith, I.J., and Dodd, S.L. (2007). Calpain activation causes a proteasome-dependent increase in protein degradation and inhibits the Akt signalling pathway in rat diaphragm muscle. *Exp Physiol* 92, 561-573.

Snapper, S.B., Meelu, P., Nguyen, D., Stockton, B.M., Bozza, P., Alt, F.W., Rosen, F.S., von Andrian, U.H., and Klein, C. (2005). WASP deficiency leads to global defects of directed leukocyte migration in vitro and in vivo. *J Leukoc Biol* 77, 993-998.

Snapper, S.B., Rosen, F.S., Mizoguchi, E., Cohen, P., Khan, W., Liu, C.H., Hagemann, T.L., Kwan, S.P., Ferrini, R., Davidson, L., *et al.* (1998). Wiskott-Aldrich syndrome protein-deficient mice reveal a role for WASP in T but not B cell activation. *Immunity* 9, 81-91.

Stewart, D.M., Tian, L., and Nelson, D.L. (1999). Mutations that cause the Wiskott-Aldrich syndrome impair the interaction of Wiskott-Aldrich syndrome protein (WASP) with WASP interacting protein. *J Immunol* 162, 5019-5024.

Stewart, M.P., McDowall, A., and Hogg, N. (1998). LFA-1-mediated adhesion is regulated by cytoskeletal restraint and by a Ca²⁺-dependent protease, calpain. *J Cell Biol* 140, 699-707.

Suen, P.W., Ilic, D., Cavegion, E., Berton, G., Damsky, C.H., and Lowell, C.A. (1999). Impaired integrin-mediated signal transduction, altered cytoskeletal structure and reduced motility in Hck/Fgr deficient macrophages. *Journal of cell science* 112 (Pt 22), 4067-4078.

Suetsugu, S., Miki, H., and Takenawa, T. (1999). Identification of two human WAVE/SCAR homologues as general actin regulatory molecules which associate with the Arp2/3 complex. *Biochem Biophys Res Commun* 260, 296-302.

Swanson, J.A. (2008). Shaping cups into phagosomes and macropinosomes. *Nat Rev Mol Cell Biol* 9, 639-649.

Symons, M., Derry, J.M., Karlak, B., Jiang, S., Lemahieu, V., McCormick, F., Francke, U., and Abo, A. (1996). Wiskott-Aldrich syndrome protein, a novel effector for the GTPase CDC42Hs, is implicated in actin polymerization. *Cell* 84, 723-734.

Thanabalu, T., and Munn, A.L. (2001). Functions of Vrp1p in cytokinesis and actin patches are distinct and neither requires a WH2/V domain. *EMBO J* 20, 6979-6989.

Thrasher, A.J. (2002). WASp in immune-system organization and function. *Nat Rev Immunol* 2, 635-646.

Thrasher, A.J. (2009). New insights into the biology of Wiskott-Aldrich syndrome (WAS). *Hematology Am Soc Hematol Educ Program*, 132-138.

Thrasher, A.J., Burns, S., Lorenzi, R., and Jones, G.E. (2000). The Wiskott-Aldrich syndrome: disordered actin dynamics in haematopoietic cells. *Immunol Rev* 178, 118-128.

Thrasher, A.J., and Burns, S.O. (2010). WASP: a key immunological multitasker. *Nat Rev Immunol* 10, 182-192.

Tompa, P., Buzder-Lantos, P., Tantos, A., Farkas, A., Szilagyi, A., Banoczi, Z., Hudecz, F., and Friedrich, P. (2004). On the sequential determinants of calpain cleavage. *J Biol Chem* 279, 20775-20785.

Torres, E., and Rosen, M.K. (2003). Contingent phosphorylation/dephosphorylation provides a mechanism of molecular memory in WASP. *Mol Cell* 11, 1215-1227.

Torres, E., and Rosen, M.K. (2006). Protein-tyrosine kinase and GTPase signals cooperate to phosphorylate and activate Wiskott-Aldrich syndrome protein (WASP)/neuronal WASP. *J Biol Chem* 281, 3513-3520.

Tsai, M.Y., Wang, S., Heidinger, J.M., Shumaker, D.K., Adam, S.A., Goldman, R.D., and Zheng, Y. (2006). A mitotic lamin B matrix induced by RanGTP required for spindle assembly. *Science (New York, NY)* 311, 1887-1893.

Tsuboi, S. (2007). Requirement for a complex of Wiskott-Aldrich syndrome protein (WASP) with WASP interacting protein in podosome formation in macrophages. *J Immunol* 178, 2987-2995.

Tsuboi, S., and Meerloo, J. (2007). Wiskott-Aldrich syndrome protein is a key regulator of the phagocytic cup formation in macrophages. *J Biol Chem* 282, 34194-34203.

Tsukada, S., Saffran, D.C., Rawlings, D.J., Parolini, O., Allen, R.C., Klisak, I., Sparkes, R.S., Kubagawa, H., Mohandas, T., Quan, S., *et al.* (1993). Deficient expression of a B cell cytoplasmic tyrosine kinase in human X-linked agammaglobulinemia. *Cell* 72, 279-290.

Villa, A., Notarangelo, L., Macchi, P., Mantuano, E., Cavagni, G., Brugnani, D., Strina, D., Patrosso, M.C., Ramenghi, U., Sacco, M.G., *et al.* (1995). X-linked thrombocytopenia and Wiskott-Aldrich syndrome are allelic diseases with mutations in the WASP gene. *Nat Genet* 9, 414-417.

Volkman, B.F., Prehoda, K.E., Scott, J.A., Peterson, F.C., and Lim, W.A. (2002). Structure of the N-WASP EVH1 domain-WIP complex: insight into the molecular basis of Wiskott-Aldrich Syndrome. *Cell* 111, 565-576.

Wang, K.K., Villalobo, A., and Roufogalis, B.D. (1989). Calmodulin-binding proteins as calpain substrates. *Biochem J* 262, 693-706.

Ward, M.E., Wu, J.Y., and Rao, Y. (2004). Visualization of spatially and temporally regulated N-WASP activity during cytoskeletal reorganization in living cells. *Proceedings of the National Academy of Sciences of the United States of America* 101, 970-974.

Weiler, M.C., Smith, J.L., and Masters, J.N. (1996). CR16, a novel proline-rich protein expressed in rat brain neurons, binds to SH3 domains and is a MAP kinase substrate. *J Mol Neurosci* 7, 203-215.

Welch, M.D., and Mullins, R.D. (2002). Cellular control of actin nucleation. *Annual review of cell and developmental biology* 18, 247-288.

Westerberg, L., Wallin, R.P., Greicius, G., Ljunggren, H.G., and Severinson, E. (2003). Efficient antigen presentation of soluble, but not particulate, antigen in the absence of Wiskott-Aldrich syndrome protein. *Immunology* 109, 384-391.

Westerberg, L.S., Meelu, P., Baptista, M., Eston, M.A., Adamovich, D.A., Cotta-de-Almeida, V., Seed, B., Rosen, M.K., Vandenberghe, P., Thrasher, A.J., *et al.* (2010). Activating WASP mutations associated with X-linked neutropenia result in enhanced actin polymerization, altered cytoskeletal responses, and genomic instability in lymphocytes. *J Exp Med* 207, 1145-1152.

Wiche, G. (1998). Role of plectin in cytoskeleton organization and dynamics. *Journal of cell science 111 (Pt 17)*, 2477-2486.

Wu, M., Yu, Z., Fan, J., Caron, A., Whiteway, M., and Shen, S.H. (2006). Functional dissection of human protease mu-calpain in cell migration using RNAi. *FEBS Lett 580*, 3246-3256.

Yamaguchi, H., Miki, H., Suetsugu, S., Ma, L., Kirschner, M.W., and Takenawa, T. (2000). Two tandem verprolin homology domains are necessary for a strong activation of Arp2/3 complex-induced actin polymerization and induction of microspike formation by N-WASP. *Proceedings of the National Academy of Sciences of the United States of America 97*, 12631-12636.

Zeng, R., Cannon, J.L., Abraham, R.T., Way, M., Billadeau, D.D., Bubeck-Wardenberg, J., and Burkhardt, J.K. (2003). SLP-76 coordinates Nck-dependent Wiskott-Aldrich syndrome protein recruitment with Vav-1/Cdc42-dependent Wiskott-Aldrich syndrome protein activation at the T cell-APC contact site. *J Immunol 171*, 1360-1368.

Zhang, J., Shehabeldin, A., da Cruz, L.A., Butler, J., Somani, A.K., McGavin, M., Kozieradzki, I., dos Santos, A.O., Nagy, A., Grinstein, S., *et al.* (1999). Antigen receptor-induced activation and cytoskeletal rearrangement are impaired in Wiskott-Aldrich syndrome protein-deficient lymphocytes. *J Exp Med 190*, 1329-1342.

Zicha, D., Dunn, G., and Jones, G. (1997). Analyzing chemotaxis using the Dunn direct-viewing chamber. *Methods Mol Biol 75*, 449-457.

Appendix 1

Plasmids used in this study:

Plasmid	Description	Expression host	Reference
YEplac112	TRP1 2µm ORI plasmid	Yeast	Results 3.1
YEplac181	LEU2 2µm ORI plasmid	Yeast	Results 3.1
YEplac195	URA3 2µm ORI plasmid	Yeast	Results 3.1
pFIV	pFIV-CMV-copGFP	Mammalian	Results 3.2 & 3.3
PEPCG	PEPCG-Cop-Neo	Mammalian	Results 3.2 & 3.3
pACT2	LEU2 vector with Gal4p DNA activation domain	Yeast	Results 3.3
pAS2-1	TRP1 vector with Gal4p DNA binding domain	Yeast	Results 3.3
WASP reporter	YEplac112 with NLS-YFP ₁₋₁₅₄ -WASP-YFP ₁₅₅₋₂₃₈	Yeast	Results 3.1
N-control-WASP	YEplac112 with NLS-YFP ₁₋₁₅₄ -WASP	Yeast	Results 3.1
C-control-WASP	YEplac181 with NLS-WASP-YFP ₁₅₅₋₂₃₈	Yeast	Results 3.1
N-control-WASP-GFP	YEplac112 with NLS-YFP ₁₋₁₅₄ -WASP-GFP	Yeast	Results 3.1
C-control-WASP-GFP	YEplac181 with NLS-WASP-YFP ₁₅₅₋₂₃₈ -GFP	Yeast	Results 3.1
NLS-WIP	YEplac181 with NLS-WIP	Yeast	Results 3.1
NLS-WIRE	YEplac181 with NLS-WIRE	Yeast	Results 3.1
NLS-CR16	YEplac181 with NLS-CR16	Yeast	Results 3.1
NLS-WIP-GFP	YEplac181 with NLS-WIP-GFP	Yeast	Results 3.1
NLS-WIRE-GFP	YEplac181 with NLS-WIRE-GFP	Yeast	Results 3.1
NLS-CR16-GFP	YEplac181 with NLS-CR16-GFP	Yeast	Results 3.1
NLS-Toca1	YEplac181 with NLS- Toca1	Yeast	Results 3.1
NLS-Nck1	YEplac181 with NLS- Nck1	Yeast	Results 3.1
NLS-Cdc42 ^{G12V} Δcaax	YEplac181 with NLS- Cdc42 ^{G12V} Δcaax	Yeast	Results 3.1
NLS-Toca1-GFP	YEplac181 with NLS- Toca1-GFP	Yeast	Results 3.1
NLS-Nck1-GFP	YEplac181 with NLS- Nck1-GFP	Yeast	Results 3.1
NLS-Cdc42 ^{G12V} Δcaax-GFP	YEplac181 with NLS- Cdc42 ^{G12V} Δcaax-GFP	Yeast	Results 3.1
NLS-Toca1 (Ura)	YEplac195 with NLS- Toca1	Yeast	Results 3.1
NLS-Nck1 (Ura)	YEplac195 with NLS- Nck1	Yeast	Results 3.1
NLS-Cdc42 ^{G12V} Δcaax (Ura)	YEplac195 with NLS- Cdc42 ^{G12V} Δcaax	Yeast	Results 3.1

WASP ^{A134T} sensor	YEplac112 with NLS-YFP ₁₋₁₅₄ -WASP ^{A134T} -YFP ₁₅₅₋₂₃₈	Yeast	Results 3.1
WASP ^{G187C} sensor	YEplac112 with NLS-YFP ₁₋₁₅₄ -WASP ^{G187C} -YFP ₁₅₅₋₂₃₈	Yeast	Results 3.1
WASP ^{L270P} sensor	YEplac112 with NLS-YFP ₁₋₁₅₄ -WASP ^{L270P} -YFP ₁₅₅₋₂₃₈	Yeast	Results 3.1
WASP ^{P373S} sensor	YEplac112 with NLS-YFP ₁₋₁₅₄ -WASP ^{P373S} -YFP ₁₅₅₋₂₃₈	Yeast	Results 3.1
WASP ^{D485N} sensor	YEplac112 with NLS-YFP ₁₋₁₅₄ -WASP ^{D485N} -YFP ₁₅₅₋₂₃₈	Yeast	Results 3.1
WASP ^{Y291E} sensor	YEplac112 with NLS-YFP ₁₋₁₅₄ -WASP ^{Y291E} -YFP ₁₅₅₋₂₃₈	Yeast	Results 3.1
WASP ^{Y291F} sensor	YEplac112 with NLS-YFP ₁₋₁₅₄ -WASP ^{Y291F} -YFP ₁₅₅₋₂₃₈	Yeast	Results 3.1
WASP ^{L270P/Y291E} sensor	YEplac112 with NLS-YFP ₁₋₁₅₄ -WASP ^{L270P/Y291E} -YFP ₁₅₅₋₂₃₈	Yeast	Results 3.1
WASP ^{L270P/Y291F} sensor	YEplac112 with NLS-YFP ₁₋₁₅₄ -WASP ^{L270P/Y291F} -YFP ₁₅₅₋₂₃₈	Yeast	Results 3.1
pFIV-WASP reporter	pFIV with NLS-YFP ₁₋₁₅₄ -WASP-YFP ₁₅₅₋₂₃₈	Mammalian/HEK 293T	Results 3.1
pFIV-WASP ^{A134T} sensor	pFIV with NLS-YFP ₁₋₁₅₄ -WASP ^{A134T} -YFP ₁₅₅₋₂₃₈	Mammalian/HEK 293T	Results 3.1
pFIV-WASP ^{L270P} sensor	pFIV with NLS-YFP ₁₋₁₅₄ -WASP ^{L270P} -YFP ₁₅₅₋₂₃₈	Mammalian/HEK 293T	Results 3.1
pFIV-WASP ^{Y291E} sensor	pFIV with NLS-YFP ₁₋₁₅₄ -WASP ^{Y291E} -YFP ₁₅₅₋₂₃₈	Mammalian/HEK 293T	Results 3.1
pFIV-WASP ^{Y291F} sensor	pFIV with NLS-YFP ₁₋₁₅₄ -WASP ^{Y291F} -YFP ₁₅₅₋₂₃₈	Mammalian/HEK 293T	Results 3.1
pFIV-WASP ^{L294T} sensor	pFIV with NLS-YFP ₁₋₁₅₄ -WASP ^{L294T} -YFP ₁₅₅₋₂₃₈	Mammalian/HEK 293T	Results 3.1
pFIV-WASP ^{AVCA} sensor	pFIV with NLS-YFP ₁₋₁₅₄ -WASP ^{AVCA} -YFP ₁₅₅₋₂₃₈	Mammalian/HEK 293T	Results 3.1
pFIV-WIP	pFIV with WIP-His	Mammalian/HEK 293T	Results 3.1
pFIV-WIRE	pFIV with WIRE-His	Mammalian/HEK 293T	Results 3.1
pFIV-CR16	pFIV with CR16-His	Mammalian/HEK 293T	Results 3.1
YFP-WIP	pFIV with YFP-WIP	Mammalian/HEK 293T	Results 3.1
WASP-CFP	pFIV with WASP-CFP	Mammalian/HEK 293T	Results 3.1
WASP-His	pFIV with WASP-His	Mammalian/HEK 293T	Results 3.2
WASP ^{L270P} -His	pFIV with WASP ^{L270P} -His	Mammalian/HEK 293T	Results 3.2
WASP ^{Y291E} -His	pFIV with WASP ^{Y291E} -His	Mammalian/HEK 293T	Results 3.2
WASP ^{Y291F} -His	pFIV with WASP ^{Y291F} -His	Mammalian/HEK 293T	Results 3.2
WASP ^{L270P/Y291E} -His	pFIV with WASP ^{L270P/Y291E} -His	Mammalian/HEK 293T	Results 3.2
WASP ^{L270P/Y291F} -His	pFIV with WASP ^{L270P/Y291F} -His	Mammalian/HEK 293T	Results 3.2

BTK-GFP	pFIV with BTK-GFP	Mammalian/HEK 293T	Results 3.2
HCK-GFP	pFIV with HCK-GFP	Mammalian/HEK 293T	Results 3.2
Tec-GFP	pFIV with Tec-GFP	Mammalian/HEK 293T	Results 3.2
ITK-GFP	pFIV with ITK-GFP	Mammalian/HEK 293T	Results 3.2
Fyn-GFP	pFIV with Fyn-GFP	Mammalian/HEK 293T	Results 3.2
WASP	YEplac112 with WASP	Yeast	Results 3.2
WASP ^{L270P}	YEplac112 with WASP ^{L270P}	Yeast	Results 3.2
WASP ^{Y291E}	YEplac112 with WASP ^{Y291E}	Yeast	Results 3.2
WASP ^{Y291F}	YEplac112 with WASP ^{Y291F}	Yeast	Results 3.2
WASP ^{L270P/Y291E}	YEplac112 with WASP ^{L270P/Y291E}	Yeast	Results 3.2
WASP ^{L270P/Y291F}	YEplac112 with WASP ^{L270P/Y291F}	Yeast	Results 3.2
WIP	YEplac181 with WIP	Yeast	Results 3.2
W7si (lentiviral)	pFIV-H1/U6-W7	Mammalian/Jurkat	Results 3.2
W8si (lentiviral)	pFIV-H1/U6-W8	Mammalian/Jurkat	Results 3.2
W7 (lentiviral)	pFIV-H1-W7	Mammalian/Jurkat	Results 3.2
W8 (lentiviral)	pFIV-H1-W8	Mammalian/Jurkat	Results 3.2
W7-W7 (lentiviral)	pFIV-H1-W7-W7	Mammalian/Jurkat	Results 3.2
W8-W8 (lentiviral)	pFIV-H1-W8-W8	Mammalian/Jurkat	Results 3.2
S1-S1 (lentiviral)	pFIV-H1-S1-S1	Mammalian/Jurkat	Results 3.2
EBV-W7 (lentiviral)	pFIV-EBV-W7	Mammalian/Jurkat	Results 3.2
EBV-W8 (lentiviral)	pFIV-EBV-W8	Mammalian/Jurkat	Results 3.2
S1 (retroviral)	pSIR-U6-S1	Mammalian/Jurkat	Results 3.2
N-WASP-GFP	pFIV with N-WASP-GFP	Mammalian/HEK 293T	Results 3.2
WASP-GFP	pFIV with WASP-GFP	Mammalian/HEK 293T	Results 3.2
RFP	PEPCG with RFP	Mammalian/Jurkat	Results 3.2
WASP _R	PEPCG with WASP _R -RFP	Mammalian/Jurkat	Results 3.2
WASP _R ^{L270P}	PEPCG with WASP _R ^{L270P} -RFP	Mammalian/Jurkat	Results 3.2
WASP _R ^{Y291E}	PEPCG with WASP _R ^{Y291E} -RFP	Mammalian/Jurkat	Results 3.2
WASP _R ^{Y291F}	PEPCG with WASP _R ^{Y291F} -RFP	Mammalian/Jurkat	Results 3.2
WASP _R ^{L270P/Y291E}	PEPCG with WASP _R ^{L270P/Y291E} -RFP	Mammalian/Jurkat	Results 3.2
WASP _R ^{L270P/Y291F}	PEPCG with WASP _R ^{L270P/Y291F} -RFP	Mammalian/Jurkat	Results 3.2
GFP	pFIV with GFP	Mammalian/ N-WASP ^{-/-}	Results 3.2
WIP	pFIV with WIP	Mammalian/ N-WASP ^{-/-}	Results 3.2
WIP-GFP	pFIV with WIP-GFP	Mammalian/ N-WASP ^{-/-}	Results 3.2
WASP-GFP	pFIV with WASP-GFP	Mammalian/ N-WASP ^{-/-}	Results 3.2
WASP ^{Y291E} -GFP	pFIV with WASP ^{Y291E} -GFP	Mammalian/ N-WASP ^{-/-}	Results 3.2

WASP ^{Y291F} -GFP	pFIV with WASP ^{Y291F} -GFP	Mammalian/ N-WASP ^{-/-}	Results 3.2
WASP ^{L270P/Y291E} -GFP	pFIV with WASP ^{L270P/Y291E} -GFP	Mammalian/ N-WASP ^{-/-}	Results 3.2
WASP ^{L270P/Y291F} -GFP	pFIV with WASP ^{L270P/Y291F} -GFP	Mammalian/ N-WASP ^{-/-}	Results 3.2
WASP ^{ΔWH1} -GFP	pFIV with WASP ¹³⁸⁻⁵⁰³ -GFP	Mammalian/ HEK 293T	Results 3.3
pAS2-1-WASP	pAS2-1 with WASP	Yeast	Results 3.3
pAS2-1-WASP ⁵⁰⁻⁵⁰³	pAS2-1 with WASP ⁵⁰⁻⁵⁰³	Yeast	Results 3.3
pAS2-1-WASP ⁹⁵⁻⁵⁰³	pAS2-1 with WASP ⁹⁵⁻⁵⁰³	Yeast	Results 3.3
pAS2-1-WASP ¹⁰⁰⁻⁵⁰³	pAS2-1 with WASP ¹⁰⁰⁻⁵⁰³	Yeast	Results 3.3
pAS2-1-WASP ¹⁰⁰⁻⁵⁰³	pAS2-1 with WASP ¹⁰⁰⁻⁵⁰³	Yeast	Results 3.3
pAS2-1-WASP ¹¹⁴⁻⁵⁰³	pAS2-1 with WASP ¹¹⁴⁻⁵⁰³	Yeast	Results 3.3
pAS2-1-WASP ¹²⁷⁻⁵⁰³	pAS2-1 with WASP ¹²⁷⁻⁵⁰³	Yeast	Results 3.3
pAS2-1-WASP ^{ΔWH1}	pAS2-1 with WASP ¹³⁸⁻⁵⁰³	Yeast	Results 3.3
pAS2-1-WASP ⁹⁵⁻⁵⁰³ Y102W/Y107W	pAS2-1 with WASP ⁹⁵⁻⁵⁰³ Y102W/Y107W	Yeast	Results 3.3
pACT2-WIP	pACT2 with WIP	Yeast	Results 3.3
GST-WASP ⁹⁵⁻³²⁰	pGEX with GST-WASP ⁹⁵⁻³²⁰	Bacteria	Results 3.3
GST-WASP ⁹⁵⁻³²⁰ WRG	pGEX with GST-WASP ⁹⁵⁻³²⁰ WRG	Bacteria	Results 3.3
WASP ^{T111P} -GFP	pFIV with WASP ^{T111P} -GFP	Mammalian/HEK 293T	Results 3.3
WASP ^{Δ50} -GFP	pFIV with WASP ^{Δ50} -GFP	Mammalian/HEK 293T	Results 3.3
WASP ^{Δ100} -GFP	pFIV with WASP ^{Δ100} -GFP	Mammalian/HEK 293T	Results 3.3
WASP ⁹⁵⁻⁵⁰³ Y102W/Y107W-GFP	pFIV with WASP ⁹⁵⁻⁵⁰³ Y102W/Y107W-GFP	Mammalian/HEK 293T	Results 3.3
WASP ⁹⁵⁻⁵⁰³ -GFP	pFIV with WASP ⁹⁵⁻⁵⁰³ -GFP	Mammalian/HEK 293T	Results 3.3
WASP ¹¹⁴⁻⁵⁰³ -GFP	pFIV with WASP ¹¹⁴⁻⁵⁰³ -GFP	Mammalian/HEK 293T	Results 3.3
WASP ¹²⁷⁻⁵⁰³ -GFP	pFIV with WASP ¹²⁷⁻⁵⁰³ -GFP	Mammalian/HEK 293T	Results 3.3
WASP ^{Δ82-95} -GFP	pFIV with WASP ^{Δ82-95} -GFP	Mammalian/HEK 293T	Results 3.3
WASP ^{Δ82-109} -GFP	pFIV with WASP ^{Δ82-109} -GFP	Mammalian/HEK 293T	Results 3.3
WASP ^{Δ82-114} -GFP	pFIV with WASP ^{Δ82-114} -GFP	Mammalian/HEK 293T	Results 3.3
WASP ^{Y88W} -GFP	pFIV with WASP ^{Y88W} -GFP	Mammalian/HEK 293T	Results 3.3
WASP ^{Y102W} -GFP	pFIV with WASP ^{Y102W} -GFP	Mammalian/HEK 293T	Results 3.3
WASP ^{Y107C} -GFP	pFIV with WASP ^{Y107C} -GFP	Mammalian/HEK 293T	Results 3.3
WASP ^{Y107W} -GFP	pFIV with WASP ^{Y107W} -GFP	Mammalian/HEK 293T	Results 3.3
WASP ^{Y88W/Y102W} -GFP	pFIV with WASP ^{Y88W/Y102W} -GFP	Mammalian/HEK 293T	Results 3.3
WASP ^{Y102W/Y107W} -GFP	pFIV with WASP ^{Y102W/Y107W} -GFP	Mammalian/HEK 293T	Results 3.3
WASP ^{T111R/P112G} -GFP	pFIV with WASP ^{T111R/P112G} -GFP	Mammalian/HEK 293T	Results 3.3
WASP ^{WRG} -GFP	pFIV with WASP ^{Y102W/T111R/P112G} -GFP	Mammalian/HEK 293T	Results 3.3
WASP ^{S103N/S108N} -GFP	pFIV with WASP ^{S103N/S108N} -GFP	Mammalian/HEK 293T	Results 3.3

WASP ^{S103N/S108NT111R/P112G} -GFP	pFIV with WASP ^{S103N/S108NT111R/P112G} -GFP	Mammalian/HEK 293T	Results 3.3
WASP ^{95-503 102F/T111R/P112G} -GFP	pFIV with WASP ^{95-503 102F/T111R/P112G} -GFP	Mammalian/HEK 293T	Results 3.3
WASP ^{WRG} sensor	YEplac112 with NLS-YFP ₁₋₁₅₄ - WASP ^{Y102W/T111R/P112G} -YFP ₁₅₅₋₂₃₈	Yeast	Results 3.3
WASP ^{WRG}	YEplac112 with WASP ^{WRG}	Yeast	Results 3.3
WASP ^{WRG} -GFP	pFIV with WASP ^{WRG} -GFP	Mammalian/ N-WASP ^{-/-}	Results 3.3
WASP _R ^{WRG}	PEPCG with WASP _R ^{WRG} -RFP	Mammalian/Jurkat	Results 3.3

Appendix 2

Primers used in this study:

Primers	Sequence 5'-3'	Remarks	Reference
WAS-F	CAT GCC ATG GGA ATG AGT GGG GGC CCA ATG GGA G	1-22 of WASP cDNA	-
WAS-R	CGC GGA TCC GTC ATC CCA TTC ATC ATC TTC ATC TTC	1480-1506 of WASP cDNA	-
YFP ¹⁻¹⁵⁴ -F	GTCGACCTCTAGAATGGTGAGCAAGGGCGAGGAGCTG	Forward primer YFP ¹⁻¹⁵⁴	Results 3.1
YFP ¹⁻¹⁵⁴ -R	CATATGTCCCATGGCTCCTCCTCCTCCGGCCATGATAT AGACGTTGTGGCTG	Reverse primer YFP ¹⁻¹⁵⁴	Results 3.1
YFP ¹⁵⁵⁻²³⁸ -F	CTCGAGTGGATCCGGAGGAGGAGGAGACAAGCAGAA GAACGGCATCAAGG	Forward primer YFP ¹⁵⁵⁻²³⁸	Results 3.1
YFP ¹⁵⁵⁻²³⁸ -R	GCGATTAAGTTGGGTAACGCCAGG	Reverse primer YFP ¹⁵⁵⁻²³⁸	Results 3.1
WAS ^{A134T} -F	GCA GAC GAG GAC GAG ACC CAG GCC TTC CGG GCC	Forward primer mutation Ala88Phe	Results 3.1
WAS ^{A134T} -R	GGC CCG GAA GGC CTG GGT CTC GTC CTC GTC TGC	Reverse primer mutation Ala88Phe	Results 3.1
WAS ^{G187C} -F	GGT GGA GAC CAA GGA TGC CCT CCA GTG GGT CCG	Forward primer Mutation Gly187Cys	Results 3.1
WAS ^{G187C} -R	CGG ACC CAC TGG AGG GCA TCC TTG GTC TCC ACC	Reverse primer Mutation Gly187Cys	Results 3.1
WAS ^{L270P} -F	CCA GAT CTG CGG AGT CCG TTC TCC AGG GCA GGA	Forward primer Mutation Leu270Pro	Results 3.1
WAS ^{L270P} -R	TCC TGC CCT GGA GAA CGG ACT CCG CAG ATC TGG	Reverse primer Mutation Leu270Pro	Results 3.1
WAS ^{P373S} -F	CCA CCA CCA CCC CCT TCA GCT ACT GGA CGT TCT	Forward primer Mutation Pro270Phe	Results 3.1
WAS ^{P373S} -R	AGA ACG TCC AGT AGC TGA AGG GGG TGG TGG TGG	Reverse primer Mutation Pro270Phe	Results 3.1
WAS ^{D485N} -F	GCC ATC CAC TCC TCC AAC GAA GGG GAG GAC CAG	Forward primer Mutation Asp485Asn	Results 3.1
WAS ^{D485N} -R	CTG GTC CTC CCC TTC GTT GGA GGA GTG GAT GGC	Reverse primer Mutation Asp485Asn	Results 3.1
WAS ^{I294T} -F	CTT ATC TAC GAC TTC ACT GAG GAC CAG GGT GGG	Forward primer Mutation Ile294Tyr	Results 3.1
WAS ^{I294T} -R	CCC ACC CTG GTC CTC AGT GAA GTC GTA GAT AAG 3	Reverse primer Mutation Ile294Tyr	Results 3.1
WAS ^{Y291E} -R	GTC CTC AAT GAA GTC CTC GAT AAG TTT AGA GGT	Forward primer Mutation Tyr291Glu	Results 3.2
WAS ^{Y291E} -F	ACC TCT AAA CTT ATC TTC GAC TTC ATT GAG GAC	Forward primer Mutation Tyr291Phe	Results 3.2
WAS ^{Y291E} -R	GTC CTC AAT GAA GTC GAA GAT AAG TTT AGA GGT	Forward primer Mutation Tyr291Phe	Results 3.2
BTK-F	CC CAC ATG TTA GCC GCA GTG ATT CTG GAG AGC	129-149 of BTK cDNA	Results 3.2

BTK-R	CGC GGA TCC GGA TTC TTC ATC CAT GAC ATC TAG	2079-2102 of BTK cDNA	Results 3.2
HCK-F	TGC TCT AGA CTG GGG GGG CGC TCA AGC TG	124-143 of HCK cDNA	Results 3.2
HCK-R	TCA ACC GGT TGG CTG CTG TTG GTA CTG GCT C	1680-1701 of HCK cDNA	Results 3.2
Tec-F	CCC ACA TGT CCA TGA ATT TTA ACA CTA TTT TGG AGG AG	1-27 of Tec cDNA	Results 3.2
Tec-R	CGG GAT CCT CTT CCA AAA GTT TCT TCA CAT TCA ACT AG	1864-1893 of Tec cDNA	Results 3.2
Itk-F	CAT GCC ATG GCC ATG AAC AAC TTA TCC TCC TGG AAG AA	1-27 of Itk cDNA	Results 3.2
Itk-R	CGG GAT CCA AGT CCT GAT TCT GCA ATT TCA GCC	1836-1860 of Itk cDNA	Results 3.2
Fyn-F	CAT GCC ATG GGC TGT GTG CAA TGT AAG GAT	1-24 of Fyn cDNA	Results 3.2
Fyn-R	CGG GAT CCC AGG TTT TCA CCA GGT TGG TAC TG	1423-1426 of Fyn cDNA	Results 3.2
W7si-F	AAAG TGA GAT GCT TGG ACG AAAA	Forward primer W7 siRNA	Results 3.2 (Olivier et al., 2006)
W7si-R	AAAA TTTT CGT CCA AGC ATC TCA	Reverse primer W7 siRNA	Results 3.2 (Olivier et al., 2006)
W8si-F	AAAG TCT CAG TTC TCT TCA CTCA	Forward primer W8 siRNA	Results 3.2 (Olivier et al., 2006)
W8si-R	AAAA TGAG TGA AGA GAA CTG AGA	Reverse primer W8 siRNA	Results 3.2 (Olivier et al., 2006)
W7-F	GAT CCC CTG AGA TGC TTG GAC GAA AAT TCA AGA GAT TTT CGT CCA AGC ATC TCA TTT TTG	Forward primer W7 shRNA	Results 3.2 (Olivier et al., 2006)
W7-R	AAT TCA AAA ATG AGA TGC TTG GAC GAA AAT CTC TTG AAT TTT CGT CCA AGC ATC TCA CG	Reverse primer W7 shRNA	Results 3.2 (Olivier et al., 2006)
S1	CAA TCT CTT GAA TTG TTC AGC TGA ATT CCC TGC TTT TTA GAG TGG TCT CAT ACA G	Forward primer S1 shRNA	Results 3.2
WASP _R	GAT CAA ATC CGG CAA GGT ATC CAA CTGA ACA AGA CCC CT	1306-1344 of WASP cDNA	Results 3.2
WASP ⁹⁵⁻⁵⁰³	CAT GCC ATG GGG CTG CTC TGG GAA CAG GAG CTG	281-303 of WASP cDNA	Results 3.3
WASP ¹¹⁴⁻⁵⁰³	CAT GCC ATG GGA TTC CAC ACC TTC GCT GGA GAT GAC	340-363 of WASP cDNA	Results 3.3
WASP ¹²⁷⁻⁵⁰³	CAT GCC ATG GGA AAC TTT GCA GAC GAG GAC GAG GCC	379-402 of WASP cDNA	Results 3.3

WASP ^{Δ82-109} -F	CTA GCT AGC CCC ACC CCC TTC TTC CAC ACC	327-348 of WASP cDNA	Results 3.3
WASP ^{Δ82-109} -R	CTA GCT AGC CTT CTG GGG GTT ATC CTT CAC GAA	220-243 of WASP cDNA	Results 3.3
WASP ^{Y88F} -F	TAC TTC ATC CGC CTT TGG GGC CTT CAG GCT GGT	Forward primer mutation Tyr88Phe	Results 3.3
WASP ^{Y88F} -R	ACC AGC CTG AAG GCC CCA AAG GCG GAT GAA GTA	Reverse primer mutation Tyr88Phe	Results 3.3
WASP ^{Y102W} -F	TGG GAA CAG GAG CTG TGG TCA CAG CTT GTC	Forward primer mutation Tyr102Trp	Results 3.3
WASP ^{Y102W} -R	GAC AAG CTG TGA CCA CAG CTC CTG TTC CCA	Reverse primer mutation Tyr102Trp	Results 3.3
WASP ^{Y107C} -F	TAC TCA CAG CTT GTC TGC TCC ACC CCC ACC CCC	Forward primer mutation Tyr102Cys	Results 3.3
WASP ^{Y107C} -R	GGG GGT GGG GGT GGA GCA GAC AAG CTG TGA GTA	Reverse primer mutation Tyr102Cys	Results 3.3
WASP ^{Y107W} -F	TAC TCA CAG CTT GTC TGG TCC ACC CCC ACC CCC	Forward primer mutation Tyr107Trp	Results 3.3
WASP ^{Y107W} -R	GGG GGT GGG GGT GGA CCA GAC AAG CTG TGA GTA	Reverse primer mutation Tyr107Trp	Results 3.3
WASP ^{S103N/S108N} -F	CTG TAC AAC CAG CTT GTC TAT AAC ACC CCC	Forward primer mutation Ser103Asn + Ser108Asn	Results 3.3
WASP ^{S103N/S108N} -R	GGG GGT GTT ATA GAC AAG CTG GTT GTA CAG	Reverse primer mutation Ser103Asn + Ser108Asn	Results 3.3
WASP ^{T111R/P112G} -F	GTC TAC TCC ACC CCC CGC GGC TTC TTT CAC ACC TTC	Forward primer mutation Tyr103Arg + Pro112Gly	Results 3.3
WASP ^{T111R/P112G} -R	GAA GGT GTG AAA GAA GCC GCG GGG GGT GGA GTA GAC	Reverse primer mutation Tyr103Arg + Pro112Gly	Results 3.3

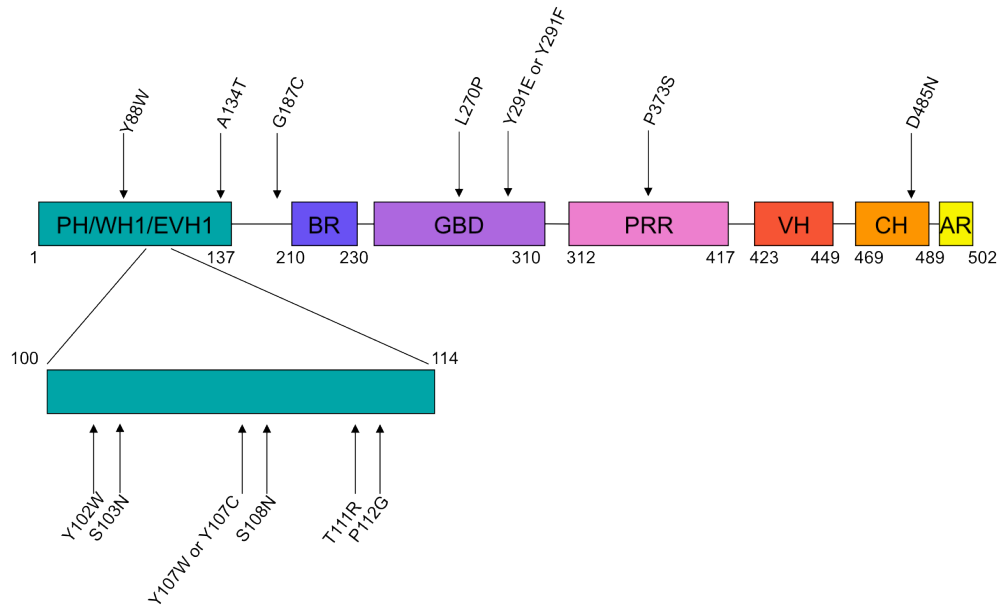


Figure A1 Schematic figure of WASP with point mutations generated in this study.

Appendix 3

Protein sequence of WASP

```

1  msggpmggrp ggrgapavqq nipstllqdh enqrlfemlg rkcltlata vqlylalppg
61  aehwtkehcg avcfvkdnpg ksyfirlygl qagrllweqe lysqlvystp tpffhtfagd
121 dcqaglnfad edeaqafra1 vqekiqrnq rsgdrrqlp ppptpaneer rgglpplplh
181 pggdgggppv gplslglatv diqnpditss ryrglpapgp spadkkrsgk kkiskadiga
241 psgfkvhshv gwdpqngfdv nnldpdlrs1 fsragiseaq ltdaetskli ydfiedgggl
301 eavrqemrrq eplpppppps rggnglprpp ivggknkgrsg plppvplgia pppptprgpp
361 ppgrggpppp pppatgrsgp lpppppgagg ppmppppppp ppppssngnp appplppalv
421 pagglapggg rgalldqirg giqlnktpga pessalqppp qsseglvgal mhvmqkrsra
481 ihssdegedq agdededdeu dd

```

cDNA sequence of WASP

```

1  atgagtgggg gcccaatggg aggaaggccc gggggccgag gagcaccagc ggttcagcag
61  aacataccct ccaccctcct ccaggaccac gagaaccagc gactctttga gatgcttgga
121 cgaaaatgct tgacgctggc cactgcagtt gttcagctgt acctggcgct gccccctgga
181 gctgagcact ggaccaagga gcattgtggg gctgtgtgct tcgtgaagga taacccccag
241 aagtcctact tcatccgcct ttacggcctt caggctgggtc ggctgctctg ggaacaggag
301 ctgtactcac agcttgtcta ctccaccccc acccccttct tccacacctt cgctggagat
361 gactgccaag cggggctgaa ctttgacagc gaggacgagg cccaggcctt ccgggcccctc
421 gtgcaggaga agatacaaaa aaggaatcag aggcaaagtg gagacagacg ccagctaccc
481 ccaccaccaa caccagccaa tgaagagaga agaggagggc tccccccctt gcccctgcat
541 ccaggtggag accaaggagg ccctccagtg ggtccgctct ccctggggct ggcgacagtg
601 gacatccaga accctgacat cacgagttca cgataccgtg ggctcccagc acctggacct
661 agcccagctg ataagaaacg ctcagggaag aagaagatca gcaaagctga tattggtgca
721 cccagtggat tcaagcatgt cagccacgtg ggggtggacc cccagaatgg atttgacgtg
781 aacaacctcg acccagatct gcggagtctg ttctccaggg cagggaatcag cgaggcccag
841 ctcaccgacg ccgagacctc taaacttata tacgacttca ttgaggacca ggggtgggctg
901 gaggtgtgtc ggcaggagat gaggcgccag gagccacttc cgccgcccc accgccatct
961 cgaggaggga accagctccc ccggccccct attgtggggg gtaacaaggg tcgttctggt
1021 cactgcccc ctgtaccttt ggggattgcc ccacccccac caacaccccg gggaccccca
1081 cccccaggcc gagggggccc tccaccacca cccctccag ctactggacg ttctggacca
1141 ctgccccctc caccctctgg agctggtggg ccaccatgc caccaccacc gccaccaccg
1201 ccaccgccc ccagctccgg gaatggacca gcccctcccc cactccctcc tgctctggtg
1261 cctgccgggg gcctggcccc tgggtggggg cggggagcgc ttttgatca aatccggcag
1321 ggaattcagc tgaacaagac ccctggggcc ccagagagct cagcgtgca gccaccacct
1381 cagagctcag agggactggt gggggccctg atgcacgtga tgcagaagag aagcagagcc
1441 atccactcct ccgacgaagg ggaggaccag gctggcgatg aagatgaaga tgatgaatgg
1501 gatgactga

```

Analysis of conformational changes in WASP using a split YFP

Rina Pei Zhi Lim, Ashish Misra, Zhihao Wu, Thirumaran Thanabalu *

School of Biological Sciences, Nanyang Technological University, 60 Nanyang Drive, Singapore 637551, Republic of Singapore

Received 20 August 2007

Available online 30 August 2007

Abstract

WASP (Wiskott–Aldrich syndrome protein) has been proposed to adopt a closed conformation (autoinhibited conformation) due to interaction between the carboxy terminal and the GTPase binding domain. Various WASP-interacting proteins have been suggested to relieve this autoinhibition. We have used the split YFP (Yellow Fluorescent Protein) to analyze the conformation of WASP. *Saccharomyces cerevisiae* cells expressing YFP_{1–154}–WASP–YFP_{155–238} were found to exhibit YFP fluorescence while cells expressing of YFP_{1–154}–WASP and WASP–YFP_{155–238} did not suggesting an intramolecular complementation of the YFP molecule. The fluorescence signal of YFP_{1–154}–WASP–YFP_{155–238} was enhanced in the presence of WIP (WASP-interacting protein) however this is not due to the increased stability of YFP_{1–154}–WASP–YFP_{155–238}. Expression of Toca-1 and Nck1 reduced the YFP fluorescence from YFP_{1–154}–WASP–YFP_{155–238} even in the presence of WIP suggesting that binding of Toca-1 or Nck1 altered the conformation of YFP_{1–154}–WASP–YFP_{155–238}. Thus both Nck1 and Toca-1 can relieve the autoinhibition of the WASP molecule.

© 2007 Elsevier Inc. All rights reserved.

Keywords: Wiskott–Aldrich syndrome; WASP-interacting protein; WASP; WIP; Las17p; Arp2/3 complex; Toca-1; Nck1

Wiskott–Aldrich Syndrome (WAS) is a genetic disorder caused by mutations in the Wiskott–Aldrich Syndrome protein (WASP) gene [1]. WASP is expressed predominantly in the hematopoietic cells while its homologue, N-WASP (Neural) with two V domains, is expressed ubiquitously [2,3]. WASP is an actin associated protein with five discrete domains. They are a WASP homology (WH1) domain, a basic region (BR), a GTPase binding domain (GBD), a proline rich sequence and the Verprolin Cofilin Acidic (VCA) region [2]. WASP and N-WASP adopt an autoinhibited conformation, the carboxy terminal interacts with the GTPase binding domain [4] and the autoinhibition can be relieved by Cdc42 and phospholipids [5,6].

N-WASP and WASP interact with a number of proteins including Toca-1 (Transducer of Cdc42 activation) [7], WIP (WASP-Interacting Protein) [8] in addition to Cdc42 [9]. WIP belongs to the verprolin family of proteins, which include WICH/WIRE and CR16 [10–12]. Majority of WASP in the cell is present as a complex with WIP [13] and 50% of the missense mutations in WASP are found in the WH1 domain [14], with some of the mutation abolishing WASP–WIP interaction [15], suggesting that WASP–WIP interaction is crucial for WASP's activity. However, it has been suggested that WIP stabilizes N-WASP/WASP in its inactive conformation [16] and phosphorylation of WIP releasing WASP from WIP inhibition [13]. It is still not clear whether Toca-1 knocks WIP from N-WASP–WIP complex before activating N-WASP [7].

The conformational changes in N-WASP induced by Cdc42 were assessed by analyzing FRET efficiency between YFP and CFP fused to the termini of N-WASP [17]. However, it would be difficult to determine whether the observed reduction of FRET efficiency is due to

Abbreviations: WASP, Wiskott–Aldrich syndrome protein; WIP, WASP-interacting protein; Toca-1, Transducer of Cdc42 activation; Nck1, Novel cytoplasmic protein; Cdc42, Cell division cycle 42.

* Corresponding author. Fax: +65 6791 3856.

E-mail address: thirumaran@ntu.edu.sg (T. Thanabalu).

direct interaction between Cdc42 and N-WASP. We have analyzed the conformation of WASP using BiMolecular Fluorescence Complementation [18] in *Saccharomyces cerevisiae* cells which is devoid of the mammalian interactors of WASP family of protein. *S. cerevisiae* cells expressing NLS-YFP_{1–154}-WASP-YFP_{155–238} had a distinct fluorescence signal in the nucleus. This fluorescence signal was enhanced in the presence of WIP and WIRE but not in the presence of CR16. The enhanced fluorescence is not due to increased stability of NLS-YFP_{1–154}-WASP-YFP_{155–238}. The observed enhanced fluorescence in the presence of WIP was reduced in the presence of either Toca-1 or Nck1 but not in the presence of Cdc42. This suggests that WIP stabilizes the auto inactivated form of WASP while both Toca-1 and Nck1 can relieve the autoinhibition.

Materials and methods

Strains, plasmids, media, and reagents. YPUAD (Yeast Extract, Peptone and Dextrose) supplemented with 40 µg/ml adenine and 20 µg/ml uracil. *S. cerevisiae* cells were transformed with plasmid DNA using the lithium acetate protocol [19].

DNA techniques and plasmid construction. DNA encoding YFP_{1–154} (N-YFP) and YFP_{155–289} (C-YFP) were amplified using polymerase chain reaction and fused to DNA encoding WASP at the N-terminus and C-terminus, respectively. The SV40 NLS sequence was fused to the N-terminus of all the constructs to target the fusion proteins to the nucleus. The fusion constructs were expressed using two micron plasmids, YEplac112 (Trp), YEplac195 (Ura), and YEplac181 (Leu) [20].

Western blot. Total protein extract from *S. cerevisiae* cells were prepared as described [21]. The proteins were resolved by 10% SDS-PAGE gel, electroblotted onto nitrocellulose membrane and probed with appropriate primary antibody and secondary antibody conjugated to horseradish peroxidase (HRP) and detected with PICO (Pierce).

Fluorescence microscopy. Exponentially growing cells were harvested and washed once with PBS. The cell pellet was resuspended in PBS and the cell suspension was applied to a microscope slide. Fluorescence was visualized by bright field microscopy using an Olympus microscope with CoolSNAP^{HQ} camera (Roper Scientific). The fluorescence intensity in the nucleus on 100 cells was quantified using metamorph software.

Results

YFP fluorescence is reconstituted by intramolecular complementation

WASP adopts an autoinhibited conformation and is a weak activator of the Arp2/3 complex [22] due to masking of the acidic domain by the GBD domain and this autoinhibition can be relieved by activated Cdc42 binding to the GBD [4]. In order to analyze the conformation of WASP we used the Bimolecular Fluorescence Complementation assay [18]. We have previously found that WASP localizes to punctate cortical patches in the presence of WIP and that WASP is not stable in the cytoplasm in the absence of WIP [23] thus we decided to target our sensor molecule to the nucleus. We transformed the plasmid expressing YFP_{1–154}-WASP-YFP_{155–238} (Trp) into *S. cerevisiae* and selected transformants using SD plates lacking tryptophan and subsequently analyzed the cells using fluorescence microscopy. Cells expressing YFP_{1–154}-WASP-YFP_{155–238} were found to have fluorescence in the nucleus (Fig. 1A). The observed fluorescence could be due to either inter molecular complementation or intra molecular complementation (Fig. 1B). To resolve between the two possibilities we made two additional constructs, YFP_{1–154}-WASP (Leu) and WASP-YFP_{155–238} (Trp). Cells expressing these two constructs did not exhibit any fluorescence (Fig. 1A). This suggests that the observed fluorescence in cells expressing YFP_{1–154}-WASP-YFP_{155–238} (Trp) is due to intramolecular complementation, thus WASP adopts an autoinhibited form in *S. cerevisiae* cells.

Expression of WIP and WIRE enhance the YFP fluorescence

We have previously shown that human WASP suppresses the growth defects of *las17Δ* in the presence of WIP [23].

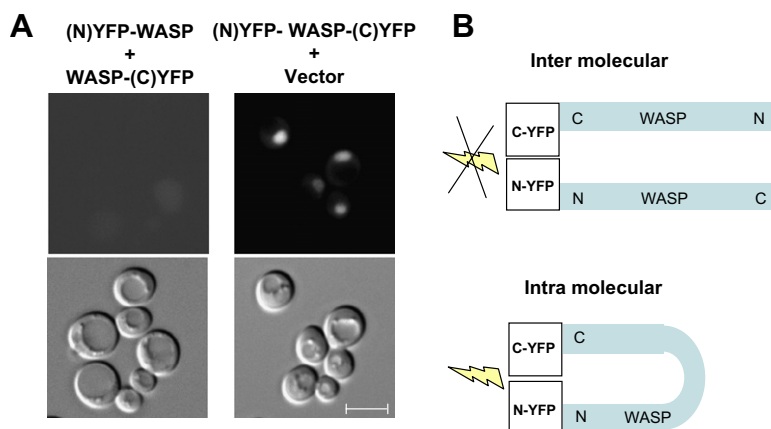


Fig. 1. WASP adopts an autoinhibited conformation in *S. cerevisiae* cells. (A) *S. cerevisiae* cells expressing YFP_{1–154}-WASP-YFP_{155–238} or expressing YFP_{1–154}-WASP-YFP_{155–238} and WASP-YFP_{155–238} were grown in selective media to exponential phase at 24 °C and were analyzed by fluorescence microscopy. Bar = 5 µm. (B) Two possible models of reconstitution of split YFP. The N- and C-terminal halves of YFP can be brought together by either intermolecular or intramolecular interactions.

The observed suppression is due to enhanced stability of WASP as well as localization of WASP in the presence of WIP [23]. In order to analyze the effect of the three proteins (WIP, WIRE, and CR16) from the verprolin family of proteins we introduced the plasmid expressing YFP_{1–154}-WASP-YFP_{155–238} (Trp) together with plasmid (Leu) expressing one of the verprolin proteins. The transformants were grown in selective media (SD minus Trp and Leu) and analyzed by fluorescence microscopy. Expression of YFP_{1–154}-WASP-YFP_{155–238} together with either WIP or WIRE resulted in the enhancement of the YFP fluorescence while expression of YFP_{1–154}-WASP-YFP_{155–238} together with CR16 did not result in any change in the fluorescence intensity (Fig. 2A and B). This suggests that both WIP and WIRE stabilize the closed conformation of WASP while CR16 does not have any effect on the conformation of WASP.

Toca-1 and Nck1 reduce the YFP fluorescence even in the presence of WIP

WASP and N-WASP have been found to bind to a number of proteins, which regulate their function. These include the well characterized Cdc42 as well as Nck1 and Toca-1. Initial work based on in vitro actin polymerization suggested that Cdc42 together with phospholipids can relieve the autoinhibition [5] however this model of WASP

activation has been revised and it has been proposed that Cdc42 acts through Toca-1 [7]. In order to analyze the effect of Toca-1, Nck1 and Cdc42, cells expressing YFP_{1–154}-WASP-YFP_{155–238} and WIP were transformed with plasmids expressing Toca-1, Nck1 or Cdc42 G12VΔcaax (to prevent membrane association). The transformants were analyzed using fluorescence microscopy (Fig. 3A). Analysis of the fluorescence intensity revealed (Fig. 3B) that both Toca-1 and Nck1 reduced the fluorescence from WASP sensor molecule while Cdc42 G12V had no effect. The reduced fluorescence is not due to reduced expression of the sensor molecule (Fig. 3C). This suggests that both Toca-1 and Nck1 alter the conformation of WASP and relieve the autoinhibition while Cdc42 does not.

Discussion

WASP and its homologue N-WASP are proline rich proteins which adopt an autoinhibited conformation with the acidic C-terminal interacting with the GTPase binding region which consists of some basic amino acids [4]. In this conformation WASP and N-WASP are weak activators of the Arp2/3 complex [22]. FRET analysis using YFP and CFP fused to the termini of N-WASP revealed the presence of a conformation in which the two fluorescent proteins were in the range of 6.3 nm [17]. FRET

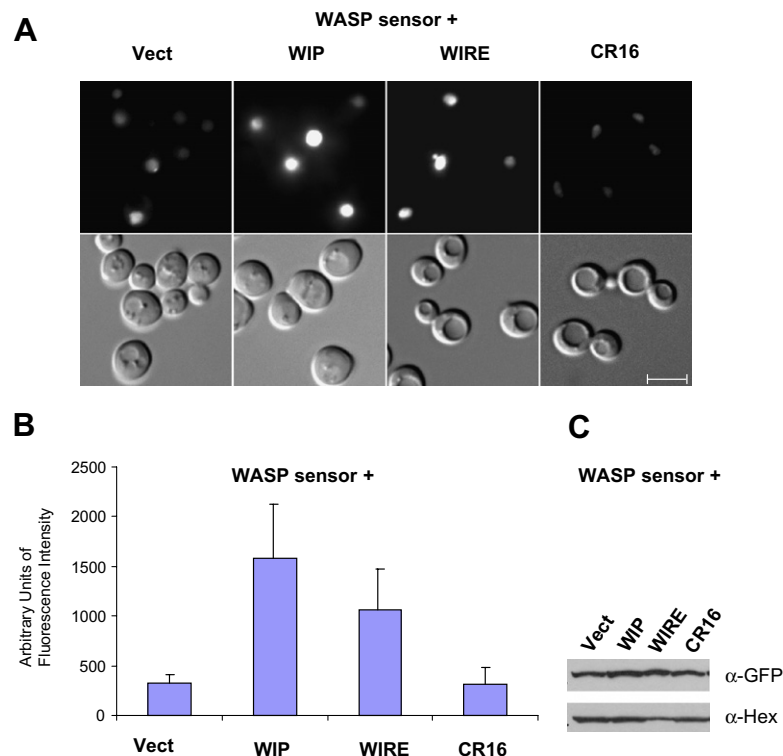


Fig. 2. WIP and WIRE enhance the YFP fluorescence. (A) *S. cerevisiae* cells expressing YFP_{1–154}-WASP-YFP_{155–238} together with (1) Vector (2) WIP (3) WIRE (4) CR16 were grown in selective media to exponential phase at 24 °C and analyzed by fluorescence microscopy. Bar = 5 μm. (B) Quantification of fluorescence intensity of cells expressing *S. cerevisiae* cells expressing NLS-YFP_{1–154}-WASP-YFP_{155–238} together with (1) Vector (2) WIP (3) WIRE (4) CR16. (C) Western blot analysis *S. cerevisiae* cells expressing of YFP_{1–154}-WASP-YFP_{155–238} together with (1) Vector (2) WIP (3) WIRE (4) CR16 using anti-GFP (α-GFP) and anti-hexokinase (α-Hex) serum.

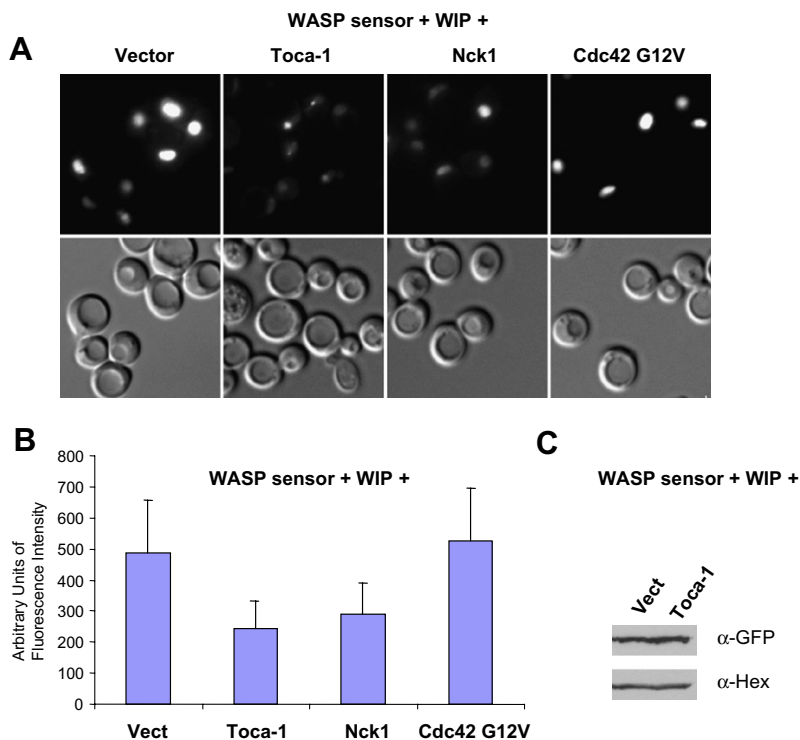


Fig. 3. Toca-1 and Nck1 can relieve the autoinhibition of WASP even in the presence of WIP. (A) *S. cerevisiae* cells expressing YFP_{1–154}-WASP-YFP_{155–238} + WIP together with (1) Vector (2) Toca-1 (3) Nck1 (4) Cdc42 G12V were grown in selective media to exponential phase at 24 °C and analyzed by fluorescence microscopy. Bar = 5 μm. (B) Quantification of fluorescence intensity of cells expressing *S. cerevisiae* cells expressing YFP_{1–154}-WASP-YFP_{155–238} together with (1) Vector (2) WIP (3) WIRE (4) CR16. (C) Western blot analysis *S. cerevisiae* cells expressing of YFP_{1–154}-WASP-YFP_{155–238} + WIP with (1) Vector (2) Toca-1 using anti-GFP (α-GFP) and anti-Hexokinase (α-Hex) serum.

efficiency was reduced in the presence of constitutively active Cdc42 but not in the presence of dominant negative mutant of Cdc42. However, as the analysis was carried out in metazoan cells with the full complement of N-WASP binding partners it would be difficult to determine whether the reduction in FRET efficiency in the presence of Cdc42 is due to direct binding of Cdc42 to N-WASP. This is especially so in light of the identification of Toca-1 [7] which has been suggested to form the connecting bridge between Cdc42 and N-WASP.

We have used the split YFP to analyze the conformational changes of WASP using *S. cerevisiae*, which does not have genes encoding any of the known interactors (Nck1, Grb2, Toca1, WIP, WIRE, CR16) of WASP. *S. cerevisiae* cells expressing NLS-YFP_{1–154}-WASP-YFP_{155–238} had fluorescence signal in the nucleus suggesting that WASP is an autoinhibited conformation. This is the first demonstration of the existence of autoinhibited conformation of WASP using the whole molecule.

We have shown that the growth defects of *las17Δ* strain of *S. cerevisiae* can be suppressed by the expression of WASP and WIP but not by the expression of WASP alone or by the expression of WASP and CR16 [23]. Co-expression of YFP_{1–154}-WASP-YFP_{155–238} with WIP or WIRE enhanced the YFP fluorescence while co-expression of YFP_{1–154}-WASP-YFP_{155–238} with CR16 did not enhance the YFP fluorescence consistent with the functional data.

We have previously shown that WASP is localized to cortical patches by binding to WIP [23]. This data suggests that WASP in the WASP–WIP complex localized at the cortical patches could be in a closed conformation raising the interesting possibility that the WASP in the closed conformation is still able to activate the Arp2/3 complex to suppress the growth defect of *las17Δ* strain.

Expression of Cdc42 with YFP_{1–154}-WASP-YFP_{155–238} did not affect the YFP fluorescence significantly while expression of Toca-1 reduced the YFP fluorescence. This supports the model in which Cdc42 activates WASP through Toca-1 [7]. We find that Toca-1 can alter the WASP conformation even in the absence of Cdc42, however it is possible that Toca-1 together with activated Cdc42 can induce a more pronounced conformational change. We also find that Nck1 can also reduce the YFP fluorescence suggesting that binding of proteins with SH3 domain (Toca-1 and Nck1) to the proline rich region of WASP can induce conformational changes and open up the WASP molecule leading to enhanced activation of the Arp2/3 complex.

Acknowledgments

This work was supported by Agency for Science, and Technology and Research (A*STAR), Biomedical Research Council grant A*STAR 05/1/22/19/392.

References

- [1] J.M.J. Derry, H.D. Ochs, U. Francke, Isolation of a novel gene mutated in Wiskott–Aldrich syndrome, *Cell* 78 (1994) 635–644.
- [2] T. Takenawa, H. Miki, WASP and WAVE family proteins: key molecules for rapid rearrangement of cortical actin filaments and cell movement, *J. Cell Sci.* 114 (2001) 1801–1809.
- [3] H. Miki, K. Miura, T. Takenawa, N-WASP, a novel actin-depolymerizing protein, regulates the cortical cytoskeletal rearrangement in a PIP2-dependent manner downstream of tyrosine kinases, *EMBO J.* 15 (1996) 5326–5335.
- [4] A.S. Kim, L.T. Kakalis, N.A. Manan, G.A. Liu, M.K. Rosen, Autoinhibition and activation mechanisms of the Wiskott–Aldrich syndrome protein, *Nature* 404 (2000) 151–158.
- [5] R. Rohatgi, H.Y. Ho, M.W. Kirschner, Mechanism of N-WASP activation by CDC42 and phosphatidylinositol 4,5-bisphosphate, *J. Cell Biol.* 150 (2000) 1299–1310.
- [6] H.N. Higgs, T.D. Pollard, Activation by Cdc42 and PIP(2) of Wiskott–Aldrich syndrome protein (WASP) stimulates actin nucleation by Arp2/3 complex, *J. Cell Biol.* 150 (2000) 1311–1320.
- [7] H.Y. Ho, R. Rohatgi, A.M. Lebensohn, M. Le, J. Li, S.P. Gygi, M.W. Kirschner, Toca-1 mediates Cdc42-dependent actin nucleation by activating the N-WASP–WIP complex, *Cell* 118 (2004) 203–216.
- [8] N. Ramesh, I.M. Anton, J.H. Hartwig, R.S. Geha, WIP, a protein associated with Wiskott–Aldrich syndrome protein, induces actin polymerization and redistribution in lymphoid cells, *Proc. Natl. Acad. Sci. USA* 94 (1997) 14671–14676.
- [9] M. Symons, J.M. Derry, B. Karlak, S. Jiang, V. Lemahieu, F. McCormick, U. Francke, A. Abo, Wiskott–Aldrich syndrome protein, a novel effector for the GTPase CDC42Hs, is implicated in actin polymerization, *Cell* 84 (1996) 723–734.
- [10] H.Y. Ho, R. Rohatgi, L. Ma, M.W. Kirschner, CR16 forms a complex with N-WASP in brain and is a novel member of a conserved proline-rich actin-binding protein family, *Proc. Natl. Acad. Sci. USA* 98 (2001) 1306–1311.
- [11] P. Aspenstrom, The WASP-binding protein WIRE has a role in the regulation of the actin filament system downstream of the platelet-derived growth factor receptor, *Exp. Cell Res.* 279 (2002) 21–33.
- [12] M. Kato, H. Miki, S. Kurita, T. Endo, H. Nakagawa, S. Miyamoto, T. Takenawa, WICH, a novel verprolin homology domain-containing protein that functions cooperatively with N-WASP in actin-microspike formation, *Biochem. Biophys. Res. Commun.* 291 (2002) 41–47.
- [13] Y. Sasahara, R. Rachid, M.J. Byrne, M.A. Fuente, R.T. Abraham, N. Ramesh, R.S. Geha, Mechanism of recruitment of WASP to the immunological synapse and of its activation following TCR ligation, *Mol. Cell* 10 (2002) 1269–1281.
- [14] K. Imai, S. Nonoyama, H.D. Ochs, WASP (Wiskott–Aldrich syndrome protein) gene mutations and phenotype, *Curr. Opin. Allergy Clin. Immunol.* 3 (2003) 427–436.
- [15] D.M. Stewart, L. Tian, D.L. Nelson, Mutations that cause the Wiskott–Aldrich syndrome impair the interaction of Wiskott–Aldrich syndrome protein (WASP) with WASP interacting protein, *J. Immunol.* 162 (1999) 5019–5024.
- [16] N. Martinez-Quiles, R. Rohatgi, I.M. Anton, M. Medina, S.P. Saville, H. Miki, H. Yamaguchi, T. Takenawa, J.H. Hartwig, R.S. Geha, N. Ramesh, WIP regulates N-WASP-mediated actin polymerization and filopodium formation, *Nat. Cell Biol.* 3 (2001) 484–491.
- [17] M. Lorenz, H. Yamaguchi, Y. Wang, R.H. Singer, J. Condeelis, Imaging sites of N-wasp activity in lamellipodia and invadopodia of carcinoma cells, *Curr. Biol.* 14 (2004) 697–703.
- [18] C.D. Hu, Y. Chinenov, T.K. Kerppola, Visualization of interactions among bZIP and Rel family proteins in living cells using bimolecular fluorescence complementation, *Mol. Cell* 9 (2002) 789–798.
- [19] T. Thanabalu, A.L. Munn, Functions of Vrp1p in cytokinesis and actin patches are distinct and neither requires a WH2/V domain, *EMBO J.* 20 (2001) 6979–6989.
- [20] R.D. Gietz, A. Sugino, New yeast-*Escherichia coli* shuttle vectors constructed with *in vitro* mutagenized yeast genes lacking six-base pair restriction sites, *Gene* 74 (1988) 527–534.
- [21] L. Meng, R. Rajmohan, S. Yu, T. Thanabalu, Actin binding and proline rich motifs of CR16 play redundant role in growth of *vrp1* Δ cells, *Biochem. Biophys. Res. Commun.* 357 (2007) 289–294.
- [22] A.J. Thrasher, WASP in immune-system organization and function, *Nat. Rev. Immunol.* 2 (2002) 635–646.
- [23] R. Rajmohan, L. Meng, S. Yu, T. Thanabalu, WASP suppresses the growth defect of *Saccharomyces cerevisiae* las17 Δ strain in the presence of WIP, *Biochem. Biophys. Res. Commun.* 342 (2006) 529–536.